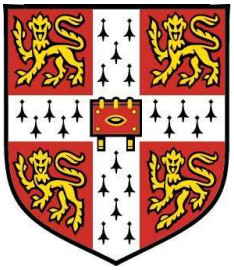

UNIVERSITY OF CAMBRIDGE

IMPROVED PRODUCTION OF POLY(HYDROXYBUTYRATE) AND RELATED ENZYMES

by

Nicholas Maitland Thomson

SIDNEY SUSSEX COLLEGE

This dissertation is submitted for the degree of
Doctor of Philosophy

MMXII

Declaration of Authorship

This dissertation is the result of my own work and includes nothing which is the outcome of work done in collaboration except where specifically indicated in the text. Its length does not exceed 60,000 words.

Some parts of this thesis have been published or are awaiting publication in the following peer-reviewed journal articles: -

1. Thomson, N.M., Roy, I., Summers, D.K. and Sivaniah, E. (2010) *In vitro* production of polyhydroxyalkanoates: achievements and applications; *Journal of Chemical Technology and Biotechnology* **85**:760–767.

2. Thomson, N.M., Summers, D.K. and Sivaniah, E. (2010) Synthesis, properties and uses of bacterial storage lipid granules as naturally occurring nanoparticles; *Soft Matter* **6**:4045–4057.

3. Thomson, N.M., Channon, K., Mokhtar, N.A., Staniewicz, L., Rai, R., Roy, I., Sato, S., Donald, A.M., Summers, D.K. and Sivaniah, E. (2011) Imaging internal features of whole, unfixed bacteria; *Scanning* **33**:59–68.

4. Thomson, N.M., Saika, A., Sangiambut, S., Ushimaru, K., Tsuge, T., Summers, D.K. and Sivaniah, E. (2013) Efficient production of active polyhydroxyalkanoate synthase in *E. coli* by co-expression of molecular chaperones; *Applied and Environmental Microbiology*; accepted.

Acknowledgements

I have spent four enjoyable and inspiring years in Cambridge and far too many people have helped me in various ways for me to name them all, much as I would like to. If you happen to be reading this and I have not thanked you personally, please rest assured that I am grateful for your help, advice and friendship.

I would not have started my Ph.D. without the help of my supervisors, Drs. Easan Sivaniah and David Summers, and without their guidance, encouragement and insight I certainly would not have finished. I would like to thank them for their constant support, for the inspiration and ideas, for challenging me to reach further, and particularly for their criticism. I have learnt an immeasurable amount from both of them. I would also like to thank Dr. Ipsita Roy for welcoming me into her laboratory at the beginning of my first year and for her help and encouragement in scaling the initial learning curve.

I was fortunate to be surrounded by a wonderful group of fellow students, who I hope will remain friends for a long time: Simon, Joakim, Elodie, Sarra, Oliver, Lorenz, Lars, Himantha, Catalin and Anders. Thank you all for the interesting discussions, help with 'physics stuff', procrastination, parties and banter.

Wonderful people were also to be found in the Sivaniah, Summers and Roy research groups, and their comments and suggestions about my work were both helpful and appreciated. Particular thanks are due to Smith Sangiambut, Chih-Chin Chen, Noor Azlin Mokhtar, Duncan Rowe and Pooja Basnett for numerous helpful discussions, insightful questions and help with experiments. Thanks also to Lech Staniewicz for help with wet STEM.

The support staff both in BSS and in Sidney Sussex College all deserve far more frequent thanks than they receive. Their good-natured assistance makes a huge contribution to the smooth running of the University and made my job as a researcher much easier. Tracy, Stef, Sarah, Owen, Pete, Suresh and Suzannah: thank you.

Prof. Takeharu Tsuge and all the members of his laboratory at the Tokyo Institute of Technology gave me a warm welcome and great assistance during my three-month stay in Japan. I learnt so much from them and had such a brilliant time that my only regret is I couldn't stay longer. Particular thanks to Ayaka Hiroe and Satoshi Tomizawa for their help during my stay and to Azusa Saika and Kazunori Ushimaru for their productive work during their visits to Cambridge. Arigatō Gozaimashita!

Finally, I would like to thank my family for always being on the end of a phone or train line, everyone I have played football with for helping me to let off steam, and the 'Green Bullet Firm' for some legendary away days.

I received funding from the Engineering and Physical Sciences Research Council (grant number EP/P504120/1), Tokyo Institute of Technology Global Center of Excellence, the Cambridge Philosophical Society and Sidney Sussex College.

Abstract

IMPROVED PRODUCTION OF POLY(HYDROXYBUTYRATE) AND RELATED ENZYMES

by Nicholas Maitland Thomson

Polyhydroxyalkanoates (PHAs) are biodegradable, thermoplastic polymers that are produced by a wide range of bacteria in response to nutrient limitation and function as carbon and energy storage molecules. They have a wide range of potential applications ranging from direct replacements for traditional plastics in packaging, industry and agriculture to new markets such as drug delivery, tissue engineering and environmental remediation.

This thesis begins with a review of PHA metabolism and uses, in which they are compared to other carbon storage compounds. The most common method of production at present is within bacteria, particularly transgenic *Escherichia coli*. However, bacterial production is expensive and limits the range of monomers that can be incorporated. This makes it difficult to fine-tune the physical properties to the desired applications. This thesis aims to address both of these problems, using polyhydroxybutyrate as a simple model.

To simplify the purification of the polymer and to broaden the range of potential monomers, PHA can be produced *in vitro*. To achieve this on a commercial scale would require the production of large quantities of the polymerase enzyme, $PhaC_{Re}$. Therefore, a novel *Escherichia coli* cell factory, which can enter a non-growing but metabolically active quiescent state, was tested for high-efficiency $PhaC_{Re}$ production.

Although the cells produced more $PhaC_{Re}$, the majority of the enzyme was accumulated in insoluble and inactive deposits. Therefore, chaperone proteins were co-expressed with $PhaC_{Re}$ to facilitate its correct folding. This resulted in an approximately three-fold increase in the yield of $PhaC_{Re}$.

Another strategy for controlling the physical properties of PHAs is to blend them with other polymers. *E. coli* typically produces very high molecular weight PHA, so small-chain alcohols were investigated for their efficiency in reducing the molecular weight to allow easier blending. Methanol and ethanol were shown to reduce the molecular weight by up to 70% at concentrations that are non-toxic to the cells. Both are cheap and readily available chemicals, and could therefore be easily used in commercial-scale production.

Finally, to understand better the mechanisms that take place within bacterial cells during PHA production, a new electron microscopy technique was investigated: wet scannning-transmission electron microscopy allows the interior features of unfixed, unstained and hydrated cells to be quickly and easily viewed at high resolution, with a limit of 15–20 nm. This was the first time the technique had been used to view the cytoplasmic contents of bacteria and demonstrated its potential as an intermediate between light microscopy and more damaging (but higher resolution) electron microscopy techniques. The technique was also used to view triacylglyceride and polyphosphate inclusions bodies within cells.

Contents

Declaration of Authorship i

Acknowledgements ii

Abstract iii

List of Figures ix

List of Tables xi

Abbreviations xiii

1 Introduction 1
- 1.1 *Escherichia coli* as the workhorse of the biotechnology industry . . . 3
- 1.2 Scope and outline of this thesis . . . 4

2 A review of bacterial carbon storage compounds 7
- 2.1 Introduction . . . 7
- 2.2 Polyhydroxyalkanoates . . . 9
  - 2.2.1 Metabolic pathways . . . 10
  - 2.2.2 Granule-associated proteins . . . 10
  - 2.2.3 Granule formation . . . 11
  - 2.2.4 Poly(thioesters) . . . 12
- 2.3 Triacylglycerides . . . 13
  - 2.3.1 Metabolic pathways . . . 14
  - 2.3.2 Granule-associated proteins . . . 14
  - 2.3.3 Granule formation . . . 16
- 2.4 Wax esters . . . 17
  - 2.4.1 Metabolic pathways . . . 17
  - 2.4.2 Granule structure and associated proteins . . . 18
  - 2.4.3 Granule formation . . . 18
- 2.5 PHA synthases . . . 19
- 2.6 Material properties and applications of Polyhydroxyalkanoates . . . 21
- 2.7 Methods of PHA production . . . 22
  - 2.7.1 Production in microorganisms . . . 22
    - 2.7.1.1 Bacteria . . . 22

2.7.1.2 Archaea . . . 23
2.7.1.3 Photosynthetic microorganisms . . . 24
2.7.1.4 Yeast . . . 25
2.7.2 Chemical synthesis . . . 25
2.7.3 Production in plants . . . 26
2.7.4 *In vitro* production . . . 27
2.8 Visualisation of PHAs in bacteria . . . 28
2.8.1 Light microscopy . . . 28
2.8.2 Atomic force microscopy . . . 30
2.8.3 Electron microscopy . . . 31
2.9 Non-lipidic bacterial storage compounds . . . 32
2.9.1 Polysaccharides . . . 32
2.9.2 Inorganic storage compounds . . . 33

3 Materials and methods 35
3.1 Bacterial strains and plasmids . . . 35
3.1.1 Strains . . . 35
3.1.2 Plasmids . . . 36
3.2 Plasmid construction . . . 37
3.2.1 Plasmid purification . . . 37
3.2.2 Polymerase chain reaction . . . 38
3.2.3 Agarose gel electrophoresis . . . 39
3.2.4 DNA ligation . . . 40
3.3 DNA sequencing . . . 41
3.4 Transformation of *E. coli* . . . 41
3.4.1 Preparation of competent cells . . . 42
3.4.2 Transformation . . . 42
3.5 Growth conditions . . . 43
3.5.1 Monitoring cell growth by measurement of optical density . . . 43
3.5.2 Q-cell growth . . . 44
3.5.3 $PhaC_{Re}$ production . . . 44
3.5.4 PHB production . . . 45
3.6 Protein purification and analysis . . . 45
3.6.1 Preparation of cell fractions for SDS-PAGE . . . 46
3.6.2 Western blotting . . . 47
3.6.3 Cobalt-affinity purification . . . 48
3.6.4 $PhaC_{Re}$ activity assay . . . 48
3.7 PHB purification and analysis . . . 49
3.7.1 Methanolysis . . . 50
3.7.2 Gas chromatography . . . 50
3.7.3 PHB purification . . . 50
3.7.4 Gel permeation chromatography analysis . . . 50
3.8 Wet STEM imaging of bacterial cells . . . 51
3.8.1 Sample preparation . . . 51
3.8.2 Imaging conditions . . . 51
3.8.3 Pump-down procedure . . . 52
3.8.4 Cell viability study . . . 52

3.8.4.1 Optical density method . . . 52
3.8.4.2 Colony counting method . . . 53
3.9 TEM sample preparation and imaging . . . 53
3.10 Chemical stock solutions . . . 54
3.11 Growth Media . . . 54
3.11.1 Luria-Bertani Medium (LB) . . . 55
3.11.2 Nutrient-Rich Medium (NR) . . . 55
3.11.3 Nitrogen-Limited Mineral Salts Medium (MS) . . . 55
3.11.4 Mineral Salts Medium for *Rhodococcus opacus* PD630 (MMR) . . . 56
3.11.5 Mineral Salts Medium for *Pseudomonas mendocina* (MMP) . . . 57
3.11.6 SOC Medium . . . 57
3.12 Buffers . . . 57
3.12.1 Inoue transformation buffer . . . 57
3.12.2 10× Tris-acetate-EDTA . . . 58
3.12.3 10× Tris-glycine buffer . . . 58
3.12.4 3× SDS-PAGE sample buffer . . . 58
3.12.5 Western blotting Anode Buffer I (pH 10.4) . . . 59
3.12.6 Western blotting anode buffer II (pH 10.4) . . . 59
3.12.7 Western blotting cathode buffer (pH 9.4) . . . 59
3.12.8 Lysis/binding buffer for protein purification (pH 8.0) . . . 60
3.12.9 Elution buffer for protein purification (pH 8.0) . . . 60
3.12.10 Desalting buffer for protein solutions (pH 8.0) . . . 60

4 The Quiescent-cell expression system for PHA synthase production 61
4.1 Introduction . . . 61
4.1.1 The development of the Quiescent-cell system . . . 62
4.1.2 The use of indole to induce quiescence . . . 63
4.2 Bacterial strains and plasmids . . . 65
4.3 Results . . . 66
4.3.1 Construction of pASG1$phaC_{\mathrm{Re}}$ . . . 66
4.4 $\mathrm{PhaC_{Re}}$ expression at 37 °C . . . 67
4.4.1 Basic analysis of Q-cell performance . . . 67
4.4.2 Timing of induction . . . 68
4.4.3 Length of induction . . . 70
4.4.4 Concentration of indole . . . 71
4.4.5 Summary of optimisation at 37 °C . . . 72
4.5 $\mathrm{PhaC_{Re}}$ expression at 30 °C . . . 73
4.5.1 Effect of density at inoculation on final cell density . . . 73
4.5.2 Effect of inoculum density on $\mathrm{PhaC_{Re}}$ production . . . 74
4.5.3 Larger-scale $\mathrm{PhaC_{Re}}$ production, purification and activity testing . . . 75
4.5.4 Protein solubility check . . . 76
4.6 Discussion . . . 77

5 Efficient production of active polyhydroxyalkanoate synthase in *E. coli* by co-expression of molecular chaperones 81
5.1 Introduction . . . 81
5.2 Bacterial strains and plasmids . . . 85

5.3 Results . . . 85
5.3.1 Production and purification of $PhaC_{Re}$ . . . 85
5.3.2 The effect of chaperones on $PhaC_{Re}$ solubility . . . 88
5.3.3 The influence of chaperone co-expression on PhaC activity . . . 89
5.3.4 The effect of chaperones on PHB production . . . 90
5.4 Discussion . . . 91

6 Polyhydroxybutyrate molecular weight control 95
6.1 Introduction . . . 95
6.1.1 Measuring polymer molecular weight . . . 96
6.1.2 Methods of controlling PHA molecular weight in *E. coli* . . . 98
6.2 Bacterial strains and plasmids . . . 100
6.3 Results . . . 101
6.3.1 Characterisation of growth and PHB production . . . 101
6.3.2 Molecular weight of PHB produced in the presence of indole . . . 103
6.3.3 Molecular weight of PHB in the presence of short-chain alcohols . 105
6.3.4 Effects of indole and alcohols on $PhaC_{Re}$ activity . . . 109
6.3.5 Other hydroxylated molecules and acetic acid . . . 109
6.4 Discussion . . . 111

7 Imaging internal features of whole, unfixed bacteria by 'wet scanning-transmission electron microscopy' 115
7.1 Introduction . . . 115
7.2 Bacterial strains . . . 119
7.3 Results . . . 119
7.3.1 Comparison of wet STEM and TEM . . . 119
7.3.2 Optimisation of imaging pressure . . . 121
7.3.3 Imaging of intracellular inclusions in bacteria . . . 123
7.3.4 Cell viability during imaging . . . 125
7.4 Discussion . . . 128
7.5 Conclusions . . . 131

8 Conclusions and future perspectives 133
8.1 The Quiescent-cell system . . . 133
8.2 Chaperone protein co-expression . . . 135
8.3 Control of PHB molecular weight . . . 135
8.4 Visualising granules within cells by wet STEM . . . 136

List of Figures

1.1 PHA granules accumulating in *R. eutropha* 2

2.1 Biochemical pathways for PHA production 11
2.2 The two proposed mechanisms for PHA granule production in bacteria . . 12
2.3 Biochemical pathways for the production of bacterial storage lipids 15
2.4 The mechanism of TAG and WE formation in bacteria 17
2.5 The four classes of PHA synthase 19
2.6 Examples of images of bacterial storage lipids 29

4.1 Tryptophan catabolism by tryptophanase 64
4.2 Basic analysis of Q-cell performance 68
4.3 Optimisation of the time of protein expression induction 69
4.4 Optimisation of the length of induction 71
4.5 Optimisation of indole concentration for Q-cell cultures 72
4.6 Effect of density at inoculation on final density of Q-cell cultures 74
4.7 Effect of inoculum density on productivity of Q-cell cultures 75
4.8 Purification of $PhaC_{Re}$ produced in Q-cells 76
4.9 Solubility of $PhaC_{Re}$ produced in Q-cells 77

5.1 Mechanisms of action of three chaperone protein systems 83
5.2 SDS-PAGE gels used to identify contaminants in purified $PhaC_{Re}$ 87
5.3 Distribution of $PhaC_{Re}$ between soluble and insoluble fractions 88
5.4 Specific activity and yield of $PhaC_{Re}$ co-expressed with chaperones 89

6.1 Cell growth and PHB accumulation in the presence of indole 102
6.2 Effect of indole concentration on dry cell weight of W3110$hns\Delta$93 103
6.3 $M_w$reduction caused by indole 104
6.4 $M_n$reduction and variation in PDI caused by indole 105
6.5 Effect of short-chain alcohols on cell growth 106
6.6 $M_w$reduction caused by ethanol and methanol 107
6.7 $M_n$reduction and variation in PDI caused by ethanol and methanol 108

7.1 Illustration of wet STEM experimental setup 117
7.2 Comparison of TEM & wet STEM Images 120
7.3 Morphology of samples at various pressures 122
7.4 Illustration of beam damage in samples 123
7.5 Wet STEM images of lipid storage inclusions in three species of bacteria . 124
7.6 Survival of *R. eutropha* at a range of pressures following wet STEM preparation 128

List of Tables

3.1 Bacterial strains used for this thesis 35
3.2 Plasmids used for this thesis 36
3.3 Details of chemical stock solutions 54

4.1 Bacterial strains and plasmids for Chapter 4 65

5.1 Bacterial strains and plasmids for Chapter 5 85
5.2 The effect of chaperone co-expression on yields of soluble $PhaC_{Re}$ 86
5.3 Production of PHB during overexpression of chaperone proteins 91

6.1 Bacterial strains and plasmids for Chapter 6 101
6.2 Growth and molecular weight control characteristics of all additives . . . 110

7.1 Bacterial strains for Chapter 7 119
7.2 Growth of *R. eutropha* H16 after wet STEM preparation procedure and exposure to low pressure for 10 minutes 126
7.3 Colony forming units (CFU) of *R. eutropha* following wet STEM preparation procedure and exposure to low pressure for 10 minutes 127

Abbreviations

ADP–glucose	Adenosine Diphosphate–glucose
AFM	Atomic Force Microscopy
AHT	Anhydrotetracycline
ATP	Adenosine Triphosphate
$\mathbf{A}_x$	Absorbance at a wavelength of x nm
CFU	Colony Forming Units
CoA	Coenzyme A
DCW	Dry Cell Weight
dd$\mathbf{H_2O}$	Double-distilled Water
ESEM	Environmental Scanning Electron Microscopy
GC	Gas Chromatography
GFP	Green Fluorescent Protein
GPC	Gel Permeation Chromatography
IPTG	Isopropyl β–D–1–thiogalactopyranoside
LB	Luria-Bertani growth medium
MS	Mineral Salts growth mediu
NR	Nutrient Rich growth Medium
$\mathbf{OD}_{600}$	Optical Density at a wavelength of 600 nm
PEG	Poly(ethylene glycol)
PHA	Polyhydroxyalkanoate
$\mathbf{PHA}_{\mathrm{MCL}}$	Medium Chain-Length Polyhydroxyalkanoate
$\mathbf{PHA}_{\mathrm{SCL}}$	Short Chain-Length Polyhydroxyalkanoate
PHB	Poly(3–hydroxybutyrate)
P4HB	Poly(4–hydroxybutyrate)
PHBV	Poly(3–hydroxybutyrate–*co*–3–hydroxyvalerate)

PHHx	Poly(3–hydroxyhexanoate)
PHO	Poly(3–hydroxyoctanoate)
PHV	Poly(3–hydroxyvalerate)
PPI	Peptidyl–Prolyl *cis/trans* Isomerase
PTE	Poly(thioester)
Q-cells	Quiescent-cell Expression System
SDS-PAGE	Sodium Dodecyl Sulphate–Polyacrylamide Gel Electrophoresis
SEM	Scanning Electron Microscopy
TAG	Triacylglyceride
TEM	Transmission Electron Microscopy
WE	Wax Ester
wet STEM	Wet Scanning–Transmission Electron Microscopy
WS/DGAT	Wax ester Synthase/acyl-CoA:Diacyclglycerol Acyltransferase

Chapter 1

Introduction

Over the last century enormous changes have been made in the human lifestyle, facilitated by technological improvements in raw material provision, manufacturing and the innovation of new products. Perhaps the principal effector of these advancements has been the availability of synthetic plastics, of which common examples such as polystyrene, polypropylene, polyethylene, polyurethane, and polyamides are universally known and recognised.

It is almost impossible to think of an area of modern life that does not depend in some way on one or more plastic. A brief consideration of their properties makes it clear why they are so useful: They are readily available, cheap and hard-wearing; a wide range of types can be selected from in order to suit countless applications; they can be processed into sheets, films, fibres, filaments and latexes; they generally weigh less than natural alternatives such as wood and leather, and they are resistant to a wide range of chemicals.

Unfortunately, over the same time-frame the disadvantages of society's reliance on synthetic plastics have also become apparent. The vast majority of plastics used at present are derived from crude oil. This is a finite resource and as it becomes scarcer it will also become more difficult and expensive to acquire. The longevity of petrochemical plastics also causes a problem as they accumulate in the environment after disposal and may become a health risk to wildlife.[1,2]

In response to the economical and environmental concerns surrounding petrochemical plastics, more sustainable sources have been sought for materials with similar properties. Chemically synthesised but degradable polymers such as poly(lactic acid), poly(butylene succinate) and polycaprolactone are commercially available.[3–5] However, polymers that are produced by biological organisms are of particular interest because the production

process can be mediated by the organisms themselves, often requiring only the input of simple carbon sources and other nutrients.[5] These macromolecules are known as biopolymers, and include modified polysaccharides such as starch, cellulose and chitosan, and lipid-like polymers such as polyhydroxyalkanoates (PHAs).

The definition of a biopolymer is rather broad, and generally encompasses polymers that require an organism or an isolated enzyme-catalysed reaction for at least one stage of their production. For example, chitosan requires chitin (the structural element of fungal cell walls and of arthropod and insect exoskeletons) as the starting material, which is then deacetylated in a chemical step to produce chitosan. PHAs, on the other hand, are truly biopolymers in the strictest sense as they are produced entirely within bacteria and need only to be extracted and purified from the cells for use. This relative ease of production and the ability of bacteria to grow quickly on a wide range of carbon sources make PHAs one of the most promising candidates for replacing petrochemical plastics.[6]

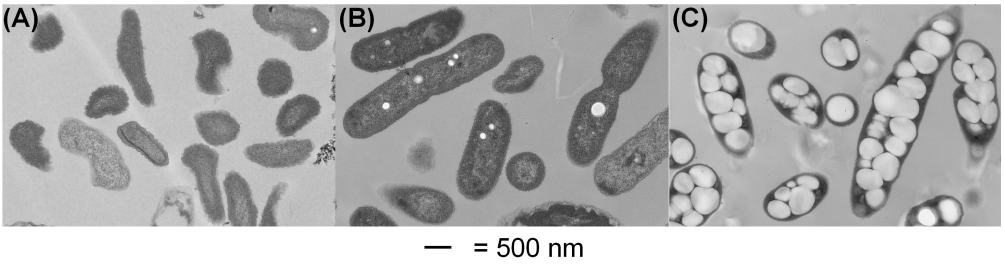

Figure 1.1: Transmission electron microscopy images of PHA granules accumulating in *R. eutropha*. (A) Cells grown with all nutrients required for growth, with no PHA. (B) Early stages of PHA granule growth (small white inclusions) as nutrients are depleted. (C) Large granules fill the cytoplasm after extended growth with low nitrogen concentration and excess fructose.

PHAs are also the focus of this thesis. They are a class of aliphatic polyester and are produced by a wide range of bacterial species as a carbon and energy storage compound. Many bacteria live in environments in which nutrient supply is not constant. Therefore, when a carbon source is plentiful but some other nutrient is in limited supply, PHA-producing species sequester the carbon for later use in the form of cytoplasmic granules of PHA (Figure 1.1).[7] Other species produce related compounds such as wax esters and triacylglycerides for the same reason.[8] All of these bacterial carbon storage compounds have commercial uses, but only PHAs have the necessary physical properties to be used as alternatives to petrochemical plastics.

1.1 *Escherichia coli* as the workhorse of the biotechnology industry

PHAs have found some niche applications in the medical industry because they are biocompatible (do not induce an immune response) and can be degraded within the body.[9] However, their adoption for mass-market applications such as packaging or for the production of disposable products has so far been limited.[5] The two main reasons for this are that the cost of PHA production makes it uncompetitive with the petrochemical industry (even if consumers are willing to spend more for a more environmentally friendly product) and that it is difficult to produce polymers with the necessary physical properties to meet the manufacturing and usage specifications.

To improve on existing manufacturing techniques, it is useful to study a relatively simple model system. Therefore, the work in this thesis is based on the production of poly(3-hydroxybutyrate) (PHB) in *Escherichia coli*. PHB is the simplest of the family of PHAs as it is a homopolymer whose monomers consist of four carbon atoms. It is also the most commonly found PHA in the natural environment and can be produced with very high yields from glucose.[10]

E. coli is the best known and most widespread model organism for bacterial microbiology and genetics, and is routinely used in industry for the production of proteins, pharmaceuticals and other chemicals.[11] It does not naturally produce any carbon storage compounds, but can easily be engineered to produce PHB by the insertion of a plasmid containing the required genes.[12] The combination of PHB and *E. coli* therefore make a convenient model system that can be easily manipulated and used to test new ideas.

The characteristics that made *E. coli* an attractive subject for microbiological studies are its convenient availability, interesting symbiotic relationship with humans, relevance to human health, fast growth under easily obtainable conditions, and versatile metabolism. These traits are still valuable and now, due to the long history of study of all aspects of *E. coli* biology, a vast wealth of knowledge has been accumulated. The relatively recent ability to manipulate the genes of organisms, and particularly to express foreign genes in host organisms, has resulted in a wide array of molecular biology tools that facilitate the further generation of knowledge. The innate benefits of using *E. coli* combined with the knowledge that has built up around it make it the default choice for expression of heterologous proteins and production of a wide range of chemicals in the biotechnology, chemical and food industries.

Fermentation of *E. coli* for the production of chemicals such as biofuels is only possible because of our detailed understanding of how to manipulate metabolic pathways. This has also driven an interest in developing methods for extremely high cell density fermentation (>100 g dry cell weight per litre) to extract greater yields.[13] Further optimisation is also achieved by careful selection of strain, vector and promoter.[14] In recent years, the use of recombinant proteins for therapeutic applications has increased dramatically, and *E. coli* has been the bacterium of choice for production.[11] Approximately 150 recombinant proteins are recommended by the U.S. Food and Drug Administration and/or the European Medicines Agency, including hormones, growth factors, colony stimulating factors, interferons, interleukins, human serum albumin and antibodies, of which 30% are produced in *E. coli*.[15]

There are disadvantages to the use of *E. coli* as a cell factory, particularly for pharmaceutical products. Being Gram-negative, it produces lipopolysaccharide (LPS) that can contaminate the final product and lead to immune responses in humans.[16] This has been a significant problem for the production of PHAs for medical purposes.[17] A potential solution that will be discussed in greater detail in Chapters 4 and 5 is to use *E. coli* for the production of the necessary enzymes, but to allow the polymerisation reaction to progress *in vitro*.

Unfortuately, overexpressed proteins frequently misfold and are deposited in the cytoplasm as insoluble inclusion bodies. Although it is sometimes possible to recover and refold this protein, this adds expense and complexity to the production.[18] Strategies to prevent inclusion body formation include using weaker induction of protein expression, growth at reduced temperatures, co-expression of chaperone proteins to assist folding, and fusion of hydrophilic 'solubility tags' to the ends of proteins.[19] Alternatively, some proteins can be secreted, either to the periplasm or entirely out of the cell, to increase yields and facilitate purification.[20] However, *E. coli* does not naturally secrete many proteins so the process can be rather inefficient and dependent on protein sequence. Therefore, there is growing interest in using alternative expression hosts. The Gram-positive *Bacillus* spp. and *Corynebacterium glutamicum* are particularly promising due to their lack of LPS and superior ability to secrete protein.[21] The problem of heterologous protein solubility in *E. coli* is also considered further in Chapters 4 and 5.

1.2 Scope and outline of this thesis

The overall aim of this thesis is to provide some potential solutions to the problems of cost and material properties in the production of PHAs. Two main approaches will be described. The first is to facilitate the production of PHA *in vitro* by improving the

productivity of the polymerase enzyme (PhaC). PHA synthases are the most important enzymes in the PHA metabolic cycle because they control which monomers are incorporated and the molecular weight of the final polymer. PhaC tends to aggregate at high concentrations and is therefore difficult to produce in commercially-relevant quantities. Therefore, it is hoped that by improving the yields of PhaC larger scale *in vitro* production will become a possibility. This should allow simpler purification of the polymer to reduce cost, and better control of the polymer composition to improve the material properties.

The second approach is to utilise existing knowledge of the control of molecular weight *in vivo* so that the natural mechanisms can be exploited, optimised and improved by controlling culture conditions and supplementing the culture with chain transfer agents. The molecular weight of a polymer is one of the key determinants of its physical properties and so can be used either to directly influence the properties of PHA or to facilitate the production of blends and composites (mixtures of PHA with other materials). This could allow cheap but mechanically poor PHAs such as PHB to be improved by blending with more flexible polymers and could reduce costs by 'bulking up' the production of expensive PHA with cheaper polymers such as cellulose.

This work deals exclusively with the production of PHB and uses *E. coli* as the principal species for production of proteins and the polymer. These were chosen because they are simple to work with, can produce high yields under a variety of growth conditions, and have been studied and characterised extensively (both individually and together). The hope and intention is to develop production methods that could be widely applied to the production of any of the large family of PHA polymers, and to bacterial hosts other than *E. coli*.

Chapter 2 provides an overview of all three types of bacterial carbon storage molecule. The focus is on PHAs, to which the triacylglycerides and wax esters are compared, in order to highlight the many similarities between the metabolic pathways, granule structure and commercial production of each. Greater focus is then placed on the production of PHAs. The PHA synthase enzymes are described in more detail, to illustrate their importance in PHA anabolism. Many different methods for PHA production have been tested, including chemical synthesis, production in microorganisms, production in plants and *in vitro* synthesis. These are also reviewed. The chapter concludes with a review of the different methods that have been used to visualise PHA granules within bacteria, in an attempt to understand the processes that occur within the cells during PHA production.

Chapter 3 provides details of the experimental methods that were used for the following chapters. Some background is given on the theory of the techniques, and where

appropriate there is a discussion of why a particular technique was chosen ahead of any alternatives. The chapter also collates the details of the bacterial strains, plasmids, growth media and chemical stocks required for the experiments.

Chapter 4 describes an investigation into the production of PHA synthase using a novel *E. coli* cell factory called the Quiescent-cell expression system (Q-cells). Q-cells are cultures of a specific strain of *E. coli* that has been engineered to respond to the addition of a chemical signal, indole, by ceasing growth but maintaining metabolic activity. They are therefore able to produce larger quantities of protein than standard cultures, as their energy is expended on protein synthesis rather than generation of additional biomass.

Chapter 5 also focuses on the provision of larger quantities of high-quality synthase enzyme for *in vitro* production. In the approach described here, chaperone proteins are co-expressed with the synthase. Chaperones are native *E. coli* proteins that assist in the folding and solubility of nascent polypeptides. The expectation was that the chaperone proteins would increase the fraction of PhaC that was properly folded, and therefore increase the yield. The effect of chaperone co-expression on PHB yield and molecular weight is also tested.

Chapter 6 switches the attention to the production of PHB in *E. coli*. Current methods for controlling the molecular weight of PHAs either use poly(ethylene glycol) (PEG) as an additive to the culture medium, or post-processing steps to reduce the weight of the final polymer. PEG is thought to reduce the molecular weight by binding to the growing PHA chain, terminating polymerisation and initiating a new chain. In this chapter, alcohols with low carbon numbers are investigated and characterised as cheaper alternatives to PEG.

Chapter 7 was inspired by a desire to understand the mechanism of PHA granule production within the natural PHB producer, *Ralstonia eutropha*. A novel electron microscopic technique known as wet scanning-transmission electron microscopy (wet STEM) was tested for its ability to image the granules within cells as they grow. Compared to more conventional electron microscopic techniques, wet STEM requires little sample preparation and allows whole cells to be imaged with minimal damage while remaining hydrated, unfixed and unstained.

Chapter 8 finally draws together the conclusions from the previous chapters, and discusses the potential for further work to develop the ideas presented in this thesis.

Chapter 2

A review of bacterial carbon storage compounds

2.1 Introduction

Three main groups of carbon storage compounds are commonly produced by bacteria. These are polyhydroxyalkanoates (PHAs), triacylglycerides (TAGs) and wax esters (WEs). All three groups share many similarities in terms of how they are manufactured and stored by bacteria, their material properties and their biochemical function. They are inherently inert and water insoluble due to containing long hydrocarbon chains, which also give them superior energy density compared to carbohydrates and proteins. Therefore, they are excellent stores of carbon and energy.[22]

Although some transient production is common,[23,24] storage compounds are generally accumulated under conditions of nutrient imbalance, frequently to well over 50% of the dry cell weight (DCW).[25] Typically, when carbon is readily available but another nutrient (often either nitrogen or oxygen) is not, the carbon source will be converted into one or more lipid storage compounds and stored in the cytoplasm in the form of granules. This is accompanied by a halt in cell division, although the cells may increase in size to accommodate as much of the storage compound as possible.[26] When the nutrient balance becomes more favourable for growth, the storage compound can be broken down and used as an energy source. Many species of bacteria live in highly changeable environments, and nutrient-limited conditions are probably in many cases the 'normal' scenario. Therefore, by sequestering carbon to protect it from competing organisms, the bacteria gain a competitive advantage.[27]

As a group, bacterial carbon storage compounds are often referred to as lipid inclusions. However, only TAGs and WEs are *stricto sensu* lipids, while PHAs are hydrophobic polymers with similar physical characteristics. TAGs belong to the class of lipids known as glycerolipids, as they are composed of three fatty acids attached to glycerol via ester bonds. WEs are similar molecules, but are formed by the esterification of fatty acids with long-chain alcohols rather than glycerol. PHAs are formed from monomers of acyl-coenzyme A (acyl-CoA), derived from the same biochemical pathways as fatty acids, but are joined to each other via ester bonds and so form much larger, polymeric molecules.

PHAs have been the most rigorously studied of the three types of carbon storage compounds, primarily because they are the most common and widespread of the three. They also have a multitude of potential biotechnological applications ranging from biodegradable plastics to medical devices, tissue engineering scaffolds and drug delivery systems.[9,25,28–32] Although TAGs and WEs are less common in bacteria, potential applications have also been found for them. These are generally as alternatives to similar lipids produced in animals, plants or eukaryotic microorganisms. TAGs are ubiquitous in eukaryotes,[25,28,33,34] while WEs are produced by many animals and microorganisms, but only used as an energy source by one plant: Jojoba (*Simmondsia chinensis*).[35] TAGs are commonly used as edible fats and oils[33] and as pharmaceutically neutral emulsifiers and carriers for drug delivery.[36] WEs are common ingredients in a range of commercial products including candles, coatings and lubricants.[37]

The structure of the granules for each type of storage compound are also very similar. They take the form of well-defined cytoplasmic structures, 200–500 μm in diameter, with an amorphous lipid core surrounded by a layer of phospholipids and protein.[25,28,38] However, the mechanisms of their production are thought to differ,[28] and the type and quantity of protein attached to the granule surface varies substantially between different types of inclusions and between kingdoms.[22] In this introductory section, a brief overview will be provided of each type of inclusion. More detailed reviews of lipid inclusions in plants,[39–41] animals[42,43] and microorganisms[44] can be found in the articles cited herein.

The focus of this thesis is on the production of PHAs. Therefore, the other types of inclusions will only be considered in comparison to PHAs to illustrate the diversity in bacterially-produced storage compounds that exist despite the overall similarities between their methods of production. Following the broad overview, PHA production and uses will be considered in greater detail.

2.2 Polyhydroxyalkanoates

PHAs are long-chain polyesters with material properties ranging from hard, brittle, crystalline thermoplastics through to soft elastomers. Their material properties depend on the constituent monomers, of which over 150 examples are known.[30,45] They can be broadly divided into the short chain length PHAs (PHA_{SCL}), which consist of monomers with 4 or 5 carbon atoms, and the medium chain length PHAs (PHA_{MCL}), with 6 or more carbon atoms in each monomer.[46–48] The type of PHA produced by a particular bacterial species is determined by the substrate specificity of the PHA synthase enzyme (PhaC), which catalyses the polymerisation of (R)-hydroxyacyl-CoenzymeA (HA-CoA) monomers.[49–51] The stereo-selectivity of the PhaC enzyme is a universal property throughout all known PHA synthases, and provides an advantage over chemical synthesis, which is only able to produce a recemic mixture of (R)- and (S)-isomers.

The most common PHA is poly((R)-3-hydroxybutyrate) (PHB), which is produced by the model organism for PHA production, *Ralstonia eutropha*, as well as by other numerous and diverse species.[30] Note that the official name of *R. eutropha* is *Cupriavidus necator*. However, the species has been re-named many times when new taxonomic information has become available. It has also previously been known as *Wautersia eutropha* and *Alcaligenes eutrophus*. The majority of journal articles in the field refer to *R. eutropha*, so for convenience the species will be referred to throughout this thesis as *R. eutropha*.

PHB is polymerised from the simplest possible 3HA monomer, with a side-chain consisting of a methyl group. When purified, its high degree of crystallinity leads to it being very brittle, and conseqently of little commercial interest.[52] By incorporating monomers with longer side-chains—including PHA_{MCL} which is studied predominantly in *Pseudomonas* spp.—the material properties can be altered to approximate those of poly(ethylene) or to become even more elastomeric.[46]

Although short oligomers (200 monomers) of PHB complexed with proteins are ubiquitous components of membrane channels for all cells, only bacteria produce long polymers for storage purposes.[28,53] However, metabolic engineering of yeast[54,55] and plants[56–58] has shown that eukaryotic cells are capable of such production when endowed with the correct enzyme activity (if only in relatively small quantities).

2.2.1 Metabolic pathways

The metabolic pathways for producing PHAs divert intermediates of other, more central, pathways and convert them into the requisite monomers. It is essential for the functioning of the synthase that the monomer is attached to a CoA.[59,60] In the case of PHA_{SCL}, acetyl-CoA or related compounds such as valeryl-CoA are diverted from the respiratory pathway by PhaA, which condenses two such molecules (Figure 2.1). The resulting acetoacetyl-CoA (or similar) is then reduced by PhaB to form the monomer, which is polymerised by PhaC.[61] PHA_{MCL} monomers arise from either fatty acid biosynthesis or β-oxidation and are modified by other enzymes, including PhaG and PhaJ before polymerisation (Figure 2.1).[61,62]

2.2.2 Granule-associated proteins

In addition to the synthase (PhaC), which is bound to the granule surface during and after polymerisation,[63] a number of other proteins have been found to be associated with the PHA granule surface. Together with phospholipids, these proteins form a 4 nm thick monolayer around the core of the granule. It is thought that they protect the hydrophobic core from the cytoplasm, and play a role in regulating the number and size of granules produced.[32,64,65]

The most abundant granule-associated proteins form a class of small (11–25 kDa), amphiphilic proteins known as phasins, of which at least four types (PhaP1–4) are present in *R. eutropha*, with PhaP1 the most numerous.[66–69] Mutants deficient in PhaP1 produce less PHA, which is accumulated in only one large granule.[68,70] Overexpression results in many small granules.[64] Therefore, it is thought that phasins are responsible for regulating PHA accumulation, and prevent the coalescence of nascent granules by forming a proteinaceous barrier between the surfaces of adjacent polymer cores.[64] PhaR, a regulatory protein is also associated with the granule surface. This is thought to bind preferably to PHA granules. However, when a critical concentration is reached and no more binding sites are available it binds instead to the *phaP1* and *phaR* gene promoters, downregulating transcription and consequently reducing the rate of PHA production.[71–73]

Depending on the species, varying numbers of PHA depolymerases have also been identified as granule-bound proteins.[74–76] It still remains to establish how a balance is reached between polymerisation and depolymerisation, if both enzymes are present simultaneously.[77] Overall, it is evident that PHA granules are rather complex, dynamic structures. In fact, Uchino *et al.*[78] and Jendrossek[79] have both argued that PHA

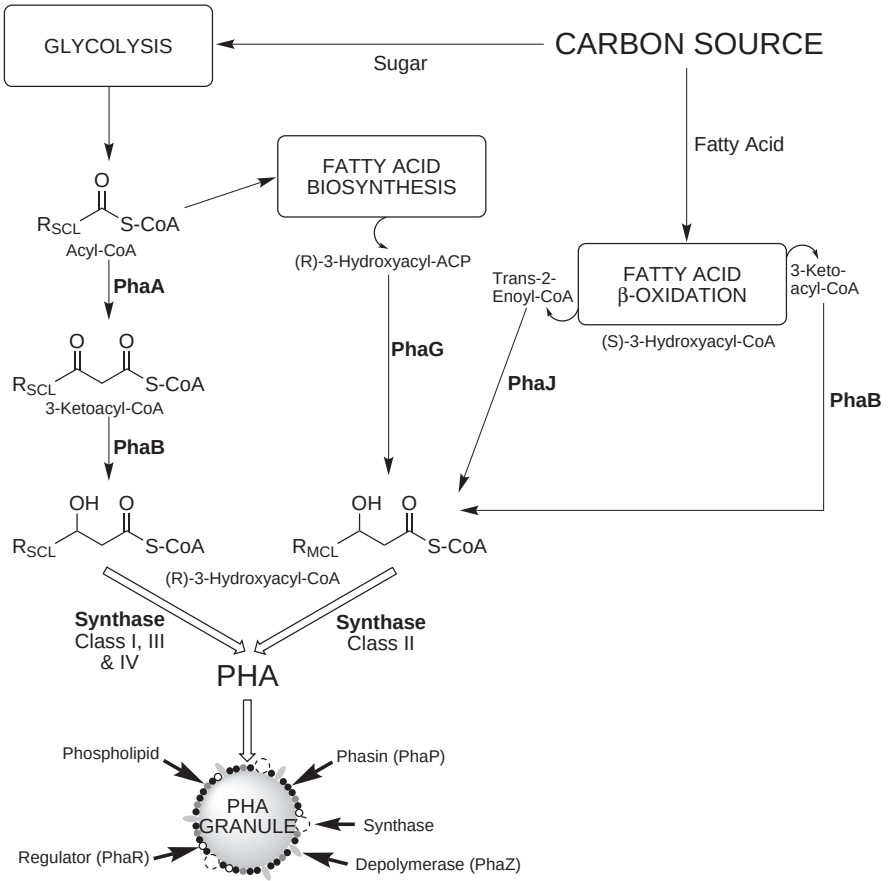

Figure 2.1: The main steps involved in the production of short chain-length PHAs (PHA_{SCL}) and medium chain-length PHAs (PHA_{MCL}), and granule formation. PHA_{SCL} monomers are derived from products of sugar respiration, such as acetyl-CoA and have side-chains (R_{SCL}) composed of 1–3 carbon atoms. PHA_{MCL} monomers are made by diverting intermediates of fatty acid metabolism and contain side-chains (R_{MCL}) of 4–11 carbon atoms. Enzyme names are in bold type: **PhaA** is β-ketothiolase, **PhaB** is acetoacetyl-CoA reductase, **PhaG** is acyl-ACP-CoA transacylase, **PhaJ** is 2-enoyl-CoA hydratase.

granules are complex enough to be considered bacterial organelles, on a par with carboxysomes and magnetosomes.

2.2.3 Granule formation

There are two competing models for the formation of PHA granules, both of which are applicable to PHA_{SCL} or PHA_{MCL}.[28,64] The first (Figure 2.2 (A)) is the 'budding model.' It is favoured at present as it better explains the observed phospholipid monolayer and has been supported more strongly by experimental data.[62,66,80] In this scenario, nascent granules are located adjacent to or even bound to the inner side of the

cytoplasmic membrane. Their growth causes the membrane to fold around them, until eventually they become large enough to 'pinch off' taking part of the membrane with them.[64]

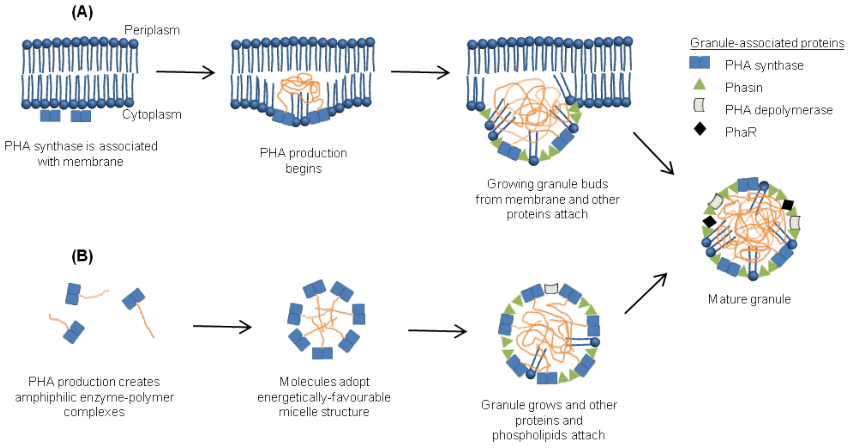

Figure 2.2: The two proposed mechanisms for PHA granule production in bacteria. (A) The budding model, in which early PHA synthesis is associated with the cytoplasmic side of the membrane. (B) The micelle model, in which PHA is initially dispersed within the cytoplasm and forms spherical inclusions due to hydrophobic interactions between polymer chains.

The second model (Figure 2.2 (B)) is known as the 'micelle model.' This proposes that the naturally amphiphilic properties of the synthase-polymer complex cause aggregation of growing polymer chains. As these aggregations grow, they begin to take the form of a spherical micelle with the hydrophobic polymer shielded from the cytoplasm by the hydrophilic outer domains of synthase molecules. Nascent granules are then further coated with the additional proteins and phospholipids and assume their final constitution.[64] This model does not explain how phospholipids become attached to the granule, as granules do not necessarily come into proximity with the membrane.

2.2.4 Poly(thioesters)

Wild-type *R. eutropha*, when grown under PHA accumulation conditions in the presence of thiochemicals such as 3-mercaptopropionic acid, produces a subclass of carbon storage compound.[81] These are copolymers of PHA_{SCL} monomers and novel sulphur-containing monomers. Because of the presence of thioester bonds between the thiol group of the sulphur-containing monomers and the carboxy group of neighbouring monomers the polymers are termed poly(thioesters) (PTEs). Homopolymers of 3-mercaptopropionate,

3-mercaptobutyrate, or 3-mercaptovalerate have also been produced, utilising a non-natural pathway in genetically modified *E. coli*.[82,83]

It appears that PTEs form very similar granule structures to PHAs.[81,82,84] This is to be expected, as the PHA synthase enzyme is also responsible for the polymerisation of PTEs, and so the reaction presumably follows the same mechanism (Figure 2.2). Tessmer *et al.* found that in *E. coli* capable of producing PHA or PTE but not phasins, the 16 kDa heat-shock protein HspA could functionally replace phasins.[84] This explains why many granules are found in PHA and PTE producing *E. coli*, rather than the single large granule produced by phasin-negative *R. eutropha*.

PTEs have interesting properties compared to PHAs: they exibit low crystalline order, and have higher glass transition and melting temperatures.[82,85] This could provide opportunities to produce more commercially-desirable plastics with improved material properties and processability. However, perhaps the most interesting property of PTEs is that they are the first example of a non-biodegradable biopolymer,[86,87] although it remains to be seen whether this property can be usefully exploited.

2.3 Triacylglycerides

TAGs are the predominant storage lipid in eukaryotes. They are trioxoesters of glycerol and long-chain fatty acids (Figure 2.3 (A)). In bacteria, they are almost exclusively synthesised in species belonging to the Gram-positive actinomycetes group, although a few Gram-negative producers have also been identified.[33,34] Nevertheless, TAG production is widespread, because actinomycetes are the most numerous bacteria in soil.[23] Members of the group include *Mycobacterium*, *Rhodococcus*, *Nocardia* and *Streptomyces*, many of which are medically (e.g. *Mycobacterium tuberculosis*) or commercially (e.g. *Streptomyces coelicolor*) important.

Rhodococcus opacus strain PD630 has emerged as the model organism for bacterial TAG production, due to its ability to accumulate large quantities.[88] In common with other TAG accumulating bacteria, *R. opacus* PD630 also produces small amounts of diacylglycerols, free fatty acids and wax esters.[88–90] However, it is only capable of accumulating neutral lipids, whereas many other TAG producers can simultaneously produce PHAs. Most notably, *R. ruber* and *Nocardia corallina* can produce a commercially attractive copolymer poly(3-hydroxybutyrate)-*co*-(3-hydroxyvalerate) from simple sugars.[89]

2.3.1 Metabolic pathways

TAGs are synthesised from glycerol-3-phosphate (G3P) and fatty acids bound to acyl carrier protein (ACP). G3P is a component of the phospholipid production pathway and a precursor of glyceraldehyde-3-phosphate, which is an intermediate in glycolysis.[91] The fatty acids are diverted from the fatty acid biosynthesis or β-oxidation pathways, much like during PHA production. Figure 2.3 demonstrates that acyl-CoAs are the key chemicals for the production of PHAs, TAGs and WEs, whether derived from respiration or fatty acid metabolism pathways. G3P is sequentially acylated by two fatty acid-ACPs to form diacylglycerol in the Kennedy pathway, by a mechanism similar to that found in eukaryotes.[92–94]

The final acylation is mediated by a wax ester synthase/acyl-CoA:diacylglycerol acyltransferase (WS/DGAT) to convert diacylglycerol to TAG (Figure 2.3 (A)). As the name suggests, this enzyme is also responsible for the final stage of WE production (see Section 2.4.1).[23] The first WS/DGAT to be identified was AtfA from *Acinetobacter baylyi* sp. ADP1.[95] As described in detail by Wältermann *et al.* almost 100 homologues have since been identified, all unrelated to known acyltransferases in eukaryotes.[8] Those that have been studied in detail seem to posess extremely low substrate specificity, and also exhibit acyl-CoA:monoacylglycerol acyltransferase activity, and accept a wide range of linear, cyclic and aromatic fatty alcohols.[96]

Although AtfA homologues are now known to be widespread in neutral lipid accumulators, and are the primary enzyme in TAG accumulation, additional pathways have been suggested.[34,95,97] For example, Arabolaza *et al.* identified three AtfA homologues in *S. coelicolor*. A triple mutant strain, defective in all three homologues, was still able to produce TAG.[97] The residual DGAT activity was suggested to result from an alternative, acyl-CoA-dependent pathway. Moreover, another pathway was also found in which phospholipids are used instead of acyl-CoAs as acyl donors. This phospholipid:diacylglyerol acetyltransferase (PDAT) pathway is a new discovery in bacteria, but analogous to plants and yeast, which also have both DGAT and PDAT pathways.

2.3.2 Granule-associated proteins

TAG inclusions have been comprehensively studied in eukaryotes. However, some differences exist between the production and composition in eukaryotes and those in prokaryotes. In eukaryotes (particularly plants), TAG inclusions are similar to prokaryotic PHA inclusions, but the variety of proteins bound to the surface appears to be reduced.[25] Notably, the enzymes responsible for TAG synthesis in eukaryotes have no similarity

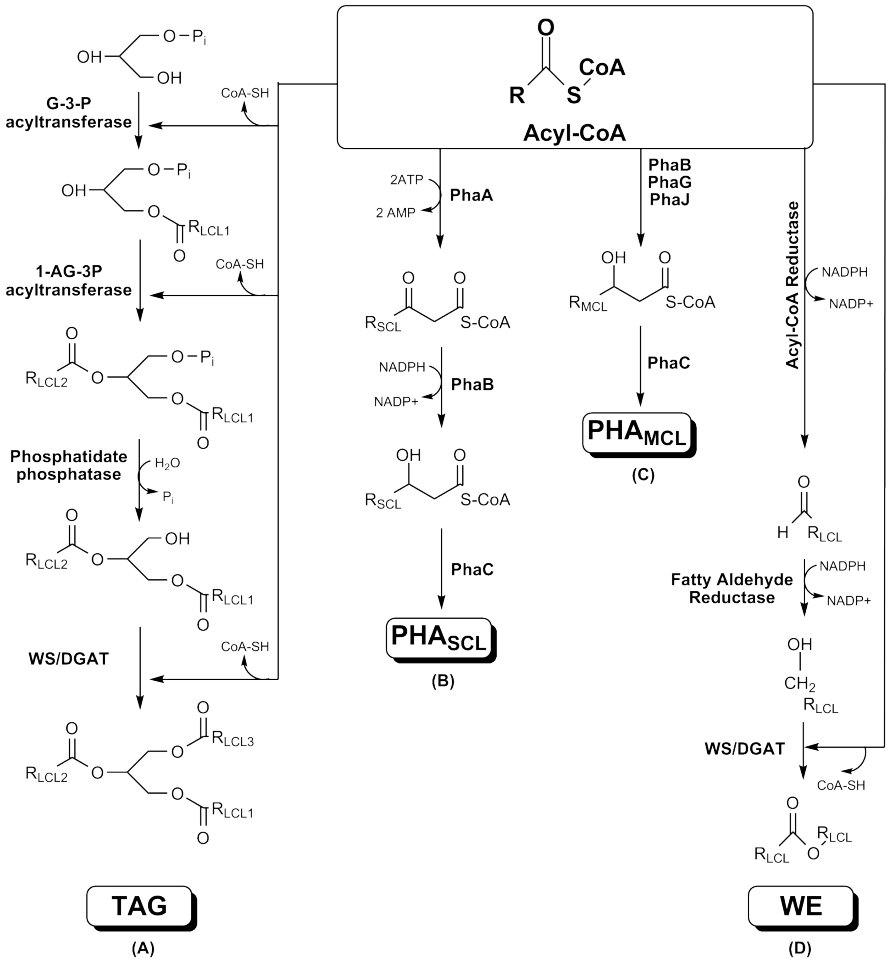

Figure 2.3: Biochemical pathways for the production of bacterial storage lipids. Note the importance of acyl-CoAs to every pathway. (A) Triacyclglycerides (TAG) are produced by addition of long chain-length acyl-CoAs to glycerol-3-phosphate (G3P). 1-AG3P is 1-acylglycerol-3-phosphate. (B) Short chain-length polyhydroxyalkanoates (PHA_{SCL}) are produced from short chain-length acyl-CoAs derived from the respiratory pathways. (C) Medium chain-length acyl-CoAs are intermediates of fatty acid metabolism. They are diverted and modified by PHA enzymes to produce hydroxyacyl-CoAs for medium chain-length polyhydroxyalkanoate (PHA_{SCL}) biosynthesis. (D) During wax ester (WE) production, long chain-length acyl-CoAs are reduced to fatty alcohols, which are then joined to another acyl-CoA.

to those in bacteria.[97] Higher eukaryotes are also able to confine TAG accumulation to specialised tissue: typically white adipose tissue in mammals and seeds in plants.[22] However, small amounts are found in almost all cell types, where they assist with processes such as vesicle formation and cell signalling.[22] Eukaryotic microorganisms accumulate TAG inclusions with similar structures to those in higher eukaryotes, and utilise similar pathways for their production but accumulation is usually triggered by nutrient limitation as in bacteria.[22]

Efforts have been made to identify TAG granule-associated proteins in prokaryotes. Although TAG granules are likely to be dynamic entities much like PHA granules, there is so far no confirmed TAG degrading enzyme associated with the granule. However, Stöveken *et al.* reported some WS/DGAT activity associated with TAG granules in addition to the cytoplasmic membrane.[96] Kalscheuer *et al.* analysed the proteins copurified with TAG granules from *R. opacus* and *R. ruber*, and identified unspecifically, weakly, and strongly bound proteins.[74] However, the most strongly bound proteins were very similar to ribosomal proteins and therefore unlikely to be associated with the granules *in vivo*.

Therefore it would appear that very few, if any, proteins are located on the surface of mature TAG granules. Interestingly, this suggests a lack of structural proteins, and is in strong contrast to PHA granules (which have phasins) and plant TAG granules (which have oleosins that are structurally similar to phasins).[25,33,64] However, the similar physical properties of PHAs and TAGs could mean that PHA granule-associated proteins are able to bind to TAGs.

2.3.3 Granule formation

Formation of TAG granules in bacteria proceeds by a process distinct from that of PHA and of lipid bodies in eukaryotes, but is probably similar to WE granule formation.[22,23] Lipid formation and WS/DGAT enzymes are known to be predominantly membrane associated.[23,96] As shown in Figure 2.4, TAG formation by membrane-bound WS/DGAT results in small lipid droplets (SLDs), formed by hydrophobic lipid-lipid and lipid-enzyme interactions.[23,98] According to the model proposed by Wältermann *et al.* many of these SLDs form an oleogenous layer on the inside of the membrane, with hydrophilic regions between SLDs through which metabolites for other membrane-associated processes may pass.[23] Because of the association with the membrane, phospholipids also become attached to this layer. SLDs then begin to accumulate into a more stable aggregation

known as a lipid prebody, surrounded by phospholipids. Finally, aggregation of individual SLDs within a lipid prebody results in a mature granule with a homogeneous inner core.

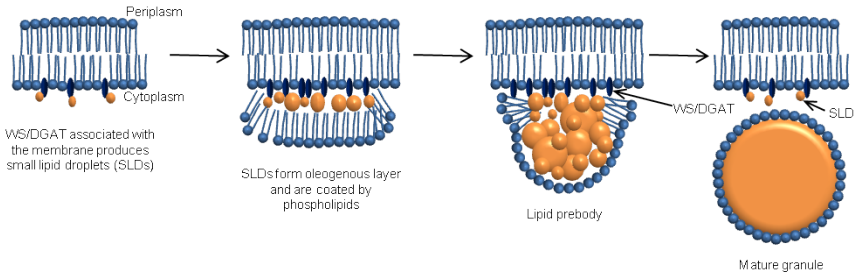

Figure 2.4: The mechanism of TAG and WE formation in bacteria. The key enzyme, WS/DGAT remains in the cytoplasmic side of the cell membrane throughout the process, in contrast to PHA synthase, which becomes incorporated in the boundary layer of the granule. Small lipid droplets (SLDs) form an oleogenous layer on the inner membrane, then coalesce as they grow until the granule becomes large enough to bud off into the cytoplasm.

2.4 Wax esters

While TAGs are predominantly associated with the actinomycetes, wax esters are more widespread.[37] However, they are most associated with Gram-negative *Acinetobacter* spp. and the hydrocarbon-degrading marine organism *Alcanivorax borkumensis*.[23,90,99] WEs are oxoesters of long chain alcohols and long chain fatty acids (Figure 2.3 (D)). Although they share many similarities with TAGs, they are almost exclusive to bacteria and within eukaryotes are only known to be accumulated intracellularly in the seeds of the Jojoba plant.[35]

2.4.1 Metabolic pathways

WE production begins with long-chain acyl-CoAs from the fatty acid metabolism pathways, in common with PHA_{MCL} and TAGs.[8] However, in this case they are first reduced by an acyl-CoA reductase to form fatty aldehydes, and then again by a fatty aldehyde reductase to give long chain fatty alcohols.[100] One of these fatty alcohols is then joined to an acyl-CoA with the release of CoA-SH by the WS/DGAT (see Figure 2.3 (D)).[8]

WEs are often produced by alkane-degrading bacteria, and long-chain alkanes such as hexadecane are fed into the lipid metabolism pathways. Ishige *et al.* found that the

composition of the WE produced by *Acinetobacter* sp. strain M-1 had a direct dependence on the chain length of the alkane on which the bacterium was grown.[37] For example, when grown on hexadecane, under nitrogen limitation, the resulting WE contained 98% hexadecyl hexadecanoate and 2% hexadecyl myristate. This suggests that the corresponding properties of the WEs could be tightly regulated, simply by changing the feedstock composition. Alvarez *et al.* also discovered that WEs produced by *R. opacus* PD630 grown on phenyldecane was predominantly phenyldecane phenyldecanoate, suggesting that the relationship between feedstock and WE chain length is not limited to *Acinetobacter* and that novel, aromatic WEs can be produced.[33]

2.4.2 Granule structure and associated proteins

Little is known about the protein content of WE bodies in bacteria, but it would appear to be similar to that for TAGs; i.e. no granule-associated depolymerases or structural proteins have been reported, although WS/DGAT might be present in small amounts.

WEs are usually accumulated in spherical granules, but unlike PHAs or TAGs have also been found in other conformations. Ishige *et al.* reported disk-shaped inclusions with diameters similar to that of the cell and consisting of stacks of a few inclusions.[100] The completion of one disk led to the formation of the next, seemingly from the same area of the cytoplasmic membrane.[100] This would suggest that the WS/DGAT enzymes remain bound to the membrane, rather than staying attached to the lipid bodies. Singer *et al.* have also reported small, rectangular WE inclusions.[101]

In the case of the disk-shaped inclusions, no limiting membrane was found to surround the structures at all. However, other WE inclusions have been reported to include phospholipid-rich monolayer membranes and it appears to be the normal case that WEs display a similar ultrastructure and morphogenesis to TAGs.[23,100,101]

2.4.3 Granule formation

The mechanism of WE granule formation is thought to be the same as for TAGs and to follow the model proposed by Steinbüchel's group (see Section 2.3.3 and Figure 2.4).[23] It is easy to see how the usual spherical inclusions could follow the same mechanism of formation as TAG granules, but the disk-shaped and rectangular inclusions seem less likely to arise spontaneously with no structural proteins to stabilise their shape. In defence of their model (Figure 2.4), Steinbüchel and co-workers have suggested that the two-dimensional nature of these inclusions arises from their tight association with the flat surface of the cytoplasmic membrane during their synthesis.[28] Particularly if these

inclusions occured in a crystalline state, a lack of aggregation of SLDs to form lipid prebodies could result in the shapes observed.

2.5 PHA synthases

The key enzymes in the production of PHAs are the PHA synthases. Their substrate specificity determines which monomers can be incorporated into the polymer, while their concentration dictates the molecular weight of the polymer chains.[49] Both of these aspects provide the basis for engineering new or improved types of polymer: synthases can be expressed in heterologous hosts engineered to provide the appropriate monomers, and the level of expression can be modulated by fusing the gene to a dose-dependent promoter.

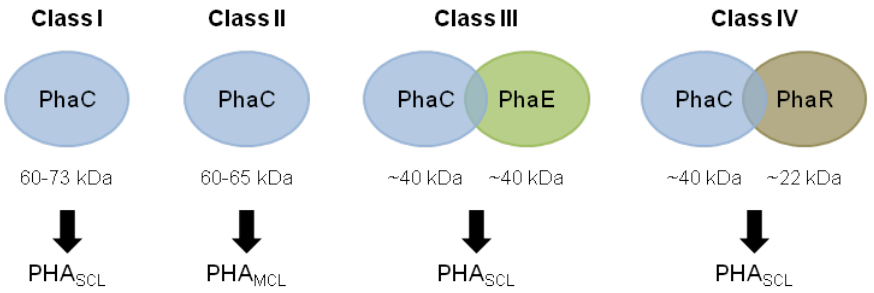

Figure 2.5: The four classes of PHA synthase. The enzymes are divided into classes based on their quaternary structures and substrate specificities.
Adapted from Rehm (2003)[102]

PHA synthases are divided into four classes on the basis of their subunit structure and their substrate specificity.[102] Figure 2.5 illustrates the basic quaternary structures of each class. Synthases belonging to class I are composed of a single subunit (PhaC) and produce exclusively PHA_{SCL} polymers. They are probably the best studied, because the synthase from *R. eutropha* falls into this class.

Class II includes the synthases from typical PHA_{MCL} producers, represented by *Pseudomonas* species such as *P. putida* and *P. oleovorans*. They do not recognise monomers with carbon chain length < 5, and have a preference for those with 6–14 carbon atoms.[102] Like class I, they also consist of one PhaC subunit.

Classes III and IV each consist of two subunits. The PhaC peptide is smaller than for the previous classes (~40 kDa as opposed to 61–73 kDa) but exhibits amino acid sequence similarity of 21–28% with type I synthases.[102,103] For class III synthases such

as from *Allochromatium vinosum*, the second subunit is a 40 kDa peptide named PhaE, while for class IV synthases from species such as *Bacillus megaterium* it is a 20 kDa unit named PhaR.[104,105] Neither PhaE nor PhaR share any sequence homology with PhaC.[102] Synthase classes III and IV both produce PHA_{SCL} polymers.

The catalytic mechanism of PHA synthases has not been definitively determined, although the currently favoured proposal is that PHA synthases operate by a similar mechanism to lipases. All four classes of synthase have strong homology to the α/β-hydrolase superfamily of enzymes, of which lipases are the member with greatest homology.[102]

Hydrolases are characterised by the highly-conserved catalytic triad motif *active site nucleophile—acidic amino acid—histidine.*[106] In PHA synthases, three conserved residues of cysteine, aspartic acid and histidine (corresponding to C319, D480 and H508 in *R. eutropha*) are thought to form this motif.[106] However, the PHA chain elongation reaction is thought to require two thiol groups as nucleophiles, so Jia *et al.* have proposed that the active form of the enzyme is a dimer, in which C319 (or its equivalent) in each PhaC are located near to each other, and the growing polymer chain is shuttled between the two sites.[106,107]

The dimer model is consistent with *in vitro* size-exclusion chromatography findings that the synthase is present as an equilibrium between an active dimer and an inactive monomer.[108] Furthermore, when synthase activity is assayed *in vitro* there is a lag phase before the enzyme reaches its full activity, which is thought to correspond to the time taken for dimerisation.[64] No crystal structures have been generated thus far for any PHA synthase, due to low yields and the tendency of the enzyme to aggregate. Therefore, the exact structure of the catalytic site is likely to remain obscure until such a breakthrough is achieved. It is also not clear to what extent the *in vitro* findings can be assumed to apply *in vivo*.

Calculations based on the concentration of synthase and the yield and molecular weight of polymer produced *in vitro* suggest that class I and II synthases produce a single polymer chain per enzyme dimer.[109,110] The class III synthase from *A. vinosum*, however produced multiple chains per enzyme and so chain transfer reactions must have taken place.[110] In contrast to the *in vitro* results, class I synthases have been calculated to produce about 60 polymer chains each *in vivo*.[111] It is suspected that nucleophilic chain transfer agents attack in or near the active site and attach to the end of the polymer chain, terminating polymerisation.[112]

The identity of these agents is not clear, but CoA,[110,113] water,[114,115] hydroxybutyrate,[116] and various alcohols[116,117] have all been suggested. The different behaviours

in vitro and *in vivo* could be due to higher concentrations of the chain transfer agent *in vivo*, or to the lack of the natural agent *in vitro*. This might also explain the general trend for polymers synthesised *in vitro* to be of higher molecular weight, since the chain transfer reaction might occur less frequently.[109,112]

2.6 Material properties and applications of Polyhydroxyalkanoates

Due to the wide variety of monomers that can be incorporated into PHAs, there is consequently huge scope for tailoring the material properties to suit virtually any conceivable application. Unfortunately, at present, only a fairly limited range of monomers are able to be incorporated into either homo- or heteropolymers of PHA with the necessary efficiency for commercial-scale production.[9] For PHA_{SCL}, this has meant that PHB has been very well studied, despite its poor material properties, due to its ease of production. Because PHB is hard and rigid when solid but has low viscosity when melted, it is useful for injection moulding of objects with thin walls.[9]

Poly(4-hydroxybutyrate) (P4HB), an isomer of PHB, has greater tensile strength and can be stretched much further before breaking than PHB. Therefore, it has been much more widely used than PHB, particularly for medical applications such as heart valves, vascular grafts, sutures and other medical textiles, and bulking agents.[118] P4HB is typically produced from carbon sources such as 4-hydroxybutyrate (4HB), 4-butyrolactone, 1,4-butanediol or 4-chlorobutyrate, which are structurally related to the 4HB-CoA monomer but expensive. Recently, Zhou *et al.* reported production of P4HB up to 68% DCW within *E. coli* using glucose as a sole carbon source.[119]

Copolymers of 3HB with 4HB or with 3-hydroxyvalerate(3HV), in which the monomers are arranged in a random sequence, are also widely used in industry.[120] Production of polymers containing a high proportion of 3HB is more efficient than engineering a pure homopolymer of other monomers. By varying the proportion of 4HB or 3HV, the crystal structure of the polymer can be modified thus influencing its material properties: generally, the higher the proportion of other monomers, the less uniform crystal structure and the more elastic or flexible the polymer.[121] To incorporate 3HV into the polymer, the carbon source should include propionic acid, which is metabolised in a pathway parallel to the production of 3HB, in which propionyl-CoA is formed and then condensed with acetyl-CoA by a homologous β-ketothioloase to PhaA called BktB.[48] The relative proportion of 3HV units is then controlled through the proportion of propionic acid compared to glucose in a defined growth medium.[122]

Poly(3HB-*co*-3HV) (PHBV) was the first PHA to be commercialised, by Imperial Chemical Industries in the late 1980s, under the Trademark 'Biopol.'[123] Initially, Biopol was used as a biodegradable alternative to polypropylene, for products such as shampoo bottles and disposable razors.[13] However, diversification of production and processing methods has since led to a wide range of PHBV-based products including food packaging, coated cardboard, fishing lines and ropes.[9] The copolymer has also found uses in cardiovascular medicine for the production of stents, grafts, sutures, dressings and artificial heart valves.[9,124–126]

Another way to alter the material properties of PHAs is to produce PHA_{MCL}. Unlike PHA_{SCL}, these are usually produced as random heteropolymers with subunits composed of numerous different carbon chain lengths. The dominant fraction is usually composed of monomers with the same number of carbon atoms as the carbon source (for example, if the carbon source is decanoic acid (C_{10}) the majority of subunits will be 3-hydroxydecanoate), with lower proportions of other chain lengths (e.g. C_6, C_8, C_{12}, C_{14}) derived from the fatty acid degradation and synthesis pathways.[127,128] Therefore, by varying the carbon source it is possible to produce a wide range of different polymers.

Most PHA synthases either produce PHA_{SCL} or PHA_{MCL}, but an exception is the class I synthase from *Aeromonas caviae*, which produces a copolymer of 3HB and 3-hydroxyhexanoate (3HHx).[129] It is also possible to blend different types of PHA in various ratios to achieve a variety of characteristics in the bulk material.

2.7 Methods of PHA production

2.7.1 Production in microorganisms

2.7.1.1 Bacteria

Bacteria are the natural producers of PHAs, so it is not surprising that extensive investigations have been conducted into their potential for improving the yield and properties of PHA polymers. An enormous number of bacterial species exist, and they display huge variety in their preferred growth conditions, ability to metabolise chemicals and ease of handling in the laboratory. Some species, such as *E. coli*, *Bacillus* spp. and *Pseudomonas* spp. have well-understood genetics that make it easy to modify metabolic pathways and introduce genes for exogenous protein expression.

PHA production in wild-type strains of the model organisms (*R. eutropha*, *Pseudomonas* spp. etc.) tends to be very efficient provided the correct growth conditions are maintained. For example, *R. eutropha* is capable of accumulating enough PHB to account

for up to ~80% of the DCW in nitrogen-limited mineral salts medium.[75] In fact, *R. eutropha* formed the basis of the commercial production system for Biopol before genetic engineering became widespread and convenient.[9] However, without genetic manipulation the only real methods for process improvement are to experiment with different carbon sources or with different fermentation strategies. This has been particularly useful for the production of PHA_{MCL} from Pseudomonads, due to the relationship between carbon source and monomer carbon number, which allows different polymers to be produced simply by changing the fatty acids used as feedstock.[26,130,131] Species can also be chosen to utilise cheap waste streams from industry (such as effluent from milk, paper, sugar or chemical processing).[10] Fermentation process optimisation has also led to greater efficiency of production, larger yields and cost reduction.[132–135]

The flexibility offered by the ability to manipulate the genes of bacteria has facilitated better understanding of the metabolic pathways leading to PHA production, allowed new non-natural copolymers to be produced, and led to productivity gains in newly-discovered and diverse species.[136] Perhaps most importantly, genetic engineering has enabled *E. coli* to be used for PHA production: researchers can now benefit from the deep understanding of *E. coli* biology and convenient tools for its manipulation (see Section 1.1). This is illustrated by the switch in production of Biopol from *R. eutropha* at ICI to its current production in *E. coli* by Metabolix.[137]

2.7.1.2 Archaea

Bacteria are not the only microorganisms capable of producing PHAs. Halophilic archaea from marine environments have also been shown to naturally produce PHA_{SCL} (reviewed by Quillaguamán *et al.*).[138] Marine archaea express PHA synthases belonging to class III with close homology to the type III synthases of PHA-producing marine bacteria. This suggests that horizontal gene transfer has occurred between bacteria and archaea.[138]

Archaeal synthases have since diverged from their common ancestors, and display some unique properties. For example, the PhaC from *Halopiger aswanensis* is tolerant of temperatures up to 60 °C and of up to 30% (w/v) NaCl.[139] The most studied archaea for PHA production is *Haloferax mediterrani*, which has been shown to accumulate up to 73% DCW PHA when grown on hydrolysed whey.[140] The polymer was identified as PHBV, putting *H. mediterrani* into a small group of species naturally able to produce PHBV from unrelated carbon sources.[141] Although the PHA content was impressive, *H. mediterrani* only accumulates PHA during the exponential growth phase, so the

volumetric productivity of cultures (volume of PHA produced per litre of culture per hour) is much lower than in *E. coli.*[138]

Halophilic archaea may prove to be a source of new and useful PHA production strategies, but at present they are relatively poorly studied and hampered by difficult fermentation conditions such as their requirement for high salt concentration.

2.7.1.3 Photosynthetic microorganisms

Feedstock cost remains one of the most prohibitive cost barriers to mass-market commercialisation of PHAs.[142–145] Therefore, there is interest in using photosynthetic organisms to convert CO_2 and light energy into PHA in a cheap and carbon-neutral manner. The majority of research in this area has been focussed on production in plants, as discussed in Section 2.7.3. However, photosynthetic microorganisms have also been used with some success. Cyanobacteria* are photosynthetic prokaryotes, some of which are naturally able to accumulate small quantities of PHA.[146]

Spirulina platensis,[147] *Synechococcus* MA19,[148] and *Nostoc muscorum*[149] have all been shown to accumulate PHB from carbon dioxide, with the greatest yield being ~10% DCW for *N. muscorum*. With supplementation of external carbon sources such as glucose and acetate, the yield for *N. muscorum* was increased to 21.5% DCW in 8 days.[149] A PHA non-producer, *Synechococcus* sp. PCC7941 was engineered to contain the PHB biosynthesis genes of *R. eutropha* and was capable of producing 25% DCW under nitrogen-limited conditions and with acetate supplementation.[148]

Eukaryotic algae are not naturally capable of producing PHA, but have recently been genetically engineered to do so. This was first accomplished by Wang *et al.* by transferring the *phaB* and *phaC* genes of *R. eutropha* into the genome of *Chlamydomonas reinhardtii* CC-849 (a native PhaA analog is known to be expressed).[150] The complete *R. eutropha* PHB pathway has also been expressed in the diatom *Phaeodactylum tricornutum*, resulting in up to 10.6% DCW PHB being produced.[151] In both cases, the PHB accumulated in the cytoplasm. It may be possible to follow the example of improved production in plants by targetting production to the chloroplasts (Section 2.7.3).

*Cyanobacteria are often called blue-green algae. This is a relic of their previous taxonomic classification, in which they were grouped with true, eukaryotic, algae due to being photosynthetic. They are now classified as bacteria, in recognition of their lack of membrane-bound organelles.

2.7.1.4 Yeast

Some yeast species are able to produce PHAs, but only enough to comprise a few percent of their total mass.[152] Production does not occur in model species such as *Saccharomyces cerevisiae* and *Pichia pastoris* but like in bacteria, much of the work to improve production has been carried out in genetically engineered strains of species that are fast growing, convenient to handle and amenable to genetic manipulation. The first genetically engineered yeast to produce PHB was *S. cerevisiae*.[153] Leaf *et al.* reported that only the *phaC* gene from *R. eutropha* was necessary for PHB accumulation, indicating that endogenous yeast enzymes are capable of synthesising the 3HB-CoA monomers. However, only 0.5% DCW was accumulated. When the whole *R. eutropha* PHB operon was expressed, the yield of PHB increased to 9% DCW on average although there was significant heterogeneity in PHB content of individual cells, ranging from 0 to ~50% of the cell volume.[154]

Small amounts of PHA_{MCL} have been produced in both *S. cerevisiae* and *P. pastoris* by expressing the PHA synthase from *Pseudomonas aeruginosa* with a peptide signal to target the enzyme to the peroxisomes.[54,155] A PHA_{SCL} heteropolymer of predominantly 3HV with a small proportion of 3HB has also been produced in the non-conventional yeast *Arxula adeninivorans* expressing the whole *R. eutropha* PHB biosynthesis system.[55] This suggests that a more thorough screening of yeasts could uncover species with interesting and useful capabilities.

Some efforts have also been made to control the monomer composition of yeast-produced PHA. In *S. cerevisiae* an engineered cytosolic β-oxidation pathway was created to provide PHA_{MCL} monomers (with carbon chain length related to the fatty acid supplied to the culture) to the *Pseudomonas oleovorans* PhaC.[156] In *Yarrowia lipolytica* expressing *P. oleovorans* PhaC, the inactivation of (R)-3-hydroxyacyl-CoA dehydrogenase activity in the peroxisome resulted in the production of homopolymers with monomer chain lengths corresponding to the carbon source.[157] Overall, it appears that commercial-scale production in yeast will not be feasible, but that they could be used as a convenient model system to understand and improve production in higher eukaryotes.

2.7.2 Chemical synthesis

It is possible to synthesise PHAs chemically through ring-opening polymerisation of β-lactones.[158] This method has the advantages of being easier to use at an industrial scale than fermentation, having greater control over the polymerisation conditions (and therefore over the final product) and allowing the incorporation of chemically-synthesised

monomers and, therefore, a wider range of options for the design of novel polymers. In particular, it is easier to control the molecular weight of the polymer through chemical synthesis.

Chemical synthesis also makes it possible to produce polymers for which bacterial synthesis is not yet a viable option, and to test it at the laboratory scale to identify promising candidates for further study in bacteria.[159] On the other hand, the chemical synthesis of monomers (especially if only one stereo-isomer is desired) is expensive and cannot be achieved from cheap, readily-available feedstocks as with fermentation.[158] However, research in the area is continuing and new catalysts are being developed to enable stereo-selective production in large volumes.[160]

2.7.3 Production in plants

The use of genetically-engineered plants is theoretically a cheap, convenient and environmentally friendly method for PHA production: using crop plants would make efficient use of existing infrastructure, and the process would be powered by sunlight and carbon dioxide through photosynthesis.[56,58,61] Although PHA_{MCL} and PHBV production has been reported in plants, most of the research to date has focused on PHB production as a relatively simple model.[57,161–164] All plants express an endogenous β-ketothiolase (PhaA homolog) in their cell cytoplasm, so the simplest route to PHB production in plants is to express PhaB and PhaC.[57] This was first achieved by Poirier *et al.* in 1992 in the model plant *Arabidopsis thaliana*.[165,166] Unfortunately, the cytoplasm contains low concentrations of acetyl-CoA so it is not possible to produce large enough quantities of PHB by this method for commercial production.[56] Additionally, the diversion of acetyl-CoA from other pathways leads to stunted plant growth and reduced seed production.[165]

Much greater quantities of acetyl-CoA are available in the plastids, as these are the sites of fatty acid biosynthesis in plants. Nawrath *et al.* were the first to target PHB synthesis enzymes to this cell compartment, and reported yields of up to 14% DCW with only slight chlorosis (yellowing of the leaves).[167] It was necessary to express all three genes from the PHB biosynthesis pathway as the plastids do not contain an endogenous PhaA homolog.

An array of agriculturally-relevant plants have been investigated for the production of PHA. The plastids (or, sometimes, peroxisomes) have remained the organelles of choice for targetted gene expression, and the strategies employed have been broadly the same as described above for *A. thaliana*, although different gene promoters and protein targetting sequences were adopted by each investigator. Maize,[168–170] oilseed rape,[162,171]

potato,[172,173] sugar beet,[174] sugar cane,[175–177] flax[178] and cotton[179,180] have all been investigated, with oilseed rape producing the greatest quantity (~9% DCW).[171]

A commonly quoted target to make PHA production in plants commercially viable is to accumulate sufficient polymer to comprise 15% DCW without negatively affecting plant growth.[161] The inability to reach this level in the plants mentioned above has reduced the interest in plant-based production. However, Metabolix received a $15 million grant from the U.S. government to pursue production in switchgrass, and are also concentrating on production in tobacco.[9,181]

Switchgrass is considered particularly promising as it rapidly produces large quantities of biomass and is able to grow on poor soil that is not used for other crops.[58] The highest yield so far reported for switchgrass was 3.7% leaf DCW by Somleva *et al.*[182] Therefore, it would appear that tobacco is presently the most promising candidate, as Bohmert-Tatarev *et al.* recently reported up to 17.3% leaf DCW production.[181] However, production in plants will probably face strong competition from algae, which have already been shown to accumulate similar yields of PHB, do not occupy valuable farmland and have much shorter growth times.

2.7.4 *In vitro* production

Production of PHAs *in vitro* has been suggested as a potential method to reduce costs, by disconnecting the synthesis of PHA from the generation of biomass. Isolated enzymes can be immobilised and used more easily than free-swimming bacteria in continuous production systems. They are also more amenable to rational modification, and may be able to accept a wider range of monomers without the constraints imposed by the conflicting needs of other metabolic processes within cells. Furthermore, since the reaction mixture is simpler and more closely regulated than bacterial culture broth, recovery of the polymer could be facilitated.

In vitro synthesis of PHB was first demonstrated in 1995.[109] Significantly, the study showed that the only requirements for the reaction to occur are an active PHA polymerase and suitable (R)-hydroxyacyl-CoA monomers, although usually a phosphate buffer for pH control is also employed.[183] Granules of PHB form *in vitro* despite the lack of phasins and other granule shell components, but they tend to be around five times larger than intracellular granules.[184,185] The molecular weight of polymer produced *in vitro* is highly dependent on the synthase concentration, displaying an inverse correlation.[109] Usually, the molecular mass *in vitro* is around an order of magnitude larger than *in vivo* suggesting that a regulatory component may be missing and that chain transfer consequently does not occur.[109]

Large scale *in vitro* production is currently prohibited by the difficulty of manufacturing both enough PHA synthase and (R)-hydroxyacyl-CoA. PHA synthases are difficult to express in high concentrations because they tend to aggregate and form inactive, insoluble inclusion bodies within the cells. The soluble fractions of some, such as PhaC from *R. eutropha* can be purified in the presence of weak non-ionic detergents such as 6-O-(N-Heptylcarbamoyl)-methyl-α-D-glucopyranoside (Hecameg) or TritonX-100.[60,64] Alternatively, the inclusion bodies can be purified, denatured by guanidine hydrochloride and allowed to refold into an active conformation.[186] However, neither technique allows reliable, economic production on the commercial scale. Chemical synthesis of monomers is expensive due to the necessity to supply CoA, and incapable of producing enantiomerically pure products.[187,188] Therefore, multiple-enzyme systems have been developed to synthesize monomers from cheap building blocks such as acetate, catalyse the polymerisation of PHA, and recycle the CoA for further monomer production.[110,185,189] Such systems are so far only feasible at the laboratory scale, however.

Although *in vitro* systems are a long way from commercial production at present, they do allow the study of the mechanism of synthase function and interactions between polymer and synthase. These studies will lead to better understanding of how the PHA production machinery works, and allow further refinements of production techniques both *in vitro* and *in vivo* to improve yields, control molecular weight and create tailor-made polymers for particular applications.

2.8 Visualisation of PHAs in bacteria

Much effort has been expended to understand and accurately describe the physical structure of bacterial lipid inclusions. Various microscopic techniques have contributed significantly to the state of knowledge in this area, some examples of which are given in Figure 2.6. Each has particular advantages and drawbacks, but when used in combination they have provided useful evidence of the structures of bacterial lipid granules, and how they are formed.

2.8.1 Light microscopy

Due to their similar structure and light refracting properties, all three types of lipid granule may be viewed easily with phase contrast light microscopy. They appear as highly refractive inclusions within the more transparent cytoplasm. However, in species that produce more than one type of lipid inclusion, such as *R. ruber* which produces PHA and TAG, it is not possible to distinguish between different types.[89]

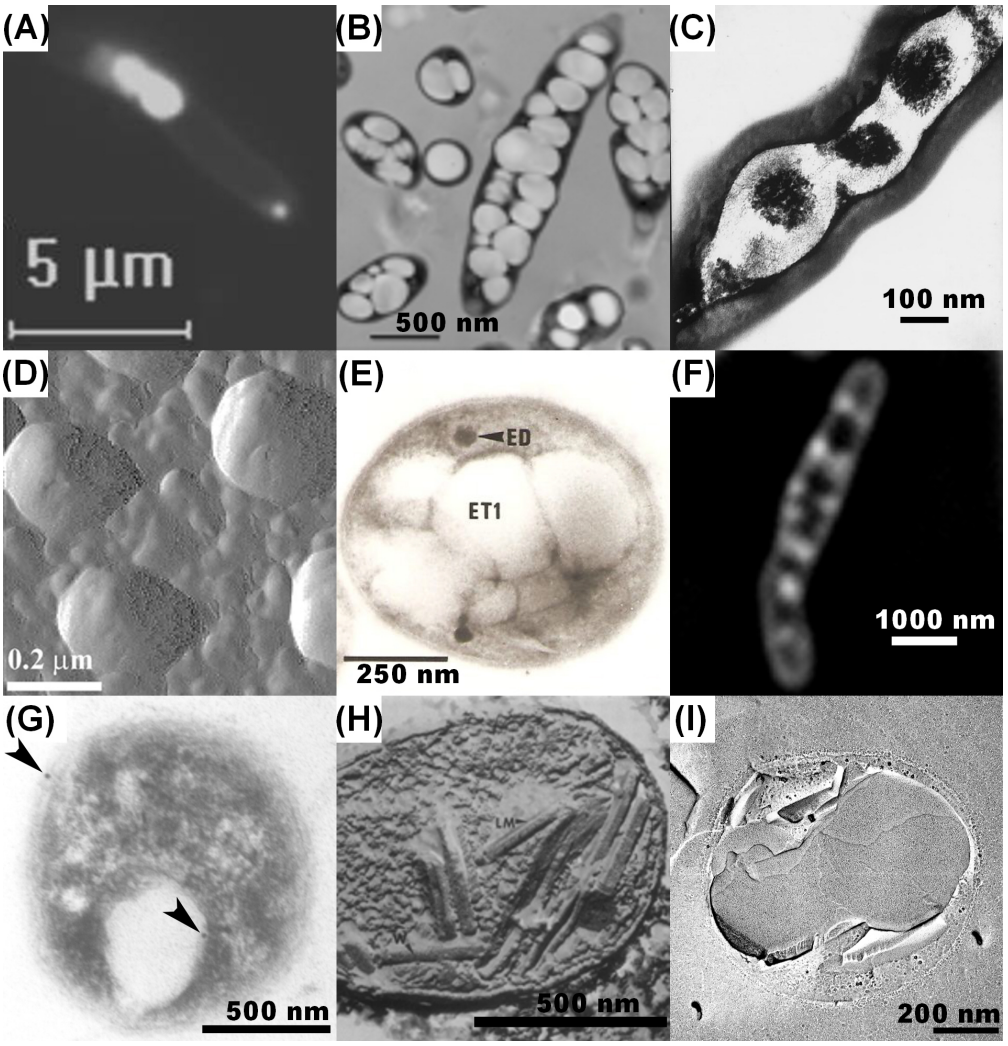

Figure 2.6: Examples of images of bacterial storage lipids. (A) GFP-tagged PHA synthase in recombinant *E. coli* showing localisation at cell poles.[190] (B) TEM of *R. eutropha* producing large quantities of PHB. (C) TEM of *R. eutropha* producing phase-separated granules of PHA with a dark-stained copolymer centre surrounded by PHB homopolymer stained grey.[191] (D) AFM image of PHA granules grown *in vitro* by purified PHA synthase.[192] (E) TEM of *R. opacus* producing large, electron lucent granules of TAG (ET1). Note the smaller, electron-dense polyphosphate inclusions (ED).[88] (F) Fluorescence image of TAG granules growing at the cell membrane of *Mycobacterium smegmatis*, stained with Nile Red.[193] (G) TEM of *Acinetobacter* producing spherical WE granules. The arrows show gold nanoparticles targeted to WS/DGAT at the cell membrane and granule surface.[96] (H) TEM of rectangular WE inclusions, prepared by the freeze-fracture, replica method.[101] (I) TEM of a disk-shaped WE inclusion from *Acinetobacter* prepared by freeze-fracture.[100] Images reproduced with kind permission from Elsevier (A), (C), (D); Springer Science+Business Media (E); Society for General Microbiology (F) and American Society for Microbiology (G-I).

Commonly, Nile red is used to stain any lipid inclusion within bacteria, and can be used as a quick screen for lipid accumulating strains (Figure 2.6 (F)).[194] More specificity for PHAs can be achieved through the use of the related dye Nile blue.[195] Greater specificity is available by fusing green fluorescent protein (GFP) or some other fluorescent protein to a granule-associated protein, such as a PHA phasin or synthase (Figure 2.6 (A)).[196,197]

Fluorescent staining clearly shows the relationship of TAG inclusions with the cytoplasmic membrane,[98,193] but has been less effective for determining which of the two models of PHA synthesis is correct. Although studies with fluorescence microscopy have repeatedly found nascent granules to be located near the membranes and cell poles, in agreement with the budding model,[80,196,197] higher-resolution electron microscopic studies have suggested a cell centre localisation.[24,111] This has not been considered a problem for the model of neutral lipid synthesis, partly because not many electron microscopic studies have been conducted and because it is well established that the WS/DGAT enzymes are membrane associated, making it more likely that granule synthesis begins near the membrane.

2.8.2 Atomic force microscopy

Native lipid granules may also be visualised by atomic force microscopy (AFM). Sudesh *et al.* were the first to view PHA granules by this method.[192] The granules had a surprisingly smooth surface considering that they were expected to be covered with a variety of proteins and phospholipids. However, as shown in Figure 2.6 (D), a second study in which purified PhaP and PhaR were allowed to bind to PHB single crystals showed a clear affinity of both proteins for the polymer, and their arrangement on model granules *in vivo*.[198] Dennis *et al.* also used AFM to image native PHB granules.[199] They saw two types of granules: rough, ovoid granules and smooth, spherical granules. When treated with sodium lauryl sulphate, the rough granules appeared the same as the smooth ones, suggesting that the boundary layer of some granules was damaged during purification and that the smooth surface was the exposed PHB.

Hiraishi *et al.* used AFM to visualise PHA granule formation *in vitro* following polymerisation by a purified PHA synthase.[200] This showed the genesis of granules by a similar mechanism to the micelle model. Of course, this does not give unequivocal support to this model, since the reaction was carried out in unnatural conditions. However, it does confirm the ability of the polymer-enzyme complex to self-assemble into a spherical structure through hydrophobic interactions. The study also revealed globular structures

of 20–30 nm apparent width, corresponding to the expected size of the synthase enzyme. This suggests that AFM has the capability to resolve granule-bound proteins and to study their arrangement on the granule surface.

2.8.3 Electron microscopy

As far back as the 1960s, TEM was used to image PHB granules in thin sections of *Bacillus* spp.[38,201,202] Studies such as these, together with techniques such as NMR, X-ray scattering and neutron scattering have provided the basis of our knowledge of lipid granule structure. While Kawaguchi and Doi revealed the amorphous nature of the inner core of granules by X-ray scattering,[203] TEM studies allowed cross-sections through granules that revealed the single phospholipid membrane and presence of associated proteins (Figure 2.6 (B,E,G)).[38,201,204]

The freeze-fracture technique of preparing samples has been of particular importance in the study of bacterial lipid bodies (Figure 2.6 (H,I)).[205] This involves rapid freezing of the sample prior to fracturing with an ultramicrotome. The fracture plane is then visualised by vacuum deposition of platinum-carbon to form a replica that can be viewed in the TEM. Fracturing often occurs along membranes, and so provides a good view of their structure. This feature has been exploited by many investigators to reveal the structure of the boundary membrane.[88,101,202] Freeze-fracture also provided an excellent view of the disk-shaped WE inclusions discovered by Ishige *et al.* (Figure 2.6 (I)).[100]

The major advantage of electron microscopy over light microscopy is the vastly superior resolution. However, it is still difficult to distinguish between different types of granule in the same cell. Additionally, the ability to see finer detail reveals non-lipid inclusions such as polyphosphates and glycogen, which could further confuse the issue. Note, however that polyphosphate inclusions are generally far more electron dense than glycogen or lipids (Figure 2.6 (E)).[88,206] Specificity can be gained by immunogold labelling. This has been used extensively in studies of PHAs,[23,25] and was instrumental in showing that phasins bind to PHA granules.[68] Stöveken *et al.* reinforced the results of thin-layer chromatography experiments to determine the location of WS/DGAT by immunogold labelling of TEM samples of *Acinetobacter* sp. ADP1 as shown in Figure 2.6 (G).[96] This confirmed that the majority of the enzyme is membrane associated, with smaller amounts associated with the granule surface and in the cytoplasm.

Electron microscope studies are not limited to visualisation of granules within cells. Whole lipid bodies can be extracted from cells and purified by centrifugation in a density gradient.[207] These so called 'native' granules can then be visualised by TEM[208,209] or SEM[110,210,211] in order to reveal more of the features of their surface. Care must be

taken to account for any artefacts caused by the preparation process, such as non-specific binding of proteins and phospholipids.

As with all biological samples, lipid granules are not ideally suited to observation by electron microscopy. It is necessary to fix whole cells or dry isolated granules, to allow them to withstand the low pressures involved. Additionally, since most biological materials are electron transparent, it is necessary to stain samples for TEM or to coat SEM samples with a thin layer of a heavy metal to increase contrast and resolution. These can all introduce artefacts which prevent the representation of the natural state of the granule. A rather under-used technique that might overcome these drawbacks is environmental scanning electron microcopy (ESEM). This uses relatively high pressure (1-5 torr) water vapour in the microscope chamber to maintain samples in a hydrated state,[212] eliminating the need for fixing. ESEM has been used to view PHA tissue engineering scaffolds for artificial heart valves,[124] but has otherwise not been used for the study of bacterial lipid structure or function.

2.9 Non-lipidic bacterial storage compounds

2.9.1 Polysaccharides

In addition to storage as lipid granules, carbon is also commonly stored as polysaccharides by a wide range of bacterial species. The two most common bacterial storage polysaccharides are glycogen and trehalose. In very general terms, storage polysaccharides play the same role as lipids. They are typically more quickly mobilised, but have a lower energy density than lipids; therefore, they are perhaps more suitable for short- to medium-term storage, while lipids are more suitable for long-term storage.

Much like the lipid compounds described above, glycogen is usually accumulated in response to an excess of carbon and deficiency in some other nutrient, and is stored in cytoplasmic granules.[213,214] It is a branched polymer of α–glucose molecules, joined by α1,4–linkages. The branches are attached via α1,6–linkages.[213] To synthesise glycogen, bacteria first manufacture adenosine diphosphate–glucose (ADP–glucose) from ATP and α–glucose–1–phosphate, catalysed by ADP–glucose pyrophosphorylase. The glucosyl unit from ADP–glucose is then transferred to a pre-existing α1,4–glucan molecule by glycogen synthase. The branching reaction is mediated by α1,4–glucan:α1,4–glucan–6–glycosyltransferase.

Trehalose is a soluble disaccharide formed by α,α–1,1–glucoside bonds between two α–glucose units, and does not form inclusion bodies.[215] Although it can be used as

an energy source, its primary function is to protect the cell against osmotic stress: trehalose production is triggered by increases in the osmotic strength of the growth medium.[216,217] Trehalose is produced in a two-step process. In the first stage, uridine diphosphate–glucose (UDP-glucose) and glucose–6–phosphate are converted to trehalose–6–phosphate by trehalose–6–phosphate synthase. This is hydrolysed by trehalose–6–phosphate phosphatase to give trehalose.[215] Interestingly, recent data have suggested that glycogen and trehalose can be inter-converted by complementary pathways in many species of bacteria, suggesting an important role for cycling between the two compounds.[218]

2.9.2 Inorganic storage compounds

Some bacteria also produce storage granules of various inorganic compounds. The composition and quantity varies significantly depending on the environmental conditions and metabolic requirements of each species. The best known such compound is polyphosphate, which is present to a greater or lesser extent in all cells and serves as a reserve of phosphate for production of ATP and related molecules.[219] Sulphur and nitrates can also be stored in granules, particularly by phototrophic and lithotrophic bacteria that require them for biosynthesis and respiration.[220] Nitrogen can also be stored in the form of cyanophycin.[221] This is a polypeptide-like polymer consisting of a backbone of α–linked aspartic acid residues joined to arginine residues via their α–amino groups.

This thesis is concerned primarily with the production of PHAs, so only the above, brief, discussion of non-lipidic storage compounds will be entered into here. For further information on the subject, the interested reader is recommended to consult the book *Inclusions in Prokaryotes*, edited by Jessup M. Shively (2006; ISBN 978-3-540-26205-3).

Chapter 3

Materials and methods

3.1 Bacterial strains and plasmids

3.1.1 Strains

Table 3.1 summarises the genotype and source of each bacterial strain used in this thesis. Details of the purposes and growth conditions are provided in the relevant chapters and in the following sections of this chapter.

Table 3.1: Bacterial strains used for this thesis

Strain	Genotype	Source
Escherichia coli BL21(DE3)	*E. coli* B F- *ompT rB- mB-* (λDE3)	Novagen, USA
E. coli DH5α	*E. coli* K12 F- Φ80*lacZ*ΔM15 Δ(*lacZYA-argF*) U169 *recA*1 *endA*1 *hsdR*17 (rK-, mK+) *phoA supE*44 *lambda- thi*-1 *gyrA*96 *relA*1	Bioline
*E. coli*W3110 wild-type	*E. coli* K12 F- λ- *rph-1* INV(*rrnD, rrnE*)	Summers lab.
E. coli W3110*hns*Δ93	As for W3110 wild-type, with *hns*Δ93 mutation; Kn^r	Chen (2010) [222]
E. coli W3110Δ*tnaA*	As for W3110 wild-type, with Δ*tnaA* mutation; Kn^r	Summers lab.
Ralstonia eutropha H16	Wild-type	ATCC 17699
R. eutropha PHB^-4	As for *R. eutropha* H16, $PhaC_{Re}$ mutant so unable to produce PHB	DSMZ 541
Rhodococcus opacus PD630	Wild-type	DSMZ 44193
Pseudomonas mendocina	Wild-type	ATCC 25411

For short-term storage (up to ~1 month), bacteria were streaked onto plates of solid medium. To solidify the medium, agar (15 g L^{-1}) was added before autoclaving. *E. coli* were kept on Luria-Bertani agar, and all other species were kept on Nutrient Rich agar. The recipes for the media can be found in Section 3.11.

For long-term storage, overnight cultures (~16 hours) were grown in the appropriate medium (as above) and 700 μl aliquots were mixed with sterile 50% glycerol in sterile 1.7 ml screw-capped storage vials. The vials were stored at −80 °C.

3.1.2 Plasmids

Table 3.2 summarises the relevant features and source of each bacterial strain used in this thesis. Details of the purposes and expression conditions are provided in the relevant chapters and in the following sections of this chapter.

Table 3.2: Plasmids used for this thesis

Plasmid	**Relevant features**	**Source**
pET15*phaC*$_{Re}$	Expression vector providing N-terminal His$_6$-tag containing *phaC*$_{Re}$; T7 promoter; Ap^r	Normi (2005) [223]
pENTRY10	Linearised, dephosphorylated entry vector for StarGate cloning; no promoter; Kn^r	IBA (Germany)
pASG-IBAwt1	Destination vector for StarGate cloning; *tet* promoter; Ap^r	IBA (germany)
pASG1*phaC*$_{Re}$	Expression vector containing *phaC*$_{Re}$ with C-terminal His$_6$-tag; *tet* promoter; Ap^r	Chapter 4
pTrc*phaCAB*	Expression vector containing *C. necator phaCAB* operon; *trc* promoter; Ap^r	Kahar (2005) [224]
pGro7	Expression vector for GroEL/GroES; *araB* promoter; Cm^r	Clontech, USA
pTf16	Expression vector for Tf; *araB* promoter; Cm^r	Clontech, USA
pG-Tf2	Expression vector for GroEL/GroES/Tf; *pzt1* promoter; Cm^r	Clontech, USA
pKJE7	Expression vector for DnaK/DnaJ/GrpE; *araB* promoter; Cm^r	Clontech, USA
pG-KJE8	Expression vector for GroEL/GroES with *pzt1* promoter; DnaK, DnaJ, GrpE with *araB* promoter; Cm^r	Clontech, USA

During growth of cultures that contained plasmids, antibiotics were added to prevent plasmid loss. Retention of plasmids within bacterial cells carries a small but significant metabolic burden, which slows the growth of the host strain. Plasmids are partitioned randomly between daughter cells during cell division, so there is a possibility of producing daughter cells that do not contain a plasmid. [225] In the absence of any selective pressure, the plasmid-free cells would be able to replicate faster than those with plasmids, and would soon dominate the culture leading to a loss of productivity for the plasmid-encoded proteins. Therefore, each plasmid contains an antibiotic-resistance gene, the loss of which prevents cell growth in the presence of the appropriate antibiotic.

3.2 Plasmid construction

To express foreign proteins in *E. coli*, the genes for those proteins are usually encoded on a plasmid, which is then inserted into the production strain. A plasmid is an autonomously replicating circle of DNA that is able to survive within bacterial cells by providing genetic material that is not contained on the chromosome, but which confers a survival advantage on the plasmid-containing strain. Most of the necessary plasmids for the experiments described here were available commercially or from other laboratories (Table 3.2). However, the plasmid pASG1$phaC_{\mathrm{Re}}$ for the expression of *R. eutropha* $\mathrm{PhaC_{Re}}$ ($phaC_{\mathrm{Re}}$) with a C-terminal $\mathrm{His_6}$-tag, used in Chapters 4 and 5, had to be constructed using standard molecular biology techniques, details of which are provided in the following sections of this chapter and Section 4.3.1.[226]

3.2.1 Plasmid purification

For genetic engineering to be successful, it is important to obtain highly pure, undamaged DNA. This ensures the various enzymes are able to work efficiently and specifically on the intended target sequence. Plasmid DNA was purified using a GeneJET miniprep kit (Fermentas, UK). A culture (5–10 ml) of the required *E. coli* strain was grown overnight in LB medium with the appropriate antibiotics for plasmid selection. Cells were separated from the growth medium by centrifugation, and the medium was discarded. The cell pellet was resuspended in resuspension buffer (250 μl) containing RNAse and transferred to a 2 ml microcentrifuge tube. Lysis buffer (250 μl) was added, and the solution was gently mixed to allow complete lysis of the cells. Lysis buffer contains sodium dodecyl sulphate to solubilise cell membranes and denature proteins, and NaOH to denature DNA.

Precipitation buffer (350 μl) was then added, and the mixture was again mixed gently before separating the precipitated cell debris by centrifugation at $17,000\times$g for 10 minutes. The precipitation buffer contains potassium acetate to decrease the pH. This allows the small plasmid DNA to re-anneal and dissolve into the buffer, while larger genetic DNA and proteins are precipitated out. The supernatant containing plasmid DNA but not chromosomal DNA or proteins was tranferred to a silica spin column, washed twice with ethanol-containing washing buffer (700 μl each time) to remove the final traces of salts and other small molecules, and then eluted into a clean 1.5 ml microcentrifuge tube in elution buffer (50 μl). Recovered DNA was quantified using a Nanodrop spectrophotometer (Fisher Scientific, UK) by measuring the absorbance at 260 nm.

3.2.2 Polymerase chain reaction

The $phaC_{Re}$ gene was amplified by the polymerase chain reaction (PCR) using a TC512 thermal cycler (Techne, UK). PCR works by mimicking DNA replication *in vitro*. DNA polymerases can only bind to double-stranded DNA. Therefore, a template containing the desired sequence is denatured at high temperature, then allowed to anneal to two short sequences of synthetic DNA known as primers. The primers are designed to selectively bind at each end of the desired sequence, and therefore only allow DNA polymerase to replicate the sequence between the primers.

The reaction was optimised according to the length of the required target and the melting (denaturing) temperature of the primers. Phusion polymerase (Fisher Scientific, UK) was found to be particularly reliable, yielding large quantities of accurately copied DNA (visualised by agarose gel electrophoresis) with short reaction times when used according to the manufacturer's instructions. PHA synthases typically contain high proportions of G-C base pairs, which decrease the efficiency of PCR. Dimethyl sulphoxide (DMSO) and Betaine (both from Sigma-Aldrich, UK) help to stabilise the annealing of primers to the template, and were found to increase the efficiency of PHA synthase gene amplification.

Primers were designed using the PrimerBLAST program* (National Centre for Biotechnology Information) and were manufactured by Invitrogen (UK).

The PCR mixture for $phaC_{Re}$was: -

Per 20 μl reaction: -

6 μl	ddH_2O
4 μl	Phusion HF buffer
2 μl	Primer 1 (10 μM)
2 μl	Primer 2 (10 μM)
1.5 μl	Template DNA (10 ng μl^{-1})
0.5 μl	40 mM dNTP mix (10 mM each nucleotide)
4 μl	5 M Betaine solution
0.2 μl	Phusion DNA polymerase

The formation of non-specific products was reduced by employing a 'touchdown PCR' protocol, in which the annealing temperature is progressively reduced during the first few cycles, from a very high starting point, to favour primer annealing only to the intended target. This is not always necessary, so most PCR protocols specify a constant annealing

*Available at http://www.ncbi.nlm.nih.gov/tools/primer-blast/

temperature. However, touchdown PCR produced almost no non-specific products (a feat not achieved with a standard protocol) and is therefore recommended in this case. The touchdown PCR protocol for $phaC_{\mathrm{Re}}$ amplification was: -

Initial denaturation:	30 seconds	98 °C
9 cycles of:	10 seconds	98 °C
	30 seconds	80 °C (−1 °C per cycle)
	30 seconds	72 °C
21 cycles of:	10 seconds	98 °C
	30 seconds	72 °C
Final elongation:	3 minutes	72 °C
Storage:	Indefinite	4 °C

Including the time taken to change between temperatures, one reaction took approximately 3 hours. The success of PCR reactions was verified by agarose gel electrophoresis (Section 3.2.3). As no contaminating fragments were present when the touchdown PCR protocol was employed, the polymerase enzyme and oligonucleotide primers were removed using a QIAquick PCR purification kit (Qiagen, UK) according to the manufacturer's instructions.

3.2.3 Agarose gel electrophoresis

DNA length and quality following PCR was analysed by agarose gel electrophoresis. The phosphate group on each nucleotide gives DNA an overall negative charge, so the molecule is attracted to the positive electrode when placed in a solution with an electrical charge applied. For electrophoresis, each sample of DNA is placed into a well at one end of a slab of agarose gel (placed near the negative electrode), through which the electrical charge is conducted. The DNA is forced to travel through the matrix of agarose molecules, which hinders the progression of larger DNA fragments more than smaller fragments. Therefore, as the DNA travels through the gel, the fragments of DNA are sorted according to their size. The concentration of agarose in the gel affects the density of the matrix and so can be varied to optimise the separation of fragments in a particular size range.

For $phaC_{\mathrm{Re}}$, samples (1–10 μl containing 100–500 ng DNA) were electrophoresed through a 0.8% agarose gel in tris-acetate-EDTA buffer (TAE). The buffer maintains a slightly alkaline pH (pH 8.0) to preserve the negative charge on the DNA, and provides a conducting medium to establish an electrical current. TAE was used as running buffer and

for the production of the agarose gel. The sample was mixed with 6× Fermentas loading buffer (1 μl), which contains glycerol to help the DNA to sink into the well, and an electrophoretic dye to help track the progress of DNA through the gel. After samples were pipetted into wells in the gel, an electric potential of 80 V was applied across the gel for 1 hour.

The DNA was stained by soaking in ethidium bromide solution (0.5 μg ml^{-1}) for 15–30 minutes and visualised on a GelDoc-It ultraviolet light transilluminator system (UVP). Ethidium bromide is a fluorescent dye that is able to intercalate between the bases of double-stranded DNA. When illuminated with ultraviolet light, it fluoresces with an orange colour, and the fluorescence is ~20× stronger when the dye is bound to DNA. For approximate sizing of DNA strands, bands on the gel were compared to a control sample of GeneRuler 1 kb DNA ladder (Fermentas, UK), consisting of a mixture of DNA fragments of different, known, lengths. The ladder was run on the same gel to control for slight variations in migration speeds between gels.

3.2.4 DNA ligation

Following PCR amplification and purification of the target DNA, the $phaC_{\mathrm{Re}}$ gene was ligated to a linearised plasmid with T4 DNA ligase (Fermentas, UK). DNA ligases catalyse the formation of phosphodiester bonds between the 3′ hydroxyl end of one DNA strand and the 5′ phosphate end of another. For the cloning of $phaC_{\mathrm{Re}}$ into pENTRY10, the plasmid was purchased in linearised form with the 5′ phosphates removed from each end. This prevented the plasmid from being re-circularised unless the insert was present to provide a phosphate for the joining reaction. Neither the plasmid nor the insert were digested with restriction enzymes, and therefore did not have overhanging 'sticky ends' of single-stranded DNA. So called 'blunt-ended' reactions such as this are less efficient than those with sticky ends, as there are is no hydrogen bonding to stabilise the construct before ligation occurs.

The ligation reaction was carried out in a 20 μl volume, and allowed to proceed overnight at 22 °C. The reaction mix was: -

Per 20 μl reaction: -

x μl	ddH_2O (to make up correct volume)
2 μl	DNA ligase reaction buffer
1-10 μl	Linearised plasmid DNA (approx. 100 ng)
1-10 μl	Cleaned, digested insert DNA (to give 3:1 insert:plasmid ratio)
1 μl	T4 DNA ligase

3.3 DNA sequencing

The sequences of newly-constructed plasmids (pENTRY10:$phaC_{\mathrm{Re}}$ and pASG1$phaC_{\mathrm{Re}}$) were verified by Sanger sequencing, carried out by Geneservice (Cambridge, UK). Plasmids were purified as described in Section 3.2.1 and eluted in ddH_2O (50 μl). If necessary, the solution was diluted to 100 ng μl^{-1} with further ddH_2O. Sequencing primers were manufactured by Invitrogen (UK), and were shipped together with the plasmid as 3.2 ng μl^{-1} aqueous solutions.

3.4 Transformation of *E. coli*

The uptake of DNA by bacteria is known as transformation. Some bacteria, such as *Streptococcus pneumoniae* are able to do this naturally, and so can gain beneficial genes from their environment.[227] Bacteria that are able to take up DNA are described as competent. *E. coli* are not naturally competent, but can be temporarily induced into competency by disrupting the cell membrane to create small holes. DNA can pass through these holes, which are then repaired by the cells' membrane repair system to allow the bacteria to continue growing.

Two methods are commonly used to induce competence in *E. coli*. The first is to apply a short, high-voltage electrical current through the cells. This requires specially-designed conductive cells and an appropriate electrical source, which were not available. Therefore the second method was chosen. This involves treating the cells with a solution of divalent cations (Mn^{2+} and Ca^{2+}) before rapidly heating them from 0–42 °C to make them competent. The divalent cations associate with the negatively-charged phospholipids and lipopolysaccharides in the cell membrane, providing a shield for the DNA, which is also negatively charged. The heating step disrupts the cell membrane sufficiently to allow DNA to pass into the cells.

The protocols for the preparation of competent cells and for the transormation itself are provided in the following sections.

3.4.1 Preparation of competent cells

E. coli were transformed by the Inoue method [226]. A single colony of the strain to be transformed was inoculated into LB medium (5 ml) with the appropriate antibiotics, and incubated for 8 hours at 37 °C while shaking at 250 rpm. From the resulting culture, 2 ml was used to inoculate SOB medium (50 ml) in a 250 ml Erlenmeyer flask. SOB medium uses the same recipe as SOC medium, but the glucose is omitted. The new culture was grown for approximately 16 hours at 18 °C while shaking at 250 rpm. The cells were then pelleted by centrifugation at 4000×g and 4 °C. The supernatant was removed, and the cells were gently resuspended in ice-cold Inoue transformation buffer (16 ml). The cells were again pelleted by centrifugation, and the supernatant was replaced with fresh Inoue transformation buffer (4 ml).

Unless used immediately, cells were stored in aliquots at −80 °C until needed. To do so, dimethyl sulphoxide (DMSO, 300 μl) was added to the cell suspension, which was then stored on ice for 10 minutes. 50 μl aliquots were dispensed into 1.5 ml microcentrifuge tubes, frozen in liquid nitrogen and then transferred to the freezer for storage.

3.4.2 Transformation

To transform the cells, aliquots were removed from the −80 °C freezer and thawed on ice. Plasmid DNA (10–25 ng) was added, and the tubes were stored on ice for 30–45 minutes. The cells were then heat-shocked at 42 °C for 45 seconds by transferring the tubes to a pre-warmed heating block with water in the wells to aid heat transfer. The tubes were transferred back to the ice bath for 2 minutes. SOC medium (800 μl) was then added, and the cells were allowed to recover and to express the antibiotic resistance marker encoded by the plasmid at 37 °C for 45-60 minutes. Finally, cells (300 μl) were spread onto LB agar plates containing the appropriate antibiotics and incubated overnight at 37 °C.

3.5 Growth conditions

3.5.1 Monitoring cell growth by measurement of optical density

A simple and convenient method to monitor the growth of bacterial cultures is to measure the optical density at various time-points using a spectrophotometer. A spectrophotometer is an instrument that shines light of a particular wavelength through a sample and detects the fraction of light that is able to travel through the entire sample. The sample is usually held in a cuvette with a width of 1 cm to ensure that the distance travelled by the light through each sample is the same. If the sample contains particles that absorb or scatter light, the amount of light detected will be reduced by an amount that is proportional to the concentration of the particles.

Bacterial cells tend to scatter light with a wavelength of approximately 600 nm. Therefore, as the cells divide and multiply, the amount of light scattered by a sample of the culture will increase and the amount of light detected will decrease. The ability of a sample to scatter light is known as its optical density. The optical density for a wavelength of 600 nm is written OD_{600}.

Measurements of OD_{600} were widely used throughout the experiments for this thesis. Protein production often depends on the density of cells in the culture at the time that protein expression is induced. Therefore, the OD_{600} before induction must be carefully monitored to ensure that protein expression is induced at the same cell density for each culture. The relationship between OD_{600} and cell density is typically linear up to values of 0.8–1.0. Therefore, samples were appropriately diluted in fresh LB medium prior to measuring, to give a maximum absorbance of 0.8.

OD_{600} is also important for characterising the growth of Q-cell cultures. Standard cultures follow a well-known growth curve of three phases: in the stationary phase, the cells are at low density and are adapting to their new growth conditions, having recently been inoculated. They might need to express a different set of genes to utilise a new carbon source, to resist an antibiotic or to adapt to a new temperature. Therefore they grow slowly. When they have adapted to the conditions, they begin to grow and divide exponentially. Therefore the second phase is known as the exponential growth phase, and is recognised by a rapid increase in OD_{600}. Finally, having begun to exhaust the available resources, growth slows and the culture enters the stationary phase at an OD_{600} of $\sim$4.

Q-cell cultures are prevented from growing during the early exponential phase. Therefore, they follow a different growth curve in which the OD_{600} continues to increase slowly

for 4–6 hours, then remains at 0.6–0.8 for the remainder of the culture time. The characteristic growth curve of Q-cells is the most convenient indicator that cultures have become quiescent.

3.5.2 Q-cell growth

Q-cell cultures were grown in 50 ml Erlenmeyer flasks. Some experiments were carried out in a laboratory in Japan (see Chapter 4 for details) and used flasks with baffles to assist aeration of the medium. A 20 ml pre-culture of *E. coli* W3110*hns*Δ93 containing pASG1*phaC*$_{\mathrm{Re}}$ was prepared by inoculating Luria-Bertani (LB) medium containing ampicillin (100 μg ml^{-1}) and kanamycin (30 μg ml^{-1}) with 200 μl of an overnight culture. Ampicillin was for plasmid selection and kanamycin was to ensure selection for the W3110*hns*Δ93 strain of *E. coli*, which contains a kanamycin-resistance cassette to produce the *hns*Δ93 mutation. The pre-culture was grown at 37 °C, shaking at 180 rpm on a reciprocal shaker until OD_{600} reached 0.25 ± 0.05.

Meanwhile, 18 ml aliquots of fresh LB medium (plus appropriate antibiotics) were prepared by adding an appropriate volume of 0.5 M indole stock solution dissolved in ethanol. Indole is poorly soluble in water, so the stock solution was added by submerging the tip of a sterile pipette in the growth medium and expelling the solution slowly, while gently swirling the contents of the flask. 2 ml of the pre-culture were added to each aliquot to begin the Q-cell culture and the time of this inoculation was defined as $t = 0$. The growth of the cultures was monitored by measuring OD_{600} at regular intervals for the first 8–10 hours, and finally after 24 hours, at which time the culture was harvested. PhaC$_{\mathrm{Re}}$ expression was induced by the addition of anhydrotetracycline (AHT, 0.4 μg ml^{-1}). The time of induction varied according to the experiment, as described in Chapter 4.

3.5.3 PhaC$_{\mathrm{Re}}$ production

For PhaC$_{\mathrm{Re}}$ co-expression with chaperone proteins, strains were grown in 1 L Erlenmeyer flasks with 200 ml of LB medium supplemented with ampicillin (100 μg ml^{-1}) and chloramphenicol (30 μg ml^{-1}) as necessary for plasmid selection. Overnight cultures in LB medium (2 ml) were used for inoculation, and the cultures were then incubated at 37 °C while shaking at 250 rpm until the OD_{600} was approximately 0.6. At this point, PhaC$_{\mathrm{Re}}$ production was induced by the addition of isopropyl β-D-1-thiogalactopyranoside (IPTG, 1mM) or AHT (0.4 μg ml^{-1}), depending on the plasmid, and the incubation temperature was reduced to 30 °C for a further 6 hours. The cells were harvested by centrifugation at 4000×g for 15 minutes, washed once with deionised

water and stored at −80 °C with 100,000 U lysozyme and 10 μl protease inhibitor for His-tagged proteins (both from Sigma-Aldrich, UK).

The N-terminal-tagged $PhaC_{Re}$ was expressed from the T7 promoter by addition of IPTG (1 mM). When chaperone proteins were co-expressed (see Chapter 5), they were allowed to accumulate before the start of $PhaC_{Re}$ expression by adding arabinose (0.5 mg ml^{-1}) and/or AHT (0.2 μg ml^{-1}), depending on the promoter(s) used, at the time of inoculation. The C-terminal-tagged $PhaC_{Re}$ was expressed from the *tet* promoter, which is also induced by AHT. Therefore, in this case only those chaperones controlled by the *araB* promoter were induced from inoculation, while $PhaC_{Re}$ and the remaining chaperones were induced by addition of AHT (0.2 μg ml^{-1}) when OD_{600} measured 0.6.

3.5.4 PHB production

For high-yield production of PHB, cultures (100 or 200 ml) were grown in 1 L Erlenmeyer flasks in LB medium supplemented with glucose (20 g L^{-1}). A variety of W3110 strains were used, but all strains contained the plasmid pTrc*phaCAB* for expression of the *R. eutropha* PHB operon from the IPTG-inducible *trc* promoter. Glucose acts as the primary carbon source for the production of PHB. Ampicillin (100 μg ml^{-1}) and chloramphenicol (30 μg ml^{-1}) were added as required for plasmid selection. When W3110*hns*Δ93 or W3110Δ*tnaA* were used, kanamycin (30 μg ml^{-1}) was also added due to the kanamycin-resistance cassettes in the chromosomes. PHB production was induced at the time of inoculation by addition of IPTG (1 mM). Cultures were incubated at either 30 or 37 °C with shaking at 250 rpm for 72 hours. Cells were harvested by centrifugation at 4000×g for 15 minutes, washed once with deionised water, transferred to pre-weighed polypropylene tubes and frozen at −80 °C overnight. The cells were freeze-dried for 72 hours and then weighed to determine dry cell weight (DCW). When chaperone proteins were co-expressed, arabinose (0.5 mg ml^{-1}) and, if necessary, AHT (0.2 μg ml^{-1}) were added to the culture medium at the time of inoculation.

3.6 Protein purification and analysis

Yields of $PhaC_{Re}$ were compared semi-quantitatively by examining the intensity of bands on sodium dodecyl sulphate-polyacrylamide gel electophoresis (SDS-PAGE) gels. The principle behind SDS-PAGE is the same as for agarose gel electrophoresis (Section 3.2.3) but polyacrylamide gels are used because they have a smaller, more uniform pore size. SDS denatures proteins and equalises the mass:charge ratio, which usually varies depending on which amino acids are present. Therefore, the separation during electrophoresis

is assumed to be on the basis of protein size with negligible contributions from charge and folding conformation.

$PhaC_{Re}$ often accumulates in insoluble intracellular deposits. For rapid screening of the productivity under different culture conditions, the total cell protein was compared. For more detailed analysis of the solubility of $PhaC_{Re}$, the protein samples were divided into the soluble and insoluble fractions, which were compared side-by-side.

Quantitative analyses were conducted if the improvements in $PhaC_{Re}$ production were felt to be sufficient for further investigation. For this, cobalt-affinity chromatography was performed to purify the $PhaC_{Re}$. The purified $PhaC_{Re}$ was quantified by measuring the concentration, based on its absorbance of light with a wavelength of 280 nm (A_{280}). The activity of the purified enzyme was also assayed (Section 3.6.4).

Cobalt-affinity chromatography exploits the affinity for divalent metal ions shown by histidine. To achieve high-affinity binding with the necessary specificity, a sequence of histidine molecules is introduced to one end of the protein of interest by modification of its gene. Typically, 6 histidines are added so the extra amino acids are known as a His_6-tag. Other metal ions such as nickel can also be used, but Co^{2+} has been found to have the highest specificity.[228] The ions are immobilised within a gel matrix in a gravity-driven chromatography column. A mixture containing the soluble proteins from a lysed cell culture is loaded onto the column in a buffer with a low concentration of imidazole. The majority of proteins flow directly through the column and are washed away, while His_6-tagged proteins and some contaminants (proteins with naturally high histidine content) are retained. The concentration of imidazole in the buffer is then gradually increased to elute first the contaminating proteins and then the purified protein of interest. Elution occurs because imidazole competes with the His_6-tag for binding to Co^{2+}.

3.6.1 Preparation of cell fractions for SDS-PAGE

Total cell protein samples were prepared from 1 ml samples of each culture. The samples were centrifuged for 5 minutes at $17,000\times$g to recover the cells and the supernatant was discarded. The cells were resuspended in an appropriate volume of 1% aqueous sodium dodecyl sulphate (SDS) solution. The volume of SDS solution was calculated from the final OD_{600} of the culture to give a density of cells in the SDS solution equivalent to $OD_{600} = 5$. This normalised the protein concentration in each sample to control for variations in cell growth. After briefly vortexing to ensure complete lysis, a 50 μl sample was taken and mixed with 100 μl of $3\times$ SDS-PAGE loading buffer, heated at 95 °C

for 10 minutes to completely dentaure the protein, and 10 μl was loaded on a 10% SDS-PAGE gel.

For soluble protein fractions, 1 ml samples of cell culture were centrifuged at $17,000\times$g for 5 minutes to recover the cells. The supernatant was discarded and the cells were re-suspended in an appropriate volume of BugBuster protein extraction reagent (Novagen, USA), equivalent to $OD_{600} = 5$. The mixture was incubated at 30 °C for 30 minutes to allow complete cell lysis. The lysed cell mixture was centrifuged at $17,000\times$g for 15 minutes at 4 °C to remove cell debris. a 50 μl sample of the supernatant was taken and mixed with 100 μl of 3× SDS-PAGE loading buffer. The samples were heated at 95 °C for 10 minutes and 10 μl was loaded on a 10% SDS-PAGE gel.

For the insoluble fraction, the pellet from the final centrifugation step for separating soluble proteins was retained after removing the remaining supernatant. The pellet was resuspended in 1% SDS solution (the same volume as of BugBuster) and vortexed vigorously to solubilise the contents. If necessary, the samples were shaken at room temperature overnight to ensure complete solubilisation. A 50 μl sample was analysed by SDS-PAGE as above.

All SDS-PAGE gels were run at 125 V, with a maximum current of 30 mA for 100 minutes. Proteins were visualised by staining with PageBlue colloidal Coomassie Blue protein staining solution (Fermentas, UK).

3.6.2 Western blotting

To compare the density of $PhaC_{Re}$ bands without interference from other proteins, $PhaC_{Re}$ was selectively visualised by western blotting. This involved transferring separated proteins from a SDS-PAGE gel onto the surface of a polyvinylidene difluoride (PVDF) membrane. Here, the His_6-tag on $PhaC_{Re}$ was selectively targetted by horseradish peroxidase conjugated to a His_6-specific antibody. The horseradish peroxidase catalysed the oxidation of 3,3′-Diaminobenzidine by hydrogen peroxide to form a dark precipitate, which marked the presence of $PhaC_{Re}$.

Samples of cell culture (10 ml) were taken prior to harvesting. The cells were recovered by centrifugation and washed once in deionised H_2O. The cell pellet was resuspended in 500 μl BugBuster cell lysis buffer (Novagen, USA) with 250 μl of Benzonase nuclease (Sigma-Aldrich, UK), and shaken at room temperature for 30 minutes. The lysis mixture was centrifuged at $17,000\times$g for 30 minutes at 4 °C. The supernatant constituted the soluble protein fraction, and the pellet (the insoluble fraction) was dissolved in 500 μl of 1% (w/v) SDS. The samples were prepared for SDS-PAGE as described previously.

The volume of sample to load onto the gel was calculated from the final culture OD_{600} so that each lane contained the same quantity of protein.

The proteins were separated by SDS-PAGE as described in Section 3.6.1, and transferred to a PVDF membrane using a Trans-Blot semi-dry blotting system (Bio-Rad, USA). His_6-tagged $PhaC_{Re}$ was specifically stained using the HisProbe HRP conjugate kit and metal-enhanced DAB substrate (Fisher Scientific, UK) according to the manufacturers instructions. Densitometry analysis was performed using the gel analysis function of ImageJ[†] (National Institutes of Health).

3.6.3 Cobalt-affinity purification

Cells were grown as described, then recovered by centrifugation and washed once with deioised water. They were transferred to a 15 ml centrifuge tube and resuspended in 5 ml of lysis/binding buffer (Section 3.12.8). Cells were ruptured by 5 cycles of sonication using a Sonopuls HD2200 sonicator (Bandelin, UK) and MS73 tip, set to 30 seconds duration, 10% duty and 10% power, with 5 minutes on ice between cycles. Cell debris was removed by centrifugation at 4 °C followed by filtration of the supernatant with a cellulose acetate syringe filter with 0.44 μm pore size. TALON His-Tag purification resin (Clontech, USA) was used for cobalt-affinity protein purification according to the manufacturer's instructions, with 2 ml of resin per column. Lysis/binding buffer was used to equilibrate and wash the column, and purified $PhaC_{Re}$ was eluted using elution buffer (Section 3.12.9). Elution fractions containing $PhaC_{Re}$ were combined, concentrated, and the buffer exchanged for desalting buffer (Section 3.12.10) using centrifugal filters with a molecular weight cut-off of 10 kDa.

3.6.4 $PhaC_{Re}$ activity assay

The final protein concentration of each sample was determined by measuring the absorbance at 280 nm (A_{280}) with a Nanodrop spectrophotometer (Fisher Scientific, UK). The molar extinction coefficient was taken to be 162,000 M^{-1} cm^{-1}.[104] Enzyme activity was determined by measuring the decrease in A_{236} resulting from the cleavage of the thioester bond with CoA. An extinction coefficient of 4500 M^{-1} cm^{-1} was used.[229] The reaction mixture consisted of 50 mM phosphate buffer, 200 μM (D,L)-3-hydroxybutyryl-CoA (Sigma-Aldrich), 4 μg $PhaC_{Re}$ and double distilled water (ddH_2O) with a total volume of 400 μl. The phosphate buffer and water were added to the cuvette first and used to zero the spectrophotometer. Next, the (D,L)-3-hydroxybutyryl-CoA was added

[†]ImageJ is available to download at http://rsbweb.nih.gov/ij/index.html

to establish a preliminary absorbance reading. Continuous recording of the absorbance was started, and finally the $PhaC_{Re}$ was added to the mixture to begin the reaction. Each assay lasted ~5 minutes.

The activity of the enzyme was determined by the maximum rate of absorbance decrease during the reaction. One enzyme unit was defined as the amount of enzyme that catalysed the release of 1 μmol CoA per minute (expressed as U mg^{-1} protein).

An alternative method for the activity of PhaC uses (5,5′-dithiobis-(2-nitrobenzoic acid) (DTNB; also known as Ellman's reagent), and has been recommended ahead of the A_{236} method.[106] It relies on the binding of DTNB to the thiol group of free CoA, released during PHA polymerisation, which can be measured spectrophotometrically at a wavelength of 212 nm with an absorption coefficient of 14,150 M^{-1} cm^{-1}. Note that this absorption coefficent is higher than for the A_{236} assay, so the DTNB test is more sensitive. However, DTNB can also react with thiol groups on proteins (including in the active site of PhaC) and therefore this assay can not be conducted continuously. For the analysis of many samples, it is thus more convenient and efficient to use the A_{236} assay.

3.7 PHB purification and analysis

For Chapters 5 and 6, gas chromatography (GC) and gel permeation chromatography (GPC) were used to analyse the productivity and molecular weight of PHB. GC separates small molecules in a gaseous mobile phase by virtue of their interactions with a liquid or polymer stationary phase at the wall of the column. After exiting the column, the analytes are detected by a flame ionisation detector, each resulting in a peak in the chromatograph at a characteristic time, and with an area that reflects its concentration. For the analysis of polymers such as PHB, it is necessary to degrade them into their monomers. This was achieved by methanolysis to form methyl esters of butyric acid.

GPC is a form of liquid chromatography, in which analytes are separated by flowing through a stationary phase that consists of porous beads with a carefully selected range of pore sizes. Larger molecules cannot fit through all of the pores and so pass rapidly through the spaces between beads and are eluted soon. Small molecules follow a longer route through the column in which they pass through many of the pores, and so elute later. Unlike GC, GPC works with polymers, but it was necessary to purify the PHB to remove large molecules that could interfere with the signal, and small molecules that could block the column. The following sections contain the protocols that were used for the methanolysis, gas chromatography, purification and gel permeation chromatography of PHB.

3.7.1 Methanolysis

Cells were grown under PHB production conditions as described in Section 3.5.4 and freeze-dried. Approximately 20 mg of dried cells were used for methanolysis to convert PHB into its methyl ester. The cells were mixed with HPLC-grade chloroform (2 ml) and methanol/sulphuric acid (85:15 v/v, 2 ml) in a glass, screw-capped tube. The mixture was vortexed to mix thoroughly then heated to 100 °C for 140 minutes in a block heater (Grant, UK).[230] After addition of 1 ml ddH_2O to induce phase separation, the lower chloroform layer was filtered (0.2 μm PVDF syringe filter) and used for gas chromatography.

3.7.2 Gas chromatography

The filtered chloroform fraction from methanolysis (0.5 ml) was combined in equal parts with a 0.1% solution of methyl benzoate (final concentration 0.05%) in HPLC-grade chloroform, in a 1.7 ml screw-capped vial with a rubber septum in the cap. The mixture was used for gas chromatography (GC) analysis with a GC2014 gas chromatograph (Shimadzu, Japan) fitted with an autosampler. Methyl benzoate served as an internal standard of constant concentration in order to calculate the accumulated PHB amount. A standard curve was constructed by methanolysing and analysing a range of known quantities of purified PHB (Sigma-Aldrich, UK).

3.7.3 PHB purification

PHB was extracted from dried cells by stirring with 50 ml chloroform per 100 mg PHB for 72 hours. After filtering to remove cell debris (either with a 0.4 μm PVDF syringe filter or Advantec No. 1 filter paper (Cole Parmer, UK)), the polymer was precipitated by slowly dropping the chloroform solution into methanol and recovered by a further filtration step with Advantec No. 5B ashless filter paper (Cole Parmer, UK). After drying, the purified polymer was then re-dissolved in chloroform at a concentration of 1 mg ml^{-1} for gel permeation chromatography (GPC) to determine the molecular weight.

3.7.4 Gel permeation chromatography analysis

The GPC analysis was conducted using a PL-GPC 50 liquid chromatography system (Polymer Labs, UK) fitted with two PL-Gel MiniMix-B separation columns and a PL-Gel MiniMix-B guard column (all from Polymer Labs, UK). Chloroform was used as the eluent at a flow rate of 0.3 ml min^{-1} and the analysis was conducted at a temperature

of 40 °C. Polystyrene standards with low polydispersity (1.3×10^3 to 7.5×10^6 Da) were used to construct a standard curve using the same conditions.

3.8 Wet STEM imaging of bacterial cells

Samples of *R. eutropha* for imaging in the wet STEM investigation were grown in either nutrient rich (NR) medium (for initial growth or for low accumulation of PHB) or nitrogen-limited mineral salts (MS) medium (for high accumulation of PHB). *Rhodococcus opacus* and *Pseudomonas mendocina* were grown in mineral salts media appropriate for each species (MMR and MMP, respectively). The recipes for the growth media are given in Section 3.11. The growth conditions varied depending on the experiment, and so are described in more detail in the relevant sections of Chapter 7. Following growth, each sample was prepared and imaged according to the same procedures, as described in the following sections.

3.8.1 Sample preparation

Samples were prepared for imaging by removing an aliquot (300 μl) of the cell suspension and adding refrigerated ddH_2O (1000 μl). This sample was then centrifuged at 6000×g for 10 minutes at 4 °C. The supernatant was removed and the pellet resuspended in ddH_2O (1000 μl). The sample was centrifuged and resuspended in 1000 μl water a final time before being placed on ice until deposition for imaging. Typically, samples remained on ice for between 30 minutes and 2 hours before imaging.

3.8.2 Imaging conditions

Samples were imaged in a XL30 ESEM (FEI, USA), equipped with a field-emission electron source, and operated in bright-field mode at the Cavendish Laboratory. A 0.5 μl sample, prepared as in Section 3.8.1, was deposited onto carbon-coated 300-mesh copper TEM grids and loaded directly into the ESEM for imaging. All transmission-mode images were acquired with an accelerating voltage of either 20 or 25 kV, beam current of 150–180 pA and spot diameter of 3 nm. The gas path length varied between 1–2 mm, and the sample-detector distance was fixed at 7 mm. Transmitted electrons were collected using a split-diode detector, placed under the sample as shown in Figure 7.1 (B). The microscope was equipped with a Peltier-cooled stage to maintain the sample temperature at 1 °C. Four small drops of water at room temperature were placed close to the sample

in the chamber to prevent complete evaporation of the sample during the pump-down phase.

3.8.3 Pump-down procedure

For routine operation, the microscope sample chamber was subjected to a number of pumping and flooding cycles as part of the pump-down procedure. This process successively replaces air in the chamber with water vapour at the target vapour pressure. Pumping to the beginning of the first flooding cycle was accomplished in approximately 30 seconds and the completion of all the flooding cycles required (approximately) a further 90 seconds. A standard, optimised pump-down procedure was designed to minimise water loss from the sample, following the guidelines of Cameron and Donald (1994).[231] The microscope chamber was pumped from atmospheric pressure to 6 Torr and then flooded to 9 Torr, before being pumped to 6 Torr again. This pumping/flooding cycle was repeated 8 times, before the imaging chamber was finally pumped to the target pressure.

To enable the imaging of samples at higher resolution, samples were partially dehydrated by deliberately using a pumping/flooding cycle that was less effective at preserving the hydrated environment, and by conducting the procedure without controlling the sample temperature (~20 °C). The chamber was pumped from atmospheric pressure to 2.0 Torr, flooded with water vapour to 9.0 Torr and then pumped to 2.0 Torr again. This cycle was repeated 5 times, before the sample chamber was pumped to the working pressure of 1.5 Torr.

3.8.4 Cell viability study

3.8.4.1 Optical density method

R. eutropha H16 (0.5 μl), prepared as for imaging but resuspended in a final volume of 300 μl water, was placed on a carbon-coated gold TEM grid and mounted in the Peltier-cooled sample holder, held at 1 °C. Pressures of 4.5, 3.0 and 1.5 Torr were chosen as a representative range. Following de-pressurisation, samples were held at the target pressure with the beam on for 10 minutes, before being returned to room temperature and pressure. Samples were immediately placed in 50 μl NR medium in a 2 ml microcentrifuge tube and held on ice until all target pressures had been acquired.

Negative controls consisted of medium only and a clean grid incubated in medium without a sample. To control for the effect of drying the sample onto the grid, a sample

of each strain was placed on a grid, allowed to dry at room temperature and pressure, and then incubated as described. Positive controls were also included, consisting of 0.5 μl of either strain introduced directly to 50 μl NR medium. After pressure-cycling, an initial OD_{600} was recorded for each sample and controls, using a Nanodrop ND2000 spectrophotometer (Thermo Scientific, USA) before being incubated at 30 °C and shaking at 200 rpm. The OD_{600} of samples and controls was measured after 40 hours, and compared to the pre-incubation measurement.

3.8.4.2 Colony counting method

R. eutropha H16 cells were prepared as described in Section 3.8.4.1. To allow three samples to be tested in parallel, a copper insert for the Peltier stage was used to provide a flat, cooled surface on which to place samples. This allowed the use of small pieces of thin glass (approximately 0.5 × 0.5 cm cut from standard cover slips with a diamond-tipped cutter) on which to deposit samples, to reduce cost. The pieces of cover slip were autoclaved and then cooled on ice in a sealed container before use. For each pressure, 1 μl of cell suspension was pipetted onto each cover slip, resting on the Peltier stage with the temperature set to 1 °C. Using the standard pumpdown procedure (Section 3.8.3), the microscope chamber was depressurised to 5.0 Torr and held at the target pressure for 10 minutes. The cover slips were then transferred into ice-cold NR medium (1 ml) in a 2 ml microcentrifuge tube and stored on ice until all samples were collected. The procedure was repeated for pressures of 4.0, 3.5, 3.0, 2.5, 2.0 and 1.0 Torr, and controls were also prepared as in Section 3.8.4.1.

Cells were dislodged from the cover slips by vigorous vortexing for at least 30 seconds. A sample of the resulting cell suspension was then diluted 10× and 200 μl was spread onto a NR agar plate. The plates were incubated at 30 °C for 16 hours. The number of viable cells in each suspension was estimated by counting the colonies on each plate and multiplying by the dilution factor (5×10^4). For the positive control and 5.0 Torr samples, larger dilution factors were necessary due to the large number of viable cells.

3.9 TEM sample preparation and imaging

Pellets of *R. eutropha* destined for observation by TEM were fixed by resuspending in 2% glutaraldehyde in 0.1 M piperazine-N,N'-bis(2-ethanesulfonic acid) (PIPES) buffer for 2 hours. Further processing was carried out at the Multi-Imaging Centre, Cambridge University (Cambridge, UK). Samples were rinsed in PIPES buffer, treated with 1% osmium tetroxide for one hour and rinsed in deionised water before staining with 2%

uranyl acetate in 0.05 M maleate buffer. The pellet was dehydrated in an ascending series of ethanol solutions from 70% to 100%, rinsed twice in acetonitrile and infiltrated with Quetol epoxy resin. The resin was cured at 60 °C for 48 hours. Thin sections were cut using a Leica ultracut UCT ultramicrotome, mounted on 300 mesh copper grids and stained with uranyl acetate and lead citrate. Samples were viewed in a Technai G2 TEM (FEI, USA) operated at 120 kV and images were recorded with a XR60B digital camera (Deben, UK).

3.10 Chemical stock solutions

Table 3.3 gives the details of stock solutions of chemicals that were kept for use when required. All aqueous solutions were sterilised by passing through a 0.22 μm cellulose acetate filter. There is no need to sterilise solutions in ethanol.

Table 3.3: Details of chemical stock solutions

Chemical	**Solvent**	**Stock conc.**	**Final conc.**	**Comments**
Ampicillin	Water	100 mg ml^{-1}	100 μg ml^{-1}	Store at −20 °C
Kanamycin	Water	30 mg ml^{-1}	30 μg ml^{-1}	Store at −20 °C
Chloramphenicol	Ethanol	30 mg ml^{-1}	30 μg ml^{-1}	Store at −20 °C
Anhydrotetracycline	Ethanol	0.4 mg ml^{-1}	0.4 μg ml^{-1}	Store at −20 °C
X-gal[a]	DMF[b]	100 mg ml^{-1}	50 μg ml^{-1}	Store at −20 °C
IPTG[c]	Water	1 M	1 mM	Store at −20 °C
Indole	Ethanol	0.5 M	0.2–3.0 mM	Store at 4 °C
PIPES[d] (pH 6.7)	Water	0.5 M	10 mM	Adjust pH with 5 M KOH Store at −20 °C
$MgSO_4 \cdot 7\,H_2O$	Water	200 g L^{-1}	0.2 g L^{-1}	
Glucose	Water	500 g L^{-1}	20 g L^{-1}	
Fructose	Water	500 g L^{-1}	20 g L^{-1}	
Arabinose	Water	200 g L^{-1}	0.5 g L^{-1}	

[a]X-gal is 5-Bromo-4-chloro-3-indolyl β-D-galactopyranoside
[b]DMF is dimethylformamide
[c]IPTG is isopropyl β-D-1-thiogalactopyranoside
[d]PIPES is piperazine-1,2-bis[2-ethanesulfonic acid]

3.11 Growth Media

The recipes for every type of growth medium and buffer used in this thesis are given in the following sections. Note that the recipes for media are for growth of liquid cultures in shake-flasks. For growth on plates, simply add agar (15 g L^{-1}) before autoclaving. The standard autoclave sterilisation cycle maintained a temperature of 121 °C for 30 minutes.

3.11.1 Luria-Bertani Medium (LB)

Per litre: -

10.0 g	Tryptone
5.0 g	Yeast extract
5.0 g	NaCl

Dissolve the ingredients in deioinised water and sterilise by autoclaving.

3.11.2 Nutrient-Rich Medium (NR)

Per litre: -

10.0 g	Tryptone
10.0 g	Meat extract
2.0 g	Yeast extract

Dissolve the ingredients in deioinised water and sterilise by autoclaving.

3.11.3 Nitrogen-Limited Mineral Salts Medium (MS)

Per litre: -

9.0 g	$Na_2HPO_4 \cdot 12\,H_2O$		
1.5 g	KH_2PO_4		
0.5 g	NH_4Cl		
0.2 g	$MgSO_4 \cdot 7\,H_2O$		
As required	Carbon source		
1.0 ml	Trace elements solution		
	consisting of (per litre): -	9.7 g	$FeCl_3$
		7.8 g	$CaCl_2$
		0.218 g	$CoCl_2 \cdot 6\,H_2O$
		0.156 g	$CuSo_4 \cdot 5\,H_2O$
		0.118 g	$NiCl_3 \cdot 6\,H_2O$
		0.105 g	$CrCl_3 \cdot 6\,H_2O$
		0.1 M	HCl

Dissolve the $Na_2HPO_4 \cdot 12\,H_2O$, KH_2PO_4 and NH_4Cl in an appropriate volume of deionised water to allow for the later addition of $MgSO_4 \cdot 7\,H_2O$, trace elements and

carbon source. Sterilise the solution by autoclaving in the culture flask. $MgSO_4 \cdot 7\,H_2O$ and trace elements ($1,000\times$ stock solutions) should be prepared separately (Section 3.10), filter sterilised and added to the growth medium before inoculation. The carbon source should also be filter sterilised and added before inoculation: the type and quantities are specified for each experiment separately.

3.11.4 Mineral Salts Medium for *Rhodococcus opacus* PD630 (MMR)

Per litre: -

10.0 g	Sodium gluconate		
3.98 g	K_2HPO_4		
1.65 g	KH_2PO_4		
1.0 g	$MgSO_4 \cdot 7\,H_2O$		
0.05 g	NH_4Cl		
1.0 ml	Trace elements solution		
	consisting of (per litre): -	15.0 g	$CaCl_2 \cdot 2\,H_2O$
		5.0 g	$FeNa \cdot EDTA$
		2.0 g	$NaMoO_4$
		0.5 g	$FeSO_4 \cdot 7\,H_2O$
		0.4 g	$ZnSO_4 \cdot 7\,H_2O$
		0.25 g	EDTA
		0.05 g	$CoCl_2 \cdot 6\,H_2O$
		0.02 g	$MnSo_4 \cdot H_{20}$
		0.015 g	H_3BO_3
		0.01 g	$NiCl_2 \cdot 6\,H_2O$
		0.005 g	$CuCl_2 \cdot 2\,H_2O$

Autoclave K_2HPO_4, KH_2PO_4 and NH_4Cl together in the culture flask. $MgSO_4 \cdot 7\,H_2O$ ($1,000\times$ stock solution) and sodium gluconate are prepared separately, sterilised by filtration, and added to the growth medium before inoculation. The trace elements solution should be filter sterilised.

3.11.5 Mineral Salts Medium for *Pseudomonas mendocina* (MMP)

Per litre: -

3.8 g	Na_2HPO_4
3.3 g	Sodium octanoate
2.65 g	KH_2PO_4
0.5 g	$(NH_4)_2SO_4$
0.4 g	$MgSO_4 \cdot 7\,H_2O$
1.0 ml	Trace elements solution (as for MS medium)

Autoclave $Na_2HPO_4 \cdot 12\,H_2O$, KH_2PO_4 and $(NH_4)_2SO_4$ together in the culture flask. $MgSO_4 \cdot 7\,H_2O$ ($1,000\times$ stock solution) and sodium octanoate are autoclaved separately and added to the growth medium before inoculation. The trace elements solution should be filter sterilised.

3.11.6 SOC Medium

Per litre: -

20.0 g	Tryptone
5.0 g	Yeast extract
0.5 g	NaCl
10.0 ml	250 mM KCl

Adjust the pH of the medium to 7.0 with 5 N NaOH and make up to the final volume. Sterilise by autoclaving and allow to cool. Add 5 ml of sterile 2 M $MgCl_2$ and 20 ml of sterile 1 M glucose.

3.12 Buffers

3.12.1 Inoue transformation buffer

Per litre: -

18.65 g	KCl
10.88 g	$MnCl_2 \cdot 4\,H_2O$
2.20 g	$CaCl_2 \cdot 2\,H_2O$
20 ml	Piperazine-1,2-bis[2-ethanesulfonic acid] (PIPES) (0.5 M, pH 6.7)

Dissolve the components in approx. 800 ml of double-distilled water (ddH_2O). Add PIPES (pH 6.7, 20 ml), then transfer to a measuring cyliner and make up to 1 L with ddH_2O. Sterilise by filtration through a 0.22 μm pore-size cellulose acetate filter. Divide into 20 ml aliquots and store at -20 °C. When needed, individual aliquots should be thawed overnight at 4 °C then transferred to an ice bucket before use.

3.12.2 10× Tris-acetate-EDTA

Running buffer for agarose gel electrophoresis. Dilute the stock solution with deionised water before use.
Per litre: -

48.4 g	Tris(hydroxymethyl)aminomethane (Tris base)
11.4 g	Glacial acetic acid (17.4 M)
3.7 g	EDTA disodium salt

Dissolve all the components in approx. 800 ml of deionised water. Transfer to a measuring cylinder and make up to 1 L with deionised water.

3.12.3 10× Tris-glycine buffer

Running buffer for polyacrylamide gel electrophoresis. Dilute the stock solution with deionised water before use.
Per litre: -

144.13 g	Glycine
30.28 g	Tris(hydroxymethyl)aminomethane (Tris base)
10.0 g	Sodium dodecyl sulphate

Dissolve all the components in approx. 800 ml of ddH_2O. Transfer to a measuring cylinder and make up to 1 L with deionised water.

3.12.4 3× SDS-PAGE sample buffer

Add 1 part sample buffer to 2 parts protein solution to achieve the correct final concentration. β-mercaptoethanol should be added immediately before use to prevent loss

from evaporation.
Per litre: -

240.0 g	Glycerol
60.0 g	Sodium dodecyl sulphate
1.5 g	Bromophenol blue
300 ml	1M Tris solution (pH 6.8, adjusted with HCl)

Dissolve the components and make up to the correct volume with ddH_2O.

3.12.5 Western blotting Anode Buffer I (pH 10.4)

Per litre: -

36.34 g	Tris(hydroxymethyl)aminomethane (Tris base)
100 ml	Methanol

Dissolve the components and make up to 1 L in ddH_2O.

3.12.6 Western blotting anode buffer II (pH 10.4)

Per litre: -

3.03 g	Tris(hydroxymethyl)aminomethane (Tris base)
100 ml	Methanol

Dissolve the components and make up to 1 L in ddH_2O.

3.12.7 Western blotting cathode buffer (pH 9.4)

Per litre: -

3.03 g	Tris(hydroxymethyl)aminomethane (Tris base)
3.0 g	Glycine
100 ml	Methanol

Dissolve the components and make up to 1 L in ddH_2O.

3.12.8 Lysis/binding buffer for protein purification (pH 8.0)

Per litre: -

17.53 g	NaCl
6.72 g	Na_2HPO_4
0.68	Imidazole
0.50 g	6-O-(N-Heptylcarbamoyl)-methyl-α-D-glucopyranoside (Hecameg)
0.41 g	NaH_2PO_4
50 ml	Glycerol

Dissolve the components and make up to 1 L in ddH_2O. Store at 4 °C.

3.12.9 Elution buffer for protein purification (pH 8.0)

Per litre: -

17.53 g	NaCl
6.80 g	Imidazole
6.72 g	Na_2HPO_4
0.50 g	6-O-(N-Heptylcarbamoyl)-methyl-α-D-glucopyranoside (Hecameg)
0.41 g	NaH_2PO_4
50 ml	Glycerol

Dissolve the components and make up to 1 L in ddH_2O. Store at 4 °C.
Note, the only difference between this and the lysis/binding buffer is the concentration of imidazole. The higher concentration in elution buffer increases the competition for binding to Co^{2+} and so displaces the His_6-tagged protein from the column.

3.12.10 Desalting buffer for protein solutions (pH 8.0)

Per litre: -

6.72 g	Na_2HPO_4
0.50 g	6-O-(N-Heptylcarbamoyl)-methyl-α-D-glucopyranoside (Hecameg)
0.41 g	NaH_2PO_4
50 ml	Glycerol

Dissolve the components and make up to 1 L in ddH_2O. Store at 4 °C.

Chapter 4

The Quiescent-cell expression system for PHA synthase production

4.1 Introduction

Currently, most production of PHAs is performed *in vivo* using bacterial hosts.[134] Although it is recognised that *in vitro* production has significant potential to reduce production costs and allow for more convenient fine-tuning of the physical properties of PHAs, a major obstacle to its acceptance as a routine and prevalent production technique is the difficulty of producing large quantities of PHA synthase.[185] Inclusion body formation is a widely known problem in heterologous protein expression by *E. coli*.[11,15,19,232] Furthermore, PHA synthases are particularly prone to aggregation due to a hydrophobic, polymer-binding domain.[64,186]

The technical difficulties associated with PHA synthase purification have also so far prevented the acquisition of a crystal structure for any of the known synthases, and this has frustrated attempts to elucidate the polymerisation mechanism.[233] Therefore, any technique that could increase the yield of soluble PHA synthase could greatly assist the improvement and scale-up of *in vitro* production, and lead to greater understanding of the molecular structure and catalytic mechanism of PHA synthases.

Despite the difficulties involved with PhaC production, little work has been reported on improving the efficiency of the process. When $PhaC_{Re}$ was first purified in 1994, it was established that expression at reduced temperature (typically 30 °C) helps to prevent inclusion body formation, and that addition of a mild non-ionic detergent such as

6-O-(N-heptylcarbamoyl)-methyl-α-D-glucopyranoside (Hecameg) prevents aggregation of the enzyme during and after purification.[108] Some attempts have also been made to re-solubilise inclusion bodies formed by the type II synthases from *Pseudomonas oleovorans* using S-Sepharose[234] and from *P. putida* by denaturing with 6 M guanidine hydrochloride, followed by refolding.[186]

In this chapter, the Quiescent-cell expression system (Q-cells) is investigated as a potential host for improved PHA synthase expression, using PhaC from *R. eutropha* ($PhaC_{Re}$) as a model protein. Q-cells are a modified version of *E. coli* strain W3110, which can be induced to stop dividing and enter a 'quiescent' state in which they remain metabolically active, by the addition of indole. The strain was developed in the laboratory of David Summers (Genetics Department, University of Cambridge) as a product of their work on the control of the cell cycle and plasmid replication in *E. coli*.[235,236] Proof-of-principle experiments have shown Q-cells to produce greater quantities of a human antibody fragment and green fluorescent protein (GFP) than standard W3110 in shake-flask and fermenter cultures.[222,237]

4.1.1 The development of the Quiescent-cell system

The Q-cell system emerged from the work of David Summers' group on the resolution of plasmid dimers in *E. coli*. The multimerisation (most commonly dimerisation) of plasmids through homologous recombination is a well-known phenomenon that leads to plasmid loss. Dimers replicate faster than monomers because they contain two origins of replication.[238] Since increased numbers of replication origins results in fewer copies of the plasmid per cell, the proliferation of dimers can rapidly lead to a complete loss of the plasmid from cells in what is known as the 'dimer catastrophe'.[239]

The antidote to the dimer catastrophe is the resolution of dimers through site-specific recombination to form two separate monomers. The best studied system for plasmid resolution is the Xer/*cer* system of the naturally-occurring ColE1 plasmid in *E. coli*.[238,240] When only monomers are present in the cell, two chromosomally-encoded proteins called XerC and XerD bind to the *cer* site of the plasmid and repress the P_{cer} promoter.[241] The repression is lifted in the presence of plasmid dimers, allowing the transcription from P_{cer} of a 70-nucleotide RNA called Rcd.[242,243]

When Rcd is overexpressed in an *hns*-205 mutant strain, cell growth ceases within 2–3 hours.[235]. The *hns*-205 mutant produces a truncated version of the Histone-like Nucleoid Structuring protein (H-NS), consisting of only the first 93 amino acids out of the usual 137. H-NS is a global gene regulator involved in chromosomal organisation

and packing.[244] Significantly, other *hns* mutations and the full-length protein do not have the same effect.[235]

Realising that it would be beneficial to produce a cell factory that channelled more energy into product formation rather than generation of biomass, the productivity of the new strain was tested by expressing a human antibody fragment, 3PF12.[237] The genes for 3PF12 and a temperature-sensitive repressor, *c*I*ts*857, were both expressed from the same plasmid (pCMT2b-ScFv) while Rcd was expressed from pRcd1. Expression of 3PF12 and Rcd were both controlled by the λ-P_R promoter, so that at 30 °C, *c*I*ts*857 would repress both of their expression. When the culture was shifted to 42 °C, the cessation of growth and the production of 3PF12 were both stimulated. 3PF12 was also fused to a PelB secretion signal peptide, so that the protein was targeted for secretion to the supernatant. Over a 24 hour culture, the new strain remained at an OD_{600} of 20 and produced 150 mg L^{-1} of 3PF12. A control culture without the pRcd1 plasmid reached an OD_{600} of 80, but was unable to produce more than 35 mg L^{-1} of 3PF12.

Microscopic examination revealed that the cells grew to about four times their original length and that the chromosomes were extremely compacted. Therefore, the increased production of 3PF12 in non-growing cells suggested that the compaction of the chromosome resulted in major down-regulation of chromosomal genes, but that production of the plasmid-encoded 3PF12 protein continued. The analogy with eukaryotic cells entering a non-growing but metabolically active 'quiescent' state during the G_0 phase of the cell cycle—in which they specialise in the production of only a few proteins—gave rise to the name Q-cells.

4.1.2 The use of indole to induce quiescence

Rcd has been shown to bind to tryptophanase and to increase its activity.[245] Tryptophanase produces indole by hydrolysis of the amino acid tryptophan in a reaction yielding pyruvate, indole and ammonia (Figure 4.1).[246] Pyruvate is channelled into the TCA cycle, and ammonia is either recycled to produce new amino acids or excreted as a waste product, while indole is not further metabolised.[247] Indole is a bicyclic aromatic hydrocarbon, consisting of a 6-membered benzene ring fused to a 5-membered, nitrogen-containing pyrrole ring. It is known to be produced by over 85 species of Gram-positive and Gram-negative bacteria, and is thought to be an important intracellular and intercellular signalling molecule.[248] Recently, indole was shown to inhibit *E. coli* cell division in response to the accumulation of plasmid dimers, showing that Rcd acts by up-regulating indole production.[245,249]

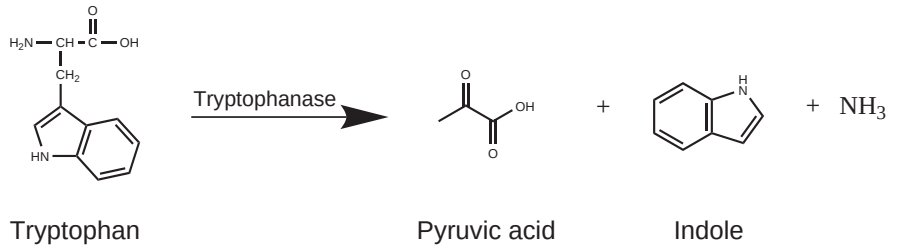

Figure 4.1: Tryptophan catabolism by tryptophanase yields pyruvic acid, indole and ammonia.

Until recently, it was thought that indole transport across the cell membrane required protein influx and efflux pumps. However, it has recently been demonstrated that indole can pass freely across *E. coli* membranes with no transporter protein involvement.[249] Furthermore, Chimerel *et al.* have shown that indole carries protons across the membrane and is thus an ionophore with the ability to equalise the electrical potential across the membrane and therefore to disrupt the proton motive force PMF that is responsible for ATP production.[250] Other ionophores, such as carbonyl cyanide m-chloro phenylhydrazine (CCCP) are known to prevent cell division by the same effect, but do not occur naturally.[251] Ionophores halt cell division by preventing the localisation of divisome proteins such as FtsA, MreB and MinD.[250,252] When dimers have been resolved, Rcd production stops and indole production is reduced. The existing indole can then diffuse into the growth medium, allowing the PMF to be rebuilt so that cell division can continue.

The Rcd-induced Q-cell system suffered from some serious disadvantages: The *hns205* allele was introduced by the insertion of an active Tn*10* transposon, and so is potentially unstable; the requirement for induction of protein expression at 42 °C is not conducive to efficient protein folding or stability; it was necessary to reconstruct the strain for each run to ensure consistent results without loss of either plasmid, and if the Rcd plasmid was lost by a few cells during fermentation they could continue to grow when others had entered quiescence and so return the culture to normal growth. In response to these deficiencies, and with the knowledge that Rcd causes increased indole production, Chih-Chin Chen in her Ph.D. thesis investigated whether it was possible to induce quiescence directly by the addition of indole.[222]

A stable version of the *hns205* allele was created in *E. coli* W3110 by inserting a kanamycin resistance cassette followed by two stop codons after the nucleotides encoding the 93$^{\text{rd}}$ amino acid of H-NS. The new strain, W3110*hns*Δ93, entered quiescence within 4–5 hours when 2.5–3.0 mM indole was added to the growth medium of early-exponential

phase shake-flask cultures.[222] Indole-induced Q-cells remained metabolically active for longer than non-quiescent cells in fed-batch fermenter cultures, as indicated by a continued production of GFP and demand for oxygen for at least 8 hours after entering quiescence. Additionally, Chen showed that analogues of indole including quinoline, isoquinoline, 3-β-indoleacrylic acid and 1-acetylindoline were also able to induce quiescence at similar concentrations, with improved specific productivity of GFP, in shake-flask cultures.[222]

The aim of this chapter is to investigate the ability of the indole-induced Q-cell strain to produce PhaC_{Re}. The previous successes with producing 3PF12 and GFP suggest that more protein should be produced by Q-cells. However, the Q-cell system has not been used with proteins such as PhaC_{Re} that are prone to aggregation, so a primary concern is whether Q-cells can increase the solubility of PhaC_{Re}.

4.2 Bacterial strains and plasmids

Table 4.1 summarises the bacterial strains and plasmids used in this study, and their sources. Full details of strain genotypes are given in Table 3.1.

Table 4.1: Bacterial strains and plasmids for Chapter 4

Strain or plasmid	Purpose for study	Source
Strains		
E. coli W3110*hns*Δ93	*hns*Δ93 to allow quiescence. Used for PhaC_{Re} expression; Kn^{r}	Chen (2010)[222]
E. coli DH5α	Cloning strain used during construction of pASG1$phaC_{\text{Re}}$	Bioline
Plasmids		
pENTRY10	Linearised, dephosphorylated entry vector for StarGate cloning; no promoter; Kn^{r}	IBA (Germany)
pASG-IBAwt1	Destination vector for StarGate cloning; *tet* promoter; Ap^{r}	IBA (germany)
pASG1$phaC_{\text{Re}}$	Expression vector containing PhaC_{Re} with C-terminal His_6-tag; tet promoter; Ap^{r}	This study
pET15$phaC_{\text{Re}}$	Template for PCR of $phaC_{\text{Re}}$	Normi (2005)[223]

4.3 Results

4.3.1 Construction of pASG1*phaC*$_{\mathrm{Re}}$

At the beginning of this project, only pET15*phaC*$_{\mathrm{Re}}$was available for the expression of PhaC$_{\mathrm{Re}}$. pET15*phaC*$_{\mathrm{Re}}$controls the expression of PhaC$_{\mathrm{Re}}$ with the T7 promoter, from bacteriophage T7, which is not recognised by *E. coli* RNA polymerases. Therefore, only strains that have been engineered to express the T7 RNA polymerase are able to express proteins from the T7 promoter. Unfortunately, *E. coli* W3110 does not express the T7 polymerase, so a new plasmid was constructed to make use of a different promoter.

To create plasmid pASG1*phaC*$_{\mathrm{Re}}$ the StarGate cloning system (IBA, Germany) was utilized. The StarGate system is a two-step cloning procedure, in which the sequence of interest is first ligated into an 'entry' vector, before being transferred by recombination into the expression vector. This avoids the need for restriction enzyme digestions.

The *phaC*$_{\mathrm{Re}}$ gene was amplified by PCR using 5′-phosphorylated primers to allow blunt-ended ligation into the dephosphorylated entry vector, pENTRY10. pET15*phaC*$_{\mathrm{Re}}$was used as the template. The primers were also used to add a short combinatorial site to each end of the gene, which when ligated into pENTRY would complete a recombinase recognition target to allow site-specific recombination into the destination vector. The forward primer was:

5′ P-<u>AATG</u>GCGACCGGCAAAGGC 3′

The reverse primer additionally included the sequence for a C-terminal His$_6$-tag for cobalt-affinity purification of the protein. The sequence was:

5′ P-<u>TCCC</u>**GTGGTGGTGGTGGTGGTG**TGCCTTGGCTTTGACGTATCG 3′

where underlined sequences are the combinatorial sites and the bold sequence is the sequence to insert a His$_6$-tag.

PCR, blunt-ended ligation and electrophoresis to check the quality and length of the DNA were carried out as described in Section 3.2. The successful insertion of PhaC$_{\mathrm{Re}}$ into pENTRY10 was verified by sequencing, carried out by Geneservice (Cambridge, UK). The gene was then transferred to the destination vector, pASG-IBAwt1, by site-specific recombination following the manufacturer's instructions. The resulting expression plasmid, pASG1*phaC*$_{\mathrm{Re}}$ was sequenced to confirm the successful insertion of the *phaC*$_{\mathrm{Re}}$ gene, then transformed into *E. coli* W3110*hns*Δ93 for expression studies. pASG1*phaC*$_{\mathrm{Re}}$ confers ampicillin resistance to the expression strain, and uses the *tet*

promoter so that protein production can be induced in any *E. coli* strain by the addition of anhydrotetracycline (AHT).

4.4 $PhaC_{Re}$ expression at 37 °C

To test whether Q-cells could improve the production of soluble $PhaC_{Re}$, a series of experiments was conducted in order to optimise the necessary growth and expression conditions. Q-cells have so far only been tested at 37 °C, which is the optimum growth temperature for *E. coli*. *R. eutropha*, on the other hand, has an optimal growth temperature of 30 °C. Furthermore, it is generally accepted that unstable or difficult-to-express proteins such as $PhaC_{Re}$ are more likely to be properly folded when they are expressed at reduced temperatures.

It is possible that reduced incubation temperature would have an effect on the kinetics of entry into quiescence, and could possibly affect the yield of protein produced. Therefore, Q-cells were first studied under the 'familiar' temperature of 37 °C to compare the growth kinetics and protein production with the expected results based on previous investigators' reports. 37 °C was also used for the initial optimisation of inducer concentration, time of induction, length of expression and concentration of indole. The expectation was then to use the optimised conditions at 30 °C to achieve a further improvement in the solubiity of $PhaC_{Re}$.

4.4.1 Basic analysis of Q-cell performance

The ability to induce quiescence in the W3110*hns*Δ93 strain was verified with and without inducing the expression of $PhaC_{Re}$to provide a baseline growth curve against which the kinetics of production cultures entering quiescence could be compared. Overnight cultures of W3110*hns*Δ93 containing pASG1$phaC_{Re}$ were used to inoculate a starter culture of LB medium (20 ml) and the new culture was grown at 37 °C while shaking at 250 rpm until the OD_{600} was 0.25–0.3. Meanwhile, further fresh LB medium (18 ml) was prepared with or without 3 mM indole, and with or without 0.4 μg ml^{-1} AHT to induce protein expression. Aliquots of the starter culture (2 ml) were used to inoculate the test cultures with cells in the early-exponential growth phase. The test cultures were then incubated as before, and samples were taken at regular intervals for 24 hours for measurement of OD_{600}. Samples were also taken after 24 hours for analysis of total protein production by SDS-PAGE.

Irrespective of AHT addition, cultures with the same indole concentration behaved almost identically (Figure 4.2(A)). Those with 0 mM indole reached a stationary phase

OD_{600} of ~5. When 3 mM indole was added, the cultures stopped growing at an OD_{600} of 0.3–0.4 and followed a growth curve characteristic of entering quiescence, as described previously.[222] Although the final OD_{600} after 24 hours was lower than in previous reports (~0.8), the SDS-PAGE gel of the total protein from the cultures (Figure 4.2 (B)) indicates that substantially more $PhaC_{Re}$ was produced by cultures with 3 mM indole and 0.4 μg ml^{-1} AHT, demonstrating that quiescence was successfully established and that the quiescent cells were capable of producing more $PhaC_{Re}$ than normal cultures. Nevertheless, none of the cultures produced large amounts of $PhaC_{Re}$, illustrating the need to optimise the expression conditions.

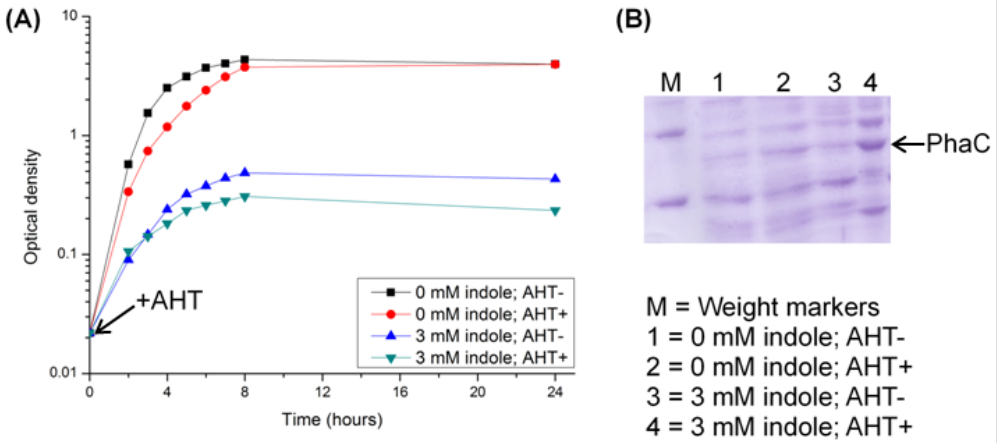

Figure 4.2: Basic analysis of Q-cell performance. To verify that the Q-cell system worked correctly in a new laboratory, cultures with and without 3 mM indole were grown with or without induction with AHT (0.4 μg ml^{-1}). + AHT indicates the time at which AHT was added to the growth medium. (A) Growth curves for the four cultures. (B) SDS-PAGE analysis of total cellular protein from the four cultures showing more $PhaC_{Re}$ in the culture containing 3 mM indole and induced with AHT (lane 4). Sample concentration was normalised for OD_{600}.

4.4.2 Timing of induction

Q-cell cultures have different growth kinetics to the normal, classical, growth curve. Therefore, it is not clear when is the appropriate time to induce the expression of a protein to obtain the maximum yield. Three possible induction times and a negative control were compared: -

i. The time of inoculation ($t = 0$ hours), defined as the time that the starter cultures were subcultured during mid-exponential phase (OD_{600} of 0.25–0.30) to create the test cultures.

ii. The time when standard cultures reached an OD_{600} of 0.8 (~2 hours, $t = 2$ hours), This was identified as the optimal time for induction of W3110*hns*Δ93 expressing $PhaC_{Re}$ from pASG1$phaC_{Re}$based on preliminary experiments (data not shown).

iii. The time that quiescence was fully attained (~8 hours, $t = 8$), defined as the time that growth completely ceased.

iv. No induction.

Cultures were grown according to the standard Q-cell protocol described in Section 3.5.2 for 24 hours, after which the total cell protein and soluble fraction of protein were analysed by SDS-PAGE. Quiescent cultures were inoculated at each of the three times. Standard cultures (no indole) were inoculated either at $t = 0$ or $t = 2$ hours.

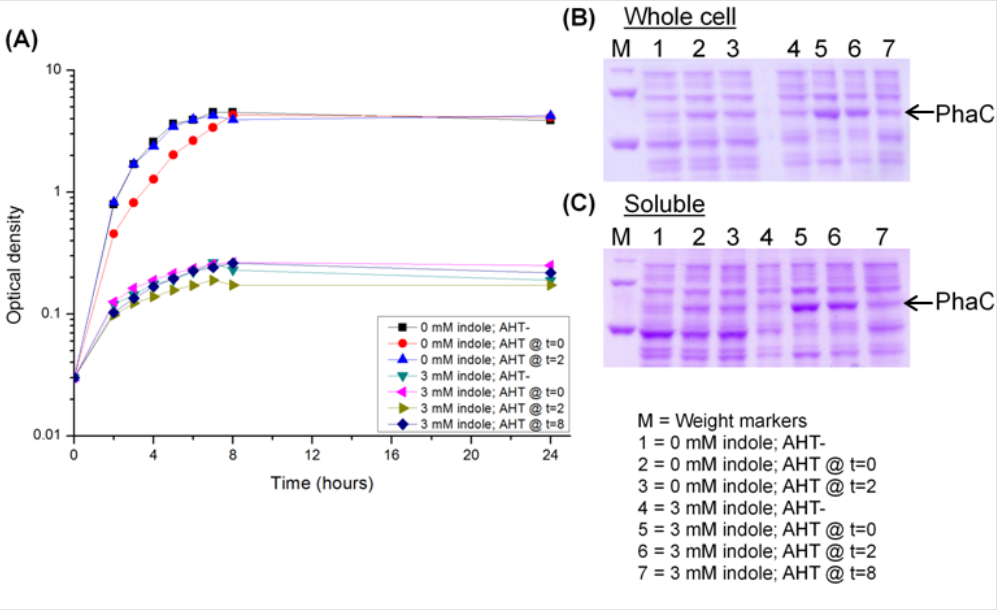

Figure 4.3: Optimisation of the time of protein expression induction. (A) Growth curves, showing time points for protein expression induction. (B) Whole cell protein SDS-PAGE analysis. (C) Soluble protein fraction SDS-PAGE analysis showing high concentration of $PhaC_{Re}$ (lanes 5 & 6).

Protein samples were normalised to the equivalent of a culture with an OD_{600} of 5. Therefore, the intensity of protein bands on the SDS-PAGE gel is indicative of the amount of protein produced per cell in each culture. The timing of induction did not affect the growth kinetics or final OD_{600} of either normal (0 mM indole) or Q-cell (3 mM indole) cultures (Figure 4.3 (A)) The analysis of total cell protein shows some leaky expression of $PhaC_{Re}$ in the absence of AHT for both standard and Q-cell cultures (Figure 4.3 (B)). Only a low level of expression was seen in the standard cultures, with

no difference between protein concentrations for induction at $t = 0$ or $t = 2$ hours. Q-cell cultures induced at $t = 0$ or $t = 2$ hours produced the most $PhaC_{Re}$ per cell (Figure 4.3 (B)). However, when AHT addition was withheld until the culture entered quiescence ($t = 8$ hours), $PhaC_{Re}$ production was severely reduced, suggesting that although Q-cells can produce more protein than standard cultures, the majority of production takes place in the period before quiescence.

The soluble protein fraction showed a very similar pattern to that of total protein (Figure 4.3 (C)). The intensity of $PhaC_{Re}$ bands is similar for total protein and soluble protein, even for the best-performing cultures (lanes 5 and 6); this suggests not only that Q-cells increase $PhaC_{Re}$ production, but that the enzyme remains soluble. Although both $t = 0$ and $t = 2$ hours soluble fractions produced similar amounts of $PhaC_{Re}$ it is more convenient to induce both standard and Q-cell cultures at $t = 0$ hours. Therefore, all subsequent experiments were carried out with the addition of AHT at the time of inoculation.

4.4.3 Length of induction

Chen's results suggested that in shake-flask cultures, Q-cells are not able to maintain their metabolic activity for longer than a few hours after entering quiescence.[222] Therefore, to determine the best length of time to allow for protein expression, cultures were grown for a short (8 hours) or long (24 hours) period, and the accumulation of $PhaC_{Re}$ was tracked by SDS-PAGE. Cultures were grown according to the standard Q-cell protocol described in Section 3.5.2. They were grown for either 8 hours or 24 hours after inoculation and samples were taken at regular intervals for analysis of protein content. The accumulation of soluble protein in samples normalised to the equivalent concentration of a culture with OD_{600} of 5 are shown in Figure 4.4.

Standard cultures produced the maximum amount of $PhaC_{Re}$ after 6–8 hours (Figure 4.4 (A)), while Q-cells took about 10 hours to reach their maximum level (Figure 4.4 (C) and (D)). The maximum quantity of $PhaC_{Re}$ produced by a standard culture in this experiment (after 6 hours) was actually higher than the maximum quantity in Q-cells (after 8 hours; figure 4.4 (C)). For both standard and Q-cell cultures, the amount of soluble $PhaC_{Re}$ reduced after the maximum, suggesting that the protein either begins to aggregate into inclusion bodies or is degraded. This also suggests that the difference in productivity seen in Section 4.4.2 is more due to protein degradation in standard cultures than to increased production in Q-cells.

Interestingly, while standard cultures began to produce large amounts of $PhaC_{Re}$ within 2 hours, the majority of protein production in Q-cells occurred from 6–10 hours. This

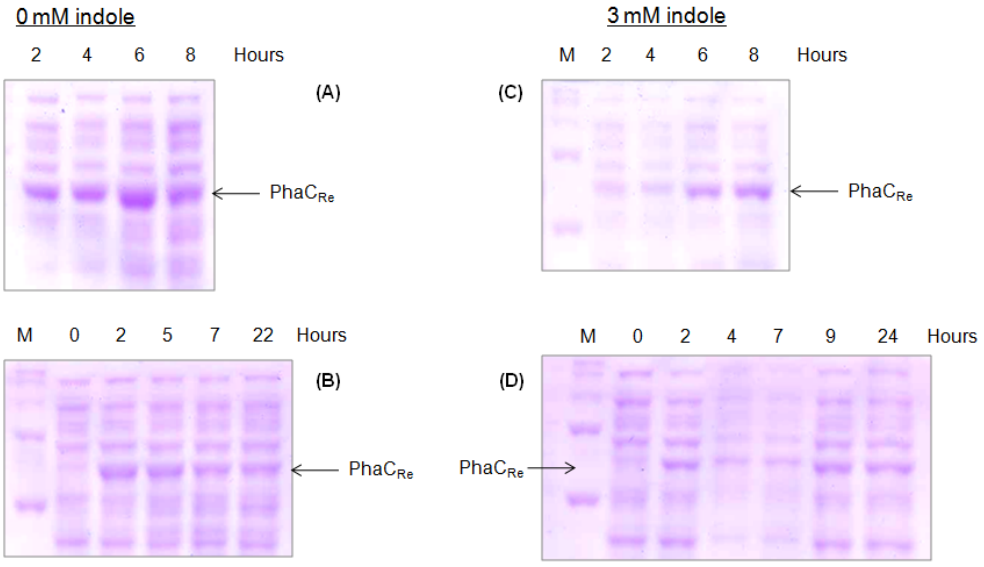

Figure 4.4: SDS-PAGE analyses to test the effects of length of induction. (A) Short and (B) long induction length experiments for cultures with 0 mM indole. (C) Short and (D) long induction length experiments for cultures with 3 mM indole. Note that protein accumulation in Q-cells is not a rapid as for standard cultures, and that total protein levels reduce by 24 hours.

might reflect the transitional period in which cell growth slows down before quiescence is reached. This is corroborated by the finding that the optimum induction strategy was immediate addition of AHT rather than at the point of entering quiescence. Based on these results, the optimal length of induction was determined to be 6 hours for standard cultures and 10 hours for Q-cell cultures.

4.4.4 Concentration of indole

Although the ideal concentration of indole to induce quiescence of W3110*hns*Δ93 was reported by Chen to be 3 mM, strains can behave differently under different growth conditions.[222] The level of protein production was tested for cultures containing 0, 2.0, 2.5 and 3.0 mM indole to determine the optimal concentration under the growth conditions described in this study. Indole concentrations above 3.0 mM result in complete, immediate inhibition of cell growth and consequently destroy the productivity of cultures (Figure 4.5 (A)). The cultures were grown as before, with addition of AHT (0.4 μg ml^{-1}) at time $t = 0$ hours and were incubated for 24 hours after inoculation. Again, productivity was estimated by comparing the intensity of soluble protein bands on an SDS-PAGE gel at the end of the culture.

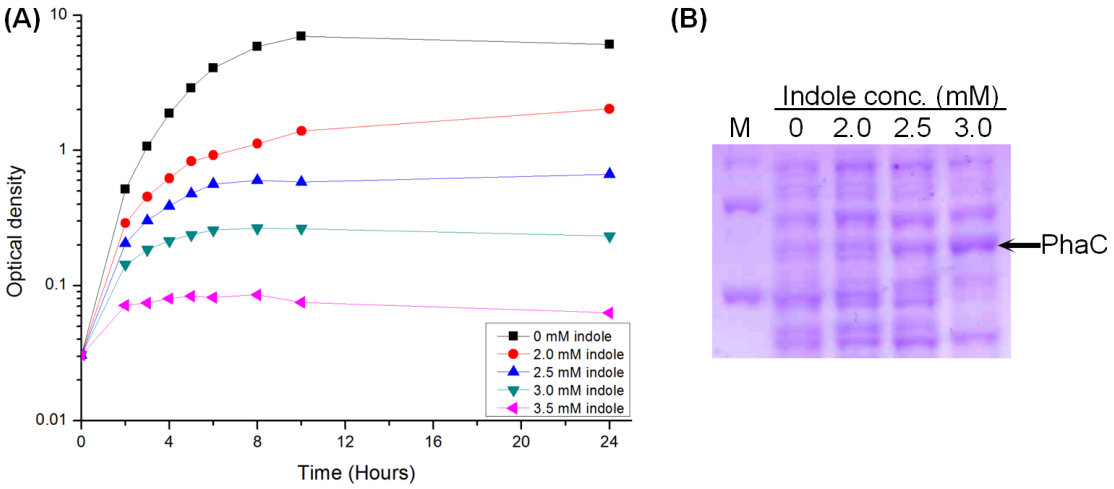

Figure 4.5: Optimisation of indole concentration for Q-cell cultures. (A) Effects of indole concentration on growth curves of W3110*hns*Δ93 containing pASG1*phaC*$_{Re}$. 2.5 and 3.0 mM indole cause cell growth to cease completely. (B) Effects of indole concentration on PhaC$_{Re}$ production in the same cultures. Note that the culture with 3 mM indole produced the most protein when samples were normalised for OD_{600}.

Cell growth was inhibited by all tested concentrations of indole, with the 2.0 mM culture reaching OD_{600}=1.5, the 2.5 mM culture reaching OD_{600}=0.6 and the 3.0 mM culture reaching OD_{600}=0.2, compared to the control culture, which grew to OD_{600}=6 (Figure 4.5 (A)). The shape of the growth curves indicate that the 2 mM culture continued to grow at a slow rate throughout the experiment, but both the 2.5 and 3.0 mM cultures stopped growing after about 6 hours. Although the growth kinetics suggest that the 2.5 mM culture entered quiescence, the soluble protein production per cell was about the same as for the 0 and 2.0 mM cultures (Figure 4.5 (B)). In comparison, the 3.0 mM culture produced more PhaC$_{Re}$ than the other cultures. This indicates that the cells with 2.5 mM indole stopped dividing, but were not able to maintain the same level of metabolic activity as a truly quiescent culture. Therefore, 3 mM was selected as the best indole concentration for further study.

4.4.5 Summary of optimisation at 37 °C

Optimisation of PhaC$_{Re}$ expression conditions was carried out in a semi-quantitative fashion by comparing the intensity of bands on SDS-PAGE gels. Based on these experiments, the best productivity for Q-cells at 37 °C should be expected when cells are:

-

i. grown from early exponential phase with protein production induced at the time of inoculation into indole-containing medium.

ii. grown for 10 hours after inoculation/induction of expression.

iii. grown in medium containing 3 mM indole.

4.5 $PhaC_{Re}$ expression at 30 °C

4.5.1 Effect of density at inoculation on final cell density

One of the primary concerns from the experiments at 37 °C was that cells entered quiescence at a very low cell density. Therefore, even if individual cells produced more protein than their counterparts grown in the absence of indole, the yield of the culture as a whole was reduced. This effect might be more pronounced in cultures grown at 30 °C as they will grow slower than at 37 °C and so might achieve an even lower cell density before entering quiescence. Therefore, a series of quiescent cultures was established using inocula of different optical densities and the growth of each culture at 30 °C was followed by measuring the OD_{600} (Figure 4.6).

An overnight culture of W3110*hns*Δ93 containing pASG1$phaC_{Re}$ was used to inoculate a starter culture (20 ml) as for the standard Q-cell cultivation procedure. The starter culture was grown at 37 °C with shaking at 250 rpm for 4 hours. Starting at 1 hour, the OD_{600} of the starter culture was recorded and a 2 ml aliquot was used to inoculate pre-warmed LB medium containing indole (20 ml final volume), and grown at 30 °C with shaking at 250 rpm. This was repeated every 30 min, so that a total of 7 Q-cell cultures were made. A control with 0 mM indole was also inoculated from the same starter culture after 1 hour. The growth of Q-cell cultures was monitored every hour for at least 8 hours, followed by a final measurement after 24 hours.

The growth rates of all Q-cell cultures were similar, and were much slower than for the 0 mM control (Figure 4.6). All cultures followed the expected growth curve, with a gradual slowing down of optical density increase until growth was halted after 6–8 hours. For the cultures inoculated after 1–2.5 hours growth, higher OD_{600} at inoculation translated to a higher final OD_{600}. 1 or 1.5 hours growth before inoculation resulted in a final OD_{600} of ~0.4, which is similar to that achieved for growth at 37 °C. Notably, after 2.5 hours the density of the inoculum had no further effect on the final OD_{600}, and there appeared to be a threshold of final $OD_{600} \approx 1$, which could not be exceeded.

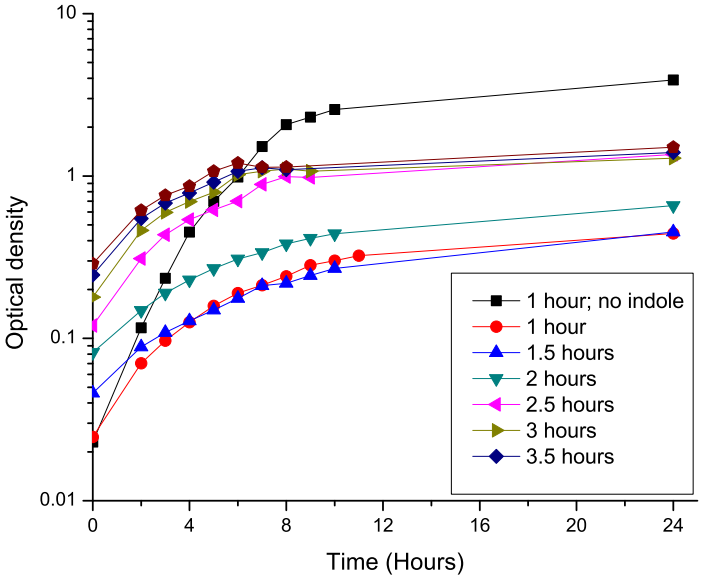

Figure 4.6: Effect of density at inoculation on final density of Q-cell cultures. A starter culture of *E. coli* W3110*hns*Δ93 was grown to stationary phase. Aliquots were taken every 30 minutes to begin Q-cell cultures, whose growth was tracked by measuring OD_{600}. There appears to be an upper limit of $OD_{600} \approx 1$, which Q-cell cultures cannot exceed.

4.5.2 Effect of inoculum density on $PhaC_{Re}$ production

The cultures from Section 4.5.1 were centrifuged to harvest the cells after 24 hours growth. Total protein and soluble protein fractions were prepared and analysed by SDS-PAGE to compare the amounts of $PhaC_{Re}$ produced. As before, the cultures were normalised to the equivalent concentration of a culture at OD_{600}=5. The total $PhaC_{Re}$ production in the earlier cultures was greater than in the later cultures (Figure 4.7). Therefore, although the cell density is very low, 'classical' Q-cell cultures are more productive per cell than those with higher densities. This parallels the finding from Section 4.4.4 that lower concentrations of indole allow slightly higher cell densities to be achieved, but result in lower productivity. Total $PhaC_{Re}$ production reduced as the starting cell density increased, further supporting the hypothesis that the majority of protein production in Q-cells occurs during the period of slow growth before growth stops.

Soluble protein production was similar for all Q-cell cultures, although the increased total production in the 1 and 1.5 hour cultures was reflected by slightly increased soluble

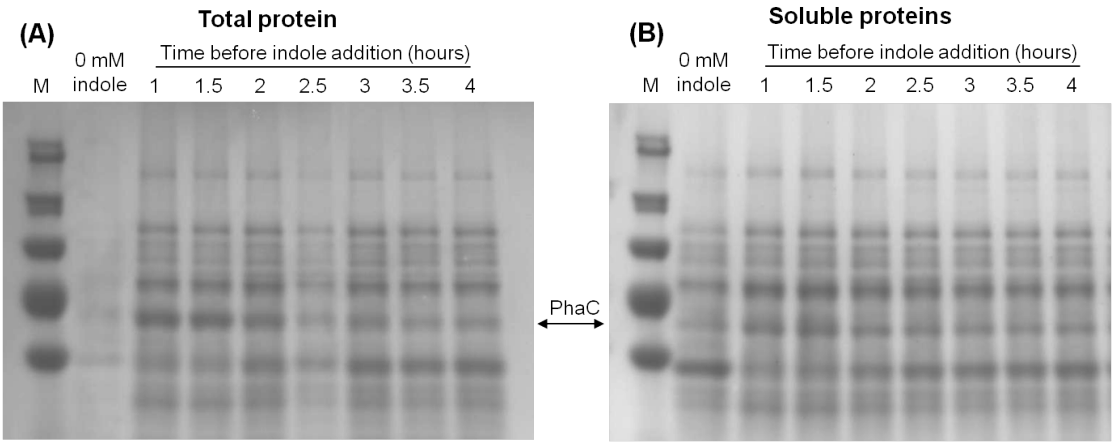

Figure 4.7: Effect of inoculum density on productivity of Q-cell cultures. Total cell protein (A) and soluble protein fraction (B) were analysed by SDS-PAGE. The soluble fractions contained less $PhaC_{Re}$ than the total protein samples, indicating that the majority of $PhaC_{Re}$ was insoluble. Cultures grown from a lower cell density were more productive than those grown from high densiy. M=Molecular weight markers; 0 mM=standard culture control.

protein yields. Q-cells produced more soluble $PhaC_{Re}$ than the control culture, but growth at 30 °C did not improve the yield of soluble protein compared to 37 °C.

4.5.3 Larger-scale $PhaC_{Re}$ production, purification and activity testing

Although some improvements in $PhaC_{Re}$ production were achieved through the optimisation experiments, the amount of protein produced was relatively low for either standard or Q-cell cultures at either 30 or 37 °C. One reason for the low apparent yields could be that Q-cell cultures only reached an OD_{600} of ~0.2. When dealing with small quantities of a dilute culture, it is difficult to maintain the correct dilution factor, as small quantities of left-over supernatant or accidental loss of some cell mass can make a significant difference to the proportion remaining.

To gain a better insight into the performance of Q-cells for $PhaC_{Re}$ production, the optimised growth protocol was scaled up to 100 ml cultures in 500 ml Sakaguchi flasks. A pre-culture (40 ml) of W3110*hns*Δ93 containing pASG1*phaC*$_{Re}$ was grown to an OD_{600} of 2.5 as described before. Half was used to inoculate a flask of LB medium containing 0 mM indole, and the other half was used for a culture containing 3.0 mM indole. Cultures were grown at 37 °C, shaking at 180 rpm on a reciprocal shaking platform. Both contained kanamycin (30 μg ml^{-1}) and ampicillin (100 μg ml^{-1}). The 0 mM culture was induced with AHT (0.4 μg ml^{-1}) when the OD_{600} reached 0.6, and

was then incubated for a further 6 hours before harvesting by centrifugation at 6000×g for 10 minutes. The cell pellet was stored at −80 °C until purification. The 3 mM culture was incubated for 10 hours after inoculation before harvesting.

$PhaC_{Re}$ was purified by Co^{2+}-affinity chromatography. Each elution fraction was analysed by SDS-PAGE (Figure 4.8 (A,B)) This confirmed that only very low amounts of $PhaC_{Re}$ were produced. Insoluble proteins that were pelleted after sonication to disrupt the cells were analysed on the same gel, and a large band corresponding to the expected size of $PhaC_{Re}$ was visible for both standard and Q-cell cultures. This suggests that the majority of the protein was accumulated as inclusion bodies. The protein concentration of each fraction was estimated by measuring the absorbance at 280 nm, but was too low to perform an assay of the activity (data not shown).

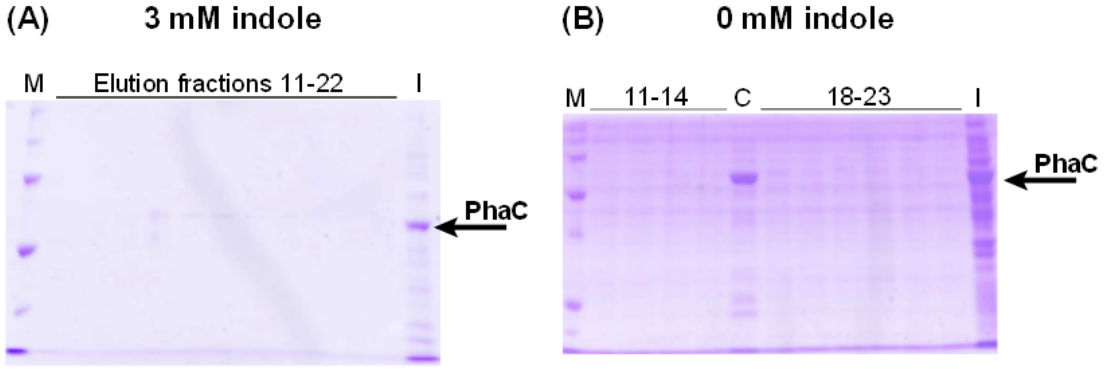

Figure 4.8: Purification of $PhaC_{Re}$ produced in Q-cells. (A) Elution fractions for His_6-purified $PhaC_{Re}$ from cultures grown with 3 mM indole. (B) Elution fractions for His_6-purified $PhaC_{Re}$ from cultures grown with 0 mM indole. M=Molecular weight markers; C=Combined fractions 15–17 with the highest concentrations of $PhaC_{Re}$; I=Insoluble fraction from lysed cells.

4.5.4 Protein solubility check

Although the results in Section 4.4.2 suggested that Q-cells might produce more $PhaC_{Re}$ in the soluble fraction than standard cultures, this result was not repeated in the later experiments. As explained previously, it is difficult to achieve the correct dilution factor with very small volume samples. Therefore, the result from the larger scale culture that most $PhaC_{Re}$ produced in Q-cells at 37 °C is insoluble was verified by growing a 20 ml culture with 0 or 3 mM indole, and with or without induction by AHT, without taking samples at intermediate times. The cultures were grown for 6 hours or 10 hours post-induction according to the optimised parameters.

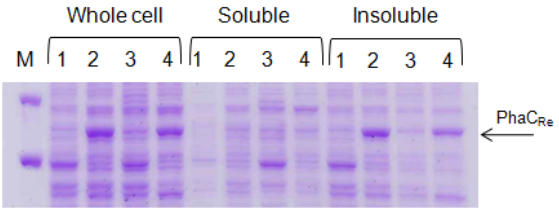

Figure 4.9: Verification of the finding that the majority of PhaC$_{Re}$ produced in Q-cells is present in the insoluble protein fraction. Note that similar levels of soluble protein are produced whether indole is present or not. For each fraction, lane 1 is 0 mM indole, −AHT; lane 2 is 0 mM indole, +AHT; lane 3 is 3 mM indole, −AHT; lane 4 is 3 mM indole, +AHT.

The entire volume was then processed to separate the soluble and insoluble fractions, which were analysed by SDS-PAGE. Only a small fraction of the PhaC$_{Re}$ was soluble (Figure 4.9). Furthermore, the bands corresponding to the soluble fraction for both 0 mM and 3 mM cultures are of equal intensity whether AHT was added or not. This indicates that some leaky expression occurred and suggests that the increased rate of protein synthesis post-induction plays a part in causing PhaC$_{Re}$to become insoluble. As before, the majority of the PhaC$_{Re}$ was insoluble as indicated by the almost equal intensity of bands corresponding to total cell protein and insoluble protein for standard or Q-cell cultures.

4.6 Discussion

Most of the previous research involving Q-cells has been carried out in Dr. Summers' laboratory (Genetics Department, Cambridge), in which it was developed. Therefore, it was encouraging to confirm that W3110*hns*Δ93 entered quiescence under the same conditions, in two different laboratories, with different equipment. Much of the experimental work for this chapter was completed in the laboratory of Dr. Takeharu Tsuge at the Toyko Institute of Technology, Tokyo, Japan during a visiting student placement from September–December 2010. This includes preliminary studies and all of the characterisation of growth at 37 °C. The growth at 30 °C was carried out in Cambridge.

Quiescence was generally maintained at a lower cell density (OD_{600}=0.4–0.5) using baffled Erlenmeyer flasks in the laboratory in Tokyo than using flasks without baffles in either laboratory in Cambridge (OD_{600}=0.7–0.8). It is difficult to say whether the reduced OD_{600} was due to a slower initial growth rate or to the establishment of quiescence at an earlier time because growth slows gradually before ceasing. Therefore, there is no

definitive point at which entry to quiescence can be defined. Since the largest difference between culture conditions in Tokyo and Cambridge was the presence of baffles—and therefore better aeration—it would be interesting to investigate further the effect of aeration on entry into quiescence.

In this study, the initial results suggested that $PhaC_{Re}$ produced in Q-cells was mainly in the soluble fraction (Figure 4.2). This supported the hypothesis that quiescent cultures devote more resources to protein production than do standard cultures, and that they are therefore better equipped to assist the folding of nascent proteins. However, the later studies reported here were unable to replicate these results. Therefore, it seems likely that some contamination of the soluble fraction occurred or that the difficulty of handling small-volume samples led to inaccuracies in the amount of protein loaded onto the gel.

Q-cells produce more $PhaC_{Re}$ per cell, as demonstrated by the total cell protein samples in figures 4.2 and 4.3 in which the sample OD_{600} was normalised. However, when comparing the soluble fractions in figure 4.9 the concentrations are roughly equal. This suggests that the cells are already solubilising as much $PhaC_{Re}$ as possible, and that any extra can only enter into the insoluble fraction. Another possibility is that proteases present in the W3110 strain of *E. coli* but absent from BL21(DE3) were able to degrade most of the soluble $PhaC_{Re}$ following cell lysis. This would further reduce the yield compared to production under standard conditions, and explains the very low specific activities as well as the lower molecular weight bands on SDS-PAGE gels. Further investigation is necessary to confirm this hypothesis. However, the problem could be easily overcome through the use of commercially-available protease inhibitor cocktails.

A more significant problem is that although Q-cells produced larger quantities of $PhaC_{Re}$, the productivity in all (standard and quiescent) cultures was low compared to other reports, particularly those seen from pET15$phaC_{Re}$ in BL21(DE3) in Chapter 5. This suggests a problem with plasmid pASG1$phaC_{Re}$ or with the expression conditions. The sequence of the plasmid was verified to be as intended, and attempts were made to optimise the expression conditions at 37 and 30 °C, as described above so these are unlikely to be resposible for the low yields.

The crucial difference is probably that pASG1$phaC_{Re}$ expresses $PhaC_{Re}$ with a C-terminal His_6-tag, and pET15$phaC_{Re}$ expresses an N-terminally tagged version. Although it was not realised during the design of pASG1$phaC_{Re}$, the modification of $PhaC_{Re}$ at the C-terminal affects its folding and reduces the activity.[253] Improperly folded $PhaC_{Re}$ is more likely to be degraded within the cell, so this could explain the low yields. If this is the case, expression of $PhaC_{Re}$ with an N-terminal His_6-tag in Q-cells should result in higher yields and may give a more reliable indication of their ability to

increase $PhaC_{Re}$ yields. This was not attempted due to the problems of low cell density and inclusion body formation that also need to be resolved.

The final cell densities of Q-cell cultures in this study were lower than those reported by Chen (0.2–0.6 here compared to ~0.8).[222] Therefore, even with the increased production of $PhaC_{Re}$, the overall productivity of Q-cells was lower than standard cultures. Whereas Chen always used an initial OD_{600} of 0.2–0.3 to inoculate Q-cell cultures, here the final OD_{600} could be controlled to a certain extent by varying the OD_{600} of the inoculum. There appeared to be a limit of $OD_{600}\approx1.0$ that Q-cell cultures could not exceed. Hannah Gaimster (Summers laboratory, Dept. of Genetics, Cambridge) has measured a spike of indole production by wild-type *E. coli* cultures at $OD_{600}\approx1.0$ that might be responsible for initiating the transition from exponential to stationary growth phase (personal communication). Therefore, the Q-cell cultures might produce additional indole at this point, accelerating their entry into quiescence.

Higher density Q-cell cultures were also slightly less productive on a per cell basis than low density cultures. This might be due to nutrient limitation in the higher density cultures. Chen reported better Q-cell productivity in fed-batch cultures than shake flask cultures.[222] Therefore, the use of more nutritious growth medium and scale-up of the cultures to the fermentor scale might also result in increased productivity and better control of final cell density.

Overall, it can be concluded that Q-cells are capable of producing larger quantities of $PhaC_{Re}$ than conventionally-grown cells, and represent a robust protein expression system that can be easily used by different laboratories. However, although each cell in a culture produces more $PhaC_{Re}$, the cell densities are lower, meaning that the overall yield of protein per culture is reduced compared to standard cultures. Combined with the loss of a substantial proportion of the protein in the insoluble fraction, and possible degradation by proteases, the current indication is that Q-cells are not a good production system for $PhaC_{Re}$.

The problems might be relieved by use of a different expression plasmid, production of an N-terminally His_6-tagged $PhaC_{Re}$, use of richer growth medium or a fed-batch protocol, and scale-up to fermentor cultures. However, these might only increase the yield of total protein, and there was no indication that $PhaC_{Re}$ solubility was improved by Q-cells. Therefore, it was decided not to pursue further the investigations into Q-cells as a protein expression platform. Chapter 5 will describe work that was conducted subsequent to the Q-cell study, in which an attempt is made to increase the proportion of $PhaC_{Re}$ that is solubilised, through the co-expression of chaperone proteins.

Chapter 5

Efficient production of active polyhydroxyalkanoate synthase in *E. coli* by co-expression of molecular chaperones

5.1 Introduction

In Chapter 4, the Q-cell system was investigated as a means to improve the production of PhaC. Although the specific productivity of individual cells may have been improved, the yield from Q-cell cultures was not better than standard cultures. Furthermore, Q-cells suffered from the problem of inclusion body formation, which drastically reduced the yield of active enzyme.

Inclusion body formation is a well-known phenomenon in heterologous protein production, particularly in *E. coli*.[19] Many methods to combat the problem have been suggested, including reducing the concentration of protein by modulating inducer quantities, expression at reduced temperatures ($\leq$30 °C), use of specialized 'folding' strains such as *E. coli* Origami, and *in vitro* refolding of proteins from isolated inclusion bodies.[254,255] However, these techniques increase the time required to obtain active protein and suffer from drawbacks including reduced protein yield and high cost.

Most bacterial proteins are assisted to fold correctly by one or more chaperone proteins.[255,256] These form a diverse family, many of which belong to the group of heat shock proteins. Chaperone production is up-regulated when the cell is under stress in order to maintain correct folding of proteins, and to target mis-folded proteins for

degradation. It is thought that when heterologous proteins are overexpressed, the increased number of protein molecules could overwhelm the native chaperone provision resulting in an accumulation of badly folded proteins. Therefore, a widely used technique to aid production of biologically active heterologous proteins is simultaneously to overexpress one or more chaperone proteins.[257] This has been used with success, particularly for eukaryotic or membrane-bound proteins (reviewed by Schlieker[258]) although the appropriate expression conditions must usually be determined experimentally on a case-by-case basis.

The co-expression of chaperones has not previously been tested in the general area of PHA research. This chapter presents the results of an investigation into chaperone-assisted $PhaC_{Re}$ expression and PHB production. Three chaperone systems were chosen for co-expression with $PhaC_{Re}$ trigger factor (abbreviated Tf; plasmid pTf16), GroEL/-GroES (plasmid pGro7) and DnaK/DnaJ/GrpE (plasmid pKJE7).[259,260] Additionally, Tf and GroEL/GroES were expressed together (plasmid G-Tf2), as were GroEL/GroES and DnaK/DnaJ/GrpE (plasmid pG-KJE8).

Trigger factor is a monomeric 56 kDa protein composed of three domains.[261,262] The N-terminal domain mediates binding to the exit tunnel of the ribosomal 50S subunit, the middle section forms a peptidyl-prolyl *cis/trans* isomerase (PPI) domain, and the C-terminal domain is responsible for mediating binding to the target peptide and the majority of the chaperone activity.[262] The PPI domain has been shown to be active *in vitro*.[261,263] PPI enzymes catalyse the rotation of the peptide bond preceding a proline residue from the *trans* to the *cis* position. This is a slow but necessary process for the correct folding of many proteins.

Although the PPI domain is active, it is not necessary for the activity of Tf.[264] The mechanism action is therefore thought to rely on the binding of the C-terminal domain to nascent peptides (Figure 5.1).[256,262] Through the N-terminal domain, the protein binds to the exit tunnel of the ribosome and scans the emerging protein chain as it is produced. Tf binds to hydrophobic residues, shielding them from the aqueous environment of the cytoplasm and preventing them from interacting with other residues in the same or nearby proteins. The chaperone activity of Tf is not thought to be an active process, as it does not bind ATP.[262] Therefore, Tf probably holds the protein in an unfolded or semi-folded state until the entire polypeptide has been released from the ribosome, and then either unbinds to allow the protein to fold spontaneously or passes it to another chaperone system.[260]

DnaK operates in a similar way to Tf, but requires the presence of two co-chaperones (DnaJ and GrpE) and is able to hydrolyse ATP to drive the folding of proteins.[259] DnaK is a monomeric heat-shock protein with a molecular weight of 70 kDa and is

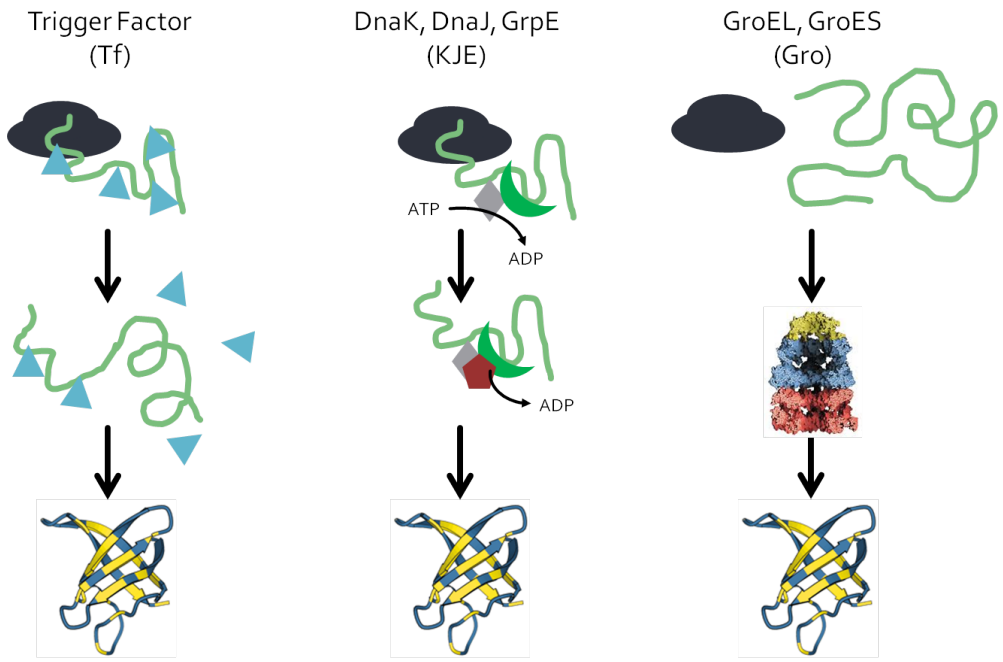

Figure 5.1: The mechanisms of action of the three chaperone protein systems used in this chapter, Trigger Factor, DnaK/DnaJ/GrpE and GroEL/GroES. Please see the main text for a full explanation of the mechanisms.

related to the eukaryotic Hsp70 protein. Rather than being a PPIase, DnaK has the similar but more general function of secondary amide peptide bond *cis*/*trans* isomerase (API; that is, it accelerates the *cis*/*trans* isomerisation of non-prolyl peptide bonds.) [265] DnaK also posseses a N-terminal ATPase domain, which is used to regulate the binding to peptides at the C-terminal. When ATP is bound, DnaK binds only transiently to hydrophobic domains of nascent proteins. In the ADP-bound state, the binding affinity is increased. [256]

The co-chaperone DnaJ also has the ability to bind to unfolded peptides and may be able to hold them in an unfolded conformation in a similar way to Tf. [266] Additionally, DnaJ increases the ATPase activity of DnaK. [267] Unlike Tf, neither DnaJ nor DnaK bind directly to the ribosome. The catalytic cycle of the DnaK/DnaJ/GrpE system begins with the binding of DnaJ to a nascent polypeptide as it exits the ribosome (Figure 5.1. DnaK-ATP also transiently binds. The interaction between DnaJ and DnaK-ATP results in hydrolysis of the ATP, and allows the transfer of the peptide chain from DnaJ to DnaK-ADP. GrpE then mediates the exchange of ADP for ATP, causing dissociation of DnaK. An individual protein can go through many rounds of DnaK binding and unbinding before reaching its fully folded conformation.

The GroEL/GroES complex (also known as the chaperonins) operates by a different but complementary mechanism to Tf and DnaK.[259] The chaperonin is composed of two heptameric rings of GroEL, joined back-to-back to form a barrel structure with two compartments.[268] One of these compartments is capped by a heptameric ring of the co-chaperonin GroES, which serves as a lid. The ring on the same side as the GroES cap is known as the *cis* ring, while that on the opposite site is termed the *trans* ring. The GroEL protein itself is a 58 kDa heat-shock protein analogous to the eukaryotic Hsp60. It is composed of three domains termed the apical, intermediate and equatorial domains.[268] The equatorial domain contains an ATP binding site. The 10 kDa GroES protein has a single domain, from which a flexible loop extends and attaches to GroEL to form a hinge.

The substrates for the chaperonin complex are partly folded and badly folded protein chains that have already detached from the ribosome.[255] The substrates may have already been acted upon by other chaperone systems such as Tf and DnaK. The mechanism of action for the chaperonin involves repeated cycles of proteins entering the cavity of the *cis* ring, conformational changes in GroEL and protein release, all driven by ATP hydrolysis.[269] The apical domains of the *cis* ring of GroEL contains many exposed hydrophobic residues, which interact with hydrophobic residues on the misfolded protein, and allow the protein to enter the central chamber. ATP then binds to the equatorial domain. This is necessary to allow the GroES cap to bind on top of the *cis* ring, so encapsulating the substrate protein and shielding it from the hydrophilic surroundings(Figure 5.1. GroES binding induces a conformational change in the *cis* ring, which increases the internal volume two-fold. ATP is then hydrolysed, providing energy for the unfolding and reorganisation of the substrate. Finally, ATP binds to the *trans* ring and is hydrolysed to drive the release of GroES and the ejection of the substrate. The current *trans* ring then becomes the substrate-binding (*cis*) ring for the next cycle.

The size of the internal cavity of GroEL limits the size of proteins that can be accomodated to a maximum of ~60 kDa.[255] However, GroEL is still capable of binding and assisting the folding of larger proteins.[270] It is thought that rather than the whole protein, only some misfolded domains are accommodated by the GroEL chamber, and that over many cycles the substrate eventually reaches the correct conformation. In this case, GroES binding and ATP hydrolysis are still necessary to drive the appropriate conformational changes, but they occur on the *trans* ring rather than the *cis* ring.[270] This may be significant for the folding of $PhaC_{Re}$, which has a molecular weight of 67 kDa when a His_6-tag is attached.

5.2 Bacterial strains and plasmids

Table 5.1 summarises the bacterial strains and plasmids used in this chapter. *E. coli* BL21(DE3) and W3110*hns*Δ93 were used as expression strains for pET15*phaC*$_{Re}$ and pASG1*phaC*$_{Re}$, respectively. Plasmids pGro7, pTf16, pG-Tf2, pKJE7 and pG-KJE8 were used in combination with the *phaC*$_{Re}$ expression plasmids to co-express a variety of chaperone proteins. Please see Table 3.1 for full details of strain genotypes.

Table 5.1: Bacterial strains and plasmids for Chapter 5

Strain or plasmid	Purpose for study	Source
Strains		
E. coli BL21(DE3)	Expression strain for production of PhaC$_{Re}$ from pET15*phaC*$_{Re}$	Novagen, USA
E. coli W3110*hns*Δ93	Expression strain for production of PhaC$_{Re}$ from pASG1*phaC*$_{Re}$ and PHB; Kn^r	Chen (2010) [222]
Plasmids		
pET15*phaC*$_{Re}$	Expression vector containing PhaC$_{Re}$ with N-terminal His$_6$-tag; T7 promoter; Ap^r	Normi (2005) [223]
pASG1*phaC*$_{Re}$	Expression vector containing PhaC$_{Re}$ with C-terminal His$_6$-tag; *tet* promoter; Ap^r	Chapter 4
pGro7	Expression vector for GroEL/GroES; *araB* promoter; Cm^r	Clontech, USA
pTf16	Expression vector for Tf; *araB* promoter; Cm^r	Clontech, USA
pG-Tf2	Expression vector for GroEL/GroES/Tf; *pzt1* promoter; Cm^r	Clontech, USA
pKJE7	Expression vector for DnaK/DnaJ/GrpE; *araB* promoter; Cm^r	Clontech, USA
pG-KJE8	Expression vector for GroEL/GroES with *pzt1* promoter; DnaK, DnaJ, GrpE with *araB* promoter; Cm^r	Clontech,USA
pTrc*phaCAB*	Expression vector containing *phaCAB* operon; *trc* promoter; Ap^r	Kahar (2005) [224]

5.3 Results

5.3.1 Production and purification of PhaC$_{Re}$

To test the productivity and activity of PhaC$_{Re}$ with or without co-expression of chaperone proteins, both the N- and C-terminally tagged proteins were purified from 200 ml shake flask cultures by cobalt-affinity chromatography (Section 3.6.3). Growth of each culture was quantified by measuring the average final OD$_{600}$ (Table 5.2). Growth was not affected by expression of GroEL/GroES (pGro7) or Tf (pTf16), but was substantially

reduced by expression of GroEL/GroES/Tf (pG-Tf2), DnaK/DnaJ/GrpE (pKJE7) and GroEL/GroES/DnaK/DnaJ/GrpE (pG-KJE8).

Table 5.2: The effect of chaperone co-expression on yields of soluble $PhaC_{Re}$

Plasmid content	**Chaperones expressed**	**Final OD_{600}[1]**	**Protein recovered (mg L^{-1})**	**Specific productivity (mg L^{-1} OD^{-1})**
N-terminal His_6-tag				
pET15*phaC*$_{Re}$ only	-	4.77	14.55	3.55
pGro7	GroEL/GroES	4.89	44.37	9.99
pTf16	Tf	4.73	36.14	8.20
pG-Tf2	GroEL/GroES/Tf	0.74	13.44	23.13
pKJE7	DnaK/DnaJ/GrpE	1.65	10.10	7.10
pG-KJE8	GroEL/GroES/ DnaK/DnaJ/GrpE	2.00	15.84	8.71
C-terminal His_6-tag				
pASG1*phaC*$_{Re}$ only	-	5.17	1.77	0.32
pGro7	GroEL/GroES	5.20	13.40	2.57
pTf16	Tf	4.93	17.67	3.58
pG-Tf2	GroEL/GroES/Tf	0.48	8.00	16.70
pKJE7	DnaK/DnaJ/GrpE	1.38	1.68	1.22
pG-KJE8	GroEL/GroES/ DnaK/DnaJ/GrpE	3.49	10.35	2.78

All values are averages of 3 cultures
[1]Optical density measured at 600 nm immediately before harvesting cells

Table 5.2 also shows the average amount of soluble $PhaC_{Re}$ recovered per litre of bacterial culture. The N-terminal His_6-tag version of $PhaC_{Re}$ (pET15*phaC*$_{Re}$) was recovered in much larger quantities than the C-terminal His_6-tag version (pASG1$PhaC_{Re}$). Within the set of strains expressing the N-terminal His_6-tag version, co-expression of GroEL/GroES or Tf resulted in approximately 3-fold increases in soluble protein with 44.37 mg L^{-1} and 36.14 mg L^{-1} respectively, compared to 14.55 mg L^{-1} for $PhaC_{Re}$ alone. The other chaperone systems resulted in either a small increase (GroEL/GroES/DnaK/DnaJ/GrpE) or a small decrease (GroEL/GroES/Tf and DnaK/DnaJ/GrpE) compared to the control.

A similar pattern was seen for the set of C-terminal tagged $PhaC_{Re}$ strains. While substantially less C-terminal tagged protein was recovered, the fold increases in recovered protein were larger. GroEL/GroES (13.40 mg L^{-1}) and Tf (17.67 mg L^{-1}) resulted in 8 to 10-fold increases compared to the control (1.77 mg L^{-1}). GroEL/GroES/Tf and GroEL/GroES/DnaK/DnaJ/GrpE co-expression resulted in 5 to 6-fold increases to 8.00 mg L^{-1} and 10.35 mg L^{-1} respectively.

To allow for the differences in final culture density, the specific productivity of $PhaC_{Re}$ (mg protein per litre per OD_{600} unit) was also calculated (Table 5.2). This confirms that the production of $PhaC_{Re}$ is far more efficient with an N-terminal His_6-tag (3.55 mg L^{-1} OD^{-1}) than a C-terminal His_6-tag (0.32 mg L^{-1} OD^{-1}). Interestingly, despite causing a serious reduction in growth, co-expression with GroEL/GroES/Tf resulted in by far the largest specific productivity for both N-terminal (23.13 mg L^{-1} OD^{-1}) and C-terminal (16.70 mg L^{-1} OD^{-1}) tagged synthase.

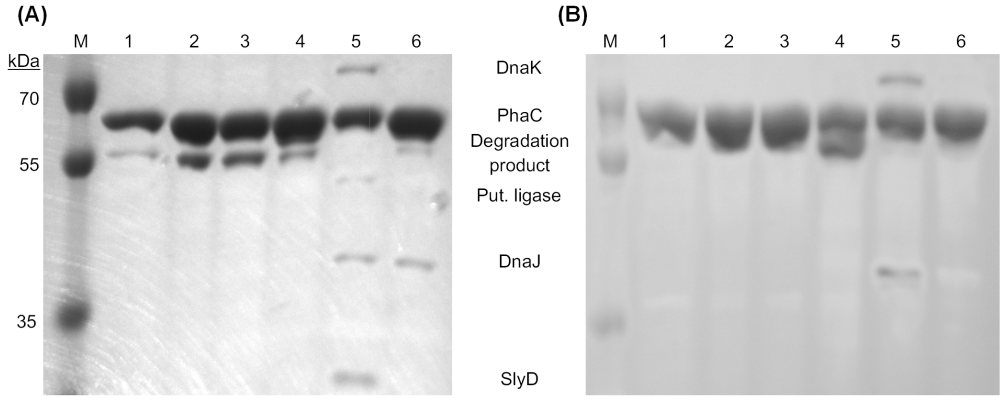

Figure 5.2: SDS-PAGE gels stained with Coomassie blue, showing $PhaC_{Re}$ purified by cobalt-affinity chromatography after expression in (A) BL21(DE3)/pET15$phaC_{Re}$ or (B) BL21(DE3)/pASG1$phaC_{Re}$ with and without chaperone protein co-expression. Bands were identified by digestion with trypsin followed by GC-MS fingerprinting. M=prestained molecular weight markers, lane 1=$PhaC_{Re}$ only, lanes 2 to 6 follow co-expression with pGro7, pTf16, pG-Tf2, pKJE7 and pG-KJE8 respectively.

Samples (approx 1.2 μg) of purified protein expressed from either pET15$phaC_{Re}$ or pASG1$phaC_{Re}$ with or without the co-expression of chaperones, were electrophoresed through a 10% polyacrylamide gel (Figure 5.2). Individual protein bands were excised and identified by trypsin digestion followed by mass spectrometry to produce a protein fingerprint. The major band in each sample was identified as $PhaC_{Re}$. Additional bands were observed, particularly in the samples with co-expression of DnaK/DnaJ/-GrpE. The most abundant of these was a ~56 kDa digestion product of $PhaC_{Re}$ which most likely resulted from cleavage between 90 and 100 amino acids from the end of the protein. Low concentrations of the DnaK and DnaJ chaperones were also detected in the samples where they were overexpressed. Two additional proteins, which were identified as a putative ligase and SlyD (a peptidyl-prolyl *cis/trans* isomerase similar to Trigger Factor), were detected in samples of $PhaC_{Re}$ expressed from pASG1$phaC_{Re}$ but not in samples from pET15$phaC_{Re}$.

5.3.2 The effect of chaperones on $PhaC_{Re}$ solubility

To find out whether the increased yield of soluble $PhaC_{Re}$ when co-expressed with chaperones was due to a net increase in $PhaC_{Re}$ synthesis or to an increase in the proportion of soluble protein, soluble and insoluble protein fractions from cells containing pET15$phaC_{Re}$ alone, or with each of the chaperone systems, were compared by SDS-PAGE. Because DnaK (70 kDa), GroEL (58 kDa) and Trigger factor (56 kDa) are all of a similar size to $PhaC_{Re}$ they could obscure the $PhaC_{Re}$ band on a SDS-PAGE gel. Therefore, the $PhaC_{Re}$ was selectively visualized by western blotting (Figure 5.3). The loading volume in each lane was normalized according to OD_{600}.

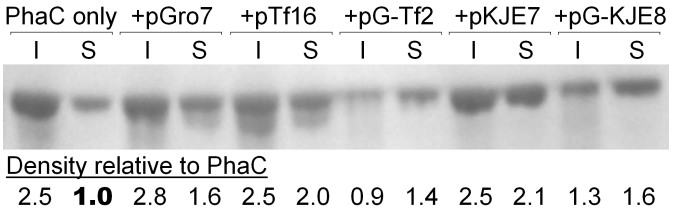

Figure 5.3: The distribution of $PhaC_{Re}$ between the insoluble (I) and soluble (S) protein fractions. $PhaC_{Re}$ was expressed from BL21 (DE3)/pET15$phaC_{Re}$ on its own or co-expressed with chaperone proteins. The relative densities were calculated using ImageJ software, and are relative to the soluble fraction of $PhaC_{Re}$ alone (bold). pGro7=GroEL/GroES, pTf16=Tf, pG-Tf2=GroEL/GroES/Tf, pKJE7=DnaK/DnaJ/GrpE, pG-KJE8=GroEL/GroES/DnaK/DnaJ/GrpE.

With the exception of protein from cells expressing GroEL/GroES/Tf, which grew very poorly making recovery of protein difficult, the intensity of the bands for each insoluble fraction was similar (ranging from 1.3–2.8× the intensity of the soluble control). However, the intensity of the bands for the soluble fractions increased when chaperone proteins were co-expressed. The two best performing systems from the purification experiment, GroEL/GroES and Tf, had 1.6- and 2.0-fold,more soluble $PhaC_{Re}$ than the control. These figures are smaller than the relative increases in soluble protein recovered during protein purification, possibly because antibody binding was inhibited by the large quantities of chaperone proteins present in the western blots. Therefore, these results should be considered only as a semi-quantitative indication of the relative amounts of $PhaC_{Re}$ in each fraction. As such, they suggest that chaperones successfully increased both the total amount of protein produced, and its solubility, although substantial amounts of protein remained in the insoluble fraction.

5.3.3 The influence of chaperone co-expression on PhaC activity

To calculate the specific activity of our $PhaC_{Re}$ preparations, the total yield of $PhaC_{Re}$ protein from each 200 ml culture was calculated from the final volume and concentration of purified protein solution after desalting. Activity assays were performed in triplicate for each sample by measuring the decrease in absorbance at 236 nm, corresponding to the 3HB-CoA thioester bond that is broken during polymerization. Analyses for statistical significance were performed using two-tailed T-tests assuming unequal sample variance.

The average specific activity of N-terminal His_6-tagged $PhaC_{Re}$ produced without chaperone protein co-expression was 12.1 U mg^{-1} protein (Figure 5.4 (A)). The cultures in which protein recovery was increased showed no significant change in specific activity ($p < 0.05$). However, the specific activity was significantly reduced ($p < 0.01$) by co-expression of GroEL/GroES/Tf (9.0 U mg^{-1} protein) and DnaK/DnaJ/GrpE (8.8 U mg^{-1} protein). When the specific activity was multiplied by the protein productivity to give the average total yield of enzyme (U L^{-1} culture), GroEL/GroES and Tf again resulted in significant ($p < 0.01$) increases (586.3 and 439.7 U L^{-1} culture respectively) compared to $PhaC_{Re}$ alone (168.7 U L^{-1} culture). Only DnaK/DnaJ/-GrpE significantly ($p < 0.01$) decreased the yield (82.4 U L^{-1} culture). Thus, the most influential effect of the GroEL/GroES and Tf systems (plasmids pGro7 and pTf16) was to increase the amount of soluble protein produced, rather than increasing its specific activity.

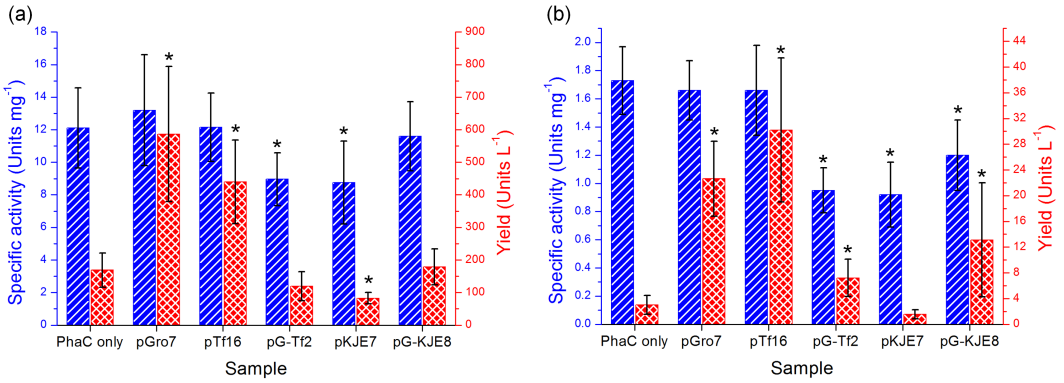

Figure 5.4: The average specific activity (blue, hatched bars) and total yield per litre (red, cross-hatched bars) for $PhaC_{Re}$ produced from (A) pET15$phaC_{Re}$ (N-terminal His_6-tag) and (B) pASG1$phaC_{Re}$(C-terminal His_6-tag) with and without co-expression of chaperone proteins. Error bars represent the standard deviation of results from cultures grown in triplicate, with three replicates of each assay. Significant differences ($p < 0.01$) from the sample expressing $PhaC_{Re}$ only are indicated by an asterisk above the bar.

It has been reported that modifications to the C-terminus of $PhaC_{Re}$ can only be introduced without affecting enzyme activity if the hydrophobic environment surrounding the C-terminus is maintained.[253] To test whether the co-expression of chaperones could prevent the reduction in $PhaC_{Re}$ activity caused by a C-terminal His_6-tag, a comparison was made between N- and C-terminal tagged protein expressed from pET15$phaC_{Re}$ and pASG1$phaC_{Re}$ respectively.

The specific activity and total yield of C-terminal tagged $PhaC_{Re}$ (expressed from pASG1$phaC_{Re}$) was significantly lower ($p < 0.01$) than the N-terminal tagged protein (Figure 5.4 (B)). Compared to an average specific activity of 1.7 U mg^{-1} protein for protein produced in cells containing pASG1$phaC_{Re}$ alone, chaperone co-expression either showed no change ($P > 0.05$) or resulted in a decrease ($p < 0.01$). Co-expression with GroEL/GroES or Tf both resulted in average specific activities of 1.7 U mg^{-1} protein. The other three chaperone combinations all resulted in decreased specific activities, with the smallest being 0.9 U mg^{-1} protein for DnaK/DnaJ/GrpE. As seen for the N-terminal His_6-tagged $PhaC_{Re}$ the differences between the yields of purified protein were more important than the variation in specific activity. The greatest yield was 30.2 U L^{-1} culture for Tf co-expression, which represents a ten-fold increase over the yield of 3.0 U L^{-1} culture when $PhaC_{Re}$ was expressed alone. Co-expression with every chaperone combination except DnaK/DnaJ/GrpE resulted in a significant increase ($p < 0.01$) in protein yield compared to $PhaC_{Re}$ alone.

5.3.4 The effect of chaperones on PHB production

In *E. coli*, the molecular weight of PHB varies in inverse proportion to the amount of $PhaC_{Re}$ produced.[271] As an initial investigation into the effects of improved $PhaC_{Re}$ production (due to chaperone co-expression) on PHB biosynthesis, *E. coli* W3110$hns\Delta 93$ carrying plasmid pTrcphaCAB alone, and equivalent strains carrying each of the five chaperone expression plasmids, were grown for 72 hours in LB medium supplemented with glucose (20 g L^{-1}) at either 30 or 37 °C.

In every case, growth (measured by dry cell weight, DCW) was better at 30 °C than at 37 °C (Table 5.3). As seen in the $PhaC_{Re}$ production experiments, chaperone protein co-expression sometimes inhibited bacterial growth and this was particularly evident when cells contained the pGro7 or pG-Tf2 chaperone expression plasmids.

There were large variations in the amount of PHB produced by each culture, both between temperatures and between chaperone expression systems. In the absence of chaperone co-expression, PHB accumulated to 65% DCW at 30 °C and to 71% DCW at 37 °C. In almost every case, co-expression of chaperone proteins substantially reduced

Table 5.3: Production of PHB during overexpression of chaperone proteins

Proteins expressed	**DCW** (**g L^{-1}**)	**PHB** (**% DCW**)	**M$_n$** ($\times 10^6$)	**M$_n$** ($\times 10^6$)	**M$_w$/M$_n$**
30 °C					
PhaCAB only	6.37	65	1.37	3.09	2.3
GroEL/GroES	2.12	27	1.29	2.78	2.2
Tf	6.85	63	1.07	2.18	2.0
GroEL/GroES/Tf	2.24	3	ND	ND	ND
DnaK/DnaJ/GrpE	7.47	49	1.42	3.00	2.1
GroEL/GroES/ DnaK/DnaJ/GrpE	7.76	59	0.86	1.93	2.2
37 °C					
PhaCAB only	2.46	71	2.34	4.46	1.9
GroEL/GroES	0.93	13	1.46	2.75	1.9
Tf	2.06	70	2.07	4.71	2.3
GroEL/GroES/Tf	1.08	1	ND	ND	ND
DnaK/DnaJ/GrpE	2.20	44	2.42	4.66	1.9
GroEL/GroES/ DnaK/DnaJ/GrpE	2.53	28	1.60	3.35	2.1

the yield of PHB. The biggest reductions were for GroEL/GroES and GroEL/GroES/Tf, with the smallest yields being for GroEL/GroES/Tf co-expression (3% and 1% at 30 and 37 °C, respectively).

The number-averaged molecular weights (M_n) were generally decreased by chaperone co-expression (Table 5.3). At 30 °C, Tf and GroEL/GroES/DnaK/DnaJ/GrpE reduced the M_n of PHB by 21.8% and 37.2% respectively. At 37 °C the largest reductions were with GroEL/GroES and GroEL/GroES/DnaK/DnaJ/GrpE (37.6% and 31.6%). Additionally, M_n for each sample was larger at 37 °C than at 30 °C. Polydispersities (defined as the ratio of M_w to M_n) were not significantly affected by chaperone protein co-expression. Due to poor growth and low PHB yield, molecular weight data were not gathered for GroEL/GroES/Tf.

5.4 Discussion

Chaperone protein co-expression was found to assist in the production of soluble $PhaC_{Re}$ in BL21(DE3). The most significant improvements were seen with the production of N-terminally tagged $PhaC_{Re}$ and chaperone expression was not able to restore reduced activity caused by a C-terminal His_6-tag. Co-expression of the GroEL/GroES operon (pGro7) or Trigger Factor (pTf16) were the most successful strategies, increasing yields

by a factor of 3.5 or 2.6 repectively. Enzyme activity was largely unaffected by chaperone protein co-expression, suggesting that soluble $PhaC_{Re}$ is correctly folded in *E. coli* BL21(DE3). The increase in yield was due to substantial increases in the quantity of soluble, active protein that could be recovered by cobalt-affinity chromatography. Therefore, the chaperone proteins assisted the folding of polypeptide chains that would otherwise have accumulated in inclusion bodies or been targeted for protein degradation.

As shown in Figure 5.3, considerable quantities of insoluble $PhaC_{Re}$ remained in each strain, although the fraction of soluble protein was increased by co-expressing chaperones. This suggests that chaperone proteins are able to allow greater quantities of $PhaC_{Re}$ to be produced in total, either by increasing production or by reducing the amount of protein that is targeted for protease degradation. This also suggests that further optimization of the expression strategy could result in even higher yields of soluble $PhaC_{Re}$.

Reduced bacterial growth, a known side-effect of chaperone protein co-expression, contributed to the difference in total protein yields between the strains used in this study. [255] Modulation of the level of chaperone expression could potentially reduce the negative effects on bacterial growth, while maintaining the beneficial effects on protein folding. The amount of protein recovered per OD_{600} unit (Table 5.2) was consistently greater when chaperone proteins were co-expressed, and the beneficial effect of GroEL/GroES/Tf, was clearly better than any of the others tested.

Small differences were noted between the specific activities of $PhaC_{Re}$ expressed with different chaperone systems. It is likely that much of the difference in specific activities is due to variations in the relative amounts of contaminating proteins in each sample. In particular, note that co-expression from pKJE7 had a larger number of co-eluting proteins than other samples, and also had a low specific activity (Figures 5.2 and 5.4). The contaminating proteins were identified as a mixture of chaperones (DnaK/J), SlyD and degradation products of $PhaC_{Re}$. Both DnaK and DnaJ, as well as SlyD, are common contaminants of His_6-tag-purified proteins due to naturally-occurring oligo(His) sequences in their primary structure. [272] Therefore, it is unsurprising to find traces of them, particularly in a strain overexpressing DnaK and DnaJ proteins.

The specific activity of $PhaC_{Re}$ has previously been reported to be 40 U mg^{-1} protein which is substantially higher than the figures reported here. [104] The protein preparation in the previous report involved an extra purification step using size-exclusion chromatography to remove soluble aggregations of $PhaC_{Re}$. Although such a procedure would be expected to increase the specific activities in this case (and to reduce variance), absolute specific activity had far less influence on relative yields between cultures than

the increase in total soluble protein. Therefore, the conclusions following a one-step purification procedure remain valid.

The C-terminal tagged protein produced from pASG1$phaC_{Re}$ had much lower specific activities than N-terminal tagged protein from pET15$phaC_{Re}$ and was also produced in lower quantities. This suggests that chaperone proteins were not able to rectify the misfolding of $PhaC_{Re}$ caused by the addition of a His_6-tag to the C-terminus. It is not clear whether the lower quantity of protein was due to differences in the expression signals and/or copy number between the plasmids, increased accumulation in inclusion bodies, or recognition of the badly-folded protein and targeting for degradation. However, since chaperone proteins were still able to increase the amount of soluble $PhaC_{Re}$ it is evident that they play a part in the folding mechanism and are at least partially successful in preventing the aggregation of badly folded protein.

Chaperone protein co-expression generally resulted in a decrease in both the number-averaged and weight-averaged molecular weights of PHB produced in *E. coli*, particularly for the GroEL/GroES, Tf, and GroEL/GroES/Dnak/DnaJ/GrpE systems. This can be attributed at least in part to the production of a larger number of active $PhaC_{Re}$ molecules. These compete for the available monomeric units and catalyse the production of a larger number of shorter chains than when only the PHB operon is expressed. Consistent with this, pKJE7 caused a small increase in M_w and was also responsible for a reduction in $PhaC_{Re}$ productivity.

Several studies have shown that the addition of exogenous hydroxy agents can usefully alter the molecular weights of *in vivo*-generated PHAs. This is considered to occur by trans-membrane migration of the agents to assist in chain termination of the polymerization process.[117,273] These results point to the use of chaperone-mediated alteration of the monomer-enzyme balance as an alternative route to altering the molecular weight distribution of the PHA product. Whilst product control by an exogenous agent can be toxicity-limited, the expression of the endogenous chaperone could be more flexibly tuned to control the molecular weight of the resulting polymer in order to suit a range of applications. One might also expect an endogenous influence to be more uniform within large fermentor volumes.

PHB production relies on an interconnected web of related biochemical pathways, including cellular respiration, which provides the acetyl-CoA that is converted into the monomeric unit for PHB. Since chaperone proteins are actively involved in folding of the majority of bacterial proteins, it is very likely that overexpression of any of the systems described in this study will simultaneously also affect the levels of the PhaA and PhaB proteins as well as many more, diverse, native proteins. This hinders any simple interpretation of the results, but suggests that the large variations in bacterial growth

and PHB accumulation could be due to imbalances in the core biochemical pathways of the cells. PHA synthase production was increased by chaperone co-expression, so the reductions in PHB yield reported here during co-expression suggest that the supply of monomers was hindered by the presence of large quantities of chaperone. Further studies are required to fully understand the reduction in PHB yield and the mechanism of PHB weight reduction during chaperone co-expression, and how this information could be translated into a commercially-relevant production process.

Chaperone protein co-expression is an effective method for increasing the yield of $PhaC_{Re}$. By using a widely-available set of expression plasmids, this study has demonstrated increases in total enzyme yield of 3–5 times without the need for costly and time-consuming processes such as expression at reduced temperature or *in vitro* protein refolding. This will facilitate the laboratory-scale study of the enzyme for the purposes of elucidating its structure and catalytic mechanism, as well as for developing *in vitro* PHB production methodologies. The method should also be easily transferable to the study of other PHA synthases.

Chapter 6

Polyhydroxybutyrate molecular weight control

6.1 Introduction

Although chapters 4 and 5 focused on the production of $PhaC_{Re}$ with a view to improving the yields for use with *in vitro* PHA production, there are still significant financial and technical barriers to overcome before large-scale *in vitro* production will be possible. Therefore in this chapter, attention is turned to overcoming a challenge for *in vivo* production by developing a strategy to control the molecular weight of PHB produced in *E. coli* W3110*hns*Δ93.

The capability exists to produce large yields of PHAs, often from cheap substrates. However, it is still difficult to control the material properties of the polymer, and this limits the range of applications for which PHAs are suitable.[10,134,143,145] As discussed in Section 2.6, the material properties depend mainly on which monomers are incorporated into the polymer and on the molecular weight of the polymer itself. Chaperone co-expression was shown in Chapter 5 to be able to reduce the molecular weight of PHB in *E. coli*. However, the Q-cell system was chosen for the present study as it was hoped that indole, as an exogenous additive, would have a more direct effect on PHB production than the rather indirect effect of chaperones, which rely on the modulation of expression levels for a large number of proteins simultaneously via chemical inducers.

The most commonly produced PHAs, including PHB tend to be too brittle for any application that demands structural integrity. Therefore, much effort has been expended to increase the efficiency of production for co-polymers with useful properties, such as PHBV, PHHx and PHO.[17,122,126] Due to the limitations of feedstock availability and

PHA synthase specificity, progress in this area has been slow. Another approach has been to increase the molecular weight of simple polymers such as PHB, to decrease the crystallinity.[224]

An alternative solution is to blend PHAs with other polymers or to produce composites of PHA with non-polymeric material.[274–277] This allows the relatively simple creation of materials with desirable properties without requiring extensive metabolic engineering, complicated processing procedures or expensive carbon sources. The ability to blend polymers depends on the thermodynamics of the molecules in question, which strongly depend on the the molecular weight of the polymers. Mixtures of small molecules have higher conformation entropy than mixtures of large molecules. Therefore, a mixture of low molecular weight polymers has greater entropy than a mixture of high molecular weight polymers, and the mixing of the former is more thermodynamically favourable. Consequently, the ability to reliably control the molecular weight of PHAs within specified limits is an important factor in developing commercial PHA-based products.

6.1.1 Measuring polymer molecular weight

Unlike small molecules, polymers are usually not all of the same molecular weight. They exist as a mixture of individual molecules with a range of numbers of monomer per polymer chain, and therefore a range of molecular weights. The distribution of weights is discrete rather than continuous because each monomer unit adds a certain, defined, weight to the polymer. For example, the molecular weight of a 3HB monomer is 86 Da; therefore, every chain of PHB will have a molecular mass that is a multiple of 86 and intermediate values are not possible.

The molecular weight of a polymer is defined by calculating an average value based on the distribution of weights. The shape of the distribution of weights within a sample of polymer will depend on many factors including how the polymer was synthesised, how it was purified and post-purification treatments such as heating or exposure to acids/alkalis. Therefore, there are many different ways to estimate the average weight, and the selection of which method to use depends on the application. The two most common estimates are the number-averaged molecular weight (M_n) and the weight-averaged molecular weight (M_w).

The most common technique for determining the distribution of weights in a polymer sample is gel permeation chromatography (GPC). This uses a column of inert polymer beads, which contains pores of varying sizes. A sample of the polymer to be analysed is dissolved in a suitable solvent and then pumped through the column at high pressure. Small molecules are able to fit through more of the pores than larger molecules and

so take a longer route through the column. In this way the molecules in the sample are separated according to their molecular weight, with larger molecules being eluted sooner than small molecules. After elution, the separated sample travels in a narrow tube (to avoid re-mixing) to a detector, which reports the concentration of sample at many time-points. By comparing the elution times to standards with known molecular weights, the weight distribution of the sample can be given. The detector usually uses either light scattering or change in refractive index of the solution to detect the presence of the sample. The GPC system used in this study used a refractive index detector (RID), which measures the change in the angle of refraction of a light beam caused by different concentrations of solute in the solvent.

Once the molecular weight distribution is known, the average molecular weight can be calculated. For M_n, the estimate is based on the number of molecules of each weight within the sample. It is equivalent to calculating the simple arithmetic mean of the distribution. If N_i is the number of molecules with molecular weight M_i then M_n is given by the formula

$$M_n = \frac{\sum_{i=1}^{\infty} N_i M_i}{\sum_{i=1}^{\infty} N_i}$$

The calculation of M_w is based on the weight of polymer chains as well as the number of each weight. The average is weighted according to the weight of each chain by replacing the term N_i with the weight of molecule having molecular weight i, denoted $N_i M_i$. This gives the formula

$$M_w = \frac{\sum_{i=1}^{\infty} N_i M_i^2}{\sum_{i=1}^{\infty} N_i Mi}$$

In this way, the chains with higher molecular weight are given greater importance to the estimation of the average. Therefore, unless every chain has exactly the same weight, M_w will always be greater than M_n. The ratio of M_w to M_n is known as the polydispersity index (PDI or M_w/M_n), which shows how widely spread the weights are within the distribution. If all weights are exactly the same, the PDI will have a value of 1. It is generally preferred for polymers to have low polydispersity (PDI of 1–3) so that the physical properties are easier to predict. PDI values for PHAs typically fall within the range 1.5–3.0.[278]

6.1.2 Methods of controlling PHA molecular weight in *E. coli*

The molecular weight of *in vivo*-synthsised PHAs is thought to be controlled by the mediation of a chain transfer reaction, which removes the synthase from a chain and causes the production of a new chain to begin.[64] PHB produced by wild-type *R. eutropha* has a typical M_w of 0.5–1.0×10^6 Da.[279] When PHB is produced *in vitro*, the molecular weight is much higher (up to 20×10^6 Da), probably because the chain transfer agent is not present.[109] Similarly, when PHB is produced in *E. coli*, the molecular weight tends to be higher than in *R. eutropha* although the reported weights vary widely depending on culture conditions.[224,271]

Kusaka *et al.* reported the production of PHB with M_w of 20×10^6 Da in *E. coli* grown in a fermentor at pH 6.0 and 37 °C.[115] This is the same weight as that reported *in vitro*, so they speculated that under these conditions, the chain transfer agent is not present in *E. coli* but that it could be produced under different conditions. Also, because *E. coli* does not naturally produce PHAs, it does not contain a PHA depolymerase enzyme and so is not able to break down the polymer that it synthesises.[280,281] *R. eutropha* on the other hand produces both a synthase and a depolymerase, which are simultaneously present on the surface of the granule and this causes degradation of the polymer both before and after purification.[24,77]

The presence—and, indeed, the identity—of a potential chain transfer agent has not been confirmed, but methods have been developed to control the molecular weight of PHAs produced by *E. coli* without the need for one. Sim *et al.* discovered that the PHA synthase enzyme activity also plays an important role in determining the weight of polymer produced.[278,282] When $PhaC_{Re}$ is expressed at high levels in *E. coli* cells also expressing the $PhaA_{Re}$ and $PhaB_{Re}$ proteins, the molecular weight of the polymer is smaller than when $PhaC_{Re}$ activity is low. This is because the presence of more enzyme molecules allows the initiation of a larger number of PHB chains at one time. If the same total amount of PHB is produced, each chain must be of lower molecular weight than if fewer chains are present. Consequently, the order of the *phaA*, *phaB* and *phaC* genes in the operon has a large effect on the yield of polymer produced and on its molecular weight.[283]

To maximise productivity and avoid the potential complications involved with genetic engineering, it is possible to process the PHB, downstream of fermentation, in such a way that the molecular weight can be controlled within the desired range. Many different methods have been used for separation of PHAs from bacterial biomass.[284] These usually involve one stage to break open the cells followed by selective dissolution and then precipitation of the PHA (see Section 3.7).

Cell lysis can be achieved by low pressure using a French press, osmotic pressure, high temperature, enzyme action, chemical disruption or spontaneous cell lysis.[284–286] All of these methods involve a certain amount of polymer degradation.[17,284] Therefore, depending on the scale of production and the intended application of the polymer, a certain method can be chosen and optimised to allow an appropriate level of molecular weight reduction.[287] If the polymer is incubated for a prolonged time under conditions favourable for degradation (for example, in the presence of depolymerases, alkaline chemicals such as NaOH, or at high temperature), (R)-3-hydroxyalkanoic acid monomers can be recovered, which are useful building blocks for chiral fine chemical synthesis.[288]

A third method for the control of PHA molecular weight is to add an exogenous chain transfer agent into the growth medium. A variety of hydroxylated compounds have been used for this purpose, of which poly(ethylene glycol) (PEG) has been studied most.[116,289] PEG is a neutral, water-soluble polymer with molecular weights of up to a few thousand Da. It is non-toxic and widely used in medical and biological research as a drug carrier, thickening agent, cross-linker, and to increase the solubility of hydrophobic chemicals and proteins.[289] PEGs with number-averaged molecular weights of 106 or 200 (PEG-106 or PEG-200) reduced the molecular weight of PHB produced by *R. eutropha* by up to 80% but longer chain-length PEGs were less effective.[117]

It is thought that the hydroxyl group of PEG can react with the carboxyl terminus of the growing PHA chain.[116] The currently accepted model for PHA chain elongation involves the thiol groups of two cysteine residues, which are acylated by the addition of 3HB-CoA, removing the CoA from the monomer. The growing PHB chain is shuttled between the two cysteines in a series of chain-transfer reactions with the addition of one monomer to the carboxyl terminus for each repetition.[106]

An endogenous chain-transfer agent such as PEG might be able to infiltrate the active site of PhaC, although it would not be able to bind to cysteine as it does not contain CoA.[60] However, the hydroxyl group could still react with the end of the PHB chain resulting in chain transfer to the PEG.[116] Since the polymer would then no longer be attached to the active site of the enzyme, elongation would cease and a new chain would be initiated. Since PEG is not produced naturally, it cannot be the natural chain transfer agent. However, it probably operates in the same way as the natural agent and is therefore a good model to study the process[273] This also makes it possible to produce PHAs with a bimodal weight distribution by adding PEG mid-way through polymer accumulation.[290]

Hydroxylated compounds that are produced naturally, such as glycerol, ethanol and methanol have also been shown to reduce the molecular weight of PHAs *in vivo*.[116] It has been noted that when glycerol is used as a carbon source for PHB production in

R. eutropha the molecular weights tend to be low.[291,292] Methanol can also be used as the sole carbon source for PHB production in some species of *Methylobacterium.*[293–295] Again, no reports have been made of the production of high molecular weight PHB in the presence of methanol. However, compared to PEG, the effects and chain transfer mechanism of endogenous hydroxylated compounds have been poorly studied.

The results of Chapter 5 suggested that co-expression of chaperone proteins and the PHB biosynthesis pathway could be used as a method to control the molecular weight by changing the ratio of synthase to monomers in the cells. However, this is rather an indirect method of effecting a change as it relies on the accurate and reproducible expression of many proteins at the correct level, simultaneously. Although Q-cells were not able to produce $\mathrm{PhaC_{Re}}$ with the necessary level of efficiency for large-scale *in vitro* synthesis, they were able to produce more protein per cell than standard cultures. Therefore, the effects on molecular weight of indole addition to cultures of W3110*hns*Δ93 expressing the $phaCAB_{\mathrm{Re}}$ operon were investigated.

Indole was expected to reduce the molecular weight of PHB produced, but this could be achieved by either of two mechanisms. Firstly, indole might alter the level of expression of enzymes in the key metabolic pathways, including the TCA cycle and PHB biosynthesis pathway, responsible for monomer production. In particular, $\mathrm{PhaC_{Re}}$ production might be up-regulated. This would then change the ratio of monomers to synthase, as in the chaperone co-expression cultures. Secondly, indole itself might play a direct role in mediating chain transfer reactions, or inhibiting the activity of the synthase enzyme. This would be analagous to the effect of adding hydroxylated compounds.

6.2 Bacterial strains and plasmids

Table 6.1 summarises the bacterial strains and plasmid used in this chapter. Three strains of *E. coli* W3110 were chosen for comparison: the wild-type strain ensured that the results were generally applicable to common laboratory strains of *E. coli*, W3110*hns*Δ93 was used to compare the effects of indole on the molecular weight of PHB produced by standard and Q-cell cultures, and W3110Δ*tnaA* was chosen as a non-indole producing strain to separate the effects of endogenous indole produced by the other two strains from the exogenous indole added to the cultures.

All three strains contained plasmid pTrc*phaCAB* for high-yield production of PHB under control of an IPTG-inducible promoter, as in Chapter 5. Please see Table 3.1 for full details of strain genotypes.

Table 6.1: Bacterial strains and plasmids for Chapter 6

Strain or plasmid	Purpose for study	Source
Strains		
E. coli W3110*hns*Δ93	Expression strain for PHB production with *hns*Δ93 for quiescence; Kn^r	Chen (2010) [222]
E. coli W3110 wild-type	Unmodified expression strain for PHB production	Summers lab.
E. coli W3110Δ*tnaA*	As for W3110 wild-type, with Δ*tnaA* to prevent indole production; Kn^r	Summers lab.
Plasmid		
pTrc*phaCAB*	Expression vector containing *phaCAB* operon; *trc* promoter; Ap^r	Kahar (2005) [224]

6.3 Results

6.3.1 Characterisation of growth and PHB production

The scattering of light by intracellular PHA granules causes cell cultures to appear far denser than at the same stage of growth without PHA accumulation. Therefore, OD_{600} is not an accurate measure of the number of cells in a culture when PHB is accumulated. Rather, at high concentrations of PHA, it correlates with the amount of PHA as that becomes the major contributor to light scattering. This presents a problem for analysing the growth of Q-cell cultures, as the established method for tracking the entry into quiescence is to follow the increase in OD_{600} over time. To investigate how the addition of indole affects the growth and productivity of W3110*hns*Δ93 cultures producing PHB, the strain was transformed with plasmid pTrc*phaCAB* to express the *R. eutropha* PHA operon under control of the IPTG-inducible *trc* promoter.

Cultures were grown in LB medium (200 ml) supplemented with 2% glucose, kanamycin (30 μg ml^{-1}), ampicillin (100 μg ml^{-1}) and IPTG (1 mM) in 1 L Erlenmeyer flasks. Indole was added at a range of concentrations from 0–3 mM and the cultures were inoculated with an overnight culture (2 ml) grown in LB medium. To control for any effects of ethanol in the indole stock solution, 0.6% ethanol (equivalent to the volume in the 3 mM culture) was added to the 0 mM culture. The cultures were incubated at 30 °C on an orbital shaker set to 250 rpm for 72 hours. Samples were periodically taken for measurement of OD_{600} (1 ml) and PHB content (20 ml). The samples for analysis of PHB content were prepared for gas chromatography (GC) analysis as described in Section 3.7.2.

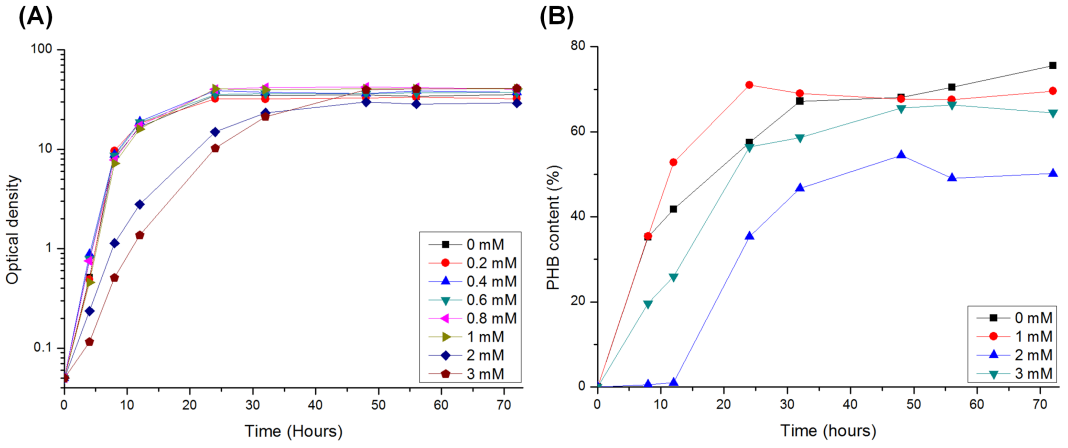

Figure 6.1: Cell growth and PHB accumulation in the presence of indole. Comparisons of the growth (A) and PHB accumulation (B) dynamics of representative cultures of *E. coli* W3110*hns*Δ93 containing plasmid pTrc*phaCAB* grown with a range of indole concentrations. Cultures were grown in LB medium supplemented with 20 g L^{-1} glucose at 30 °C for 72 hours.

As shown in Figure 6.1 (A), the cultures containing 0–1 mM indole grew according to a classical growth curve, with no difference between the growth kinetics or final density. The addition of 2 or 3 mM indole affected the rate of growth, with 3 mM indole having a greater effect. However, the final density attained by all cultures was very similar. Note that the final densities were extremely high (OD_{600} = 30–40), as expected, due to the presence of PHB granules. Although not shown in Figure 6.1, a culture with 4 mM indole failed to grow. Although it is clear that indole affects the growth rate of cells, the growth curve for the 3 mM culture does not follow the characteristic shape for entering quiescence as seen in chapter 4. Due to the extra scattering from PHB granules, it is not possible to conclude from the measurements of OD_{600} whether the culture entered quiescence.

The accumulation of PHB within cells followed a similar pattern to the growth curve (Figure 6.1 (B)). There was little difference between the rate of accumulation and final PHB content for cultures with 0 or 1 mM indole. The 3 mM culture accumulated PHB slower than with lower indole concentrations, but eventually reached a similar level (65–70% of DCW). Interestingly, the 2 mM culture accumulated PHB at the slowest rate and accumulated the least PHB (55% of DCW). Assuming that the 3 mM culture was still able to achieve quiescence, this might reflect the ability of Q-cells to maintain their metabolic activity for longer, and so to continue producing PHB. However, the amount of PHB produced by the 3 mM culture was not greater than for the 0 mM culture

and took longer to accumulate. Therefore, it is doubtful as to whether Q-cells might represent a more efficient production system for PHAs.

6.3.2 Molecular weight of PHB produced in the presence of indole

To investigate the effects of indole on PHB molecular weight in *E. coli*, 200 ml shake flask cultivations were performed on three related strains of *E. coli* W3110. The W3110*hns*Δ93 Q-cell strain was shown in the previous section to tolerate up to 3 mM indole while still producing large quantities of PHB. To test whether this ability is due to the *hns*Δ93 mutation, the wild-type W3110 strain was also grown. Finally, to separate the effects of exogenous indole from that produced by the cells themselves, the indole-negative W3110Δ*tnaA* strain (which has had the tryptophanase *tnaA* gene knocked out) was used. All three strains carried the pTrc*phaCAB* plasmid for PHB production.

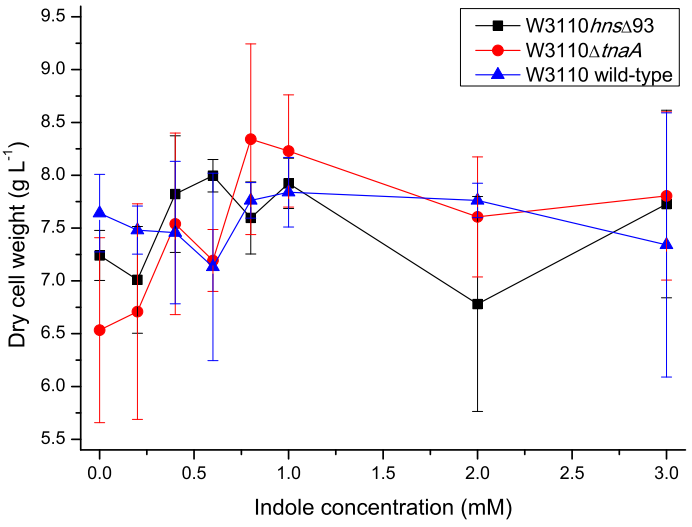

Figure 6.2: The effect of indole concentration on final dry cell weight production by *E. coli* W3110*hns*Δ93 producing PHB. Cells were grown for 72 hours in LB medium supplemented with 20 g L^{-1} glucose before freeze-drying. Data presented are the averages of three separate experiments ± standard deviation.

Cultures were grown in triplicate, as described in the previous section, in the presence of 0–3 mM indole. The 0 mM culture contained 0.6% ethanol. Following cultivation, the cells were freeze-dried and weighed to determine the total DCW produced. PHB was extracted and purified from ~65 mg dry cells by chloroform dissolution and methanol precipitation (see Section 3.7.3). The purified polymer was dissolved in chloroform

(1 mg ml^{-1}) for molecular weight estimation by gel permeation chromatography (GPC) as described in Section 3.7.4.

Figure 6.2 shows the DCW productivity of all three *E. coli* strains as the concentration of indole was varied. For the *hns*Δ93, Δ*tnaA* and wild-type strains, the mean DCW per litre (± standard deviation) across all samples were 7.51 ± 0.64, 7.47 ± 0.88 and 7.53 ± 0.58 g, respectively. Across all 27 samples, the lowest accumulation of DCW was 6.03 g L^{-1} (wild-type, 3 mM) and the largest was 9.12 g L^{-1} (Δ*tnaA*, 0.8 mM). The overall mean value was 7.51 g L^{-1} with a standard deviation of 0.70. Final dry cell weights per litre for all three strains were statistically the same ($p > 0.05$, determined by T-test). Although there was a suggestion of increased DCW accumulation from 0–1.0 mM indole, the relatively large standard deviations do not allow the identification of a significant trend within individual strains.

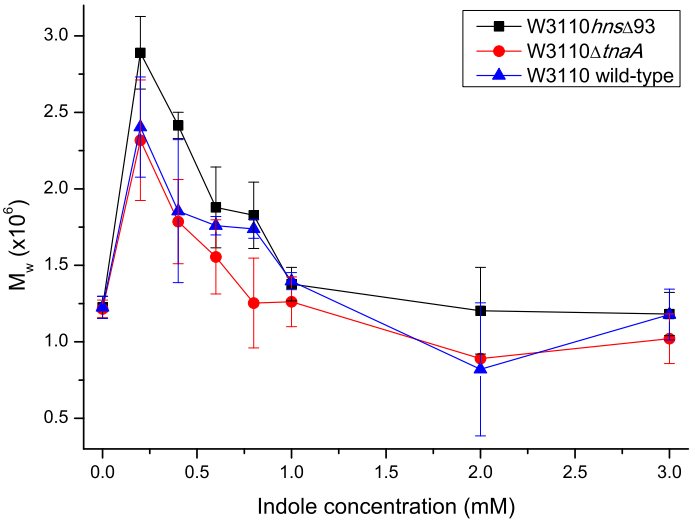

Figure 6.3: $M_w$reduction caused by indole. The effect of indole addition on the weight-averaged molecular weight (M_w) of PHB produced by *E. coli* W3110*hns*Δ93 W3110Δ*tnaA* and W3110 wild-type. The 0 mM sample contained 0.6% ethanol but no additional indole. Data presented are the averages of three independent experiments ± standard deviation.

Figure 6.3 shows the mean M_w for all three strains at each indole concentration. The trend was the same for each strain, and no significant difference ($p > 0.05$) was found between any strains. Therefore, the mutations in strains *hns*Δ93 and Δ*tnaA* had no effect on either their growth or the M_w of PHB produced. Increasing the concentration of indole was correlated with a decrease in the M_w of PHB. Although it was expected

that the highest M_w would be for the cultures with 0 mM, that concentration actually had the lowest M_w, equal with that of the 2 and 3 mM samples (1.2×10^6 Da). There was a sudden increase in M_w to ~2.5×10^6 Da when the indole concentration was increased to 0.2 mM. Thereafter, M_w decreased rapidly between 0.2–0.8 mM before plateauing at the original level until 3 mM.

The same trend was seen for M_n, although at lower values ranging from 0.5–1.3×10^6 Da (Figure 6.4 (A)). Again, no significant differences ($p > 0.05$) were found between strains. Due to the change in M_n following that of M_w, there was no overall change in polydispersity (M_w/M_n). However, as shown in Figure 6.4 (B), there was considerable variation in the individual values, which ranged from 1.8–2.4.

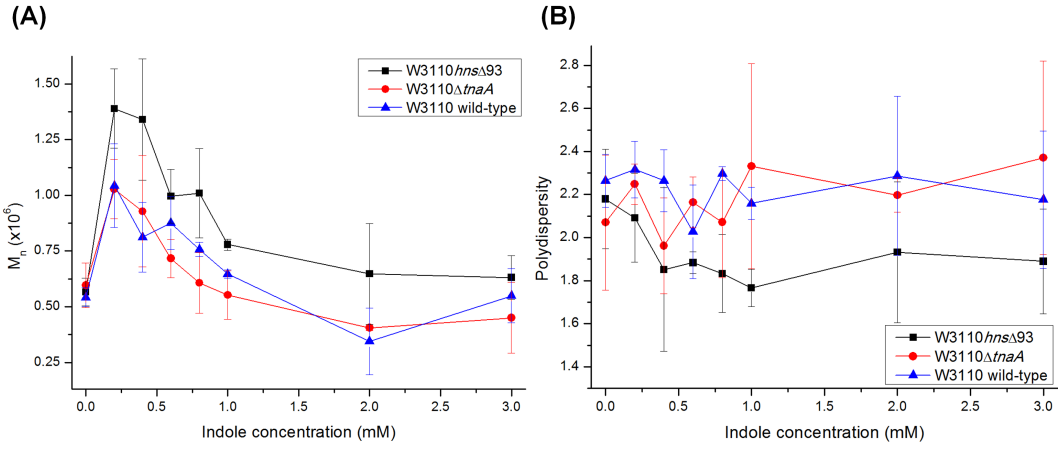

Figure 6.4: $M_n$reduction and variation in PDI caused by indole. (A) The effect of indole addition on the number-averaged molecular weight (M_n) of PHB produced by *E. coli* W3110*hns*Δ93, W3110Δ*tnaA* and W3110 wild-type. (B) Changes in the polydispersity index (PDI) of the same samples. The 0 mM samples contained 0.6% ethanol but no additional indole. Data presented are the averages of three independent experiments ± standard deviation.

6.3.3 Molecular weight of PHB in the presence of short-chain alcohols

The unusual change in molecular weight in response to indole addition prompted further investigation into why the 0 mM samples should display such low values. The only addition to these cultures was of ethanol, at a concentration equal to that added to the 3 mM cultures. As discussed in Section 6.1, hydroxylated compounds such as PEG have previously been used to reduce the molecular weight of PHAs. Considering that the 0 and 3 mM cultures contained the same concentration of ethanol and that both produced PHB of the same molecular weight, it seemed likely that the weight-reduction effect was

caused by the ethanol used to dissolve the indole, rather than indole itself. To test this hypothesis, a culture of wild-type W3110 was grown as before but in the absence of ethanol or indole. The M_w of the purified polymer was ~4.5×10^6 Da: significantly higher than any weights seen in the previous experiment (data not shown).

To further characterise the effects of ethanol on the molecular weight of PHB produced in *E. coli*, a full range of wild-type W3110 cultures (100 ml) was grown in triplicate in the same manner as before. Ethanol was added in the same concentrations as for the indole experiment, ranging from 0–0.6% (v/v). To investigate whether the carbon chain length of an alcohol affects its ability to reduce the molecular weight of PHB, a series of cultures containing 0–0.6% methanol was also grown. PEGs with fewer monomer units have a greater effect on PHA molecular weight than those with many monomers.[117] Therefore methanol, which only has one carbon atom might be more effective than ethanol, which has two.

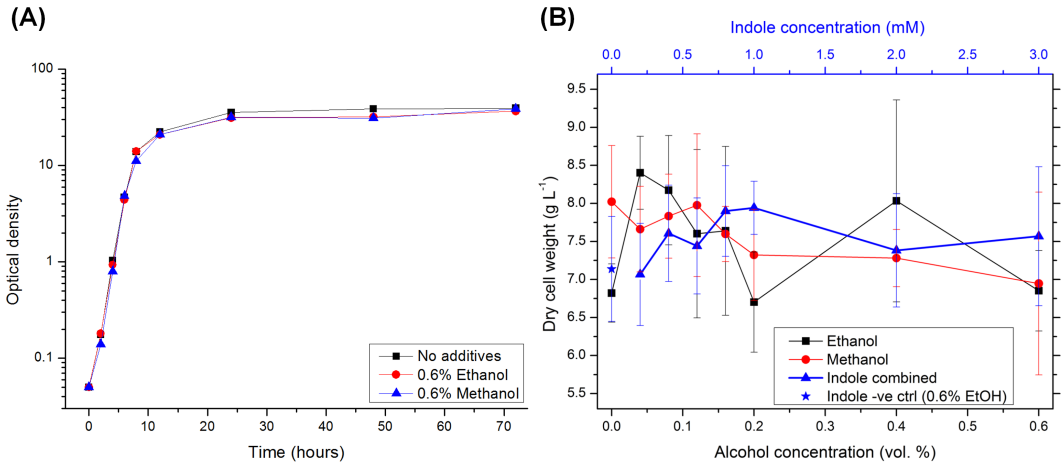

Figure 6.5: Effect of short-chain alcohols on cell growth. Cultures of *E. coli* W3110 wild-type were grown in the presence of 0–0.6% ethanol or methanol. (A) Representative cultures with 0.6% ethanol or methanol followed the same growth curve, and reached the same final OD_{600} as a control with no additives. (B) Average dry cell weight (± standard deviation) for 3 repeat cultures at each alcohol concentration, and for all 9 indole-containing cultures combined. There were no significant differences between additives or between different concentrations of the same additive.

To check that cell growth was not affected by the addition of short chain-length alcohols to the growth medium, the increase in OD_{600} was tracked throughout the growth cycle. Figure 6.5 (A) shows the growth curves for representative samples containing 0.6%

ethanol or methanol compared to a control culture with no additive. The curves demonstrate a very close correlation between each sample. Therefore, ethanol or methanol added to the growth medium at up to 0.6% had no effect on cell growth.

Similarly, the total DCW produced was the same for each strain, and there was no difference between the addition of alcohol or of indole ($p > 0.05$), as shown in Figure 6.5 (B). The average DCW per L (± standard deviation) were 7.45 g (± 0.90) for ethanol and 7.58 g (± 0.70) for methanol. Across all ethanol and methanol cultures, the DCW yields ranged from 5.97–8.89 g L^{-1}, which is in good agreement with the range when indole was added. Because there was no significant difference between strains for the accumulation of DCW with indole addition (Figure 6.2), the data for all three strains (9 series of cultures in total) were combined to produce the average results for indole shown in Figure 6.5.

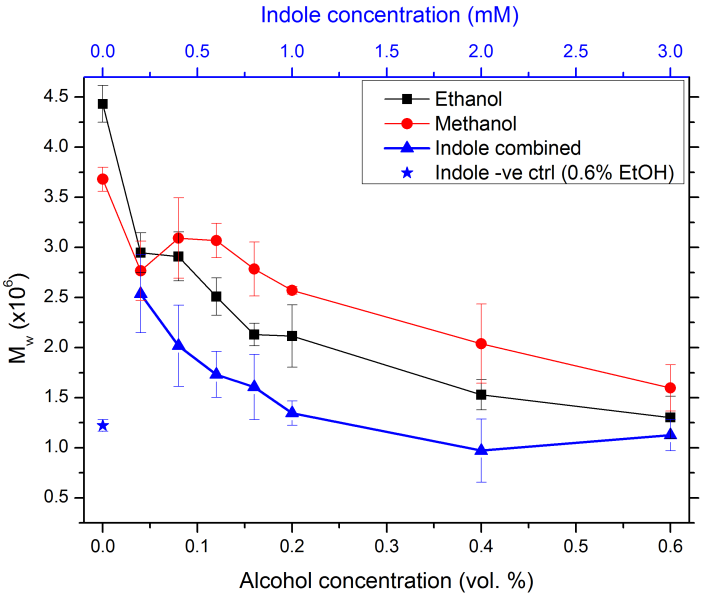

Figure 6.6: The effect of ethanol or methanol addition on the weight-averaged molecular weight (M_w) of PHB produced by *E. coli* W3110 wild-type. The data for the effect of indole are shown for comparison, as averages for all three strains combined. Data presented are the averages (± standard deviation) of three independent experiments for the addition of alcohols and nine experiments for the addition of indole.

Figure 6.6 compares the patterns of M_w reduction caused by the addition of ethanol, methanol and indole to the growth medium. The lines for ethanol and methanol represent the average of three independent experiments, while the results for indole were combined as before. In the absence of indole or alcohol, the M_w was 4.4×10^6 Da for ethanol and 3.7×10^6 Da for methanol. Between 0.04–0.20% there was a sharp decline

in molecular weight as either ethanol or methanol concentrations were increased, as seen for indole addition. By 0.60%, the M_w had stabilised around its minimum values of 1.3×10^6 Da for ethanol and 1.6×10^6 Da for methanol.

The drop in molecular weights was not as severe when either alcohol was added, compared to when indole was added due to higher than expected M_w at 0.08–0.20%, although the large standard deviations indicate that this was probably due to random fluctuations caused by the inherent inaccuracies of refractive index-based detection methods. However, perhaps indole has some synergistic effect that further reduces the molecular weight.

The patterns of M_n and polydispersity followed the same relationship to M_w as for the addition of indole (Figure 6.7). For M_n, the zero-addition controls produced PHB of the highest weight (~1.5×10^6 Da). Alcohol addition then caused a sharp decrease in molecular weight before a plateau was reached at ~0.9×10^6 Da, as seen in the M_w results. As with indole addition, the positive correlation between M_w and M_n resulted in no significant change in the polydispersity ($p > 0.05$) at any concentration. However, the polydispersity was consistently higher when alcohols (particularly ethanol) were added, compared to indole (Figure 6.7 (B)). Further repeats would be necessary to establish the significance of this observation.

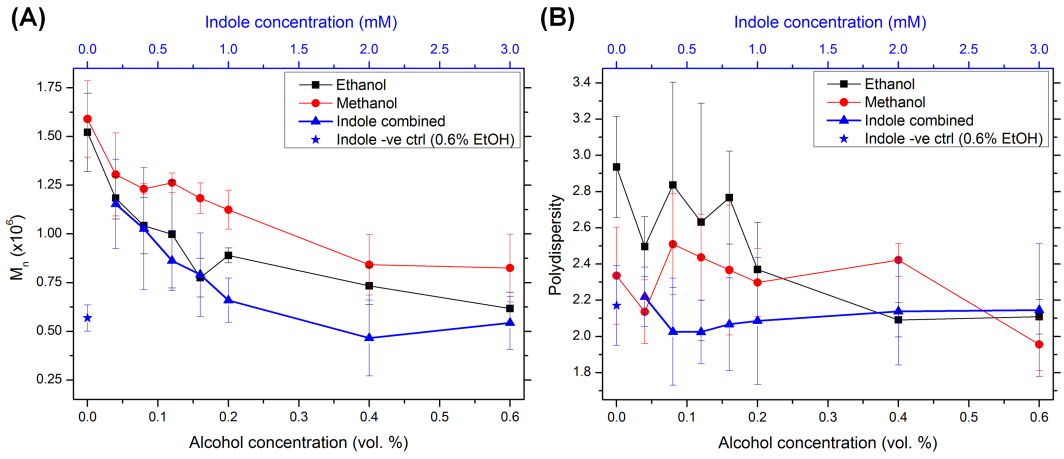

Figure 6.7: (A) The effects of ethanol and methanol addition on the number-averaged molecular weight (M_n) of PHB produced by *E. coli* W3110 wild-type. (B) Changes in the polydispersity index (PDI) of the same samples. The data for the effect of indole are shown for comparison, as averages for all three strains combined. Data presented are the averages of at least three independent experiments (± standard deviation).

6.3.4 Effects of indole and alcohols on $PhaC_{Re}$ activity

The above results showed that the ethanol from the stock solution was responsible for the change in molecular weight of PHB when cultures were grown in the presence of indole, and that methanol has a similar effect on M_w. The similarity in structure between alcohols and PEG suggests that ethanol and methanol probably operate by the same mechanism as PEG to terminate the polymerisation of PHB chains. To confirm that the effect is not caused by modulation of PHA synthase activity, $PhaC_{Re}$ purified by cobalt-affinity chromatography (as described in Section 3.7.3) was used to test the effect of the presence of indole or short-chain alcohols *in vitro*. The activity of the enzyme was determined spectrophotometrically by measuring the rate of decrease in absorption at 236 nm caused by the breaking of the thioester bond with CoA during polymerisation of PHB (see Section 3.6.4).

With no chemicals added to the reaction, the average specific activity was 11.7 U mg^{-1} protein from 4 replicates of the assay. The addition of 3 mM indole (together with 0.6% ethanol) gave an average activity of 10.9 U mg^{-1} protein, which was not significantly lower ($p > 0.05$). Similarly, there was no significant change in activity when 0.6% ethanol or methanol were added, with average values of 12.2 and 11.5 U mg^{-1} protein, respectively from four repeats. Therefore, the change in molecular weight was not due to a change in the activity of the enzyme.

6.3.5 Other hydroxylated molecules and acetic acid

Considering the indication that the change in molecular weight of PHB was due to the termination of polymer chains by reactions with the hydroxyl groups of ethanol and methanol, further investigations were carried out to test the effects of similar functional groups. Three other chemicals were tested to compare their effects on the molecular weight of PHB. Isopropanol is an alcohol with three carbon atoms, and was expected to perform in a similar fashion to methanol and ethanol. Glycerol has previously been shown to reduce the molecular weight of PHA.[294] It contains three hydroxyl groups rather than one, so might react more readily with the growing PHB chain. Finally, to establish whether other functional groups are capable of taking part in the chain transfer reaction, acetic acid was added to the growth cultures. Acetic acid is produced in large quantities by many species of bacteria, including *E. coli*, during growth on glucose.[296] The carboxylic acid functional group is similar in structure to a hydroxyl group, but also includes a C=O double bond. A previous report stated that acetic acid slightly increased the molecular weight of PHB produced by *R. eutropha*, but its effect in *E. coli* has not been studied.[116]

In the previous experiments a range of concentrations for the chemical additives was established based upon convenient concentrations for indole addition and the large decrease in M_w seen between 0–0.6% ethanol. The relationship between indole and ethanol concentrations is straightforward because indole was dissolved in ethanol, thus linking the chosen concentrations. However, if a chain transfer reaction is caused by the presence of hydroxylated compounds, the molar quantity of the compound becomes the important concentration parameter rather than volume percentage.

0.6% (v/v) ethanol is approximately 100 mM. Therefore, the volumes of isopropanol, glycerol and acetic acid were calculated to allow their addition at a concentration of 100 mM, for direct comparison to ethanol. 100 ml shake-flask cultures were prepared and grown in duplicate as before with the addition of 100 mM of each of the three additional chemicals. When glacial acetic acid was added, the culture failed to grow due to a very low pH. Therefore, sodium acetate was used to allow the pH to be controlled.

100 mM sodium acetate has a pH of 8.39 in ddH_2O. Therefore, to maintain the pH close to 7.0 the LB medium was prepared using a 100 mM phosphate buffer instead of distilled water.[226] Control cultures using phosphate-buffered LB medium but without the addition of acetate were also grown. Using these modifications, a final average DCW of 9.8 g L^{-1} was achieved. This was the largest accumulation of cell mass of any of the tested chemicals (Table 6.2), but may not be significant considering the low number of repeats and the high standard deviations reported for DCW in Section 6.3.2.

Table 6.2: Growth and molecular weight control characteristics of all additives

Additive	Dry Cell Weight (g L^{-1})	M_w ($\times 10^6$)	M_w/M_n	M_w Reduction[1] (%)
None[2]	7.4 ± 0.8	4.1 ± 0.4	2.6 ± 0.4	0
Indole[3] (3 mM)	7.6 ± 0.9	1.1 ± 0.2	2.2 ± 0.4	73.2
Ethanol (0.6%)	6.9 ± 0.5	1.3 ± 0.2	2.1 ± 0.1	68.0
Methanol (0.6%)	6.9 ± 0.6	1.6 ± 0.2	2.0 ± 0.1	60.6
Isopropanol (100 mM)	8.5 ± 0.5	1.3 ± 0.3	2.3 ± 0.3	68.5
Glycerol (100 mM)	7.0 ± 0.6	2.8 ± 0.4	1.8 ± 0.4	31.3
Acetate (0 mM)	7.3 ± 0.1	2.9 ± 0.2	2.2 ± 0.1	27.8
Acetate (100 mM)	9.8 ± 0.6	2.6 ± 0.5	2.0 ± 0.1	37.2

[1]Percentage reduction compared to no additives
[2]Average of 6 cultures of *E. coli* W3110 wild-type
[3]Average of 9 cultures using 3 strains of *E. coli* W3110
Isopropanol and glycerol results are averages of 2 repeats. All others are averages of at least 3 repeats (± standard deviation), all using *E. coli* W3110 wild-type.

The effects of each of the tested chemicals on cell growth and PHB molecular weight are summarised in Table 6.2. Isopropanol and glycerol both resulted in decreased M_w

compared to no additives, but the reduction for glycerol (31.3%) was less than for ethanol or methanol, while isopropanol had the same effect (68.5%). Acetate addition also resulted in a 37.2% decrease in M_w. However, growth in only phosphate-buffered LB medium resulted in nearly the same magnitude of decrease (27.8%), so it is not clear whether the M_w reduction was due to the addition of acetate or was a consequence of the buffered medium.

The largest reduction in M_w was caused by 3 mM indole (73.2%) and was slightly larger than for ethanol (68.0%) or methanol (60.6%). This might indicate a small additional effect of indole, although the majority of the molecular weight decrease can be attributed to ethanol. Isopropanol caused a similar decrease (68.5%) to the other alcohols, suggesting that carbon chain-length is not a factor in determining the efficiency of chain transfer agents, at least in the range of 1–3 carbons. Interestingly, glycerol decreased the M_w less (31.3%) than isopropanol. Since both molecules contain 3 carbon atoms, the number of hydroxyl groups might also be important in determining how easily each molecule can diffuse across the cell membrane.

6.4 Discussion

This investigation has revealed the striking effects of small-chain alcohols in reducing the molecular weight of PHB produced in *E. coli*. The original aim was to determine how the presence of indole in the Q-cell strain, W3110*hns*Δ93, affects the yield and properties of PHB produced therein. Indole addition reduced the rate of growth but not the final cell density or product yields. Both M_w and M_n were substantially reduced by the addition of up to 1 mM indole, with a small further reduction when the concentration was increased to 3 mM. It had the same effect in the wild-type W3110 strain, as well as in the *tnaA*-knockout strain (W3110Δ*tnaA*), which does not produce indole. This was surprising, as Δ*tnaA* should have contained lower concentrations of indole and therefore produced PHB with higher molecular weights than the other strains.

More surprising was the discovery that M_w in the 0 mM controls of each strain was as low as for the addition of 3 mM indole. This was attributed to the presence of ethanol in the control samples. An investigation into the effects of ethanol and methanol as cell culture additives gave results that agreed with those obtained for indole. Significantly, control samples containing no alcohol yielded the highest molecular weight PHB, confirming that small-chain alcohols reduce the molecular weight of PHB in *E. coli*. As discussed in Section 6.1, hydroxylated compounds are known to reduce the molecular weight of PHB, probably by mediating chain termination reactions. However, most of the attention has been on the effects of PEGs, while the M_w-reducing effects of small alcohols have only

been mentioned in passing as part of studies into PHA production using methanol as carbon source.[293–295]

Modulation of $PhaC_{Re}$ activity by the tested additives was ruled out by *in vitro* assays, which showed no change in activity up to the maximum concentrations used. It is also unlikely that low concentrations of ethanol or methanol could have a large enough effect on the expression of $PhaC_{Re}$ or the provision of 3HB-CoA to mediate the molecular weight reduction via manipulation of the enzyme:monomer ratio. Therefore, the results presented here provide support for the hypothesis that chain-transfer is mediated by hydroxylated molecules and that PEG and small-chain alcohols utilise the same mechanism.

This study focussed on the overall effect of supplementing PHB accumulation medium with hydroxylated molecules, and so can not provide further insight into the chain-transfer mechanism beyond stating that it appears to apply to a wide range of different molecules. The results for methanol, ethanol and isopropanol are in agreement with previous reports for PEG that smaller molecules induce a larger reduction in M_w. This might be because smaller molecules are more easily able to diffuse into cells through the cell membrane. Alternatively, smaller molecules might fit more easily into the active site of $PhaC_{Re}$ and so have a greater frequency of chain-transfer activity.

The smaller M_w reduction caused by glycerol in comparison to isopropanol is an interesting result. Glycerol is a molecule of similar size to isopropanol but contains three hydroxyl groups, giving it greater hydrophilicity than isopropanol. Therefore, it should cross the cell membrane less easily. The smaller effect of glycerol than of isopropanol suggests that glycerol was indeed less available for chain transfer mediation, and demonstrates that the interaction with PhaC is not the only factor that determines the efficacy of a chain transfer agent.

The data presented here demonstrate that ethanol and methanol reduce the molecular weight of PHB by up to 70%. This is in good agreement with the magnitude of weight reductions reported previously for methanol.[294] Acetate had very little effect in reducing M_w. This is also in good agreement with previous reports, which also found that succinate and lactate have little effect on M_w of PHB.[116,294] Therefore, the presence of a hydroxyl group is the most important characteristic for PHB chain transfer agents.

In comparison to PEG, both methanol and ethanol show similar maximum M_w reductions. PEG follows a similar trend to that shown in Figure 6.6 with a rapid decline in M_w followed by a plateau as the concentration increases.[117] The most effective PEG for M_w reduction is PEG-200, which is able to reduce the molecular weight by 60–80% at a concentration of 1–2 % (w/v).[117,273] A 1% solution of PEG-200 is equivalent to

approximately 50 mM. Ethanol and methanol achieved their maximum weight reduction at ~100 mM, and are therefore slightly less potent. However, they had no effect on cell growth or PHB productivity. In contrast, PEG-200 reduces viable cell counts and PHB production slightly at 50 mM and substantially at ≥100 mM.[117] Therefore short-chain alcohols have a wider operational zone than PEGs in which they can reduce M_w by the same amount without the risk of damaging productivity. Additionally, short-chain alcohols are cheaper than PEGs: at the time of writing, 100 ml of ethanol costs £3.02 while an equivalent molar quantity of PEG-200 costs £17.00 (advertised prices, Sigma-Aldrich, UK).

In conclusion, indole was shown to have no (or at least minimal) effect on the molecular weight of PHB produced by *E. coli*. The ability of short chain-length alcohols to reduce the molecular weight of PHB was confirmed and characterised. Both alcohols and PEGs share similar dynamics of molecular weight reduction, and probaly share the same mechanism. However, alcohols are less toxic to cells and significantly cheaper than PEGs and are therefore much better suited to large-scale production of low molecular weight PHAs.

Chapter 7

Imaging internal features of whole, unfixed bacteria by 'wet scanning-transmission electron microscopy'

7.1 Introduction

Despite the large amount of research into all aspects of PHA production, degradation and processing over the last four decades, one issue that is still to be fully resolved is the exact structure of the granule under natural conditions within the bacterial cytoplasm. The same is true for other types of bacterial lipid inclusions. Although the individual components of the granules (the polymer core, surrounded by proteins including various synthases, depolymerases, regulatory proteins and phasins, and possibly phospholipids) can be identified and characterised, it is still not clear in what proportions each component is present or how the components are arranged within the structure.[79] Furthermore, the initial mechanism of granule growth and the changes in structure and composition as the granule grows are also not known.

The problem is that it is difficult to obtain high resolution images of the granules, while maintaining their natural state. Optical microscopy has the advantages of easy, quick, non-invasive sample preparation but suffers from low resolution and low magnification.[80] Transmission electron microscopy provides extremely high magnification, but requires the samples to be dried, embedded in resin, cut into very thin slices and stained so as to achieve contrast between different features.[24] This makes sample preparation

an expensive and laborious undertaking, and at each stage artefacts can be introduced, which destroy any hope of maintaining the sample in its natural state.

Cryo-electron microscopy (cryo-EM) is another technique that allows high-resolution imaging of intact cells with no staining.[297] Samples are vitrified by plunging in liquid ethane cooled with liquid nitrogen. By maintaining them at liquid nitrogen temperatures, samples may be imaged under high vacuum without evaporation of water. The technique was employed by Comolli *et al.* to image PHA and polyphosphate inclusions in *Caulobacter crescentus*.[298] Although cryo-EM overcomes some of the limitations of TEM, such as the need for staining and sectioning of samples, it is necessary to use low beam currents to avoid damaging the sample and to increase contrast. This results in a low signal-to-noise ratio. Cryo-EM sample preparation is much faster than for TEM, but the success of the procedure depends greatly on the nature of the sample and on operator skill to prevent ice crystal formation. There is also the added inconvenience of maintaining samples at temperatures below $-160\,^{\circ}\mathrm{C}$. Therefore, no techniques have yet been developed that are able to quickly probe the structure of the granules within whole, hydrated, undamaged bacterial cells.

One technique that holds the potential to allow visualisation of lipid granules within the cytoplasm is wet Scanning Transmission Electron Microscopy (wet STEM).[212,299] The technique was developed as an extension of Environmental Scanning Electron Microscopy (ESEM), which was itself developed as a version of SEM that is capable of maintaining an environment around the sample to be imaged. This is achieved by pumping a gas into the imaging chamber, resulting in a substantially higher pressure than would normally be acceptable in electron microscopy (1–10 Torr). Most commonly, water vapour is chosen as it allows the preservation of the water content in hydrated samples such as biological material.[300] The water vapour also plays a direct role in imaging, by amplifying the secondary electron signal and contributing to image contrast.[212,301] In wet STEM, the environmental control mechanisms of an ESEM are used with a detector that allows the collection of electrons that have passed through a sample, thereby allowing internal structures within the sample to be imaged.

A schematic diagram of the main internal structure of an ESEM set up for wet STEM imaging is shown in Figure 7.1. The majority of the distance travelled by the electron beam after leaving the source is held at very low pressures as in standard electron microscopy (Figure 7.1 (A)). It is then focussed through two pressure-limiting apertures so that it enters the sample chamber close to the sample and only the final few millimetres of its path are in the gaseous atmosphere. The sample is deposited on a carbon-coated metal TEM grid, within a copper sample holder which sits on top of a water-cooled Peltier stage so that the temperature of the sample can be controlled. Electrons that

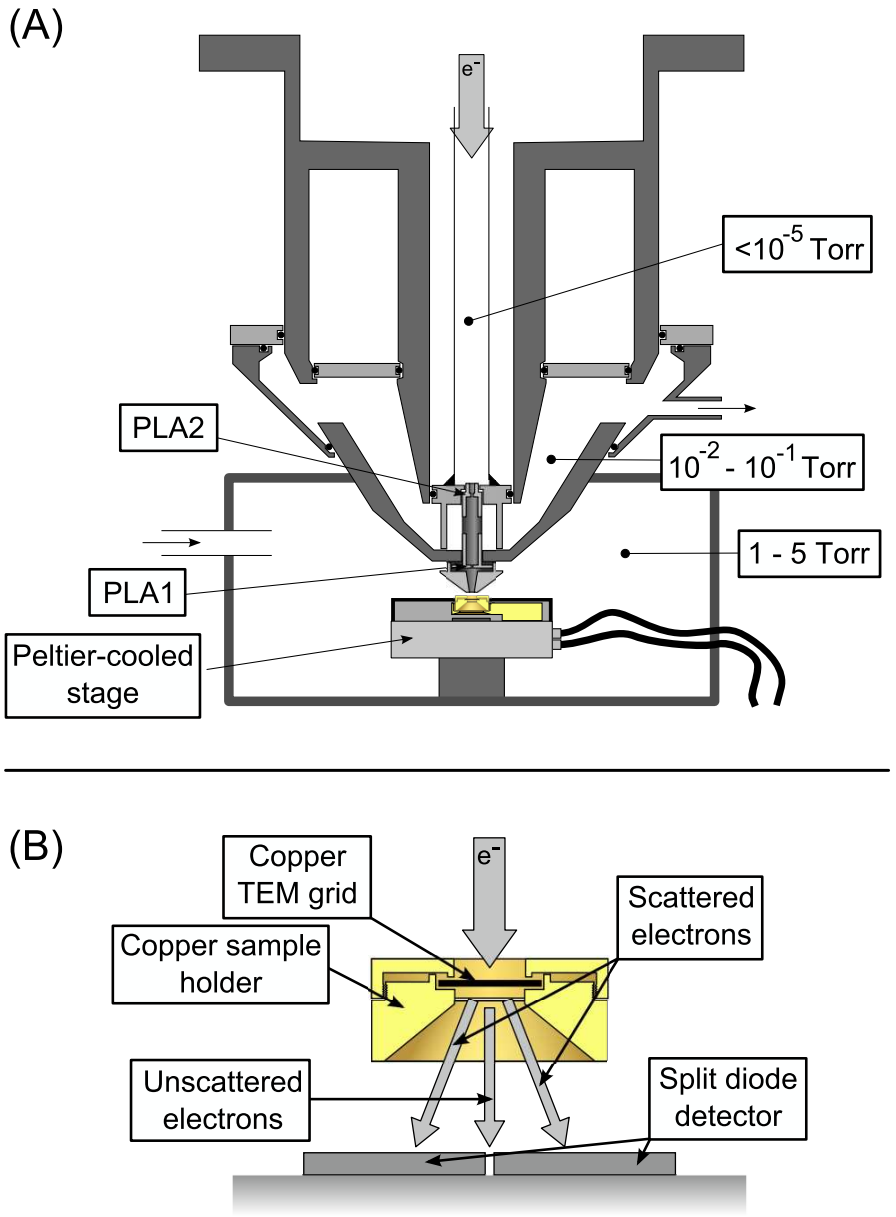

Figure 7.1: (A) Overview of the ESEM in wet STEM mode. As with secondary or backscattered electron detection, the sample chamber is maintained at a high vapour pressure relative to the majority of the electron path through the use of differential pumping and pressure-limiting apertures (PLA1 and PLA2). (B) Sample holder and detector arrangement. A copper TEM grid is held above a split-diode detector. In this setup, the relative positions of the sample and detector are fixed in the x-, y- and z-directions.

pass through the sample are gathered by a split-diode detector located below the Peltier stage, and the signal generated by the detector is converted into an image of the sample (Figure 7.1 (B)). Wet STEM has the potential to be of significant utility in many aspects of microbiology. In particular, the robust nature of bacterial cells means that they may be able to withstand the low pressure imaging environment; perhaps even to remain viable during imaging.

At present the technique is poorly characterised, especially for the study of whole bacterial cells. Despite the potential offered by the technique for easily and quickly obtaining high-resolution images of internal features of whole cells in their natural state, no such images have been reported. PHA granules are a useful exemplar to investigate the abilities and limitations of wet STEM in this respect. The inclusions vary in size from nascent agglomerations of a few nanometres to mature inclusions with diameters of 200–500 nm. This provides a good method with which to judge the resolution of wet STEM. Since PHA inclusions are composed of hydrocarbons, and are therefore of a similar density to the surrounding cell mass, they also provide a good indication of the level of contrast that is achievable.

Here, two species that are widely known to accumulate PHA were used. *R. eutropha* was chosen due to its ease of handling, high production capacity and status as the model organism for PHA_{SCL} production. The second species, *Pseudomonas mendocina*, was chosen because it produces PHA_{MCL} for comparison of granule size, structure and density. To assess the ability of wet STEM to distinguish between different lipids,TAG inclusions produced by *Rhodococcus opacus* PD630 were also imaged.

Previous studies of PHA and TAG metabolism have relied primarily on optical microscopy and transmission electron microscopy. The fluorescent stain Nile blue is known to be highly specific for PHAs, and the related Nile red and Sudan black are general lipid stains that can be used to detect TAG or PHA.[302] The inclusions can also be seen with phase contrast microscopy. However, the resolution provided by the light microscope limits the possibilities for examining the spatial distribution of inclusions, as well as making examinations of the nascent inclusions impossible. Therefore, TEM has been used for the majority of previous studies into PHA and TAG morphology. For example, cross sections viewed by TEM revealed a single phospholipid membrane and the presence of associated proteins surrounding PHA inclusions.[38,201]

Bogner *et al.* have led the way in applying wet STEM to bacterial cells.[299] However, in their technique cells remained in aqueous suspension and the only visible subcellular structure was the double membrane of *Pseudomonas syringae*. 'Liquid STEM' has also been performed on whole eukaryotic cells by containing them, suspended in liquid,

within a purpose-built microchip inside a standard scanning-transmission electron microscope.[303] However, the extra scattering caused by the surrounding liquid prevented imaging of internal features. In the study reported here, imaging conditions were selected to allow the evaporation of extraneous water, while water associated with cells remained in place. This permitted clear images of intracytoplasmic structures in hydrated, unfixed and unstained bacterial cells to be obtained. The effects of such conditions on the morphology and viability of bacterial cells were also studied.

7.2 Bacterial strains

Table 7.1 summarises the bacterial strains used in this study and their sources. The majority of the imaging, and the cell viability study were performed with *R. eutropha* H16 to examine the production of PHB. For comparison with cells containing no PHA inclusions, *R. eutropha* PHB$^-$4 was chosen: a PHA-negative mutant isolated by Schlegel *et al.*[304] To investigate the applicability of the technique to a range of species, *P. mendocina* was also used for the production of PHA_{MCL} copolymer. For imaging TAG inclusions, *R. opacus* PD630 was selected.

Table 7.1: Bacterial strains for Chapter 7

Strain	Purpose for study	Source
Ralstonia eutropha H16	Wild-type, imaging of PHB granules in cells	ATCC 17699
R. eutropha PHB$^-$4	$PhaC_{Re}$ mutant of *R. eutropha* H16 for PHB negative control	DSMZ 541
Rhodococcus opacus PD630	Wild-type, production of TAG and PHB	DSMZ 44193
Pseudomonas mendocina	Wild-type, production of PHA_{MCL}	ATCC 25411

7.3 Results

7.3.1 Comparison of wet STEM and TEM

TEM sample preparation is a lengthy process including fixing, drying, sectioning and staining. All of these can introduce artefacts. To date, TEM has been the standard method for imaging PHA inclusions within cells. Therefore, a direct comparison was made between TEM and wet STEM to establish whether wet STEM could be used as an alternative or complementary technique that would redress some of the deficiencies of TEM. A culture of *R. eutropha* was grown in nitrogen-limited mineral salts medium.

Samples taken simultaneously were imaged by either wet STEM or TEM. Representative images from both techniques are shown in Figure 7.2. The protocols for TEM and wet STEM sample preparation were as described in Chapter 3.

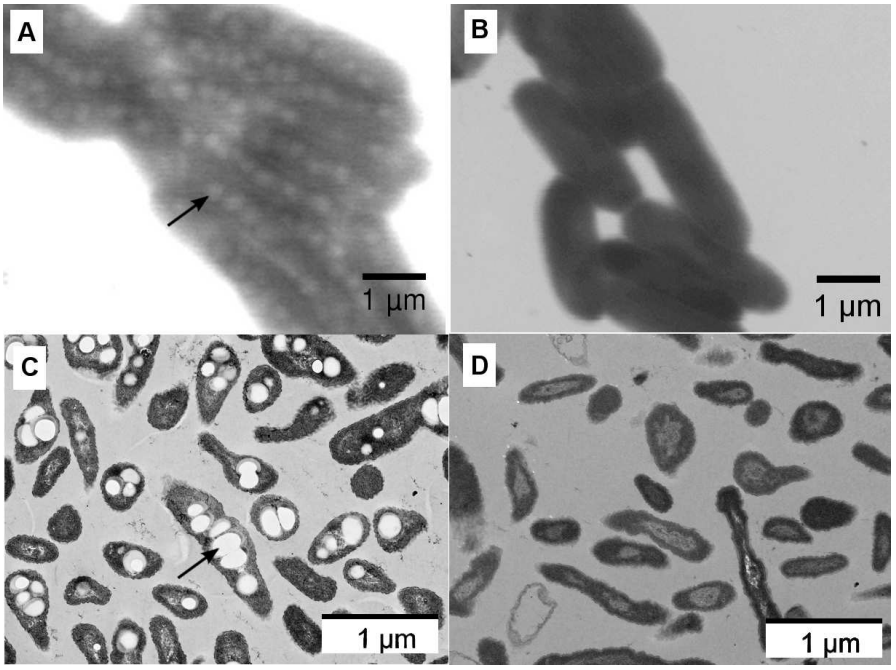

Figure 7.2: Comparison of images obtained by wet STEM and TEM. Wet STEM samples had no preparation except washing with ddH_2O, and are not stained. Images were acquired at 3.5 Torr, allowing the cells to remain hydrated. TEM samples were prepared and imaged using standard techniques (see text for details). (A) Wet STEM image of *R. eutropha* H16, containing numerous granules per cell (arrow). (B) Wet STEM image of *R. eutropha* PHB$^-$4. (C) TEM image of a section through a *R. eutropha* H16 sample, showing bacteria at a range of angles to the sectioning plane and at a range of depths. PHB granules are easily visible (arrow). (D) TEM image of a section through a *R. eutropha* PHB$^-$4 sample.

In this side-by-side comparison, the advantages and disadvantages of both techniques can be appreciated. Wet STEM (Figure 7.2 (A,B)) provides inferior absolute resolution and contrast when compared to TEM (Figure 7.2 (C,D)). However, inclusions are still clearly visible both in the wet STEM and TEM as electron-lucent patches that are not present in *R. eutropha* PHB$^-$4 (Figure 7.2). The apparent average inclusion diameters are very similar for both techniques. However, the range of diameters for wet STEM is narrower than for TEM.

While the resolution of the image is higher in the TEM, the morphology of the bacteria is substantially different. Cells imaged by wet STEM are roughly cylindrical with a smooth, uniform perimeter. Those imaged by TEM have unusual projections and areas where the membrane has pinched inwards. This is more apparent in strain PHB$^-$4

(Figure 7.2 (D)), since the presence of PHB granules physically supports the membrane in the wild-type strain (Figure 7.2 (C)). The inclusions are more resistant to this type of damage than the cell periphery, and their cross-sections appear circular (except where two granules touch) indicating that granule sizes and shapes seen in the TEM are likely to be representative of the natural state.

In the wet STEM, the cells remained hydrated throughout imaging. However, this has allowed them to aggregate more than in the TEM. Combined with the inferior resolution, this makes it difficult to distinguish between individual cells (Figure 7.2 (A)). However, as shown below, it is possible to prepare samples in such a way that individual cells can be selected and studied if necessary.

7.3.2 Optimisation of imaging pressure

Although wet STEM imaging can be performed at pressures up to ~10 Torr, there is a steady degradation in resolution and contrast as the pressure is increased, due to increased scattering of the electron beam. Therefore, a compromise must be reached between maintaining a low enough pressure to obtain good pictures and preventing damage to the cells caused by membrane disruption and dehydration. Conducting all imaging at 1 °C assists with this by reducing the vapour pressure of water in the sample.

To optimise the imaging pressure, the morphological effects of reduced pressures and electron beam exposure on bacterial samples were investigated. Samples of *R. eutropha* H16 were grown in MS medium overnight and prepared for imaging as above. The sample chamber was evacuated to 4.7 Torr, following the standard pump-down procedure. The sample was imaged at 4.7 Torr and then the beam stop was activated to reduce beam damage. This pressure was maintained for a further 10 minutes, before the chamber was pumped to the next pressure (3.7 Torr). This cycle was repeated until images of the sample had been collected at all of the target pressures. Figure 7.3 shows samples at four representative pressures: 4.7, 3.7, 2.7 and 0.7 Torr.

A low level of magnification was used to increase the number of cells that could be viewed. Since the same portion of the sample was exposed to the beam for the duration of the experiment, focus and contrast adjustments were made as rapidly as possible before images were acquired, and then exposure to the beam was terminated. Therefore, the images are not optimised to allow fine detail to be viewed. However, large PHA inclusions are visible in many of the cells at all pressures, as demonstrated by the inset to Figure 7.3 (A). The appearance of the bacteria at all pressures is very similar, with the cytoplasm apparently remaining dispersed throughout the cell. A few cells in Figure 7.3 appear very dark. These are assumed to be lying on top of other cells, so that the total

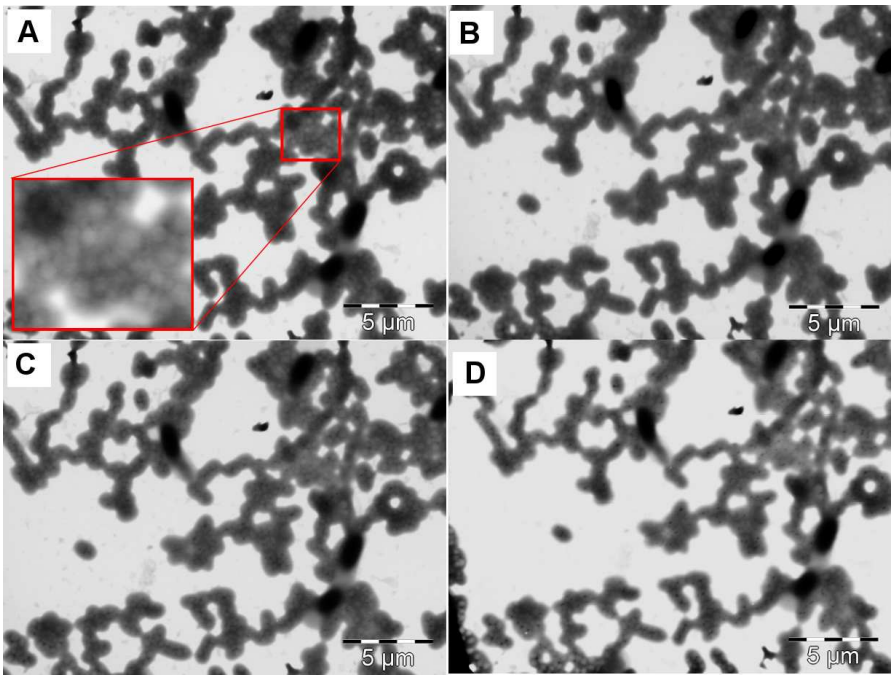

Figure 7.3: Morphology of samples at various pressures. A series of images was acquired using wet STEM mode at vapour pressures of 4.7 Torr (A), 3.7 Torr (B), 2.7 Torr (C) and 0.7 Torr (D). The inset to (A) is a magnified view of cells in which PHA inclusions are visible. All images are from a single sample of *R. eutropha* grown overnight in MS medium. There is very little apparent change in the large-scale morphology of the bacteria across the pressure range investigated here.

thickness prevents transmission of electrons. There was some reduction in the quality of the image obtained by the time the sample was imaged at 0.7 Torr. When a section of the sample grid that had been previously unexposed to the electron beam was imaged following stepwise depressurisation, the image quality was restored (Figure 7.4 (B)). This demonstrates that although the pressures used had little effect on visible cell morphology, beam damage was a significant factor. Therefore, imaging times were minimised where possible.

According to Donald[212], the critical vapour point of water at 1 °C is approximately 5 Torr. However, the experiments with bacterial cells suggested that they tend to prevent evaporation of the surrounding water, probably due to hydrophilic interactions with cell-surface molecules. Extraneous water reduces image quality, so it is preferable to employ a mildly dehydrating environment. Complete evaporation of the water droplet occurred at 3.5–4.0 Torr. Therefore, the cells in Figure 7.3 (C) and (D) were certainly dehydrated. With these considerations in mind, the optimal imaging pressure for subsequent experiments was determined to be 3.5 Torr.

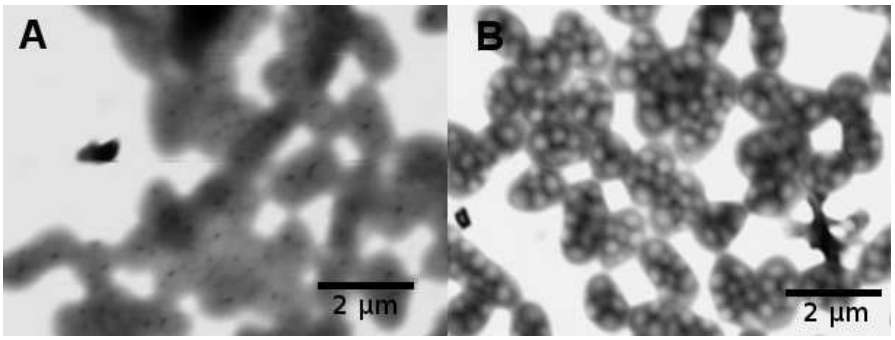

Figure 7.4: Illustration of electron beam damage incurred by the sample following repeated imaging of the same area. (A) Magnified area of the final image in the pressure series shown in Figure 7.3 (D). (B) A separate image, acquired from the same sample, under the same conditions, but from an area that had not been exposed previously to the electron beam.

7.3.3 Imaging of intracellular inclusions in bacteria

If only the intracellular structures such as PHA granules are of interest, it is possible to obtain clearer images by using lower pressures. This allows water to evaporate from the samples, causing the cytoplasm to shrink away from the cell wall, and so reduces electron scattering. To test the efficacy of this technique a modified pump-down procedure was used, in which the chamber was pumped from atmospheric pressure to 2.0 Torr, flooded with water vapour to 9.0 Torr and then pumped to 2.0 Torr again. This cycle was repeated five times, before the sample chamber was pumped to the working pressure of 1.5 Torr.

Some areas showed obvious membrane damage and cytoplasm leakage due to the low pressure, whereas other areas appeared similar to those imaged in fully hydrated conditions. In the undamaged sections, PHA or TAG inclusions were easily visible, appearing as electron-lucent patches within cells (Figure 7.5). TAG and PHA inclusions are of sufficiently similar electron density and morphology to be indistinguishable by observation alone. However, there were generally more TAG inclusions per *R. opacus* cell than for PHA inclusions per *R. eutropha*.

After prolonged accumulation time, the inclusions appeared to fill the majority of the intracellular volume. In these cases, overlapping and deformation caused by the close proximity of inclusions to one another was observable (Figure 7.5 (A)). This effect was not as pronounced for *P. mendocina*, which still had relatively small PHA inclusions

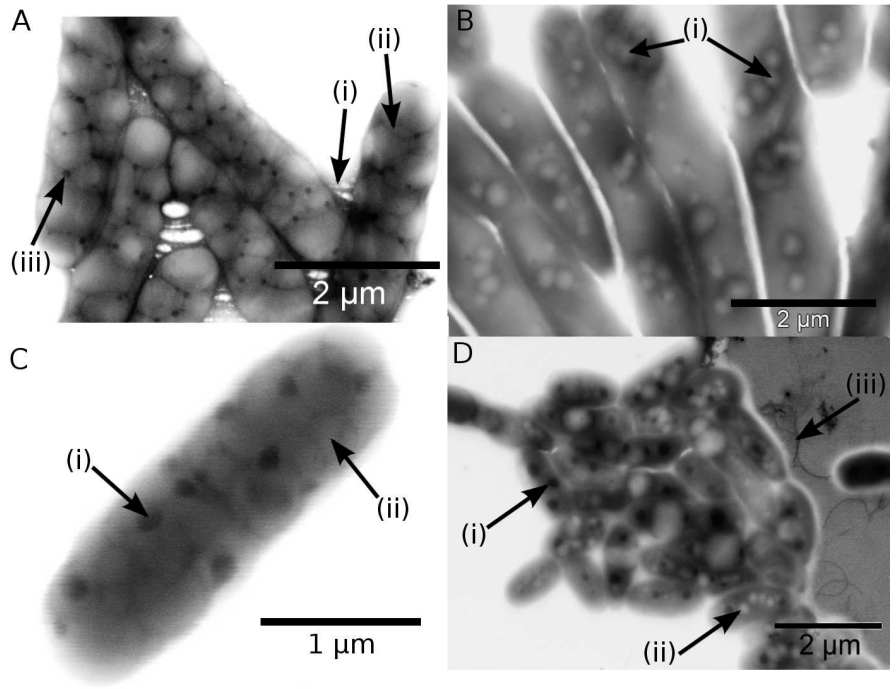

Figure 7.5: Wet STEM images of lipid storage inclusions in three species of bacteria. (A) *R. eutropha* H16 grown in MS for 72 hours. (i) extracellular polysaccharides (ii) overlapping area of two large PHB inclusions (iii) electron-dense inclusion (B) *R. eutropha* H16 grown in NR for 24 hours. (i) small PHB inclusions (C) *R. opacus* grown in MMR for 48 hours. (i) electron-dense inclusion (ii) TAG inclusion (D) *P. mendocina* grown in MMP for 48 hours. (i) electron-dense inclusion (ii) PHA inclusion (iii) flagella. The contrast on the right-hand side of this image was adjusted to show the flagella more clearly.

(approximate mean of 200 nm) after 48 hours of accumulation. Pseudomonas species including *P. mendocina* are widely known to produce copious quantities of the exopolysaccharide alginate[305,306]. Inclusions were slightly obscured, and cells appeared to be stuck together in *P. mendocina* samples by what was assumed to be a layer of alginate, which contributed to electron scattering (data not shown).

When only a small fraction of the cell volume was occupied by PHA (Figure 7.5 (B)), the dehydration of the cytoplasm allowed the membrane to collapse around the granules. This caused a variegated appearance of cells, where the electron beam could pass more easily through the reduced thickness. However, near to the inclusions the membrane was supported. This maintained some of the cell thickness, causing a dark perimeter around each inclusion. Additionally, the inclusions tended to be grouped together. This was probably due to the retracting cytoplasm pulling inclusions together as water evaporated.

Other structural features such as flagella (Figure 7.5 (D)) could also be resolved, setting

a resolution limit of 10–15 nm. All three species of bacteria additionally contained electron-dense bodies, which were assumed to be polyphosphate granules. These are known to be accumulated by the species concerned, and are often associated with PHA and TAG inclusions[302,307–309]. The electron-dense granules in *P. mendocina* and *R. opacus* (up to ~450 nm diameter) were substantially larger than those in *R. eutropha* (up to ~150 nm diameter) although all species had similar numbers per cell.

7.3.4 Cell viability during imaging

All conventional forms of electron microscopy necessitate the killing of cells during the sample preparation procedures. Due to the high doses of electron radiation experienced by cells during imaging, one can assume that any bacteria that are imaged by wet STEM are also killed in the process (D. Waller, personal communication). However, if those on other parts of the grid remain viable, it would indicate that the only significant damage incurred by cells is due to the unavoidable effects of the imaging process rather than the surmountable low-pressure environment or sample preparation.

A simple experiment was conducted to investigate the effects of the wet STEM imaging conditions on the viability of *R. eutropha* H16. Tests were carried out in duplicate. Samples were prepared as before and subjected to 10 minutes at 4.0, 3.5 or 1.5 Torr without imaging. The grid was incubated in 50 μl NR medium for 40 hours at 30 °C, and viability was assessed by measuring an increase in OD_{600} in a sample of the growth medium(Table 7.2). A sample was also allowed to dry on a grid at room temperature and pressure to control for the effects of drying. Samples that had not grown after 40 hours failed to do so upon further incubation (data not shown). Since the OD_{600} value does not give a quantitative measure of the proportion of cells that survived the low pressure environment, here the results are presented simply as positive/negative. Samples that showed a positive result for growth had reached OD_{600} = 0.4–0.8, corresponding to late exponential phase/stationary phase. Samples that failed to grow remained below OD_{600}= 0.01. Note that the OD_{600} values were recorded with a Nanodrop spectrophotometer with a sample size of 2 μl and a path-length of 0.1 cm, and are not directly comparable to those achieved with more orthodox equipment.

As shown in Table 7.2, most samples were able to grow following washing and resuspending in water, and exposure to low pressures. One air-dried sample failed to grow, suggesting that the effect of drying the sample onto the grid is likely to be more significant than low pressure. It also suggests that the pump-down procedure and presence of water vapour surrounding the cells are effective in protecting against complete dehydration of the sample. Samples were able to grow following exposure to all test pressures.

Table 7.2: Growth of *R. eutropha* H16 after wet STEM preparation procedure and exposure to low pressure for 10 minutes

Sample	Growth after 40 hours?	
	Test 1	Test 2
Medium only	✗	✗
Grid only	✗	✗
Positive control	✓	✓
Air-dried	✓	✗
4.5 Torr	✓	✓
3.0 Torr	✓	✓
1.5 Torr	✓	✓

This suggests that the cells were not severely damaged by the preparation procedure or the low pressures.

The OD_{600} after 40 hours represents the cell density of cultures that have progressed beyond the exponential growth phase, and so is not proportional to the original number of cells surviving the pressure test. This means it is not possible to calculate the proportion of surviving cells for any individual pressure. For example, if only a few cells survived a pressure of 1.5 Torr, they would still have sufficient time to reach the same final OD_{600} as a sample at higher pressure with many thousands of survivors. Therefore, the extent of the dependence of cell viability on their state of hydration is not clear. A more rigorous experiment was conducted, in which *R. eutropha* H16 cells were exposed to pressures of 5.0, 4.0, 3.5, 3.0, 2.5, 2.0 and 1.0 Torr in addition to the same controls as before. 1 μl samples were prepared as before and deposited on small pieces of glass cover slip. The previous testing conditions were employed, but the cells were then resuspended in NR medium and plated onto NR agar. Following overnight growth at 30 °C, cell survival was quantified by counting the number of colonies on each plate. 3 samples were tested for each pressure.

The colony counting method of assessing *R. eutropha* viability in the wet STEM supports the hypothesis that the most significant factor in decreasing viability is evaporation of water from the sample after placing on the grid, rather than of the low pressure. Table 7.3 shows a decrease from approximately 2×10^9 colony forming units (CFU) per ml in the positive control to approximately 3×10^7 CFU ml^{-1} in the air-dried control. Both experiments were carried out at room temperature, so the decrease in viability by a factor of 64 can be attributed to the effects of drying.

Table 7.3: Colony forming units (CFU) of *R. eutropha* following wet STEM preparation procedure and exposure to low pressure for 10 minutes

Sample	**CFU per ml** ($\times 10^7$)			
	Test 1	Test 2	Test 3	Average
Medium only	0	0	0	0
Cover slip only	0	0	0	0
Positive control	208	208	208	208[a]
Air-dried	3.04	2.62	4.08	3.25 ± 0.75
5.0 Torr	53.2	53.2	53.2	53.2[a]
4.0 Torr	3.56	4.54	6.00	4.70 ± 1.23
3.5 Torr	3.46	4.80	4.90	4.39 ± 0.80
3.0 Torr	5.06	5.22	2.93	4.40 ± 1.28
2.5 Torr	2.02	5.02	6.50	4.51 ± 2.28
2.0 Torr	2.62	2.57	4.97	3.39 ± 1.37
1.0 Torr	2.03	1.30	2.20	1.84 ± 0.48

Average figures reported ± standard deviation.
[a]Approximate figure with no standard deviation due to large numbers of colonies

This is further supported by the finding that the samples exposed to 5 Torr only suffered a 4-fold decrease in viability to approximately 5×10^8 CFU ml^{-1} (Table 7.3). 5 Torr is not a sufficiently low pressure to evaporate the water from the sample, and a droplet remained after 10 minutes exposure. Therefore, the cells were protected from the effects of drying. It is not clear whether the smaller observed decrease in viability was due to a small amount of drying (perhaps at the edges of the droplet) or to the low pressure. The 4.0 Torr samples (and all lower pressures) had evaporated after 10 minutes. However, on average, slightly more colonies were formed for all pressures except 1.0 Torr than for the air-dried control. This suggests that the controlled pumping procedure was effective in allowing the evaporation to take place gently, and that low pressure itself does not have a large effect on bacterial viability.

Figure 7.6 shows the trend for increased viability at higher pressures, particularly at pressures that are sufficient to maintain a water droplet around the cells. There was an 11-fold reduction in viability between 5.0 and 4.0 Torr, probably due to the evaporation of water. Below 4.0 Torr, there was no significant difference in viability until 2.0–2.5 Torr. The viability was again slightly reduced below this pressure, either due to rupturing of the membrane caused by low pressure, or possibly to the eventual release of water that was complexed with cell-surface molecules and thus providing some protection from total evaporation.

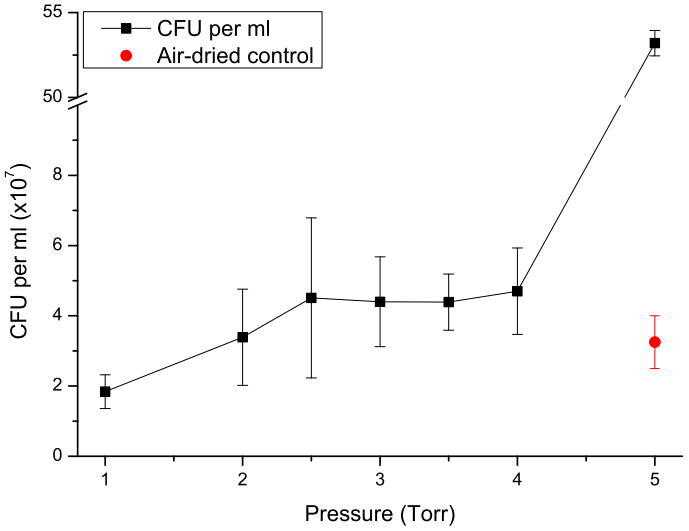

Figure 7.6: Survival of *R. eutropha* following wet STEM preparation and exposure to a range of low pressures for 10 minutes. For comparison, a point corresponding to the survival of cells in the air-dried control is also shown (red circle). Each point represents the average of three repeats, with error bars signifying the standard deviation.

No growth was seen in the negative controls for either viability experiment. This indicates that the sample handling procedures were sufficiently hygienic to avoid introducing contamination to the samples. However, since antibiotics were not used, additional measures were employed to verify the purity of the samples. Cultures that grew were subjected to Nile Blue staining and viewed by fluorescence microscopy. The presence of PHA inclusions was confirmed (data not shown), and ruled out the most likely candidates for contamination. Cultures were also successfully grown on mineral salt agar plates, with citrate as the sole carbon source (data not shown).[310] These are known to be selective for *R. eutropha*.

7.4 Discussion

Contrast in wet STEM is generated through differential scattering between areas of different mass density. Since the inclusions are only slightly less dense than the cytoplasm, this indicates that wet STEM is a sensitive technique for distinguishing between biological materials without staining. A wider range of inclusion diameters and cell

morphologies were seen for TEM than for wet STEM. This is due to the effects of sectioning during TEM sample preparation. During sectioning one cannot know which plane through a given cell (and the granules within) will be exposed. Consequently, it cannot be known at which depth a particular inclusion was sectioned, making calculation of inclusion volume almost impossible. Figure 7.2 (B) demonstrates this effect, showing sections through both the sagittal and transverse planes, and many intermediates. Tian *et al.* attempted to address this issue by estimating the actual size of inclusions from many cross-sections, using unbiased stereology[24,111]. Although very accurate, this is an extremely time-consuming method. It would also not be appropriate for examining features that are affected more by the preparation process than are PHAs.

In wet STEM, cells rest on the carbon film, so that they are all effectively in the same plane, and the image is acquired through the entire thickness of the bacterium, forming a two-dimensional projection of the cell. Since the image is effectively the average of sections at all possible heights, the apparent dimensions of the cells and any internal features therefore represent the maximum dimensions. This enables a fast and reliable measurement of the dimensions of many cells in one field of view. The combination of hydrated morphology and projected images means that wet STEM can provide information about the nature of the biological samples that can be used to complement the undoubted resolution and contrast advantages of TEM.

Although the main selling point of wet STEM for bacterial imaging is that it can maintain cells in a hydrated state, the images obtained at 3.5 Torr were rather blurry and had significantly lower resolution than the TEM images (Figure 7.2). This might be acceptable for imaging relatively large features such as PHA inclusions, but presents a barrier for imaging anything smaller than about 100 nm. As shown in Figure 7.5, one solution is to purposefully allow dehydration of the cells so that the membranes collapse inwards. This decreases the total thickness of the cells, and so allows more electrons to pass through resulting in clearer images with greater resolution.

The technique of controlled dehydration of bacterial cells for wet STEM imaging was pioneered by Staniewicz *et al.*, and its effects were studied using *E. coli.*[311] They argued that although the technique clearly introduces artefacts, it also provides structural information about the inside of bacterial cells that is not available by other means. For example wild-type and $\Delta mreC$ strains of *Salmonella enterica* serovar Typhimurium exhibited distinct patterns of light and dense material after dehydration due to the inability to anchor the actin-like cytoskeletal protein MreB to the cell membrane following the loss of expression of MreC. Using the controlled dehydration method obviously sacrifices the advantages of maintaining the hydration of cells. In this case, the main advantage is ease and speed of use. Compared to SEM or TEM, the sample preparation time and cost

are far lower. Therefore, wet STEM could be seen as a bridge between light microscopy (with its ease of use) and electron microscopy (with its high magnification).[311]

A large reduction in viability was seen when *R. eutropha* cells were exposed to low pressures in the microscope chamber (Table 7.3). However, as a similar reduction was observed simply by allowing a sample to dry at atmospheric pressure, the reduction in viability was probably due to removal of water, rather than the low pressure. The design of the pump-down procedure is therefore important to ensure that the pressure is not reduced too quickly, which causes cells to lyse. There is also evidence that a carefully optimised pumpdown procedure could provide some protection against the effects of dehydration (Figure 7.6). According to these results, only 1–2% of the cells in a sample are viable after 10 minutes at an imaging pressure of 3.5 Torr. Therefore, it is not possible to conclude that wet STEM is an appropriate technique for imaging live cells.

It is probable that the colony-counting assay for cell viability underestimated the number of viable cells. Although the cover slips were incubated on ice for ~3 hours to allow rehydration and detachment of cells and were then vortexed vigorously to further dislodge attached cells, it is likely that some cells remained attached to the glass surface. This is a possible explanation for the much larger number of cells surviving a pressure of 5.0 Torr in which fewer cells could be expected to attach to the surface (Table 7.3). It was not possible to quantify the proportion of cells remaining attached, but it can be assumed to remain constant for each pressure below 5.0 Torr. Therefore, the trend shown in Figure 7.6 probably remains valid.

An alternative method to quantify the proportion of cells remaining could be to use a live/dead cell staining kit. This method was employed by Susan Kirk (Cavendish Laboratory, Cambridge, U.K.) in a previous Ph.D. thesis using a mixture of propidium iodide (red) and CYTO-13 (green) dyes.[312] Propidium iodide stains only dead cells, while CYTO-13 stains only live cells. *E. coli* were exposed to various pressures for 10 minutes in a similar experiment to that employed here, then were stained and viewed by fluorecence light microscopy to determine the proportion of cells remaining alive. The results showed a similar pattern to that seen in Figure 7.6, with no difference in viability down to approximately 2.5 Torr and a slight decrease for pressures below this. However, the proportion of surviving cells at pressures above 2.5 Torr was ~75%. This suggests that a large proportion of the cells in the colony-counting experiment remained attached to the cover slip, leading to underestimation of the true viability.

Beyond the dehydration-induced loss of viability there was little further loss at pressures as low as 1.0 Torr. This is perhaps to be expected, as bacteria are routinely lyophilised for long-term storage with no great detriment to their viability. However, it is not yet clear how much of an effect this has on the overall structure of the cells. Further studies

are required to establish when or if deliberately allowing dehydration of bacterial samples is an appropriate method for increasing resolution. Recently, alternative forms of ESEM have been designed, which allow more controlled dehydration of samples [313]. In future, these may allow a finer balance between sample protection and imaging quality.

These cell viability results also do not take into account electron beam damage, which could be a significant problem during imaging (Figure 7.4). The total time of exposure to the beam to acquire the image in Figure 7.4 (A) was on the order of around 10 minutes. However, this was a summation of several imaging procedures at different pressures. Therefore, although care should be taken to minimise exposure to the beam, sufficient time to image samples should be available during routine operation.

7.5 Conclusions

In comparison to the more established techniques of TEM and STEM, wet STEM is disadvantaged in terms of resolution and contrast. However, being able to compare TEM images with quickly and easily obtainable images from whole, unfixed, unstained cells could be of great advantage in the study of bacterial morphology.

In this exploratory study, PHA and TAG inclusions were imaged within bacteria and it was shown that the cells are likely to remain in, or close to, their natural state provided that appropriate conditions are selected. PHAs and TAGs, as hydrocarbons, are not substantially less dense than the cytoplasm and other surrounding structures. Nevertheless, they are readily observed as more electron-lucent inclusions within cells, demonstrating the utility of wet STEM for imaging such structures without staining. Denser structures such as the polyphosphate inclusions that were frequently found to be produced simultaneously with PHAs and TAGs were also easily distinguished in the pictures. Other bacterial inclusions such as carbonosomes, magnetosomes and misfolded protein inclusion bodies could potentially also be readily studied using wet STEM.

The cell viability assay suggested that the majority of cells are killed due to dehydration at pressures below 5.0 Torr. However, there is evidence from previous studies to suggest that the colony-counting technique might lead to a gross underestimate of cell viability due to cell adhesion to the glass cover slips used to hold the sample. Further reduction of pressure only led to a small decrease in viability: therefore wet STEM provides a relatively large range of pressures in which imaging can be carried out without affecting viability. Further research should be conducted to find better methods of recovering cells after imaging, or to allow imaging while the cells remain suspended in a liquid droplet. The results presented here suggest that a pressure of 3.5 Torr should be used when

the overall structure of the cell is important, or when the introduction of artefacts is unacceptable. Clearer, high-resolution images can be obtained by controlled dehydration to allow more detailed study of the internal structure of bacteria. For this, an appropriate pressure would be in the range of 1.5–2.0 Torr.

More characterisation of the technique is necessary to overcome its limitations and realise its potential. Improvements in the detector may allow for enhanced signal-to-noise ratios and the resolution of finer structural details. Further work is also necessary to fully understand the effects of the imaging conditions on various samples and to ascertain whether unexpected artefacts are introduced. Finally, it is important to further investigate the viability of bacterial (and other) cells under these conditions and to develop techniques for re-imaging the same sample to allow the study of temporal developments.

Chapter 8

Conclusions and future perspectives

The overall aim of this thesis was to investigate ways to improve the production of polyhydroxyalkanoates and PHA synthase enzymes in *E. coli*. The general approach was to investigate new methods in a simple fashion, so the focus was on the production of PHB and on the class I synthase from *R. eutropha*. Two expression systems were investigated for improved production of $PhaC_{Re}$: Q-cells and co-expression of chaperone proteins. To help with the control of the material propeties of PHB, small-chain alcohols were used to reduce and control the molecular weight. Finally, wet STEM was investigated to assess its potential as a high resolution imaging method that causes minimal damage to cells, to understand better the dynamics of PHA granule growth.

In this final chapter, the major results of each experiment are summarised, and possibilities for future investigations in the same areas are discussed.

8.1 The Quiescent-cell system

The Q-cell system was originally developed for highly efficient protein production by uncoupling protein synthesis from the generation of biomass.[222] It had previously been used successfully for the production of a human antibody fragment and GFP, so the indications were that it was a good platform technology for the production of proteins, generally. However, despite efforts to optimise the expression of $PhaC_{Re}$ both at 30 °C and at 37 °C, the yields achieved in Chapter 4 were not sufficient to conclude that Q-cells are any better at producing $PhaC_{Re}$ than standard cultures. Q-cells were able to produce more $PhaC_{Re}$ per cell than standard cultures, but the lower cell densities

cancelled out the improvement. This is in contrast to previous studies in which Q-cells were more productive despite the lower cell density.[237]

It was disappointing that Q-cells were not more effective producers of $PhaC_{Re}$, but this does not rule out the potential for further studies to be carried out, either to further improve $PhaC_{Re}$ production or for the production of other proteins. $PhaC_{Re}$ is known to be a difficult protein to overexpress due to its propensity to aggregate, so this may have contributed to the low yields. The presence of a C-terminal His_6-tag probably also affected the stability of the protein and may also have reduced the yield.[253] Additionally, although the sequence of plasmid pASG1$phaC_{Re}$ was verified, yields in standard cultures were also low, so there is the possibility to redesign the expression plasmid to improve production.

A further strategy that would be interesting to investigate would be the secretion of proteins by Q-cells. This was employed for the production of the 3PF12 antibody fragment, which is so far the protein produced in the largest quantity by Q-cells.[237] Secretion to the culture medium by the addition of a signal peptide to $PhaC_{Re}$ or another protein would decrease interactions between individual proteins (because the volume of medium is much larger than that of the cells) and so reduce the chances of aggregation. Recovery costs could also be reduced, as there would be no need to rupture cells. The secretion strategy should be particularly effective for Q-cells because they remain metabolically active for longer than standard cultures, and so they should be able to continue secreting protein into the medium after the time that the available space inside cells would be exhausted. Fermentor cultures of Q-cells have also proved to be more productive than shake-flask cultures, possibly because of better nutrient availability.[222] Therefore, further studies should be conducted into secretion of protein such as $PhaC_{Re}$ in fed-batch fermentations of Q-cells.

The continued metabolic activity of Q-cells might also make them useful for the production of molecules other than proteins. If the central metabolic pathways such as the TCA cycle and fatty acid synthesis/degration remain active, Q-cells could be an efficient cell factory for the production of small metabolites,[314] biofuels,[315] hydrogen,[316] and drugs.[317] A relatively simple but instructive model for this investigation, related to the work in this thesis could be the production of 3-hydroxybutyrate (3HB). Production of 3HB only requires the introduction of the PhaA and PhaB enzymes to produce 3HB-CoA, and thioesterase II (TesB) to remove the CoA.[318] 3HB production in Q-cells would demonstrate the continued activity of the TCA cycle and provide a measure of the potential productivities. 3HB also has some commercial applications as a building block for the synthesis of chiral fine chemicals.[288]

8.2 Chaperone protein co-expression

Even if Q-cells had produced significantly larger quantities of $PhaC_{Re}$ than standard cultures, the indication from the SDS-PAGE analyses was that protein solubility was not improved in Q-cells. The prevention of aggregation is a significant problem in $PhaC_{Re}$ production, so a solution to the problem was sought by co-expressing chaperone proteins with $PhaC_{Re}$ to assist its folding. Of the 5 chaperone systems tested, GroEL/GroES and Trigger factor were found to be most effective, increasing the recovery of soluble protein without affecting the activity. This led to yields of $PhaC_{Re}$ that were approximately 3× those from cells expressing $PhaC_{Re}$ only (Chapter 5).

The results from Chapter 5 provide an indication of the yields that could be expected from the chaperone co-expression system. However, large quantities of $PhaC_{Re}$ remained insoluble, so there is still room for optimisation. This could be through varying the strength of induction of either $PhaC_{Re}$ or of the chaperones. For example, gentler induction of $PhaC_{Re}$ expression by lower concentrations of IPTG would be less likely to overwhelm the protein production machinery and so allow more time for individual proteins to fold correctly. It might also be interesting to study the effects of protein secretion in the presence of chaperone proteins as a method to reduce the interactions between $PhaC_{Re}$ molecules to reduce aggregation. This might also be combined with production in Q-cells, to take advantage of the increased length of metabolic activity and to further increase production capacity.

Chaperone co-expression should also be tested for the production of PHA synthases other than $PhaC_{Re}$. The technique has been used successfully for the production of other proteins,[258] so should be generally applicable to all PHA synthases. However, it would be interesting to discover whether the same chaperones would be most effective for other synthases (particularly classes II-IV) and to what extent the same expression conditions could be used. It is hoped that the increased yields of $PhaC_{Re}$ with chaperone co-expression will facilitate the production of the enzyme in order to understand its structure and function, and to produce large quantities for *in vitro* PHA production.

8.3 Control of PHB molecular weight

Hydroxylated compounds have previously been suggested to mediate chain transfer reactions during PHA synthesis *in vivo*, and therefore to reduce the molecular weight of the polymer.[116,117] However, the majority of the work thus far has focussed on poly(ethylene glycol) (PEG).[273] Therefore, in Chapter 6, the effects of ethanol and methanol on PHB molecular weight were compared to the published results for PEG.

Both of the alcohols tested were able to reduce the molecular weight of PHB by the same amount as reported for PEG, at similar concentrations. Small-chain alcohols are better candidates for chain-transfer agents in the large-scale production of PHB as they are cheaper, less toxic and potentially can be produced endogenously.

As with the previous experiments, PHB production was used here as a simple model, but the results should be widely applicable to PHA production generally. Therefore, it would be interesting to investigate the effects of small-chain alcohols on PHA produced in other species of bacteria (including natural PHA producers), particularly those that produce PHA_{MCL}. Further characterisation of the material properties of PHAs with different molecular weights should also be carried out, particularly to determine the optimal weights for the production of commercially-relevant blends and composites.

8.4 Visualising granules within cells by wet STEM

The final study utilised a new electron microscopy technique called wet STEM, which was designed to allow the study of the internal structure of hydrated samples without the need for fixing, staining and sectioning. It had only previously been used once with bacterial samples, but no significant internal structures were seen.[312] Therefore, the study of PHA, triacylglyceride and polyphosphate granules described in Chapter 7 was the first of its kind. As an exploratory study of the potential applications of wet STEM in PHA research, or in the wider field of bacteriology, Chapter 7 has developed a basic protocol for sample preparation and provided some guidelines on the ease-of-use of the microscope and its limits of resolution.

The overall conclusion was that wet STEM could be a useful intermediate tool between light microscopy and electron microscopy. It combines the benefits of simple and quick sample preparation, minimal sample damage and ability to image whole cells that are associated with light microscopy with the higher magnification of electron microscopy. However, using a colony-counting protocol it was not possible to ascertain to what extent the wet STEM can maintain the viability of cells during imaging. Only a few percent of the cells in the assay survived the test conditions; however, this is likely to be an underestimate of the viability because many cells remained attached to the glass substrate after exposure to low pressure.

As with any new technique, wet STEM requires much further optimisation and characterisation. The technique is gradually being put to more uses, including for the imaging of colloidal suspensions, polymers, mammalian cells and bacteria.[311,319] There are also alternative designs of sample chamber for the preservation of biological samples, which

should be compared to establish the relative benefits and drawbacks of each.[303,313] As the technique evolves and is improved, it is likely to become more widely used for detailed structural studies of bacterial morphologies. The greatest benefit of wet STEM is probably the straightforward sample preparation procedure. This is likely to make it of great use for structural and temporal studies of dynamic features within bacteria, particularly those that are relatively large such as lipid body inclusions, magnetosomes, and spores.

Other high-resolution imaging techniques have also been developed over the last decade, so for a particular application it is worthwhile assessing the relative merits and disadvantages of each technique. For example, cryo-electron tomography images many thin sections using TEM and reconstructs a 3-dimensional representation of the sample. This has recently been used to study the growth and localisation of PHA granules.[320] Compared to wet STEM, the technique is very slow and laborious but it has the significant advantage of producing 3-dimensional images. Super-resolution light microscopy techniques such as Stimulated Emission Depletion (STED) and Stochastic Optical Recognition Microscopy (STORM) have also become increasingly popular, but typically require relatively long times and significant computing power in addition to expensive fluorescent markers. Alternatively, single-molecule detection techniques such as Surface-Enhanced Raman Spectroscopy (SERS) can be used to build a visual representation of a sample by combining the spectroscopic information from a matrix of spectra. As with the other techniques, SERS microscopy is also relatively slow and reliant on computing power. Therefore, at present, wet STEM maintains its advantage over other techniques in its relative ease and speed of use combined with high magnification power.

Bibliography

[1] Thompson, R.C., Swan, S.H., Moore, C.J. and vom Saal, F.S. (2009) Our plastic age, *Philosophical Transactions of the Royal Society of London. Series B, Biological sciences*, **364**, 1973–1976

[2] Derraik, J.G.B. (2002) The pollution of the marine environment by plastic debris: a review, *Marine Pollution Bulletin*, **44**, 842–852

[3] Benedict, C.V., Cameron, J.A. and Huang, S.J. (1983) Polycaprolactone degradation by mixed and pure cultures of bacteria and a yeast, *Journal of Applied Polymer Science*, **28**, 335–342

[4] Nampoothiri, K.M., Nair, N.R. and John, R.P. (2010) An overview of the recent developments in polylactide (PLA) research, *Bioresource Technology*, **101**, 8493–8501

[5] Sudesh, K. and Iwata, T. (2008) Sustainability of biobased and biodegradable plastics, *CLEAN - Soil, Air, Water*, **36**, 433–442

[6] Verlinden, R.A.J., Hill, D.J., Kenward, M.A., Williams, C.D. and Radecka, I. (2007) Bacterial synthesis of biodegradable polyhydroxyalkanoates, *Journal of Applied Microbiology*, **102**, 1437–1449

[7] Lee, S.Y. (1996) Plastic bacteria? Progress and prospects for polyhydroxyalkanoate production in bacteria, *Trends in Biotechnology*, **14**, 431–438

[8] Wältermann, M., Stöveken, T. and Steinbüchel, A. (2007) Key enzymes for biosynthesis of neutral lipid storage compounds in prokaryotes: properties, function and occurrence of wax ester synthases/acyl-CoA: diacylglycerol acyltransferases, *Biochimie*, **89**, 230–242

[9] Philip, S., Keshavarz, T. and Roy, I. (2007) Polyhydroxyalkanoates: biodegradable polymers with a range of applications, *Journal of Chemical Technology and Biotechnology*, **82**, 233–247

[10] Tsuge, T. (2002) Metabolic improvements and use of inexpensive carbon sources in microbial production of polyhydroxyalkanoates, *Journal of Bioscience and Bioengineering*, **94**, 579–584

[11] Huang, C.J., Lin, H. and Yang, X. (2012) Industrial production of recombinant therapeutics in *Escherichia coli* and its recent advancements, *Journal of Industrial Microbiology and Biotechnology*, **39**, 383–399

[12] Lee, S.Y., Yim, K.S., Chang, H.N. and Chang, Y.K. (1994) Construction of plasmids, estimation of plasmid stability, and use of stable plasmids for the production of poly(3-hydroxybutyric acid) by recombinant *Escherichia coli*, *Journal of Biotechnology*, **32**, 203–211

[13] Lee, S.Y. (1996) Bacterial polyhydroxyalkanoates, *Biotechnology and Bioengineering*, **49**, 1–14

[14] Terpe, K. (2006) Overview of bacterial expression systems for heterologous protein production: from molecular and biochemical fundamentals to commercial systems, *Applied Microbiology and Biotechnology*, **72**, 211–222

[15] Ferrer-Miralles, N., Domingo-Espín, J., Corchero, J.L., Vázquez, E. and Villaverde, A. (2009) Microbial factories for recombinant pharmaceuticals, *Microbial Cell Factories*, **8**, Online journal

[16] Petsch, D. and Anspach, F.B. (2000) Endotoxin removal from protein solutions, *Journal of Biotechnology*, **76**, 97–119

[17] Rai, R., Yunos, D.M., Boccaccini, A.R. *et al.* (2011) Poly-3-hydroxyoctanoate P(3HO), a medium chain length polyhydroxyalkanoate homopolymer from *Pseudomonas mendocina*, *Biomacromolecules*, **12**, 2126–2136

[18] Ventura, S. and Villaverde, A. (2006) Protein quality in bacterial inclusion bodies, *Trends in Biotechnology*, **24**, 179–185

[19] Sorensen, H.P. and Mortensen, K.K. (2005) Soluble expression of recombinant proteins in the cytoplasm of *Escherichia coli*, *Microbial Cell Factories*, **4**, Online journal

[20] Mergulhão, F.J.M., Summers, D.K. and Monteiro, G.A. (2005) Recombinant protein secretion in *Escherichia coli*, *Biotechnology Advances*, **23**, 177–202

[21] van Wely, K.H., Swaving, J., Freudl, R. and Driessen, a.J. (2001) Translocation of proteins across the cell envelope of Gram-positive bacteria, *FEMS Microbiology Reviews*, **25**, 437–454

[22] Wältermann, M. and Steinbüchel, A. (2006) Wax ester and triacylglycerol inclusions, in: *Inclusions in Prokaryotes*, edited by J. Shively, Springer-Verlag, Berlin/Heidelberg, volume 1 of *Micobiology Monographs*, 137–166

[23] Wältermann, M., Hinz, A., Robenek, H. *et al.* (2005) Mechanism of lipid-body formation in prokaryotes: how bacteria fatten up, *Molecular Microbiology*, **55**, 750–763

[24] Tian, J., He, A., Lawrence, A.G. *et al.* (2005) Analysis of transient polyhydroxybutyrate production in *Wautersia eutropha* H16 by quantitative Western analysis and transmission electron microscopy, *Journal of Bacteriology*, **187**, 3825–3832

[25] Murphy, D.J. (2001) The biogenesis and functions of lipid bodies in animals, plants and microorganisms, *Progress in Lipid Research*, **40**, 325–438

[26] Anderson, A.J. and Dawes, E.A. (1990) Occurrence, metabolism, metabolic role, and industrial uses of bacterial polyhydroxyalkanoates., *Microbiological Reviews*, **54**, 450–472

[27] Guerrero, R. and Berlanga, M. (2007) The hidden side of the prokaryotic cell: rediscovering the microbial world, *International Microbiology*, **10**, 157–168

[28] Wältermann, M. and Steinbüchel, A. (2005) Neutral lipid bodies in prokaryotes: recent insights into structure, formation, and relationship to eukaryotic lipid depots, *Journal of Bacteriology*, **187**, 3607–3619

[29] Zinn, M., Witholt, B. and Egli, T. (2001) Occurrence, synthesis and medical application of bacterial polyhydroxyalkanoate, *Advanced Drug Delivery Reviews*, **53**, 5–21

[30] Steinbüchel, A. and Lütke-Eversloh, T. (2003) Metabolic engineering and pathway construction for biotechnological production of relevant polyhydroxyalkanoates in microorganisms, *Biochemical Engineering Journal*, **16**, 81–96

[31] Pompe, T., Keller, K., Mothes, G. *et al.* (2007) Surface modification of poly(hydroxybutyrate) films to control cell-matrix adhesion, *Biomaterials*, **28**, 28–37

[32] Grage, K., Jahns, A.C., Parlane, N. *et al.* (2009) Bacterial polyhydroxyalkanoate granules: biogenesis, structure, and potential use as nano-/micro-beads in biotechnological and biomedical applications, *Biomacromolecules*, **10**, 660–669

[33] Alvarez, H.M. and Steinbüchel, A. (2002) Triacylglycerols in prokaryotic microorganisms, *Applied Microbiology and Biotechnology*, **60**, 367–376

[34] Kalscheuer, R., Stöveken, T., Malkus, U. *et al.* (2007) Analysis of storage lipid accumulation in *Alcanivorax borkumensis*: evidence for alternative triacylglycerol biosynthesis routes in bacteria, *Journal of Bacteriology*, **189**, 918–928

[35] Yermanos, D.M. (1975) Composition of Jojoba seed during development, *Journal of the American Oil Chemists Society*, **52**, 115–117

[36] Lawrence, M.J. and Rees, G.D. (2000) Microemulsion-based media as novel drug delivery systems, *Advanced Drug Delivery Reviews*, **45**, 89–121

[37] Ishige, T., Tani, A., Sakai, Y. and Kato, N. (2003) Wax ester production by bacteria, *Current Opinion in Microbiology*, **6**, 244–250

[38] Lundgren, D.G., Pfister, R.M. and Merrick, J.M. (1964) Structure of poly-β-hydroxybutyric acid granules, *Journal of General Microbiology*, **34**, 441–446

[39] Thelen, J.J. and Ohlrogge, J.B. (2002) Metabolic engineering of fatty acid biosynthesis in plants, *Metabolic Engineering*, **4**, 12–21

[40] Voelker, T. and Kinney, A.J. (2001) Variations in the biosynthesis of seed-storage lipids, *Annual Review of Plant Biology*, **52**, 335–361

[41] Post-Beittenmiller, D. (1996) Biochemistry and molecular biology of wax production in plants, *Annual Review of Plant Biology*, **47**, 405–430

[42] Nevenzel, J.C. (1970) Occurrence, function and biosynthesis of wax esters in marine organisms, *Lipids*, **5**, 308–319

[43] Allen, W.V. (1976) Biochemical aspects of lipid storage and utilization in animals, *Integrative and Comparative Biology*, **16**, 631–647

[44] Ratledge, C. (2004) Fatty acid biosynthesis in microorganisms being used for single cell oil production, *Biochimie*, **86**, 807–815

[45] Ward, P.G. and OConnor, K.E. (2005) Bacterial synthesis of polyhydroxyalkanoates containing aromatic and aliphatic monomers by *Pseudomonas putida* CA-3, *International Journal of Biological Macromolecules*, **35**, 127–133

[46] Madison, L.L. and Huisman, G.W. (1999) Metabolic engineering of poly (3-hydroxyalkanoates): From DNA to Plastic, *Microbiology and Molecular Biology Reviews*, **63**, 21–53

[47] Steinbüchel, A., Füchtenbusch, B., Gorenflo, V. *et al.* (1998) Biosynthesis of polyesters in bacteria and recombinant organisms, *Polymer degradation and stability*, **59**, 177–182

[48] Braunegg, G., Lefebvre, G. and Genser, K.F. (1998) Polyhydroxyalkanoates, biopolyesters from renewable resources: physiological and engineering aspects, *Journal of Biotechnology*, **65**, 127–161

[49] Rehm, B.H.A. (2006) Genetics and biochemistry of polyhydroxyalkanoate granule self-assembly: the key role of polyester synthases, *Biotechnology Letters*, **28**, 207–213

[50] Stubbe, J., Tian, J., He, A. *et al.* (2005) Nontemplate-dependent polymerization processes: polyhydroxyalkanoate synthases as a paradigm, *Annual Review of Biochemistry*, **74**, 433–480

[51] Rehm, B.H.A. and Steinbüchel, A. (1999) Biochemical and genetic analysis of PHA synthases and other proteins required for PHA synthesis, *International Journal of Biological Macromolecules*, **25**, 3–19

[52] Lenz, R.W. and Marchessault, R.H. (2005) Bacterial polyesters: biosynthesis, biodegradable plastics and biotechnology, *Biomacromolecules*, **6**, 1–8

[53] Das, S., Lengweiler, U.D., Seebach, D. and Reusch, R.N. (1997) Proof for a nonproteinaceous calcium-selective channel in *Escherichia coli* by total synthesis from (R)-3-hydroxybutanoic acid and inorganic polyphosphate, *Proceedings of the National Academy of Sciences of the U.S.A.*, **94**, 9075–9079

[54] Poirier, Y., Erard, N. and MacDonald-Comber Petétot, J. (2001) Synthesis of polyhydroxyalkanoate in the peroxisome of *Saccharomyces cerevisiae* by using intermediates of fatty acid β-oxidation, *Applied and Environmental Microbiology*, **67**, 5254–5260

[55] Terentiev, Y., Breuer, U., Babel, W. and Kunze, G. (2004) Non-conventional yeasts as producers of polyhydroxyalkanoatesgenetic engineering of *Arxula adeninivorans*, *Applied Microbiology and Biotechnology*, **64**, 376–381

[56] Yunus, A.M.M., Parveez, G.K.A. and Ho, C.L. (2008) Transgenic plants producing polyhydroxyalkanoates, *Asia Pacific Journal of Molecular Biology and Biotechnology*, **16**, 1–10

[57] van Beilen, J.B. and Poirier, Y. (2008) Production of renewable polymers from crop plants, *The Plant Journal*, **54**, 684–701

[58] Snell, K.D. and Peoples, O.P. (2002) Polyhydroxyalkanoate polymers and their production in transgenic plants, *Metabolic Engineering*, **4**, 29–40

[59] Satoh, Y., Tajima, K., Tannai, H. and Munekata, M. (2003) Enzyme-catalyzed poly(3-hydroxybutyrate) synthesis from acetate with CoA recycling and NADPH regeneration *in vitro*, *Journal of Bioscience and Bioengineering*, **95**, 335–341

[60] Ushimaru, K., Sangiambut, S., Thomson, N.M., Sivaniah, E. and Tsuge, T. (2012) New insights into activation and substrate recognition of polyhydroxyalkanoate synthase from *Ralstonia eutropha*, *Applied Microbiology and Biotechnology*, **Accepted**

[61] Poirier, Y., Nawrath, C. and Somerville, C. (1995) Production of polyhydroxyalkanoates, a family of biodegradable plastics and elastomers, in bacteria and plants, *Biotechnology*, **13**, 142–150

[62] Rehm, B.H.A. (2007) Biogenesis of microbial polyhydroxyalkanoate granules: a platform technology for the production of tailor-made bioparticles, *Current Issues in Molecular Biology*, **9**, 41–62

[63] Liebergesell, M., Sonomoto, K., Madkour, M., Mayer, F. and Steinbüchel, A. (1994) Purification and characterization of the poly(hydroxyalkanoic acid) synthase from *Chromatium vinosum* and localization of the enzyme at the surface of poly(hydroxyalkanoic acid) granules, *European Journal of Biochemistry*, **226**, 71–80

[64] Stubbe, J. and Tian, J. (2003) Polyhydroxyalkanoate (PHA) homeostasis: the role of PHA synthase, *Natural Product Reports*, **20**, 445–457

[65] Jurasek, L. and Marchessault, R.H. (2004) Polyhydroxyalkanoate (PHA) granule formation in *Ralstonia eutropha* cells: a computer simulation, *Applied Microbiology and Biotechnology*, **64**, 611–617

[66] Jurasek, L. and Marchessault, R.H. (2002) The role of phasins in the morphogenesis of poly(3-hydroxybutyrate) granules, *Biomacromolecules*, **3**, 256–261

[67] Neumann, L., Spinozzi, F., Sinibaldi, R. *et al.* (2008) Binding of the major phasin, PhaP1, from *Ralstonia eutropha* H16 to poly(3-hydroxybutyrate) granules, *Journal of Bacteriology*, **190**, 2911–2919

[68] Wieczorek, R., Pries, A., Steinbüchel, A. and Mayer, F. (1995) Analysis of a 24-kilodalton protein associated with the polyhydroxyalkanoic acid granules in *Alcaligenes eutrophus*, *Journal of Bacteriology*, **177**, 2425–2435

[69] Pohlmann, A., Fricke, W.F., Reinecke, F. *et al.* (2006) Genome sequence of the bioplastic-producing "Knallgas" bacterium *Ralstonia eutropha* H16, *Nature Biotechnology*, **24**, 1257–1262

[70] York, G.M. and Stubbe, J. (2001) New insight into the role of the PhaP phasin of *Ralstonia eutropha* in promoting synthesis of polyhydroxybutyrate, *Journal of Bacteriology*, **183**, 2394–2397

[71] York, G.M., Stubbe, J. and Sinskey, A.J. (2002) The *Ralstonia eutropha* PhaR protein couples synthesis of the PhaP phasin to the presence of polyhydroxybutyrate in cells and promotes polyhydroxybutyrate production, *Journal of Bacteriology*, **184**, 59–66

[72] Maehara, A., Taguchi, S., Nishiyama, T., Yamane, T. and Doi, Y. (2002) A repressor protein, PhaR, regulates polyhydroxyalkanoate (PHA) synthesis via its direct interaction with PHA, *Journal of Bacteriology*, **184**, 3992–4002

[73] Pötter, M., Müller, H. and Steinbüchel, A. (2005) Influence of homologous phasins (PhaP) on PHA accumulation and regulation of their expression by the transcriptional repressor PhaR in *Ralstonia eutropha* H16, *Microbiology*, **151**, 825–833

[74] Kalscheuer, R., Wältermann, M., Alvarez, H.M. and Steinbüchel, A. (2001) Preparative isolation of lipid inclusions from *Rhodococcus opacus* and *Rhodococcus ruber* and identification of granule-associated proteins, *Archives of Microbiology*, **177**, 20–28

[75] York, G.M., Lupberger, J., Tian, J. *et al.* (2003) *Ralstonia eutropha* H16 encodes two and possibly three intracellular poly [D-(-)-3-hydroxybutyrate] depolymerase genes, *Journal of Bacteriology*, **185**, 3788–3794

[76] Hiraishi, T. and Taguchi, S. (2009) Enzyme-catalyzed synthesis and degradation of biopolymers, *Mini-Reviews in Organic Chemistry*, **6**, 44–54

[77] Ren, Q., de Roo, G., Ruth, K. *et al.* (2009) Simultaneous accumulation and degradation of polyhydroxyalkanoates: futile cycle or clever regulation?, *Biomacromolecules*, **10**, 916–922

[78] Uchino, K., Saito, T., Gebauer, B. and Jendrossek, D. (2007) Isolated poly(3-hydroxybutyrate) (PHB) granules are complex bacterial organelles catalyzing formation of PHB from acetyl coenzyme A (CoA) and degradation of PHB to acetyl-CoA, *Journal of Bacteriology*, **189**, 8250–8256

[79] Jendrossek, D. (2009) Polyhydroxyalkanoate granules are complex subcellular organelles (carbonosomes), *Journal of Bacteriology*, **191**, 3195–3202

[80] Jendrossek, D., Selchow, O. and Hoppert, M. (2007) Poly(3-Hydroxybutyrate) granules at the early stages of formation are localized close to the cytoplasmic membrane in *Caryophanon latum*, *Applied and Environmental Microbiology*, **73**, 586–593

[81] Lütke-Eversloh, T., Bergander, K., Luftmann, H. and Steinbüchel, A. (2001) Identification of a new class of biopolymer: bacterial synthesis of a sulfur-containing polymer with thioester linkages, *Microbiology*, **147**, 11–19

[82] Lütke-Eversloh, T., Fischer, A., Remminghorst, U. *et al.* (2002) Biosynthesis of novel thermoplastic polythioesters by engineered *Escherichia coli*, *Nature Materials*, **1**, 236–240

[83] Lütke-Eversloh, T. and Steinbüchel, A. (2004) Microbial polythioesters, *Macromolecular Bioscience*, **4**, 166–174

[84] Tessmer, N., Konig, S., Malkus, U. *et al.* (2007) Heat-shock protein HspA mimics the function of phasins *sensu stricto* in recombinant strains of Escherichia coli accumulating polythioesters or polyhydroxyalkanoates, *Microbiology*, **153**, 366–374

[85] Kawada, J., Lütke-Eversloh, T., Steinbüchel, A. and Marchessault, R.H. (2003) Physical properties of microbial polythioesters: characterization of poly(3-mercaptoalkanoates) synthesized by engineered *Escherichia coli*, *Biomacromolecules*, **4**, 1698–1702

[86] Elbanna, K., Lütke-Eversloh, T., Jendrossek, D., Luftmann, H. and Steinbüchel, A. (2004) Studies on the biodegradability of polythioester copolymers and homopolymers by polyhydroxyalkanoate (PHA)-degrading bacteria and PHA depolymerases, *Archives of Microbiology*, **182**, 212–225

[87] Kim, D.Y., Lütke-Eversloh, T., Elbanna, K., Thakor, N. and Steinbüchel, A. (2005) Poly(3-mercaptopropionate): a nonbiodegradable biopolymer?, *Biomacromolecules*, **6**, 897–901

[88] Alvarez, H.M., Mayer, F., Fabritius, D. and Steinbüchel, A. (1996) Formation of intracytoplasmic lipid inclusions by *Rhodococcus opacus* strain PD630, *Archives of Microbiology*, **165**, 377–386

[89] Alvarez, H.M., Kalscheuer, R. and Steinbüchel, A. (1997) Accumulation of storage lipids in species of *Rhodococcus* and *Nocardia* and effect of inhibitors and polyethylene glycol, *Fett/Lipid*, **99**, 239–246

[90] Alvarez, H.M., Pucci, O.H. and Steinbüchel, A. (1997) Lipid storage compounds in marine bacteria, *Applied Microbiology and Biotechnology*, **47**, 132–139

[91] Coleman, J. (1992) Characterization of the *Escherichia coli* gene for 1-acyl-sn-glycerol-3-phosphate acyltransferase (*plsC*), *Molecular and General Genetics*, **232**, 295–303

[92] Kennedy, E.P. and Weiss, S.B. (1956) The function of cytidine coenzymes in the biosynthesis of phospholipides, *Journal of Biological Chemistry*, **222**, 193–214

[93] Weiss, S.B., Kennedy, E.P. and Kiyasu, J.Y. (1960) The enzymatic synthesis of triglycerides, *Journal of Biological Chemistry*, **235**, 40–44

[94] Katavic, V., Reed, D.W., Taylor, D.C. *et al.* (1995) Alteration of seed fatty acid composition by an ethyl methanesulfonate-induced mutation in *Arabidopsis thaliana* affecting diacylglycerol acyltransferase activity, *Plant Physiology*, **108**, 399–409

[95] Kalscheuer, R. and Steinbüchel, A. (2003) A novel bifunctional wax ester synthase/acyl-CoA:diacylglycerol acyltransferase mediates wax ester and triacylglycerol biosynthesis in *Acinetobacter calcoaceticus* ADP1, *Journal of Biological Chemistry*, **278**, 8075–8082

[96] Stöveken, T., Kalscheuer, R., Malkus, U., Reichelt, R. and Steinbüchel, A. (2005) The wax ester synthase/acyl Coenzyme A:diacylglycerol acyltransferase from *Acinetobacter* sp. Strain ADP1: characterization of a novel type of acyltransferase, *Journal of Bacteriology*, **187**, 1369–1376

[97] Arabolaza, A., Rodriguez, E., Altabe, S., Alvarez, H.M. and Gramajo, H. (2008) Multiple pathways for triacylglycerol biosynthesis in *Streptomyces coelicolor.*, *Applied and environmental microbiology*, **74**, 2573–2582

[98] Christensen, H., Garton, N.J., Horobin, R.W., Minnikin, D.E. and Barer, M.R. (1999) Lipid domains of mycobacteria studied with fluorescent molecular probes, *Molecular Microbiology*, **31**, 1561–1572

[99] Fixter, L.M., Nagi, M.N., McCormack, J.G. and Fewson, C.A. (1986) Structure, Distribution and Function of Wax Esters in *Acinetobacter calcoaceticus*, *Journal of General Microbiology*, **132**, 3147–3157

[100] Ishige, T., Tani, A., Takabe, K. *et al.* (2002) Wax ester production from *n*-alkanes by *Acinetobacter* sp. strain M-1: ultrastructure of cellular inclusions and role of acyl Coenzyme A reductase, *Applied and Environmental Microbiology*, **68**, 1192–1195

[101] Singer, M.E., Tyler, S.M. and Finnerty, W.R. (1985) Growth of *Acinetobacter* sp. strain HO1-N on n-hexadecanol: physiological and ultrastructural characteristics, *Journal of Bacteriology*, **162**, 162–169

[102] Rehm, B.H.A. (2003) Polyester synthases: natural catalysts for plastics, *Biochemical Journal*, **376**, 15–33

[103] Qi, Q. and Rehm, B.H.A. (2001) Polyhydroxybutyrate biosynthesis in *Caulobacter crescentus*: molecular characterization of the polyhydroxybutyrate synthase, *Microbiology*, **147**, 3353–3358

[104] Yuan, W., Jia, Y., Tian, J. *et al.* (2001) Class I and III polyhydroxyalkanoate synthases from *Ralstonia eutropha* and *Allochromatium vinosum*: characterization and substrate specificity studies, *Archives of Biochemistry and Biophysics*, **394**, 87–98

[105] McCool, G.J. and Cannon, M.C. (2001) PhaC and PhaR are required for polyhydroxyalkanoic acid synthase activity in *Bacillus megaterium*, *Journal of Bacteriology*, **183**, 4235–4243

[106] Jia, Y., Yuan, W., Wodzinska, J. *et al.* (2001) Mechanistic Studies on Class I Polyhydroxybutyrate (PHB) Synthase from *Ralstonia eutropha): Class I and III Synthases Share a Similar Catalytic Mechanism*, *Biochemistry*, **40**, 1011–1019

[107] Griebel, R., Smith, Z. and Merrick, J.M. (1968) Metabolism of poly(β-hydroxybutyrate). I. Purification, composition, and properties of native poly(β-hydroxybutyrate) granules from *Bacillus megaterium*, *Biochemistry*, **7**, 3676–3681

[108] Gerngross, T.U., Snell, K.D., Peoples, O.P. *et al.* (1994) Overexpression and purification of the soluble polyhydroxyalkanoate synthase from *Alcaligenes eutrophus*: evidence for a required post-translational modification for catalytic activity, *Biochemistry*, **33**, 9311–9320

[109] Gerngross, T.U. and Martin, D.P. (1995) Enzyme-catalyzed synthesis of poly [(R)-(-)-3-hydroxybutyrate]: formation of macroscopic granules *in vitro*, *Proceedings of the National Academy of Sciences of the U.S.A.*, **92**, 6279–6283

[110] Jossek, R., Reichelt, R. and Steinbüchel, A. (1998) *In vitro* biosynthesis of poly(3-hydroxybutyric acid) by using purified poly(hydroxyalkanoic acid) synthase of *Chromatium vinosum*, *Applied Microbiology and Biotechnology*, **49**, 258–266

[111] Tian, J., Sinskey, A.J. and Stubbe, J. (2005) Kinetic studies of polyhydroxybutyrate granule formation in *Wautersia eutropha* H16 by transmission electron microscopy, *Journal of Bacteriology*, **187**, 3814–3824

[112] Lawrence, A.G., Choi, J.H., Rha, C., Stubbe, J. and Sinskey, A.J. (2005) *In vitro* analysis of the chain termination reaction in the synthesis of poly-(R)-β-hydroxybutyrate by the class III synthase from *Allochromatium vinosum*, *Biomacromolecules*, **6**, 2113–2119

[113] Kurja, J., Zirkzee, H.F., de Koning, G.M. and Maxwell, I.A. (1995) A new kinetic model for the accumulation of poly(3-hydroxybutyrate) in *Alcaligenes eutrophus* 1. Granule growth, *Macromolecular Theory and Simulations*, **4**, 839–855

[114] Kawaguchi, Y. and Doi, Y. (1992) Kinetics and mechanism of synthesis and degradation of poly(3-hydroxybutyrate) in *Alcaligenes eutrophus*, *Macromolecules*, **25**, 2324–2329

[115] Kusaka, S., Abe, H., Lee, S.Y. and Doi, Y. (1997) Molecular mass of poly[(R)-3-hydroxybutyric acid] produced in a recombinant *Escherichia coli*, *Applied and Environmental Microbiology*, **47**, 140–143

[116] Madden, L.A., Anderson, A.J., Shah, D.T. and Asrar, J. (1999) Chain termination in polyhydroxyalkanoate synthesis: involvement of exogenous hydroxy-compounds as chain transfer agents, *International Journal of Biological Macromolecules*, **25**, 43–53

[117] Shi, F., Ashby, R.D. and Gross, R.A. (1996) Use of poly(ethylene glycol)s to regulate poly(3-hydroxybutyrate) molecular weight during *Alcaligenes eutrophus* cultivations, *Macromolecules*, **29**, 7753–7758

[118] Martin, D.P. and Williams, S.F. (2003) Medical applications of poly-4-hydroxybutyrate: a strong flexible absorbable biomaterial, *Biochemical Engineering Journal*, **16**, 97–105

[119] Zhou, X.Y., Yuan, X.X., Shi, Z.Y. *et al.* (2012) Hyperproduction of poly(4-hydroxybutyrate) from glucose by recombinant *Escherichia coli*, *Microbial Cell Factories*, **11**, Online journal

[120] Yoshie, N. and Inoue, Y. (1999) Chemical composition distribution of bacterial copolyesters, *International Journal of Biological Macromolecules*, **25**, 193–200

[121] Wang, Y., Yamada, S., Asakawa, N. *et al.* (2001) Comonomer compositional distribution and thermal and morphological characteristics of bacterial poly(3-hydroxybutyrate-*co*-3-hydroxyvalerate)s with high 3-hydroxyvalerate content, *Biomacromolecules*, **2**, 1315–1323

[122] Chen, Q., Wang, Q., Wei, G., Liang, Q. and Qi, Q. (2011) Production in *Escherichia coli* of poly(3-hydroxybutyrate-co-3-hydroxyvalerate) with differing monomer compositions from unrelated carbon sources, *Applied and environmental microbiology*, **77**, 4886–4893

[123] Nawrath, C., Poirier, Y. and Somerville, C. (1995) Plant polymers for biodegradable plastics: cellulose, starch and polyhydroxyalkanoates, *Molecular Breeding*, **1**, 105–122

[124] Sodian, R., Hoerstrup, S., Sperling, J. *et al.* (2000) Tissue engineering of heart valves: *in vitro* experiences, *The Annals of Thoracic Surgery*, **70**, 140–144

[125] Williams, S.F., Martin, D.P., Horowitz, D.M. and Peoples, O.P. (1999) PHA applications: addressing the price performance issue I. Tissue engineering, *International Journal of Biological Macromolecules*, **25**, 111–121

[126] Hazer, D.B., Kılıçay, E. and Hazer, B. (2012) Poly(3-hydroxyalkanoate)s: Diversification and biomedical applications, *Materials Science and Engineering C*, **32**, 637–647

[127] Lageveen, R.G., Huisman, G.W., Preusting, H. *et al.* (1988) Formation of polyesters by *Pseudomonas oleovorans*: effect of substrates on formation and composition of poly-(R)-3-hydroxyalkanoates and poly-(R)-3-hydroxyalkenoates, *Applied and Environmental Microbiology*, **54**, 2924–2932

[128] Chen, G.Q., Xu, J., Wu, Q., Zhang, Z. and Ho, K.P. (2001) Synthesis of copolyesters consisting of medium-chain-length β-hydroxyalkanoates by *Pseudomonas stutzeri* 1317, *Science*, **48**, 107–112

[129] Shimamura, E., Kasuya, K.i. and Kobayashi, G. (1994) Physical properties and biodegradability of microbial poly (3-hydroxybutyrate-*co*-3-hydroxyhexanoate), *Macromolecules*, **27**, 878–880

[130] Haywood, G.W., Anderson, A.J. and Dawes, E.A. (1989) A survey of the accumulation of novel polyhydroxyalkanoates by bacteria, *Biotechnology Letters*, **11**, 471–476

[131] Sun, Z., Ramsay, J.a., Guay, M. and Ramsay, B.a. (2009) Fed-batch production of unsaturated medium-chain-length polyhydroxyalkanoates with controlled composition by *Pseudomonas putida* KT2440, *Applied Microbiology and Biotechnology*, **82**, 657–662

[132] Choi, J.H. and Lee, S.Y. (1997) Process analysis and economic evaluation for poly(3-hydroxybutyrate) production by fermentation, *Bioprocess Engineering*, **17**, 335–342

[133] Wang, F. and Lee, S.Y. (1997) Poly (3-hydroxybutyrate) production with high productivity and high polymer content by a fed-batch culture of *Alcaligenes latus* under nitrogen limitation, *Applied and Environmental Microbiology*, **63**, 3703–3706

[134] Lee, S.Y., Choi, J.H. and Wong, H.H. (1999) Recent advances in polyhydroxyalkanoate production by bacterial fermentation: mini-review, *International Journal of Biological Macromolecules*, **25**, 31–36

[135] Sun, Z., Ramsay, J.a., Guay, M. and Ramsay, B.a. (2007) Fermentation process development for the production of medium-chain-length poly-3-hyroxyalkanoates, *Applied Microbiology and Biotechnology*, **75**, 475–485

[136] Aldor, I.S. and Keasling, J.D. (2003) Process design for microbial plastic factories: metabolic engineering of polyhydroxyalkanoates, *Current Opinion in Biotechnology*, **14**, 475–483

[137] Sudesh, K., Abe, H. and Doi, Y. (2000) Synthesis, structure and properties of polyhydroxyalkanoates: biological polyesters, *Progress in Polymer Science*, **25**, 1503–1555

[138] Quillaguamán, J., Guzmán, H., Van-Thuoc, D. and Hatti-Kaul, R. (2010) Synthesis and production of polyhydroxyalkanoates by halophiles: current potential and future prospects, *Applied Microbiology and Biotechnology*, **85**, 1687–1696

[139] Hezayen, F.F., Steinbüchel, A. and Rehm, B.H.A. (2002) Biochemical and enzymological properties of the polyhydroxybutyrate synthase from the extremely halophilic archaeon strain 56, *Archives of Biochemistry and Biophysics*, **403**, 284–291

[140] Koller, M., Hesse, P., Bona, R. *et al.* (2007) Potential of various archae- and eubacterial strains as industrial polyhydroxyalkanoate producers from whey, *Macromolecular Bioscience*, **7**, 218–226

[141] Poli, A., Di Donato, P., Abbamondi, G.R. and Nicolaus, B. (2011) Synthesis, production, and biotechnological applications of exopolysaccharides and polyhydroxyalkanoates by archaea, *Archaea*, **Article ID**, Online journal

[142] Keenan, T.M., Nakas, J.P. and Tanenbaum, S.W. (2006) Polyhydroxyalkanoate copolymers from forest biomass, *Journal of Industrial Microbiology and Biotechnology*, **33**, 616–626

[143] Sudesh, K., Bhubalan, K., Chuah, J.A. *et al.* (2011) Synthesis of polyhydroxyalkanoate from palm oil and some new applications., *Applied Microbiology and Biotechnology*, **89**, 1373–1386

[144] Du, C., Sabirova, J.S., Soetaert, W. and Ki, C.L. (2012) Polyhydroxyalkanoate production from low-cost sustainable raw materials, *Current Chemical Biology*, **6**, 14–25

[145] Koller, M., Bona, R., Braunegg, G. *et al.* (2005) Production of polyhydroxyalkanoates from agricultural waste and surplus materials, *Biomacromolecules*, **6**, 561–565

[146] Sharma, N.K., Tiwari, S.P., Tripathi, K. and Rai, A.K. (2010) Sustainability and cyanobacteria (blue-green algae): facts and challenges, *Journal of Applied Phycology*, **23**, 1059–1081

[147] Campbell, J., Stevens, S.E. and Balkwill, D.L. (1982) Accumulation of poly-β-hydroxybutyrate in *Spirulina platensis*, *Journal of Bacteriology*, **149**, 361–363

[148] Asada, Y., Miyake, M., Miyake, J., Kurane, R. and Tokiwa, Y. (1999) Photosynthetic accumulation of poly-(hydroxybutyrate) by cyanobacteria–the metabolism and potential for CO_2 recycling., *International Journal of Biological Macromolecules*, **25**, 37–42

[149] Haase, S.M., Huchzermeyer, B. and Rath, T. (2011) PHB accumulation in *Nostoc muscorum* under different carbon stress situations, *Journal of Applied Phycology*, **24**, 157–162

[150] Wang, C., Hu, Z., Lei, A. and Jin, B. (2010) Biosynthesis of Poly-3-hydroxybutyrate (PHB) in the transgenic green alga *Chlamydomonas reinhardtii*, *Journal of Phycology*, **46**, 396–402

[151] Hempel, F., Bozarth, A.S., Lindenkamp, N. *et al.* (2011) Microalgae as bioreactors for bioplastic production, *Microbial Cell Factories*, **10**, Online journal

[152] Abd-El-Haleem, D.A.M. (2009) Biosynthesis of polyhydroxyalkanotes in wild type yeasts., *Polish Journal of Microbiology*, **58**, 37–41

[153] Leaf, T.A., Peterson, M.S., Stoup, S.K., Somers, D.A. and Srienc, F. (1996) *Saccharornyces cerevisiae* expressing bacterial polyhydroxybutyrate synthase produces poly-3-hydroxybutyrate, *Microbiology*, **142**, 1169–1180

[154] Carlson, R. and Srienc, F. (2006) Effects of recombinant precursor pathway variations on poly[(R)-3-hydroxybutyrate] synthesis in *Saccharomyces cerevisiae*, *Journal of Biotechnology*, **124**, 561–573

[155] Poirier, Y., Erard, N. and MacDonald-Comber Petétot, J. (2002) Synthesis of polyhydroxyalkanoate in the peroxisome of *Pichia pastoris*, *FEMS Microbiology Letters*, **207**, 97–102

[156] Zhang, B., Carlson, R. and Srienc, F. (2006) Engineering the monomer composition of polyhydroxyalkanoates synthesized in *Saccharomyces cerevisiae*, *Applied and Environmental Microbiology*, **72**, 536–543

[157] Haddouche, R., Poirier, Y., Delessert, S. *et al.* (2011) Engineering polyhydroxyalkanoate content and monomer composition in the oleaginous yeast *Yarrowia lipolytica* by modifying the β-oxidation multifunctional protein, *Applied Microbiology and Biotechnology*, **91**, 1327–1340

[158] Ikada, Y. and Tsuji, H. (2000) Biodegradable polyesters for medical and ecological applications, *Macromolecular Rapid Communications*, **21**, 117–132

[159] Noda, I., Lindsey, B.S. and Caraway, D. (2010) Nodax class PHA copolymers: their properties and applications, in: *Plastics from Bacteria: Natural Functions and Applications*, edited by G.Q. Chen, Springer Berlin Heidelberg, Berlin, Heidelberg, volume 14 of *Microbiology Monographs*, chapter 10, 238–254

[160] Carpentier, J.F. (2010) Discrete Metal Catalysts for Stereoselective Ring-Opening Polymerization of Chiral Racemic β-Lactones, *Macromolecular rapid communications*, **31**, 1696–1705

[161] Slater, S., Mitsky, T.A., Houmiel, K.L. *et al.* (1999) Metabolic engineering of *Arabidopsis* and *Brassica* for poly(3-hydroxybutyrate-*co*-3-hydroxyvalerate) copolymer production, *Nature Biotechnology*, **17**, 1011–1016

[162] Valentin, H.E., Broyles, D.L., Casagrande, L. *et al.* (1999) PHA production, from bacteria to plants, *International Journal of Biological Macromolecules*, **25**, 303–306

[163] Suriyamongkol, P., Weselake, R., Narine, S., Moloney, M. and Shah, S. (2007) Biotechnological approaches for the production of polyhydroxyalkanoates in microorganisms and plants - a review., *Biotechnology Advances*, **25**, 148–175

[164] Matsumoto, K., Murata, T., Nagao, R. *et al.* (2009) Production of short-chain-length/medium-chain-length polyhydroxyalkanoate (PHA) copolymer in the plastid of *Arabidopsis thaliana* using an engineered 3-ketoacyl-acyl carrier protein synthase III, *Biomacromolecules*, **10**, 686–690

[165] Poirier, Y., Dennis, D.E. and Somerville, C. (1992) Polyhydroxybutyrate, a biodegradable thermoplastic, produced in transgenic plants, *Science*, **256**, 520–523

[166] Poirier, Y., Dennis, D.E., Klomparens, K., Nawrath, C. and Somerville, C. (1992) Perspectives on the production of polyhydroxyalkanoates in plants, *FEMS Microbiology Reviews*, **103**, 237–246

[167] Nawrath, C., Poirier, Y. and Somerville, C. (1994) Targeting of the polyhydroxybutyrate biosynthetic pathway to the plastids of *Arabidopsis thaliana* results in high levels of polymer accumulation, *Proceedings of the National Academy of Sciences of the U.S.A.*, **91**, 12,760–12,764

[168] Hahn, J.J., Eschenlauer, A.C., Narrol, M.H., Somers, D.A. and Srienc, F. (1997) Growth kinetics, nutrient uptake and expression of the *Alcaligenes eutrophus* poly (β -hydroxybutyrate) synthesis pathway in transgenic maize cell suspension cultures, *Biotechnology Progress*, **13**, 347–354

[169] Hahn, J.J., Eschenlauer, A.C., Sleytr, U.B., Somers, D.A. and Srienc, F. (1999) Peroxisomes as sites for synthesis of polyhydroxyalkanoates in transgenic plants, *Biotechnology progress*, **15**, 1053–1057

[170] Zhong, H., Teymouri, F., Chapman, B. *et al.* (2003) The pea (*Pisum sativum* L.) rbcS transit peptide directs the *Alcaligenes eutrophus* polyhydroxybutyrate enzymes into the maize (*Zea mays* L.) chloroplasts, *Plant Science*, **165**, 455–462

[171] Houmiel, K.L., Slater, S., Broyles, D.L. *et al.* (1999) Poly (β-hydroxybutyrate) production in oilseed leukoplasts of *Brassica napus*, *Planta*, **209**, 547–550

[172] Romano, A., Vreugdenhil, D., Jamar, D. *et al.* (2003) Evidence of medium-chain-length polyhydroxyoctanoate accumulation in transgenic potato lines expressing the *Pseudomonas oleovorans* Pha-C1 polymerase in the cytoplasm, *Biochemical Engineering Journal*, **16**, 135–143

[173] Romano, A., van der Plas, L.H., Witholt, B., Eggink, G. and Mooibroek, H. (2005) Expression of poly-3-(R)-hydroxyalkanoate (PHA) polymerase and acyl-CoA-transacylase in plastids of transgenic potato leads to the synthesis of a hydrophobic polymer, presumably medium-chain-length PHAs, *Planta*, **220**, 455–464

[174] Menzel, G., Harloff, H.J. and Jung, C. (2003) Expression of bacterial poly (3-hydroxybutyrate) synthesis genes in hairy roots of sugar beet (*Beta vulgaris* L.), *Applied Microbiology and Biotechnology*, **60**, 571–576

[175] Petrasovits, L.A., Purnell, M.P., Nielsen, L.K. and Brumbley, S.M. (2007) Production of polyhydroxybutyrate in sugarcane, *Plant Biotechnology Journal*, **5**, 162–172

[176] Purnell, M.P., Petrasovits, L.a., Nielsen, L.K. and Brumbley, S.M. (2007) Spatio-temporal characterization of polyhydroxybutyrate accumulation in sugarcane, *Plant Biotechnology Journal*, **5**, 173–184

[177] Tilbrook, K., Gebbie, L., Schenk, P.M., Poirier, Y. and Brumbley, S.M. (2011) Peroxisomal polyhydroxyalkanoate biosynthesis is a promising strategy for bioplastic production in high biomass crops., *Plant Biotechnology Journal*, **9**, 958–969

[178] Wróbel, M., Zebrowski, J. and Szopa, J. (2004) Polyhydroxybutyrate synthesis in transgenic flax, *Journal of Biotechnology*, **107**, 41–54

[179] Chowdhury, B. and John, M.E. (1998) Thermal evaluation of transgenic cotton containing polyhydroxybutyrate, *Thermochimica Acta*, **313**, 43–53

[180] John, M.E. and Keller, G. (1996) Metabolic pathway engineering in cotton: biosynthesis of polyhydroxybutyrate in fiber cells, *Proceedings of the National Academy of Sciences of the U.S.A.*, **93**, 12,768–12,773

[181] Bohmert-Tatarev, K., McAvoy, S., Daughtry, S., Peoples, O.P. and Snell, K.D. (2011) High levels of bioplastic are produced in fertile transplastomic tobacco plants engineered with a synthetic operon for the production of polyhydroxybutyrate, *Plant Physiology*, **155**, 1690–1708

[182] Somleva, M.N., Snell, K.D., Beaulieu, J.J. *et al.* (2008) Production of polyhydroxybutyrate in switchgrass, a value-added co-product in an important lignocellulosic biomass crop, *Plant Biotechnology Journal*, **6**, 663–678

[183] Takase, K., Matsumoto, K., Taguchi, S. and Doi, Y. (2004) Alteration of substrate chain-length specificity of type II synthase for polyhydroxyalkanoate biosynthesis by *in vitro* evolution: *in vivo* and *in vitro* enzyme assays, *Biomacromolecules*, **5**, 480–485

[184] Nobes, G.A.R., Jurasek, L., Marchessault, R.H. *et al.* (2000) Growth and kinetics of *in vitro* poly([R]-(-)-3-hydroxybutyrate) granules interpreted as particulate polymerization with coalescence, *Macromolecular Rapid Communications*, **21**, 77–84

[185] Liu, S.J. and Steinbüchel, A. (2000) Exploitation of butyrate kinase and phosphotransbutyrylase from *Clostridium acetobutylicum* for the *in vitro* biosynthesis of poly(hydroxyalkanoic acid), *Applied Microbiology and Biotechnology*, **53**, 545–552

[186] Rehm, B.H.A., Qi, Q., Beermann, B.B., Hinz, H.J. and Steinbüchel, A. (2001) Matrix-assisted *in vitro* refolding of *Pseudomonas aeruginosa* class II polyhydroxyalkanoate synthase from inclusion bodies produced in recombinant *Escherichia coli*, *Biochemical Journal*, **358**, 263–268

[187] Tajima, K., Satoh, Y., Nakazawa, K. *et al.* (2004) Chemoenzymatic synthesis of poly(3-hydroxybutyrate) in a water-organic solvent two-phase system, *Macromolecules*, **37**, 4544–4546

[188] Sato, S., Ono, Y., Mochiyama, Y. *et al.* (2008) Polyhydroxyalkanoate film formation and synthase activity during *in vitro* and *in situ* polymerization on hydrophobic surfaces, *Biomacromolecules*, **9**, 2811–2818

[189] Satoh, Y., Murakami, F., Tajima, K. and Munekata, M. (2005) Enzymatic synthesis of poly(3-hydroxybutyrate-*co*-4-hydroxybutyrate) with CoA recycling using polyhydroxyalkanoate synthase and acyl-CoA synthetase, *Journal of Bioscience and Bioengineering*, **99**, 508–511

[190] Peters, V., Becher, D. and Rehm, B.H. (2007) The inherent property of polyhydroxyalkanoate synthase to form spherical PHA granules at the cell poles: The core region is required for polar localization, *Journal of Biotechnology*, **132**, 238–245

[191] Kelley, A.S. and Srienc, F. (1999) Production of two phase polyhydroxyalkanoic acid granules in *Ralstonia eutropha*, *International Journal of Biological Macromolecules*, **25**, 61–67

[192] Sudesh, K., Gan, Z., Maehara, A. and Doi, Y. (2002) Surface structure, morphology and stability of polyhydroxyalkanoate inclusions characterised by atomic force microscopy, *Polymer Degradation and Stability*, **77**, 77–85

[193] Garton, N.J., Christensen, H., Minnikin, D.E., Adegbola, R.A. and Barer, M.R. (2002) Intracellular lipophilic inclusions of mycobacteria *in vitro* and in sputum, *Microbiology*, **148**, 2951–2958

[194] Spiekermann, P., Rehm, B.H.A., Kalscheuer, R., Baumeister, D. and Steinbüchel, A. (1999) A sensitive, viable-colony staining method using Nile red for direct screening of bacteria that accumulate polyhydroxyalkanoic acids and other lipid storage compounds, *Archives of Microbiology*, **171**, 73–80

[195] Ostle, A.G. and Holt, J.G. (1982) Nile blue A as a fluorescent stain for poly-β-hydroxybutyrate, *Applied and Environmental Microbiology*, **44**, 238–241

[196] Jendrossek, D. (2005) Fluorescence microscopical investigation of poly(3-hydroxybutyrate) granule formation in bacteria., *Biomacromolecules*, **6**, 598–603

[197] Peters, V. and Rehm, B.H.A. (2005) *In vivo* monitoring of PHA granule formation using GFP-labeled PHA synthases, *FEMS Microbiology Letters*, **248**, 93–100

[198] Sudesh, K., Maehara, A., Gan, Z., Iwata, T. and Doi, Y. (2004) Direct observation of polyhydroxyalkanoate granule-associated-proteins on native granules and on poly(3-hydroxybutyrate) single crystals by atomic force microscopy, *Polymer Degradation and Stability*, **83**, 281–287

[199] Dennis, D.E., Liebig, C., Holley, T. *et al.* (2003) Preliminary analysis of polyhydroxyalkanoate inclusions using atomic force microscopy, *FEMS Microbiology Letters*, **226**, 113–119

[200] Hiraishi, T., Kikkawa, Y., Fujita, M. *et al.* (2005) Atomic force microscopic observation of in vitro polymerized poly[(R)-3-hydroxybutyrate]: insight into possible mechanism of granule formation, *Biomacromolecules*, **6**, 2671–2677

[201] Ellar, D., Lundgren, D.G., Okamura, K. and Marchessault, R.H. (1968) Morphology of poly-β-hydroxybutyrate granules, *Journal of Molecular Biology*, **35**, 489–502

[202] Dunlop, W.F. and Robards, A.W. (1973) Ultrastructural Study of Poly-β-Hydroxybutyrate Granules from *Bacillus cereus*, *Journal of Bacteriology*, **114**, 1271–1280

[203] Kawaguchi, Y. and Doi, Y. (1990) Structure of native poly(3-hydroxybutyrate) granules characterized by X-ray diffraction, *FEMS Microbiology Letters*, **70**, 151–156

[204] Rontani, J.F., Mouzdahir, A., Michotey, V., Caumette, P. and Bonin, P. (2003) Production of a polyunsaturated isoprenoid wax ester during aerobic metabolism of squalene by *Marinobacter squalenivorans* sp. nov, *Applied and Environmental Microbiology*, **69**, 4167–4176

[205] Severs, N.J. (2007) Freeze-fracture electron microscopy, *Nature Protocols*, **2**, 547–576

[206] Seufferheld, M.J., Vieira, M.C.F., Ruiz, F.A. *et al.* (2003) Identification of Organelles in Bacteria Similar to Acidocalcisomes of Unicellular Eukaryotes, *Journal of Biological Chemistry*, **278**, 29,971–29,978

[207] Preusting, H., Kingma, J., Huisman, G.W., Steinbüchel, A. and Witholt, B. (1993) Formation of polyester blends by a recombinant strain of *Pseudomonas oleovorans*: different poly(3-hydroxyalkanoates) are stored in separate granules, *Journal of Environmental Polymer Degradation*, **1**, 11–21

[208] Scott, C.C. and Finnerty, W.R. (1976) Characterization of intracytoplasmic hydrocarbon inclusions from the hydrocarbon-oxidizing *Acinetobacter* species HO1-N, *Journal of Bacteriology*, **127**, 481–489

[209] Stuart, E.S., Tehrani, A., Valentin, H.E. *et al.* (1998) Protein organization on the PHA inclusion cytoplasmic boundary, *Journal of Biotechnology*, **64**, 137–144

[210] Banki, M.R., Gerngross, T.U. and Wood, D.W. (2005) Novel and economical purification of recombinant proteins: intein-mediated protein purification using in vivo polyhydroxybutyrate (PHB) matrix association, *Protein Science*, **14**, 1387–1395

[211] Ramachander, T.V.N., Rohini, D., Belhekar, A. and Rawal, S.K. (2002) Synthesis of PHB by recombinant *E. coli* harboring an approximately 5 kb genomic DNA fragment from *Streptomyces aureofaciens* NRRL 2209, *International Journal of Biological Macromolecules*, **31**, 63–69

[212] Donald, A.M. (2003) The use of environmental scanning electron microscopy for imaging wet and insulating materials, *Nature Materials*, **2**, 511–516

[213] Preiss, J. (1984) Bacterial glycogen synthesis and its regulation, *Annual Review of Microbiology*, **38**, 419–458

[214] Wilson, W.a., Roach, P.J., Montero, M. *et al.* (2010) Regulation of glycogen metabolism in yeast and bacteria, *FEMS Microbiology Reviews*, **34**, 952–985

[215] Strøm, A.R. and Kaasen, I. (1993) Trehalose metabolism in *Escherichia coli* : stress protection and stress regulation of gene expression, *Molecular Microbiology*, **8**, 205–210

[216] Larsen, P.I., Sydnes, L.K., Landfald, B. and Strø m, A.R. (1987) Osmoregulation in *Escherichia coli* by accumulation of organic osmolytes: betaines, glutamic acid, and trehalose, *Archives of Microbiology*, **147**, 1–7

[217] Elbein, A.D., Pan, Y.T., Pastuszak, I. and Carroll, D. (2003) New insights on trehalose: a multifunctional molecule, *Glycobiology*, **13**, 17–27

[218] Chandra, G., Chater, K.F. and Bornemann, S. (2011) Unexpected and widespread connections between bacterial glycogen and trehalose metabolism, *Microbiology*, **157**, 1565–1572

[219] Kortstee, G.J., Appeldoorn, K.J., Bonting, C.F., van Niel, E.W. and van Veen, H.W. (1994) Biology of polyphosphate-accumulating bacteria involved in enhanced biological phosphorus removal., *FEMS Microbiology Reviews*, **15**, 137–153

[220] Mußmann, M., Hu, F.Z., Richter, M. *et al.* (2007) Insights into the genome of large sulphur bacteria revealed by analysis of single filaments, *PLOS Biology*, **5**, Online journal

[221] Obst, M. and Steinbüchel, A. (2006) Cyanophycin–an ideal bacterial nitrogen storage material with unique chemical properties, in: *Inclusions in Prokaryotes*, edited by J. Shively, Springer-Verlag, Berlin/Heidelberg, 167–193

[222] Chen, C.C. (2010) Quiescent *E.coli* as a cell factory, Ph.D. thesis, University of Cambridge

[223] Normi, Y.M., Hiraishi, T., Taguchi, S. *et al.* (2005) Characterization and properties of G4X mutants of *Ralstonia eutropha* PHA synthase for poly (3-hydroxybutyrate) biosynthesis in *Escherichia coli*, *Macromolecular Bioscience*, **5**, 197–206

[224] Kahar, P., Agus, J., Kikkawa, Y. *et al.* (2005) Effective production and kinetic characterization of ultra-high-molecular-weight poly [(R)-3-hydroxybutyrate] in recombinant *Escherichia coli*, *Polymer Degradation and Stability*, **87**, 161–169

[225] Summers, D.K. (1998) Timing, self-control and a sense of direction are the secrets of multicopy plasmid stability, *Molecular Microbiology*, **29**, 1137–1145

[226] Sambrook, J. and Russell, D.W. (2001) *Molecular cloning: A laboratory manual*, Cold Spring Harbour Press, Cold Spring Harbour, New York, 3rd edition

[227] Steinmoen, H., Knutsen, E. and Håvarstein, L.S. (2002) Induction of natural competence in *Streptococcus pneumoniae* triggers lysis and DNA release from a subfraction of the cell population, *Proceedings of the National Academy of Sciences of the U.S.A.*, **99**, 7681–7686

[228] Gaberc-Porekar, V. and Menart, V. (2001) Perspectives of immobilized-metal affinity chromatography, *Journal of Biochemical and Biophysical Methods*, **49**, 335–360

[229] Fukui, T., Yoshimoto, A., Matsumoto, M. *et al.* (1976) Enzymatic synthesis of poly-β-hydroxybutyrate in *Zoogloea ramigera*, *Archives of Microbiology*, **110**, 149–156

[230] Braunegg, G., Sonnleitner, B. and Lafferty, R.M. (1978) A rapid gas chromatographic method for the determination of poly-β-hydroxybutyric acid in microbial biomass, *Applied Microbiology and Biotechnology*, **6**, 29–37

[231] Cameron, R.E. and Donald, A.M. (1994) Minimizing sample evaporation in the environmental scanning electron microscope, *Journal of Microscopy*, **173**, 227–237

[232] Haacke, A., Fendrich, G., Ramage, P. and Geiser, M. (2009) Chaperone over-expression in *Escherichia coli*: apparent increased yields of soluble recombinant protein kinases are due mainly to soluble aggregates, *Protein Expression and Purification*, **64**, 185–193

[233] Sheu, D.s. and Lee, C.y. (2004) Altering the substrate specificity of polyhydroxyalkanoate synthase 1 Derived from *Pseudomonas putida* GPo1 by localized semirandom mutagenesis, *Journal of Bacteriology*, **186**, 4177–4184

[234] Ren, Q., de Roo, G., Kessler, B. and Witholt, B. (2000) Recovery of active medium-chain-length-poly-3-hydroxyalkanoate polymerase from inactive inclusion bodies using ion-exchange resin, *Biochemical Journal*, **349**, 599–604

[235] Rowe, D.C.D. and Summers, D.K. (1999) The quiescent-cell expression system for protein synthesis in *Escherichia coli*, *Applied and Environmental Microbiology*, **65**, 2710–2715

[236] Summers, D. (2002) A quiet revolution in the bacterial cell factory, *Microbiology Today*, **29**, 76–79

[237] Mukherjee, K.J., Rowe, D.C.D., Watkins, N.A. and Summers, D.K. (2004) Studies of single-chain antibody expression in quiescent *Escherichia coli*, *Applied and Environmental Microbiology*, **70**, 3005–3012

[238] Summers, D.K. and Sherratt, D.J. (1984) Multimerization of high copy number plasmids causes instability : ColEI encodes a determinant essential for plasmid monomerization and stability, *Cell*, **36**, 1097–1103

[239] Summers, D.K., Beton, C.W.H. and Withers, H.L. (1993) Multicopy plasmid instability: the dimer catastrophe hypothesis, *Molecular Microbiology*, **8**, 1031–1038

[240] Hodgman, T.C., Griffiths, H. and Summers, D.K. (1998) Nucleoprotein architecture and ColE1 dimer resolution: a hypothesis, *Molecular Microbiology*, **29**, 545–558

[241] Colloms, S.D., McCulloch, R., Grant, K., Neilson, L. and Sherratt, D.J. (1996) Xer-mediated site-specific recombination *in vitro*, *The EMBO Journal*, **15**, 1172–1181

[242] Patient, M.E. and Summers, D.K. (1993) ColE1 multimer formation triggers inhibition of *Escherichia coli* cell division, *Molecular Microbiology*, **9**, 1089–1095

[243] Blaby, I.K. and Summers, D.K. (2009) The role of FIS in the Rcd checkpoint and stable maintenance of plasmid ColE1, *Microbiology*, **155**, 2676–2682

[244] Tendeng, C. and Bertin, P.N. (2003) H-NS in Gram-negative bacteria: a family of multifaceted proteins, *Trends in Microbiology*, **11**, 511–518

[245] Chant, E.L. and Summers, D.K. (2007) Indole signalling contributes to the stable maintenance of *Escherichia coli* multicopy plasmids, *Molecular Microbiology*, **63**, 35–43

[246] Snell, E.E. (1975) Tryptophanase: structure, catalytic activities, and mechanism of action, in: *Advances in Enzymology and Related Areas of Molecular Biology, Volume 42*, edited by A. Meister, John Wiley and Sons, Hoboken, New Jersey, chapter 6, 287–333

[247] Newton, W.A. and Snell, E.E. (1965) Formation and interrelationships of tryptophanase and tryptophan synthetases in *Escherichia Coli*, *Journal of Bacteriology*, **89**, 355–364

[248] Lee, J.H. and Lee, J. (2010) Indole as an intercellular signal in microbial communities, *FEMS Microbiology Reviews*, **34**, 426–444

[249] Piñero Fernandez, S., Chimerel, C., Keyser, U.F. and Summers, D.K. (2011) Indole transport across *Escherichia coli* membranes, *Journal of Bacteriology*, **193**, 1793–1798

[250] Chimerel, C., Field, C.M., Piñero Fernandez, S., Keyser, U.F. and Summers, D.K. (2012) Indole prevents *Escherichia coli* cell division by modulating membrane potential, *Biochimica et Biophysica Acta - Biomembranes*, **1818**, 1590–1594

[251] Kralj, J.M., Hochbaum, D.R., Douglass, A.D. and Cohen, A.E. (2011) Electrical spiking in *Escherichia coli* probed with a fluorescent voltage-indicating protein, *Science*, **333**, 345–348

[252] Strahl, H. and Hamoen, L.W. (2010) Membrane potential is important for bacterial cell division, *Proceedings of the National Academy of Sciences of the U.S.A.*, **107**, 12,281–12,286

[253] Jahns, A.C. and Rehm, B.H.A. (2009) Tolerance of the *Ralstonia eutropha* class I polyhydroxyalkanoate synthase for translational fusions to its C terminus reveals a new mode of functional display, *Applied and Environmental Microbiology*, **75**, 5461–5466

[254] Clark, E.D. (2001) Protein refolding for industrial processes, *Current Opinion in Biotechnology*, **12**, 202–207

[255] Thomas, J.G., Ayling, A. and Baneyx, F. (1997) Molecular chaperones, folding catalysts, and the recovery of active recombinant proteins from *E. coli*, *Applied Biochemistry and Biotechnology*, **66**, 197–238

[256] Young, J.C., Agashe, V.R., Siegers, K. and Hartl, F.U. (2004) Pathways of chaperone-mediated protein folding in the cytosol, *Nature Reviews Molecular Cell Biology*, **5**, 781–791

[257] Baneyx, F. (1999) Recombinant protein expression in *Escherichia coli*, *Current Opinion in Biotechnology*, **10**, 411–421

[258] Schlieker, C., Bukau, B. and Mogk, A. (2002) Prevention and reversion of protein aggregation by molecular chaperones in the *E. coli* cytosol: implications for their applicability in biotechnology, *Journal of Biotechnology*, **96**, 13–21

[259] Nishihara, K., Kanemori, M., Kitagawa, M., Yanagi, H. and Yura, T. (1998) Chaperone coexpression plasmids: differential and synergistic roles of DnaK-DnaJ-GrpE and GroEL-GroES in assisting folding of an allergen of Japanese Cedar pollen, Cryj2, in *Escherichia coli*, *Applied and Environmental Microbiology*, **64**, 1694–1699

[260] Nishihara, K., Kanemori, M., Yanagi, H. and Yura, T. (2000) Overexpression of trigger factor prevents aggregation of recombinant proteins in *Escherichia coli*, *Applied and Environmental Microbiology*, **66**, 884–889

[261] Hesterkamp, T., Hauser, S., Lütcke, H. and Bukau, B. (1996) *Escherichia coli* trigger factor is a prolyl isomerase that associates with nascent polypeptide chains, *Proceedings of the National Academy of Sciences of the U.S.A.*, **93**, 4437–4441

[262] Merz, F., Boehringer, D., Schaffitzel, C. *et al.* (2008) Molecular mechanism and structure of Trigger Factor bound to the translating ribosome, *The EMBO Journal*, **27**, 1622–1632

[263] Stoller, G., Rücknagel, K.P., Nierhaus, K.H. *et al.* (1995) A ribosome-associated peptidyl-prolyl *cis/trans* isomerase identified as the trigger factor, *The EMBO Journal*, **14**, 4939–4948

[264] Kramer, G., Patzelt, H., Rauch, T. *et al.* (2004) Trigger factor peptidyl-prolyl *cis/trans* isomerase activity is not essential for the folding of cytosolic proteins in *Escherichia coli*, *Journal of Biological Chemistry*, **279**, 14,165–14,170

[265] Schiene-Fischer, C., Habazettl, J., Schmid, F.X. and Fischer, G. (2002) The hsp70 chaperone DnaK is a secondary amide peptide bond *cis-trans* isomerase, *Nature Structural Biology*, **9**, 419–424

[266] Mayer, M.P. and Bukau, B. (2005) Hsp70 chaperones: cellular functions and molecular mechanism, *Cellular and Molecular Life Sciences*, **62**, 670–684

[267] Schröder, H., Langer, T., Hartl, F.U. and Bukau, B. (1993) DnaK, DnaJ and GrpE form a cellular chaperone machinery capable of repairing heat-induced protein damage., *The EMBO Journal*, **12**, 4137–4144

[268] Xu, Z., Horwich, A.L. and Sigler, P.B. (1997) The crystal structure of the asymmetric GroEL-GroES-(ADP)7 chaperonin complex, *Nature*, **388**, 741–750

[269] Keskin, O., Bahar, I., Flatow, D., Covell, D.G. and Jernigan, R.L. (2002) Molecular mechanisms of chaperonin GroEL-GroES function, *Biochemistry*, **41**, 491–501

[270] Chaudhuri, T.K., Farr, G.W., Fenton, W.A., Rospert, S. and Horwich, A.L. (2001) GroEL/GroES-mediated folding of a protein too large to be encapsulated, *Cell*, **107**, 235–246

[271] Agus, J., Kahar, P., Abe, H., Doi, Y. and Tsuge, T. (2006) Molecular weight characterization of poly[(R)-3-hydroxybutyrate] synthesized by genetically engineered strains of *Escherichia coli*, *Polymer Degradation and Stability*, **91**, 1138–1146

[272] Robichon, C., Luo, J., Causey, T.B., Benner, J.S. and Samuelson, J.C. (2011) Engineering *Escherichia coli* BL21(DE3) derivative strains to minimize *E. coli* protein contamination after purification by immobilized metal affinity chromatography, *Applied and Environmental Microbiology*, **77**, 4634–4646

[273] Tomizawa, S., Saito, Y., Hyakutake, M. *et al.* (2010) Chain transfer reaction catalyzed by various polyhydroxyalkanoate synthases with poly(ethylene glycol) as an exogenous chain transfer agent, *Applied Microbiology and Biotechnology*, **87**, 1427–1435

[274] Chen, G.Q. and R.C., L. (2009) Polyhydroxyalkanoate blends and composites, in: *Biodegradable Polymer Blends and Composites from Renewable Resources*, edited by L. Yu, John Wiley and Sons, Haboken, NJ, USA, chapter 8, Chapter 8

[275] Scaffaro, R., Dintcheva, N.T., Marino, R. and La Mantia, F.P. (2011) Processing and properties of biopolymer/polyhydroxyalkanoates blends, *Journal of Polymers and the Environment*, **20**, 267–272

[276] Misra, S.K., Valappil, S.P., Roy, I. and Boccaccini, A.R. (2006) Polyhydroxyalkanoate (PHA)/inorganic phase composites for tissue engineering applications, *Biomacromolecules*, **7**, 2249–2258

[277] Gogotov, I.N., Gerasin, V.a., Knyazev, Y.V., Antipov, E.M. and Barazov, S.K. (2010) Composite biodegradable materials based on polyhydroxyalkanoate, *Applied Biochemistry and Microbiology*, **46**, 607–613

[278] Sim, S.J., Snell, K.D., Hogan, S.A. *et al.* (1997) PHA synthase activity controls the molecular weight and polydispersity of polyhydroxybutyrate *in vivo*, *Nature Biotechnology*, **15**, 63–67

[279] Agus, J., Kahar, P., Abe, H., Doi, Y. and Tsuge, T. (2006) Altered expression of polyhydroxyalkanoate synthase gene and its effect on poly[(R)-3-hydroxybutyrate] synthesis in recombinant *Escherichia coli*, *Polymer Degradation and Stability*, **91**, 1645–1650

[280] Handrick, R., Reinhardt, S. and Jendrossek, D. (2000) Mobilization of Poly(3-Hydroxybutyrate) in *Ralstonia eutropha*, *Journal of Bacteriology*, **182**, 3–6

[281] Jendrossek, D. and Handrick, R. (2002) Microbial degradation of polyhydroxyalkanoates, *Annual review of Microbiology*, **56**, 403–432

[282] Snell, K.D., Hogan, S.A., Sim, S.J., Sinskey, A.J. and Rha, C. (1998), Method for controlling molecular weight of polyhydroxyalkanoates

[283] Hiroe, A., Tsuge, K., Nomura, C.T., Itaya, M. and Tsuge, T. (2012) Rearrangement of gene order in the *phaCAB* operon leads to effective production of ultra-high-molecular-weight poly[(R)-3-hydroxybutyrate] in genetically engineered *Escherichia coli.*, *Applied and environmental microbiology*, **78**, 3177–3184

[284] Jacquel, N., Lo, C.w., Wei, Y.h., Wu, H.s. and Wang, S.S. (2008) Isolation and purification of bacterial poly(3-hydroxyalkanoates), *Biochemical Engineering Journal*, **39**, 15–27

[285] Jung, I.L., Phyo, K.H., Kim, K.C., Park, H.K. and Kim, I.G. (2005) Spontaneous liberation of intracellular polyhydroxybutyrate granules in *Escherichia coli*, *Research in Microbiology*, **156**, 865–873

[286] Resch, S., Gruber, K., Wanner, G. *et al.* (1998) Aqueous release and purification of poly(β-hydroxybutyrate) from *Escherichia coli*, *Journal of Biotechnology*, **65**, 173–182

[287] Yu, J. and Chen, L.X.L. (2006) Cost-effective recovery and purification of polyhydroxyalkanoates by selective dissolution of cell mass, *Biotechnology progress*, **22**, 547–553

[288] Chen, G.Q. and Wu, Q. (2005) Microbial production and applications of chiral hydroxyalkanoates, *Applied Microbiology and Biotechnology*, **67**, 592–599

[289] Shi, F., Gross, R.A. and Rutherford, D.R. (1996) Microbial polyester synthesis: effects of poly(ethylene glycol) on product composition, repeat unit sequence, and end group structure, *Macromolecules*, **29**, 10–17

[290] Ashby, R.D., Shi, F. and Gross, R.A. (1999) A tunable switch to regulate the synthesis of low and high molecular weight microbial polyesters, *Biotechnology and Bioengineering*, **62**, 106–113

[291] Mothes, G., Schnorpfeil, C. and Ackermann, J.U. (2007) Production of PHB from Crude Glycerol, *Engineering in Life Sciences*, **7**, 475–479

[292] Cavalheiro, J.a.M., de Almeida, M.C.M., Grandfils, C. and da Fonseca, M. (2009) Poly(3-hydroxybutyrate) production by *Cupriavidus necator* using waste glycerol, *Process Biochemistry*, **44**, 509–515

[293] Suzuki, T., Deguchi, H., Yamane, T., Shimizu, S. and Gekko, K. (1988) Control of molecular weight of poly-β-hydroxybutyric acid produced in fed-batch culture of *Protomonas extorquens*, *Applied Microbiology and Biotechnology*, **27**, 487–491

[294] Taidi, B., Anderson, A.J., Dawes, E.A. and Byrom, D. (1994) Effect of carbon source and concentration on the molecular mass of poly(3-hydroxybutyrate) produced by *Methylobacterium extorquens* and *Alcaligenes eutrophus*, *Applied Microbiology and Biotechnology*, **40**, 786–790

[295] Yezza, A., Fournier, D., Halasz, A. and Hawari, J. (2006) Production of polyhydroxyalkanoates from methanol by a new methylotrophic bacterium *Methylobacterium* sp. GW2, *Applied Microbiology and Biotechnology*, **73**, 211–218

[296] Luli, G.W. and Strohl, W.R. (1990) Comparison of growth, acetate production, and acetate inhibition of Escherichia coli strains in batch and fed-batch fermentations, *Applied and environmental microbiology*, **56**, 1004–1011

[297] Dubochet, J., McDowall, a.W., Menge, B., Schmid, E.N. and Lickfeld, K.G. (1983) Electron microscopy of frozen-hydrated bacteria, *Journal of Bacteriology*, **155**, 381–390

[298] Comolli, L.R., Kundmann, M. and Downing, K.H. (2006) Characterization of intact subcellular bodies in whole bacteria by cryo-electron tomography and spectroscopic imaging, *Journal of Microscopy*, **223**, 40–52

[299] Bogner, A., Thollet, G., Basset, D., Jouneau, P.H. and Gauthier, C. (2005) Wet STEM: a new development in environmental SEM for imaging nano-objects included in a liquid phase, *Ultramicroscopy*, **104**, 290–301

[300] Bogner, A., Jouneau, P.H., Thollet, G., Basset, D. and Gauthier, C. (2007) A history of scanning electron microscopy developments: towards "wet-STEM" imaging, *Micron*, **38**, 390–401

[301] Danilatos, G.D. (1988) Foundations of environmental scanning electron microscopy, in: *Advances in Electronics and Electron Physics*, edited by P.W. Hawkes, Academic Press, New York, 109–250

[302] Serafim, L.S., Lemos, P.C., Levantesi, C. *et al.* (2002) Methods for detection and visualization of intracellular polymers stored by polyphosphate-accumulating microorganisms, *Journal of Microbiological Methods*, **51**, 1–18

[303] de Jonge, N., Peckys, D.B., Kremers, G.J. and Piston, D.W. (2009) Electron microscopy of whole cells in liquid with nanometer resolution, *Proceedings of the National Academy of Sciences of the U.S.A.*, **106**, 2159–64

[304] Schlegel, H.G., Lafferty, R.M. and Krauss, I. (1970) The isolation of mutants not accumulating poly-β-hydroxybutyric acid, *Archiv für Mikrobiologie*, **71**, 283–294

[305] Bayer, A.S., Eftekhar, F., Tu, J., Nast, C.C. and Speert, D.P. (1990) Oxygen-dependent up-regulation of mucoid exopolysaccharide (alginate) production in *Pseudomonas aeruginosa*, *Infection and Immunity*, **58**, 1344–1349

[306] Hacking, A.J., Taylor, I.W.F., Jarman, T.R. and Govan, J.R.W. (1983) Alginate Biosynthesis by *Pseudomonas mendocina*, *Microbiology*, **129**, 3473–3480

[307] Cruden, D.L., Wolfram, J.H., Rogers, R.D. and Gibson, D.T. (1992) Physiological properties of a *Pseudomonas* strain which grows with p-xylene in a two-phase (organic-aqueous) medium, *Applied and Environmental Microbiology*, **58**, 2723–2729

[308] Lugg, H., Sammons, R.L., Marquis, P.M. *et al.* (2008) Polyhydroxybutyrate accumulation by a *Serratia* sp., *Biotechnology letters*, **30**, 481–491

[309] Walther-Mauruschat, A., Aragno, M., Mayer, F. and Schlegel, H.G. (1977) Micromorphology of Gram-negative hydrogen bacteria, *Archives of Microbiology*, **114**, 101–110

[310] Friedrich, B., Hogrefe, C. and Schlegel, H.G. (1981) Naturally occurring genetic transfer of hydrogen-oxidizing ability between strains of *Alcaligenes eutrophus*, *Journal of Bacteriology*, **147**, 198–205

[311] Staniewicz, L., Donald, A.M., Stokes, D.J. *et al.* (2012) The application of STEM and *in situ* controlled dehydration to bacterial systems using ESEM, *Scanning*, **34**, 237–246

[312] Kirk, S.E. (2008) Exploration of the use of ESEM for the study of biological materials, Ph.D. thesis, University of Cambridge

[313] Neděla, V. (2010) Controlled dehydration of a biological sample using an alternative form of environmental SEM, *Journal of Microscopy*, **237**, 7–11

[314] Almaas, E., Kovács, B., Vicsek, T., Oltvai, Z.N. and Barabási, A.L. (2004) Global organization of metabolic fluxes in the bacterium *Escherichia coli*, *Nature*, **427**, 839–843

[315] Kalscheuer, R., Stölting, T. and Steinbüchel, A. (2006) Microdiesel: *Escherichia coli* engineered for fuel production, *Microbiology*, **152**, 2529–2536

[316] Penfold, D., Forster, C. and Macaskie, L. (2003) Increased hydrogen production by *Escherichia coli* strain HD701 in comparison with the wild-type parent strain MC4100, *Enzyme and Microbial Technology*, **33**, 185–189

[317] Martin, V.J.J., Pitera, D.J., Withers, S.T., Newman, J.D. and Keasling, J.D. (2003) Engineering a mevalonate pathway in *Escherichia coli* for production of terpenoids, *Nature Biotechnology*, **21**, 796–802

[318] Liu, Q., Ouyang, S.P., Chung, A., Wu, Q. and Chen, G.Q. (2007) Microbial production of R-3-hydroxybutyric acid by recombinant *E. coli* harboring genes of *phbA*, *phbB*, and *tesB*, *Applied Microbiology and Biotechnology*, **76**, 811–818

[319] Staniewicz, L. (2011) Transmission-mode imaging in the environmental scanning electron microscope (ESEM), Ph.D. thesis, University of Cambridge

[320] Beeby, M., Cho, M., Stubbe, J. and Jensen, G.J. (2012) Growth and localization of polyhydroxybutyrate granules in *Ralstonia eutropha*, *Journal of bacteriology*, **194**, 1092–1099